Xjenza Online - Journal of Malta Chamber of Scientists
http://www.mcs.org.mt/

Editorial Board

Editor-in-Chief

Prof Giuseppe Di Giovanni
Department of Physiology and Biochemistry,
University of Malta,
Msida, Malta.
MSD 2080
Tel.: +356 2340 2776
Fax: +356 2131 0577
giuseppe.digiovanni@um.edu.mt

Associate Editors

Biomedical Sciences
Mario Valentino
valentino.mario@um.edu.mt

Cognitive and Social Sciences
Ian Thornton
ian.thornton@um.edu.mt

Economics
Ian Cassar
ian.p.cassar@um.edu.mt

Engineering Science
Philip Farrugia
philip.farrugia@um.edu.mt

Geosciences
Sebastiano D'Amico
sebastiano.damico@um.edu.mt

Information and Communication Technologies
Nicholas Sammut
nicholas.sammut@um.edu.mt

Life Sciences
Sandro Lanfranco
sandro.lanfranco@um.edu.mt

David Mifsud
david.a.mifsud@um.edu.mt

Linguistics
Ray Fabri
ray.fabri@um.edu.mt

Mathematical and Statistical Science
Liberato Camilleri
liberato.camilleri@um.edu.mt

Physics and Chemical Sciences
David Magri
david.magri@um.edu.mt

Advisory Board Members

Prof Angela A. Xuereb Anastasi, University of Malta angela.a.xuereb@um.edu.mt
Prof David Eisner, Manchester University, UK eisner@manchester.ac.uk
Prof Frank Vella, University of Saskatchewan, Canada f.vella@sasktel.net
Prof Giovanni Romeo, University of Bologna, Italy egf.giovanni.romeo@gmail.com
Prof Vincenzo Crunelli, Cardiff University, UK crunelli@cardiff.ac.uk

Project editor

Jackson Levi Said
Department of Physics,
University of Malta,
Msida MSD 2080, Malta.
jsaid01@um.edu.mt

Copy Editor

William Hicklin
Department of Physics,
University of Malta,
Msida MSD 2080, Malta.
whick01@um.edu.mt

Editorial Assistant

Stephanie Chambers
Exeter Medical School,
St Luke's Campus,
Exeter, University,
UK.
sc505@exeter.ac.uk

Web Administrator

John Gabarretta
Department of Chemistry,
University of Malta,
Msida MSD 2080, Malta.
john.gabarretta.09@um.edu.mt

Scope of Journal

Xjenza is the Journal of the Malta Chamber of Scientists and is published in an electronic format. Xjenza is a peer-reviewed, open access international journal. The scope of the journal encompasses research articles, original research reports, reviews, short communications and scientific commentaries in the fields of: mathematics, statistics, geology, engineering, computer science, social sciences, natural and earth sciences, technological sciences, linguistics, industrial, nanotechnology, biology, chemistry, physics, zoology, medical studies, electronics and all other applied and theoretical aspect of science.

The first issue of the journal was published in 1996 and the last (No. 12) in 2007. The new editorial board has been formed with internationally recognised scientists, we are planning to restart publication of Xjenza, with two issues being produced every year. One of the aims of Xjenza, besides highlighting the exciting research being performed nationally and internationally by Maltese scholars, is to provide insight to a wide scope of potential authors, including students and young researchers, into scientific publishing in a peer-reviewed environment.

Instructions for Authors
Xjenza is the journal of the Malta Chamber of Scientists and is published by the Chamber in electronic format on the website: http://www.xjenza.com. Xjenza will consider manuscripts for publication on a wide variety of scientific topics in the following categories

- (01) Communications
- (02) Research Articles
- (03) Research Reports
- (04) Reviews
- (05) Notes
- (06) News
- (07) Autobiography

Communications are short peer-reviewed research articles (limited to three journal pages) that describe new important results meriting urgent publication. These are often followed by a full Research Article.

Research Articles form the main category of scientific papers submitted to Xjenza. The same standards of scientific content and quality that applies to Communications also apply to Research Articles.

Research Reports are extended reports describing research carried out in Malta or by Maltese researchers of interest to a wide scientific audience characteristic of Xjenza. Please contact the editor to discuss the suitability of topics for Research Reports.

Review Articles describe work of interest to the wide readership characteristic of Xjenza. They should provide an in-depth understanding of significant topics in the sciences and a critical discussion of the existing state of knowledge on a topic based on primary literature. Review Articles should not normally exceed 6000 words.Authors are strongly advised to contact the Editorial Board before writing a Review.

Notes are fully referenced, peer-reviewed short articles limited to three journal pages that describe new theories, concepts and developments made by the authors in any branch of science and technology. Notes need not contain results from experimental or simulation work.

News: The News section provides a space for articles up to three pages in length describing leading developments in any field of science and technology or for reporting items such as conference reports. The Editor reserves the right to modify or reject articles for consideration as 'news items'.

Errata: Xjenza also publishes errata, in which authors correct significant errors of substance in their published manuscripts. The title should read: Erratum: "Original title" by ***, Xjenza, vol. *** (year). Errata should be as short as consistent with clarity.

Invited Articles and Special Issues: Xjenza regularly publishes Invited Articles and Special Issues that consist of articles written on invitation by the Editor or member of the editorial board.

Submission of Manuscripts

Manuscripts should be sent in electronic format (via e-mail) to the Editor of Xjenza:

Prof. Giuseppe Di Giovanni
Department of Physiology and Biochemistry
Faculty of Medicine and Surgery (On Campus)
University of Malta
Msida MSD 06
Malta
Tel: (+356) 2340 2776
e-mail: xjenza@mcs.org.mt

Referees
All manuscripts submitted to Xjenza are peer reviewed. Authors are requested to submit with their manuscript the names and addresses of three referees, preferably from overseas. Every effort will be made to use the recommended reviewers; however the editor reserves the right to also consult other competent reviewers.

Conflict of Interest
Authors are expected to disclose any commercial or other associations that could pose a conflict of interest in connection with the submitted manuscript. All funding sources supporting the work, and institutional or corporate affiliations of the authors, should be acknowledged on the title page or at the end of the article.

Policy and Ethics
The work described in the submitted manuscript must have been carried out in accordance with The Code of Ethics of the World Medical Association (Declaration of Helsinki) for experiments involving humans (http://www.wma.net/en/30publications/10policies/b3/index.html); EU Directive 2010/63/EU for animal experiments (http://ec.europa.eu/environment/chemicals/lab_animals/legislation_en.htm); Uniform Requirements for manuscripts submitted to Biomedical journals (http://www.icmje.org). This must be stated at an appropriate point in the article.

Submission, Declaration and Verification
Submission of a manuscript implies that the work described has not been published previously (except in the form of an abstract or as part of a published lecture or academic thesis), that it is not under consideration for publication elsewhere, that it has been approved for publication by all authors, and tacitly or explicitly, by the responsible authorities where the work was carried out, and that, if accepted, it will not be published elsewhere in the same form, in English or in any other language, including electronically, without the written consent of the copyright-holder.

Permissions
It is the responsibility of the corresponding author of a manuscript to ensure that there is no infringement of copyright when submitting material to Xjenza. In particular, when material is copied from other sources, a written statement is required from both the author and/or publisher giving permission for reproduction. Manuscripts in press, unpublished data and personal communications are discouraged; however, corresponding authors are expected to obtain permission in writing from at least one author of such materials.

Preparation of Manuscripts
It is important that the file be saved in the native format of the word processor used. If the LaTeX typesetting language is used to prepare the manuscript the Xjenza style, available at https://dl.dropboxusercontent.com/u/8940972/XjenzaPaperTemplate.zip, should be used. Any new commands and environments created for the manuscript should be placed in a separate file. All the files necessary to run the document should be supplied together with the rendered PDF. If another word processor is used, the text should be in single-column format and layout of the text to be kept as simple as possible. Most formatting codes will be removed and replaced on processing of the manuscript. The word processor options should not be used in order to justify text or hyphenate words. However, the use of bold face, italics, subscripts, superscripts etc. is permitted. Together with the native format of the word processor, a pdf, generated by the word processor, should be given.

Article Structure
A manuscript for publication in Xjenza will ordinarily consist of the following order: Title page with contact information, Abstract, Highlights, Keywords, Abbreviations, Introduction, Materials and Methods, Results, Discussion, Conclusions, Appendices and References.

The manuscript will be divided into clearly defined sections. Each subsection should be given a brief heading. Each heading should appear on its own separate line. Subsections should be used as much as possible when cross-referencing text: refer to the subsection by heading as opposed to simply 'the text'.

Title page
- Title should be concise yet informative. Titles are often used in information-retrieval systems. Avoid abbreviations and formulae where possible.
- Author names and affiliations. Present the authors' affiliation addresses (where the actual work was done) below the names. Indicate all affiliations with a lower-case superscript number immediately after each author's name and in front of the appropriate address. Provide full postal address of each affiliation, including the country name and, if available, the e-mail address.
- Corresponding author. Clearly indicate who will handle correspondence at all stages of refereeing and publication, including post-publication. Ensure that telephone and fax numbers (with country and area code) are provided in addition to the e-mail address and complete postal address. Contact details must be kept up to date by the corresponding author.
- Present/permanent address. If an author has changed the address since the work described, this can be indicated as a footnote to the author's name. The address at which the author actually did the work must be retained as the main, affiliation address. Superscript Arabic numerals are used for such footnotes.

Abstract
A concise and factual abstract is required of up to about 250 words. The abstract should state briefly the background and purpose of the research, the principal results and major conclusions. An abstract is often presented separately from the article, so it must be able to stand alone. For this reason, references and non-standard abbreviations should be avoided. If essential, these must be defined at first mention in the abstract itself.

Highlights
Highlights are mandatory for Xjenza. They consist of a short collection of 3-5 bullet points of a minimum of 85 characters (including spaces) each, that convey the core findings of the article and should be submitted in a separate file. Please use 'Highlights' in the file name.

Keywords
Immediately after the abstract, provide a maximum of 10 keywords to be used for indexing purposes.

Abbreviations
Define abbreviations that are not standard in this field in a footnote to be placed on the first page of the article. Such abbreviations that are unavoidable in the abstract must be defined at their first mention as well as in the footnote and should be used consistenly throughout the text.

Introduction
State the objectives of the work and provide an adequate background, avoid a detailed literature survey or a summary of the results.

Material and Methods
Provide sufficient detail to allow the work to be reproduced. Methods already published should be indicated by a reference: only relevant modifications should be described.

Results
Results should be clear and concise. Numbered/tabulated information and/or figures should also be included.

Discussion
This should explore the significance of the results of the work, yet not repeat them. Avoid extensive citations and discussion of published literature. A combined section of Results and Discussion is often appropriate.

Conclusions
The main conclusions based on results of the study may be presented in a short Conclusions section. This may stand alone or form a subsection of a Discussion or Results and Discussion section.

Appendices
Formulae and equations in appendices should be given separate numbering: Eq. (A.1), Eq. (A.2), etc.; in a subsequent appendix, Eq. (B.1) and so on. Similarly for tables and figures: Table A.1; Fig. A.1, etc.

Acknowledgements
Collate acknowledgements in a separate section at the end of the article before the references and do not, therefore, include them on the title page, as a footnote to the title or otherwise. List here those individuals who provided assistance during the research (e.g., providing language help, writing assistance or proof reading the article, etc.).

Units
Follow internationally accepted rules and conventions: use the

international system of units (SI). If other units are mentioned, please give their equivalent in SI.

Footnotes
Footnotes should be used sparingly. Number them consecutively throughout the article, using superscript Arabic numbers. Many word processors build footnotes into the text, and this feature may be used. Should this not be the case, indicate the position of footnotes in the text and present the footnotes themselves separately at the end of the article. Do not include footnotes in the Reference list.

Table Footnotes
Indicate each footnote in a table with a superscript lower case letter.

Artwork
Electronic artwork General points:

- Make sure you use uniform lettering and sizing of your original artwork.
- Save text in illustrations as 'graphics' or enclose the font.
- Only use the following fonts in your illustrations: Arial, Courier, Times, Symbol.
- Number the illustrations according to their sequence in the text.
- Name your artwork files as 'fig$x$' or 'tab$x$' where x corresponds to the sequence number in your document.
- Provide captions to illustrations separately.
- Produce images near to the desired size of the printed version.
- Make sure that the artwork has no margins and borders.
- Submit each figure as a separate file.

A detailed guide on electronic artwork is available on our website: http://www.xjenza/authorguidelines

Formats
Regardless of the application used, when your electronic artwork is finalised, please 'save as' or convert the images to one of the following formats (note the resolution requirements for line drawings, halftones, and line/halftone combinations given below):
EPS or SVG: Vector drawings. Embed the font or save the text as 'graphics'.
TIFF: Color or grayscale photographs (halftones): always use a minimum of 300 dpi.
TIFF: Bitmapped line drawings: use a minimum of 1000 dpi.
TIFF: Combinations bitmapped line/half-tone (color or grayscale): a minimum of 500 dpi is required.
Where possible use a vector format for your artwork. If this is not possible, supply files that have and adequate resolution.

Colour Artwork
Please make sure that artwork files are in an acceptable format (TIFF, EPS or SVG) and have the correct resolution.

Figure Captions
Ensure that each illustration has a caption. Supply captions separately, not attached to the figure. A caption should comprise a brief title (not on the figure itself) and a description of the illustration. Keep text in the illustrations themselves to a minimum, but explain all symbols and abbreviations used.

Tables
Number tables consecutively in accordance with their appearance in the text. Place footnotes to tables below the table body and indicate them with superscript lowercase letters. Avoid vertical rules. Be sparing in the use of tables and ensure that the data presented in tables do not duplicate results described elsewhere in the article.

References
Citation in text

Every reference cited in the text should also be present in the reference list (and vice versa). The reference list should be supplied as an Endnote (*.xml), Research Information Systems (*.ris), Zotero Library (zotero.splite) or a BiBTEX (*.bib) file. Unpublished results and personal communications are not recommended in the reference list, but may be mentioned in the text. If these references are included in the reference list they should follow the standard reference style of the journal and should include a substitution of the publication date with either 'Unpublished results' or 'Personal communication'. Citation of a reference as 'in press' implies that the item has been accepted for publication.

Web references
The full URL should be given together with the date the reference was last accessed. Any further information, if known (DOI, author names, dates, reference to a source publication, etc.), should also be given. Web references can be listed separately or can be included in the reference list.

References in a Special Issue
Please ensure that the words 'this issue' are added to any references in the list (and any citations in the text) to other articles in the same Special Issue.

Reference Style
Text: All citations in the text should refer to:
1. Single author: the name (without initials, unless there is ambiguity) and the year of publication;
2. Two authors: both names and the year of publication;
3. Three or more authors: first author's name followed by 'et al.' and the year of publication.
Citations may be made directly (or parenthetically). Groups of references should be listed first alphabetically, then chronologically.
Examples: 'as demonstrated (Allan, 2000a, 2000b, 1999; Allan and Jones, 1999). Kramer et al. (2010) have recently shown ....'
List: References should be arranged first alphabetically and then further sorted chronologically if necessary. More than one reference from the same author(s) in the same year must be identified by the letters 'a', 'b', 'c', etc., placed after the year of publication. For articles with more then five authors, only the first five should be listed followed by 'et al'.

Examples:
Reference to a Journal Publication:

Apostol, B. L., Kazantsev, A., Raffioni, S., Illes, K., Pallos, J., et al. (2003). A cell-based assay for aggregation inhibitors as therapeutics of polyglutamine-repeat disease and validation in Drosophila. *Proc. Natl. Acad. Sci. U. S. A.* 100(10), 5950–5.

Venter, J. C., Adams, M. D., Myers, E. W., Li, P. W., Mural, R. J., et al. (2001). The sequence of the human genome. *Science.* 291(5507), 1304–1351.

Reference to a Book:

Bruce, V., Doyle, T., Dench, N. and Burton, M. (1991). Remembering facial configurations. *Cognition.* 38(2), 109–144.

Reference to a Chapter in an Edited Book:

Di Giovanni G., Pierucci M., Di Matteo V. (2011). *Monitoring Dopamine in the mesocorticolimbic and nigrostriatal systems by microdialysis: relevance for mood disorders and Parkinson's disease.* In: Applications of Microdialysis in Pharmaceutical Science. Ed: Tsai T-H. John Wiley & Sons,

Inc., Hoboken, NJ, USA.

Journal Abbreviations Journal names should be abbreviated according to:
-Index Medicus journal abbreviations: http://www.nlm.nih.gov/tsd/serials/lji.html;
-List of title word abbreviations: http://www.issn.org/2-22661-LTWA-online.php;
-CAS (Chemical Abstracts Service): http://www.cas.org/sent.html.

Video data
Xjenza accepts video material and animation sequences to support and enhance the presentation of the scientific research. Authors who have video or animation files that they wish to submit with their article are strongly encouraged to include these within the body of the article. This can be done in the same way as a figure or table by referring to the video or animation content and noting in the body text where it should be placed. All submitted files should be properly labelled so that they directly relate to the video files content. This should be provided in one of our recommended file formats with a preferred maximum size of 50 MB.

Submission checklist
The following list will be useful during the final checking of a manuscript prior to sending it to the journal for review. Please consult this Guide for Authors for further details of any item.
Ensure that the following items are present:
One author has been designated as the corresponding author with contact details:

- E-mail address
- Full postal address
- Telephone and fax numbers

All necessary files have been sent, and contain:

- Keywords
- All figures are given separately in EPS, SVG of TIFF format
- Caption for figures is included at the end of the text
- All tables (including title, description, footnotes)
- The reference list XML, RIS, zotero.splite or BIB file is given

Further considerations

- Manuscript has been 'spell-checked' and 'grammar-checked'
- References are in the required format
- All references mentioned in the reference list are cited in the text, and vice versa
- Permission has been obtained for use of copyrighted material from other sources (including the Web)
- A PDF document generated from the word processor used is given

After Acceptance
Use of the Digital Object Identifier
The Digital Object Identifier (DOI) may be used to cite and link to electronic documents. The DOI consists of a unique alpha-numeric character string which is assigned to a document by the publisher upon the initial electronic publication. The assigned DOI never changes. Therefore, it is an ideal medium for citing a document, particularly 'Articles in press' because they have not yet received their full bibliographic information. When you use a DOI to create links to documents on the web, the DOIs are guaranteed never to change.

Proofs, Reprints and Copyright
Authors will normally be sent page proofs by e-mail or fax where available. A list of any necessary corrections should be sent by fax or email to the corresponding editor within a week of proof receipt to avoid unnecessary delays in the publication of the article. Alterations, other than essential corrections to the text of the article, should not be made at this stage. Manuscripts are accepted for publication on the understanding that exclusive copyright is assigned to Xjenza. However, this does not limit the freedom of the author(s) to use material in the articles in any other published works.

Xjenza Online - Journal of Malta Chamber of Scientists
www.xjenza.org

Editorial

Nicholas Sammut

Dear Readers,

Welcome to the Xjenza Online first special issue which focuses on the outcomes of the contributions made to the 6th Workshop in ICT (WICT) organised by the Faculty of ICT at the University if Malta.

With over 50 contributions, WICT reached new heights since its inception 6 years ago. 32 of these contributions were academic focusing on emerging postgraduate research in artificial intelligence, communications and computer engineering, computer information systems, computer science, Microelectronics and Nanoelectronics.

The workshop also had two specialised sessions: one on Entrepreneurship with 12 contributions and the other on microelectromechanical systems (MEMs) with 7 contributions.

6 of the best academic contributions are presented in this special issue. In the first paper, Conrad Attard, Colin Cachia and Matthew Montebello report the development of a tool intended for caregivers which helps them monitor wandering persons with dementia. Such practical systems will undoubtedly increase in use with the ever increasing impact of dementia and similar diseases on society at large.

The second paper by Jonathan Mifsud and Matthew Montebello presents a preliminary study on private social network dynamics to understand related trends. A visualisation method of the connections in the network is presented and used to indicate how skill shortages in the network can be identified. This method can have a number of applications particularly in corporations that use private social networks in their modus operandi.

The third paper by Melanie Zammit and Adrian Francalanza investigates uniqueness typing for a higher-order channel. A type system based on the concept of uniqueness asserts when it is safe to change the object type in a channel.

Adrian Francalanza this time with Mandy Zammit, also investigates formal proofs for broadcast algorithms. Two broadcast algorithms are studied and an encoding framework using a process descriptive language is presented. This framework is then used to formalise these algorithms.

Ian Cassar, Christian Colombo and Adrian Francalanza also present a paper on monitoring distributed systems with distributed PolyLarva; a language–agnostic runtime verification tool. They present a formal implementation-independent model which proves important properties such as determinism hence enabling ways of re-designing the tool in a more scalable way. Amongst other results, a prototype implementation of the distributed PolyLarva tool implements the new actor-based semantics over a language that can natively handle distribution and concurrency.

Finally Russell Farrugia, Ivan Grech, Owen Casha, Joseph Micallef, Edward Gatt, Roseanne Duca and Conrad Cachia study warpage issues in large area mould embedded technologies. This is a very important problem encountered in most MEMs. They delve into possible causes of asymmetric warpage related to dimensional and material characteristics of moulds by using finite element techniques. These results are validated through measurements which in turn are used to deduce appropriate guidelines for low warpage wafer encapsulation. Such results are very important in packaging applications of MEM devices.

We hope that you enjoy this collection of academic papers as we aspire to use such special issues to create a new channel for authors and editors in scientific fields to publish their work.

Yours Sincerely,

Nicholas Sammut;

Guest Editor Xjenza Online

Xjenza Online - Journal of The Malta Chamber of Scientists
www.xjenza.org
DOI: 10.7423/XJENZA.2014.2.01

Research Article

WanderRep: A reporting Tool for Caregivers of Wandering Persons with Dementia

Colin Cachia, Conrad Attard and Matthew Montebello
Department of Computer Information Systems, University of Malta, Msida, Malta

Abstract. Wandering behaviour is regarded as one of the most difficult to manage for Caregivers of Persons with Dementia. It also results in a lot of stress and burden for all caregivers involved, since this behaviour can result in injuries and getting lost. In this research we are proposing a tool which utilizes the currently available Smart Mobile Technologies to focus on the patients' wandering patterns whilst identifying any possible dangers pertaining to the patient. A number of findings have been collected from this research tool, through a number of studies with both formal and informal caregivers and patients at the St. Vincent de Paul Elderly Nursing Home. These findings primarily relate to: (1) The benefits which caregivers perceive when being alerted of danger relating to their patients and (2) the need for further understanding this research area through the collected data. Caregivers are also given the opportunity to give their feedback on a patient's exposure to danger, thus creating a cooperative environment between caregivers of the same patient. Preliminary tests have shown how this system achieves an 89 % specificity to danger rate, which defines the statistical performance of a binary classification test, together with showing how caregivers find this system as a positive way of reducing their burden when caring for wandering patients.

Keywords Dementia, Wandering, Burden, Smart Mobile Technology

1 Introduction

Due to the number of improvements being achieved in the areas of medicine and quality of life, amongst others, the age structure of societies worldwide is continuously changing with a constantly aging trend. As a matter of fact, the European old-age dependency ratio in 2010 amounted to 25.9 % while it is projected to grow to more than 34 % by 2025, as reported by Eurostat (n.d.). This indicates that by 2025, the European eligible work force (including people aged between 15 and 64) will consist of an average of 66 % of all the population, thus another 34 % are aged 65 and over. In the Maltese islands, this ratio is expected to reach 28 % of the population by 2050, according to Abela et al. (2007).

As a result of this increase in age, an increased frequency of age related deficiencies, such as physical and cognitive impairments, are continuously demanding a higher availability of health and social services. This is especially the case when the elder people suffer from conditions such as Dementia and Alzheimer's Disease, where they would be unable to keep on living independently in their own homes. Figures show how persons with dementia are expected to amount to 1.47 % of the whole Maltese population by 2015, while the same figure is expected to reach a staggering amount of 3.26 % by 2050 and 3.62 % by 2060, according to A. Scerri and C. Scerri (2012).

The term "successful ageing" is regarded as a fundamental goal that must be achieved to fight this ageing problem. Zhou et al. (2012) define successful ageing, which is also referred to as "ageing-in-place" by Patterson et al. (2002), across a number of elements, namely: reduced physical disability over the age of 75, good self-ratings and a greater length of a normal and independent life. Courtenay et al. (2010), however, detail two strategies that can be considered in achieving successful ageing at home:

Ageing-in-place Care provision is gradually adapted according to the user's needs inside the household;
In-Place Progression User moves within the service as his/her needs increase.

Considering the shortage in the current supply of professional care workers, helping patients achieve successful ageing has proved to be a stressful task for caregivers (both formal and informal) and family members of people with these types of cognitive impairments as Lauriks et al. (2007) and Wherton and Monk (2010) suggest. According to Hulme et al. (2010), this burden is largely due to the emotional and behavioural problems that the persons with dementia evidence, along with the decline in function and other symptoms such as aggression, depression and wandering.

Correspondence to: Colin Cachia (ccac0005@um.edu.mt)

© 2014 Xjenza Online

2 Dementia

Dementia can be divided into several types of conditions, which all include a degree of cognitive decline that influences a patient's ability to conduct activities of daily living. These include, amongst others: Alzheimer's disease, Vascular Dementia and Pick's Disease. Moreover, the condition can be divided into three main stages, each having different characteristics: Mild/Early which usually takes 2-4 years until the patient progresses to the next stage, Moderate which can take 2 up to 10 years and Severe which can endure 1 to 3 or more years (Alzheimer'sAssociation, 2011).

The caring of persons with dementia mainly involves the attending and supervision of everyday needs, together with the management of behavioural problems. The latter are in fact the most recurring issues when caring for a patient diagnosed with dementia, and require constant supervision since the person involved may end up disoriented, unable to express his/her feelings, and end up behaving disruptively. These behaviours can range from repeatedly asking the same questions to having more aggressive actions such as hitting, biting and screaming (WHO, 2012). Although not every person suffering with dementia resorts to these types of behaviours, all may face vulnerabilities to low frustration tolerance, impaired judgment, apathy and inability to initiate tasks as Zimmerman (2001) notes. On the other hand, Wherton and Monk (2010) note how persons with mild dementia face difficulties when conducting multi-step tasks due to memory impairment. Biswas et al. (2010) confirm this issue and state that conducting these daily tasks becomes problematic even though they are physically capable of doing them correctly. This matter is made worse when the patient is not capable of remembering the correct steps required in Activities of Daily Life (ADL), such as grooming, bathing, eating and taking medication on time. Mild dementia can also affect more complex activities, such as tidying, cooking and financial calculations. This concern raises the need for personal assistance and residential care in order to fight consequences such as diminished quality of life, poor self-esteem and anxiety (Hoey et al., 2011).

Apart from the several everyday activity functional deficiencies, Douglas et al. (2011) notice how cognitive decline also brings about a number of safety concerns this may cause persons with dementia, such as forgetting items on a stove and taking medication too frequently.

3 Wandering Behaviour

Research in the area of wandering has resulted into a number of definitions, most notably the one defined by Hermans et al. (2007), who explains Wandering as a set of issues related to people with dementia walking inside or away from home, with health risks related to injury, weight loss, early institutionalisation, decline of language skills, premature mortality and therefore higher caregiver burden. Another highly cited definition is given by Algase (2006) who describes the behaviour as one which incorporates, at a minimum, the amount of walking or wandering, spatial disorientation and eloping behaviour. The review by Algase also shows a relationship between agitation and wandering with these patients. Wandering can be considered as one of the most frequent and possibly hazardous behaviour malfunctions in persons with dementia, as illustrated by Vuong et al. (2011). This behaviour terminology combines a number of different complex actions without each having a reason in particular, as Faucounau et al. (2009) state. In accordance with this statement, Robinson et al. (2007) argue that there is no distinct definition for wandering, which is also dubbed as agitation or agitated behaviour and can be described according to geographical pattern, typology and neurocognitive deficits. Despite this claim, Algase (2006) reviewed literature in the area and came up with the most cited definition of wandering behaviour, as quoted below:

"*Wandering is a syndrome of dementia-related locomotion behaviour having a frequent, repetitive, temporally-disordered, and/or spatially disoriented nature that is manifested in lapping, random, and/or pacing patterns, some of which are associated with eloping, eloping attempts, or getting lost unless accompanied.*"

While wandering is still considered as dangerous and a source of distress for carers, its main consequences can also be beneficial for persons with dementia. In fact, wandering can be considered as a form of exercise which can help in the patient's blood circulation, amongst other benefits, as Robinson et al. (2007) suggest.

Despite these benefits, Faucounau et al. (2009) argue that caregivers (both formal and professional) find it very unsafe for their patients to wander on their own, since they will be more likely to stray outside, get physically hurt and even face deadly situations. On the other hand, Douglas et al. (2011) state that the prospect of injuries from wandering was found to be low as compared to the injuries suffered by the same types of patients in other situations, such as falls. Siders et al. (2004) explain how frequent wanderers face a considerably larger chance of falling, having hip fractures, facing home placement and making use of physical restraints.

The hazards from wandering can be further measured when compared to the likelihood of injury from fire and burns, where wandering behaviour was found to present a greater risk to the persons with dementia themselves. Douglas et al. (2011) also show how wandering behaviour is still reported as the most common safety problem by caregivers, whilst increased caregiver rigour is a direct result of increased patient wandering situations.

Although research has highlighted a number of hazards related to wandering, this research required further evidence of the problems which caregivers face in their day to day jobs. The section below introduces the research conducted with both caregivers and persons with dementia to achieve this goal.

4 Methodology

4.1 Participants and Instrumentation

For the purpose of this research, two main events were organised in order to gather the necessary data and elements required by this work. These events involved; (1) A

Workshop with Dementia Caregivers, and (2) Pilot Study with Dementia Patients.

The workshop was primarily organised to gather first hand insight into what care giving on a daily basis means. This helps in understanding the problems associated with patients with dementia , especially those with wandering behaviour. On the other hand, the aim of the Pilot Study was twofold: It provided the possibility of collecting wandering and movement data related to a Person with Dementia (PwD) inside the care home, as well as the opportunity to conduct interview and feedback sessions with Caregivers themselves who were given a demonstration of the final prototype and asked to evaluate the system.

The first workshop with Dementia Caregivers was organised in St. Julian's, Malta, and attracted a total of 16 formal and informal caregivers. The attendees were first given an overview of the current limitations found in research with regards to caring for dementia patients. During the second part of this workshop, attendees were offered the opportunity to contribute with their experiences and discuss ways in which their troubles might be alleviated through the use of technology.

The second event was conducted over a period of 5 days at the St. Vincent de Paul Residence in Marsa, Malta. A total of 5 Professional Caregivers participated in this study, where a prototype of the system was presented for their use. This proptotype utilised wandering pattern data collected from a Dementia Patient inside the ward during the same study. This data was collected by using indoor wireless signal Received Signal Strength (RSS) fingerprinting for indoor positioning, by using a Smartwatch device capable of recording location data relating to the patient. Caregivers were given examples of/how the system reacts to irregular wandering patterns displayed by the patients.

5 Smart mobile technology

With the utilisation of the latest smart technologies, Information and Communication Technology (ICT) can become a significant player in the creation of intelligent and automated home environments which help the elderly in their day-to-day lives while still sustaining their independence and self-sufficiency despite their ageing process.

Research has achieved the objective of ageing-in-place in a number of cases through Context Awareness, which forms part of the latest generation of computing, known as Ubiquitous Computing. This vision, otherwise known as pervasive computing, knows its foundation in research by Weiser (1991). He described this concept as one where technologies vanish into the structure of objects which people use for everyday tasks, in a way which makes it unnoticeable to its users. When this vision was published, the required technology wasn't available and eventually the vision did not materialise. However, with the advancing developments in computer hardware, sensors and their networking capabilities, Wieser's vision is becoming even more possible to emerge, as Satyanarayanan (2001) explains.

Pervasive computer systems need to continuously exploit information about the situation of their users, or the state of the actual system in order to make adaptations to their behaviour. These functions contribute to another concept of visions: those of context-aware systems, which according to Mark Wieser, will make the vision of pervasive computing possible. In fact, he describes it as a vision of personal computing through which future living environments are infused with non-interfering, seamlessly operating services which are readily available upon user's request (Weiser, 1991).

6 WanderRep

Given the highly stressful task of managing wandering dementia patients, WanderRep, as a tool, aims to help both the caregiver in managing a patient more effectively and the patient being safeguarded against possible dangers. This work utilises Mobile Computing to ultimately achieve the pre-determined objectives. In this type of model, where the computer in question is expected to be portable and transported with the user, a number of limitations arise. This is mainly due to the restricted nature of currently available mobile devices with regards to hardware specifications such as storage capacities and processing power. This work is thus basing its proposal on a general Client/Server Architecture, where different layers refer to particular functions within this eco-system which together work to overcome the limitations in current mobile devices while achieving the pre-set objectives. All components pertaining to each side will be analysed. These include: Patient Mobility Layer, Distributed Database Layer, Machine Learning Layer, Service Layer, Caregiver Mobility Layer and Client Database Layer. The overall architectural design is displayed in Figure 1.

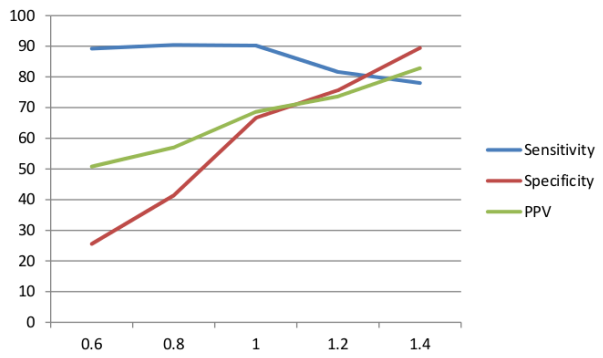

Figure 1: Technical Architecture

6.1 Server Side

This research extends the work of Vuong et al. (2011, 2011), who propose a wandering recognition process based on a less resource intensive smartphone. Given the lack of computing resources available, this method makes use of State Prediction techniques with adaptive confidence estimation in order to predict a patient's next location, which allows for a degree of certainty when predicting a future state. When it comes to analysing the user's actual patterns, Vuong et al. apply the definition introduced by Martino-Saltzman et al. (1991) in representing the user's

movement patterns as wandering or non-wandering patterns.

Assessment of a user's state is tackled through a different approach, taking machine learning methods as a solution. The wandering detection algorithm being proposed in this work involves the inclusion of the four main features, or attributes, which ultimately are involved in building the wandering profile of a patient. Based on the types of dangers to be deduced, the features chosen for this algorithm include Location, Travel Patterns, Temperature and Activity Level. All these will be coupled with their respective Time element. This structure aims to give maximum flexibility for the system to learn the user's main traits. These will be used to model the patient's profile for abnormal event detection capabilities.

The machine learning layer being proposed in this work has the objective of providing a level of intelligence capable of understanding a patient's behaviour and habits in order to be able to detect episodes whenever the patient's behaviour is considered aberrant. This work makes use of Unsupervised Learning algorithms to provide the system with a learning ability where the patient's normal behaviours are learnt, making it possible for the system to identify and detect events when the patient's behaviour does not conform to these habits. The choice falls on Unsupervised Learning since this involves a one-class approach to learning what is normal and can be used to detect what is abnormal in the user's whole presence dataset. Since anomalous data in these scenarios is highly difficult to gather, Unsupervised Learning fits in perfectly with the requirements of this project since a patient's behaviour will be assessed based on current and historical unlabelled data. Clustering and Anomaly Detection techniques are used in this case to provide for Unsupervised Learning of a patient's patterns and the discovery of abnormal data. This approach uses X-Means for clustering of data, together with Local Density Cluster-Based Outlier (LDCOF) for detection of anomalies in the patient's behaviour.

6.2 Client Side

This solution is implemented on a smart mobile device, whose main objectives are those of tracking a patient's indoor movements while being unobtrusive in the user's activities. Indoor positioning has proved to be a major research area in academia. In fact, one of the more widely accepted positioning techniques, the Global Positioning System (GPS), is efficiently used when outdoors. However, as Dale (2010) and Kamel et al. (2011) report, this system doesn't work inside homes and suffers from bad reception in areas with high buildings. For this reason, a system which makes use of a smart device and the available Wireless Local Area Networks (WLAN) was chosen to allow for indoor positioning. With the use of inexpensive and currently available WLAN access point location fingerprints, this implementation would be capable of detecting the location of a user by comparing the access point values with a fingerprint database of values related to particular predefined locations.

Given these requirements, the smart mobile device shall consist of a wearable smart watch which has the capability of scanning for WLAN access points and communicating these values wirelessly to a centralised server. This solution is ideal since it allows for indoor positioning to be realised while being less intrusive to the patients during the pilot study. The smartwatch should also be running on the Android platform, which allows for the developed solution to be used across a number of other devices. Android is an open source framework, mainly designed to be used in mobile devices, and is managed by Google. Android also provides a number of development tools which includes all the libraries needed to interface with the available hardware and to deploy the application effortlessly in the smartwatch and other compatible Android devices.

7 Results

The Caregiver Workshop provided positive outcomes as to what caregivers perceive from the use of technology in their area, especially when related to the problems and dangers caused by their patients' wandering behaviour. One of the most significant outcomes was that of caregivers considering this type of behaviour to be one of the most stressful from their daily challenges associated with caring for people suffering from dementia. This is reflected through the 100 % of results, implying that all attendees agree with this statement.

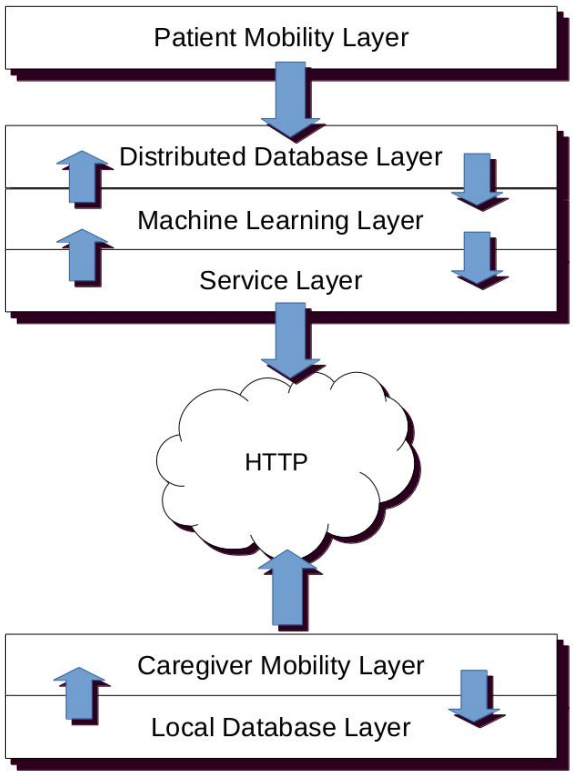

Figure 2: Sensitivity, Specificity and PPV results at the different levels of threshold

With regards to one of the major indicators of wandering

behaviour, that of tracking movement of patients, caregivers also showed positive feedback. In fact, more than 75 % of respondents state that deterioration in a patient's cognitive ability is reflected through a change in daily routines, although these routines are different according to the patient. Therefore, the tracking of changes in a patient's patterns can lead to a caregiver being alarmed of any substantial changes in a dementia patient's wandering routines. From the subsequent workshops, the features found in Table 1 were considered to be important for a Wandering Detection system to consider in order to identify danger associated with wandering.

Table 1: Features and Associated Dangers identified during Caregivers' Workshop

Feature	Danger
Location	Wandering Patterns
Temperature	Hypothermia, Sickness
Time	Sundowning, Associated time with movements
Activity Level	Fatigue, Chance of Wandering

The features identified as a result of the caregiver workshop were implemented into a proof of concept system which allowed formal caregivers to test a solution based on these outcomes. Moreover, five case scenarios were tested using the proof of concept, tackling the following patient situations: (a) Irregular Wandering Patterns, (b) Low Activity Levels, (c) High Activity Level, (d) Non-Compliance To Daily Activities, and (e) Irregular Ambient Temperatures. These case scenarios were tested for an indication of the Proof of Concept's success rate in determining dangers from a patient's wandering scenario. Three main values were identified in this case, namely Sensitivity and Specificity to Danger as a Binary Classification Test and a Positive Predictive Value as a precision value for true positive results. The following results listed in Table 2 were achieved across the five case studies.

Table 2: Case Studies Results

Sensitivity	78 %
Specificity	89 %
Positive Predictive Value	83 %

The results confirm that the five different case scenarios achieved a high specificity to danger rate at 89 %. Sensitivity reached high average scores at 78 %. This implies a high proportion of actual positives being identified as such. In this case, the system is providing high proportions when identifying real danger scenarios. This implies that fewer false alarms are generated by the system as the probability of normal activity being regarded as abnormal is lower. The precision rate in identifying dangerous scenarios, denoted as PPV, follows a similar average rate at 83 %. These results can be considered as positive due to the system's dependency on an Unsupervised Learning System for Danger Detection, as shall be explained in the following sections.

8 Conclusion

This paper describes in detail the framework used to conduct the work as part of this research. This work includes the design of a new wandering detection algorithm, its implementation through a technical architecture, together with its field evaluation together with experts in the area of Caregiving for Persons with Dementia.

8.1 Evaluation

The evaluation process involved in this work has included two main outlooks, namely: (i) the creation of five case studies each representing a particular dangerous scenario being exposed to the patient, as identified through literature and field research, and (ii) an interview session held with caregivers of Persons with Dementia at the St. Vincent de Paul residence for the elderly.

The major outcome from this evaluation involves a high percentage of accuracy when detecting dangers, as reflected by the 78 % sensitivity to danger rate shown in Figure 2. This figure can further be improved through time as extra learning data is applied to the model within the Unsupervised Learning System. These results imply the achievability of objectives such as ageing in place and in-place progression for older adults diagnosed with Dementia when utilising Smart Mobile technologies. On the other hand, caregivers' evaluation of the final prototype involves a number of positive elements with regards to the system's modelling and utilised user interface.

Despite these advantages, caregivers also suggest further improvements with the addition of further data related to the patient, such as blood pressure levels and sugar levels, together with ways of creating a suitable cooperation environment for all formal and informal caregivers caring for the same patient.

8.2 Future Research

This work utilises four main features for its learning model, namely: Temperature, Activity Level, Location and Time. These features are then modelled into the Patient Safety Wandering Profile. Given the rate by which Smart Technology is continuously progressing, increasing capabilities and sensors along the way, future research may include more features related to body sensors, such as tilt, blood pressure and body temperature. Moreover, security with regards to the sensitive nature of the data handled by these sensors also needs to be tackled in future work.

8.3 Constraints and Limitations

The major constraints in this research are related to the availability of resources, both human and technical. Apart from lacking the availability of both professional and formal caregivers. More accurate indoor positioning methods are also a limit on this research. A point of mention is also required for the difficulty encountered when conducting research with the vulnerable subjects specified in this work.

References

Abela, S., Mamo, J., Aquilina, C. and Scerri, C. (2007). Estimated prevalence of dementia in the Maltese Islands. *Malta Med. J.* 19(2), 23–26.

Algase, D. L. (2006). What's new about wandering behaviour? An assessment of recent studies. *Int J Older People Nurs.* 1(4), 226–234.

Alzheimer'sAssociation. (2011). Understanding Dementia: Signs, Symptoms, Types, Causes and Treatment.

Biswas, J., Sim, K., Huang, W., Tolstikov, A., Aung, A., et al. (2010). Sensor based micro context for mild dementia assistance. *Proc. 3rd Int. Conf. PErvasive Technol. Relat. to Assist. Environ. - PETRA '10.*

Courtenay, K., Jokinen, N. S. and Strydom, A. (2010). Caregiving and Adults With Intellectual Disabilities Affected by Dementia. *J. Policy Pract. Intellect. Disabil.* 7(1), 26–33.

Dale, Ø. (2010). Usability and Usefulness of GPS Based Localization Technology Used in Dementia Care. *Lect. Notes Comput. Sci.* 300–307.

Douglas, A., Letts, L. and Richardson, J. (2011). A systematic review of accidental injury from fire, wandering and medication self-administration errors for older adults with and without dementia. *Arch. Gerontol. Geriatr.* 52(1), e1–e10.

Eurostat. (nodate). European old-age dependency ratio.

Faucounau, V., Riguet, M., Orvoen, G., Lacombe, A., Rialle, V., et al. (2009). Electronic tracking system and wandering in Alzheimer's disease: A case study. *Ann. Phys. Rehabil. Med.* 52(7-8), 579–587.

Hermans, D. G., Htay, U. H. and McShane, R. (2007). Non-pharmacological interventions for wandering of people with dementia in the domestic setting. *Cochrane database Syst. Rev.* (1), CD005994.

Hoey, J., Plötz, T., Jackson, D., Monk, A., Pham, C. and Olivier, P. (2011). Rapid specification and automated generation of prompting systems to assist people with dementia. *Pervasive Mob. Comput.* 7(3), 299–318.

Hulme, C., Wright, J., Crocker, T., Oluboyede, Y. and House, A. (2010). Non-pharmacological approaches for dementia that informal carers might try or access: a systematic review. *Int. J. Geriatr. Psychiatry.* 25(7), 756–63.

Kamel, B. M. N., Athanasios, A., Evangelos, B. and Mary, P. (2011). Geo-enabled technologies for independent living: Examples from four European projects. *Technol. Disabil.* 23(1), 7–17.

Lauriks, S., Reinersmann, A., der Roest, H. G., Meiland, F. J. M., Davies, R. J., et al. (2007). Review of ICT-based services for identified unmet needs in people with dementia. *Ageing Res. Rev.* 6(3), 223–246.

Martino-Saltzman, D., Blasch, B. B., Morris, R. D. and McNeal, L. W. (1991). Travel Behavior of Nursing Home Residents Perceived as Wanderers and Non-wanderers. *Gerontologist.* 31(5), 666–672.

Patterson, D. J., Etzioni, O., Fox, D. and Kautz, H. (2002). Intelligent Ubiquitous Computing to Support Alzheimer's Patients: Enabling the Cognitively Disabled. In *Ubicog '02 first int. work. ubiquitous comput. cogn. aids.*

Robinson, L., Hutchings, D., Corner, L., Finch, T., Hughes, J., et al. (2007). Balancing rights and risks: Conflicting perspectives in the management of wandering in dementia. *Health. Risk Soc.* 9(4), 389–406.

Satyanarayanan, M. (2001). Pervasive computing: vision and challenges. *IEEE Pers. Commun.* 8(4), 10–17.

Scerri, A. and Scerri, C. (2012). Dementia in Malta : new prevalence estimates and projected trends. *Malta Med. J.* 24(3), 21–24.

Siders, C., Nelson, A., Brown, L. M., Joseph, I., Algase, D., et al. (2004). Evidence for implementing nonpharmacological interventions for wandering. *Rehabil. Nurs.* 29(6), 195–206.

Vuong, N. K., Chan, S., Lau, C. T. and Lau, K. M. (2011). A predictive location-aware algorithm for dementia care. *2011 IEEE 15th Int. Symp. Consum. Electron.*

Weiser, M. (1991). The Computer for the 21st Century. *Sci. Am.* 265(3), 94–104.

Wherton, J. P. and Monk, A. F. (2010). Problems people with dementia have with kitchen tasks: The challenge for pervasive computing. *Interact. Comput.* 22(4), 253–266.

WHO. (2012). *Dementia: A Public Health Priority.* World Health Organisation.

Zhou, J., Su, X., Ylianttila, M. and Riekki, J. (2012). Exploring Pervasive Service Computing Opportunities for Pursuing Successful Ageing. *Lect. Notes Comput. Sci.* 73–82.

Zimmerman, S. (2001). *Assisted living needs, practices, and policies in residential care for the elderly.* Baltimore: Johns Hopkins University Press.

Xjenza Online - Journal of The Malta Chamber of Scientists
www.xjenza.org
DOI: 10.7423/XJENZA.2014.2.02

Research Article

Dynamics of Private Social Networks

Jonathan Mifsud and Matthew Montebello
Department of Intelligent Computer Systems, University of Malta

Abstract. Social networks, have been a significant turning point in ways individuals and companies interact. Various research has also revolved around public social networks, such as Twitter and Facebook. In most cases trying to understand what's happening in the network such predicting trends, and identifying natural phenomenon. Seeing the growth of public social networks several corporations have sought to build their own private networks to enable their staff to share knowledge, and expertise. Little research has been done in regards to the value private networks give to their stake holders. This is primarily due to the fact as their name implies, these networks are private, thus access to internal data is limited to a trusted few. This paper looks at a particular online private social network, and seeks to investigate the research possibilities made available, and how this can bring value to the organisation which runs the network. Notwithstanding the limitations of the network, this paper seeks to explore the connections graph between members of the network, as well as understanding the topics discussed within the network. The findings show that by visualising a social network one can assess the success or failure of their online networks. The Analysis conducted can also identify skill shortages within areas of the network, thus allowing corporations to take action and rectify any potential problems.

Keywords Linked Data – Social Networks – Social Network Analysis – Semantic Network Analysis

1 Introduction

Social Networks have gathered significant interest, not just by the general population, who got sucked into this whole phenomenon, but also scientists, researchers and corporates. The success of major social networks such as Facebook and Twitter has seen a marked increase in the interest taken by researchers into these networks. Most research has indeed focused on trying to understand what is going on in these Social Networks by doing what is called Semantic Analysis. This allows a machine to identify topics and subjects discussed within the network, and eventually allows machines to reason about the underlying network.

Various corporates have also jumped on the social bandwagon, not just by setting up social profiles on public networks but by actually setting up internal social networks. Indeed 44 % of German SME's interviewed in (Meske and Stieglitz, 2013) indicated that they use Social Media for internal purposes, with 39.06 % having an Internal Social Network. private social networks platforms such as NationalField, Yammer (Yammer, 2014) and Zoho Connect (Z. C. P. Ltd., 2014) have come up and started to cater for enterprises. Companies such as Ebay, XEROX and DHL have successfully made private social networks part of their work, a place where ideas can thrive, and processes streamlined. Such was the effect of these networks that Obama's election campaign's success in 2008 was attributed to their use of a private social network, which led to the creation of NationalField.

Private social networks have become a place where employees of the same company, or group of companies can share information, connect and help each other regardless of the distance. Similarly to their public counterparts, they made the world a smaller place, being a single entry point for communication across the whole company. The information shared on these Private Social Network, could be very rich, allowing machines to understand the topics being discussed, thus understand which members of the network have best understanding of certain subjects.

This paper will look into the unique environment of private social networks, and how the semantics of the content posted on the network can be exploited in order to further understand aspects of the company. The paper is structured in the following manner, first giving a background of the Organisation whose network is being explored. Then understanding and finding influential figures within the company, going to helping individuals finding expertise within the corporation. Whilst Social Networks bring plenty of positives, it doesn't mean that they always work out the way it's intended to be; thus the paper also looks at problems which a Private Social Network comes across. How these problems can be tackled, and identification of when in a company's life using a private social network can be beneficial.

Correspondence to: Jonathan Mifsud (jonathan.mifsud.07@um.edu.mt)

© 2014 Xjenza Online

2 Goals

The goal of this research is to explore the phenomenon of private social networks, and their similarity to Public Social Networks. This paper looks with particular interest, towards the network structure and dynamics of the private network. Applying techniques used in public networks in order to understand who the influencers within Private Networks are, and how this relates to the structure of the Company.

The paper goes to explore further the semantics and topics discussed within the organisation, taking particular interest as to whether these can be a reliable source to identify skills within the organisation. All this whilst giving guidance on how to conduct future research on private social networks, and identifying parameters which will increase the chances of having a successful research on private networks.

3 Background Information

Conducting any research on private social networks is not necessarily straight forward, the primary stumbling block is the fact that these networks are private. Apart from the organisation who is running the network, and benefiting from what's being discussed few or none are the people with access to such information. For this research to be possible we had to partner with Impact Hub (Impact Hub, 2014), an organisation who uses a NationalField (National Field, 2014) powered private social network. A background of Impact Hub's organisational structure is provided below to aid one's understanding of the presented work.

Impact Hub, formerly The Hub, is an organisation which was founded in London back in 2005, with the purpose of fostering and promoting social innovation. The success of their model let to an unprecedented increase in their network, and currently have over 54 Impact Hubs world wide, with over 7000 members. This rapid increase both in members and size, meant that Impact Hubs were now not only a local thing, where entrepreneurs and start-ups could learn from each other but rather a global community. In order to bring closer their global community and make better use of skills located within the hub, and further understanding of why some hubs are more successful then others.

Through the platform provided by NationalField, they were partly achieving their goals, of having their whole world-wide network interconnected. This did not give them much information about the network and their users, thus a collaborative partnership was put in place allowing an analysis of their network which gives the opportunity to present this paper.

The Impact Hub Social Network structure provided by NationalField, looks very much like an earlier version of Facebook. In this social network, each member has his / her own profile page and is allowed to post status updates, comment on such updates, as well as like updates done by themselves or other individuals. The network also contained various groups, which are in themselves dependent on either the actual location of the Impact Hub that the user is a member of, or otherwise by interest in a particular group or initiative. All updates are in themselves public, thus anyone member of the network is allowed to read, and the structure of the Home Feed meant that newer posts always come up top of the network significantly increasing the reach within the network. Posts within a particular group automatically trigger an email, sharing the post to all members of the group. This inherent network structure is important to remember when conducting a Social Network Analysis as it does have an impact on the results.

4 Related Work

Social Network Analysis (SNA) is not necessarily done on online social networks (OSN) but can be conducted using various data sources. Previous research has already looked at analysing private enterprise and closed networks within organisations using SNA techniques. Kazienko et al. (2011) use SNA to improve enterprise structures, the research focuses on email to build it's model however recommends overlaying data sources, including emails and logs. This added information would give more dimensions relating to the Social Network, which would be able to map the real social network of the organisation. Zhu et al. (2008) and Golbeck and Hendler (2004) focus on trust within social networks, trust being the basic ingredient to develop relationships within the network. Zhu et al. (2008) use PageRank like technique to give value and weight to email communication, increasing trust through each communication with an individual. Whilst Golbeck and Hendler (2004) discusses how an individual will only seek reputable information through relationships which are in themselves reputable.

Of particular interest are papers on the more sociological side, such as Abreu and Camarinha-Matos (2011), where the authors look at measuring social capital. With this work focusing on an organisation whose members are other Enterprises, this paper gives light on the potential interest in our work. By understanding the skills, and values of the members in a social network or business incubator, one can far easier sell the benefits of being a member in such network. The paper goes on to propose a means of measuring capital within the network, and how easy it is to access the different types of capital available within the network.

Taking a look at online social networks most research has focused on Semantic Analysis of the networks. Twitter was the social network of choice in most research due to various favourable aspects, all updates are limited to 140 characters, and most importantly tweets are public to the whole community. The large volume of tweets, and network structure allows better semantic analysis when compared to other networks such as Facebook. Teufl and Kraxberger (2011) looks at extracting knowledge from /twitter, whilst Asur and Huberman (2010) look into predicting the future using data extracted from Twitter. Of particular interest are the works of Tao et al. (2012) and Abel et al. (2011) where both look at user modelling and semantic user profiles respectively.

Term frequency or TF/IDF could be used along other natural language processing techniques for automatic key-

word extraction. This is done by identifying the most used keywords by a particular user and then use these keywords as a means to identify the main user interests (Wang and Jin, 2011). Semantic Enrichment can also be done using techniques such as co-occurrence (Wang and Jin, 2011), relating words which often appear together. Stankovic et al. (2012) look into the effectiveness of expanding the profiles, in addition to co-occurrence (DMSR) they build their own system hyProximity (HPSR). This takes into consideration semantic relatedness between classes such as `rdf:subclassOf` and other links such as objects being part of an industry, service or are a product (Stankovic et al., 2012). Finally they also propose the use of a Pseudo Relevance-Feedback (PRF) which is used to expand searches from the result-set (Stankovic et al., 2012).

It is also possible to use external service providers such as DBPedia Spotlight, Zemanta and OpenCalais (Tao et al., 2012). These services extract semantics from the provided text according to pre-set parameters, and use linked data from well known resources such as DBPedia (Sahnwaldt, 2014), a WikiPedia linked semantic database. The resulting data can then be processed in order to filter and keep only topics for which the user seems to be an expert for building the user profile. Interest Weight to Ontology (Nakatsuji et al., 2006) could be a way to further enhance user profiles by having ontologies pass weight to their parents.

Due to network members discussing various topics, there is also the possibility of using a vector space model to represent the different interests of each of the users (Tao et al., 2012). Vectors could be also used for social connections, where the vectors would represent the number of interactions with different members within the network (Fan and Li, 2008). TUMS presented by Tao et al. (2012) is an interesting project in itself which provides a user modelling service using twitter, and provides both an API and a graphical user interface. This system uses the last 300 tweets and linked articles to obtain a good user representation.

Whilst these papers successfully argue how Semantics can be successfully extracted from Social Networks, there is still a risk of Semantic Attacks on such networks. Still using the example of Twitter Kumar and Geethakumari (2014) argue that "OSN have increased the spread of misinformation in social networks", whereby incorrect information is believed by members of the network and shared again further increasing it's reach. One cannot also discount the possibility of individuals who purposefully manipulate information posted on the social networks. This could lead the machines to extract incorrect information from the systems and understandably give an incorrect analysis. Thus correctness of any semantic information extracted is important to give trust to the underlying system.

5 Methodology

In this section we explain the methodology by which this research was conducted, and is thus essential in view of the outcomes of the research. In the previous sections a background of Impact Hub and their network structure was given, for the purposes of this research access to an API was given. The API allowed the following functions:

1. Obtain a List of Users
2. Request profile information
3. View user stream
4. View comments and likes of updates posted in the stream

With no direct stream of past historical entries, and limited number of hits on the server, it was best to hit the API periodically asking information on a user at a time. This allowed access to whatever appeared on the user's feed, thus picking up any new status updates and comments in the system. It also allowed a fool-proof way of obtaining any updates to each user's personal profiles, as users could update their description at any time. With updates set at 1 minute intervals, and considering the could of total users by the end was of nearly 5800 users, this meant a latency of up to 4 days. Whereby each user's data was updated roughly once every four days.

Whilst admittedly this approach is not practical in real-time applications, due to the restrictions we had in place this was the most appropriate solution. In an ideal world, we would have obtained a Feed which describes the latest changes to the network, then the system could investigate each one separately. Due to the relationship, between us, our partner Impact Hub and NationalField who were providing the social networking platform and API this was not possible.

The information was systematically gathered from July 2012 to January 2014, covering a period of 18 months. During this period the data was semantically analysed and stored in a database. Once we closed the data-set being used for this period we started looking at both the semantics of the system as well as conducting a SNA. Details of the semantic analysis, Social Network Analysis and results will be discussed in the later sections of this paper.

6 Semantic Analysis

For the purposes of this research using an external service provider to parse and analyse data was deemed the most appropriate. The decision was taken in the light of previous research conducted by Tao et al. (2012) which successfully used OpenCalais for semantic annotations, and building user profiles based on these annotations. OpenCalais and DBPedia Spotlight were both considered and tested on sample datasets. The flexibility afforded when using optional parameters in DBPedia Spotlight, made it a better candidate solution for this system. In addition there were two other key points which led to this decision. First all terms are listed in WikiPedia, thus individuals could easily go to topics which are being discussed. Secondly OpenCalais is a propriety system, whilst with DBPedia Spotlight being open source one can load the system on a local server, and possibly extend it should the need arise. Being able to set up locally was considered important as when analysing the data, this would otherwise be sent to

a 3rd Party, and would be subject to additional terms and conditions. Working locally ensures that Impact Hub or other enterprises which wish to use similar systems still retain full control of their data.

The Semantic Entity Extraction was then split into parts, depending on the type of content being parsed. Taking into consideration that the Biography, Status Updates and Comments are usually of different lengths and serve different purposes. The parameters used in the analysis were adjusted accordingly to increase recall whilst trying to ensure correctness. Each of the extracted entities were then stored in a database and linked to the original source, be it the biography, status update or a comment.

7 Social Network Analysis

Having captured information about the network, including who is posting, and which users were interacting with each other it was time to apply SNA techniques to see if the network structure on the social network correlates to the real-life situation. In addition to this we could augment the information with the semantic data extracted in the previous section. This allows a unique view on the network, which cannot be obtained in traditional manners.

The below table shows the total number of users, posts and comments extracted from the social network. Likes were omitted as this feature was under utilized with only around 30 likes registered within the system.

Metric	Value
Total Users	5,791
Users filled their biography	777
No of Posts	12,537
Post Edges Created	1,287
Users involved in Post	1,440
No of Comments	16,034
Node Edges Created	1,765
Users involved in Comments	2,059
Users involved in Posts or Comments	2,595

Due to a large number of inactive users within the network, highlighted above, the following sections will only focus on users who had any sort of interaction. Thus, this may not necessarily represent the actual network structure within the Impact Hub organisation. One can also notice that the large number of posts and comments within the network were mainly done through the same source and target, noticed easily when comparing the number of posts, and edges created in the network. For simplification purposes in our analysis, only users who are connected either through Posts or Comments are considered.

The first relationship which was studied was that created through Posts. Posts are usually sent from one entity to another, most of the time being users on the network, however could also possibly be directed to a group page. After converting the data into a graph entity and using a ForceAtlas algorithm for clustering the network structure found in Figure 1(a) was obtained. This visualisation shows that the users form clusters, with individuals who are the centerpoint of particular clusters. By visualising posts one can also notice that the network is interconnected and various nodes are only connected to one or two other nodes.

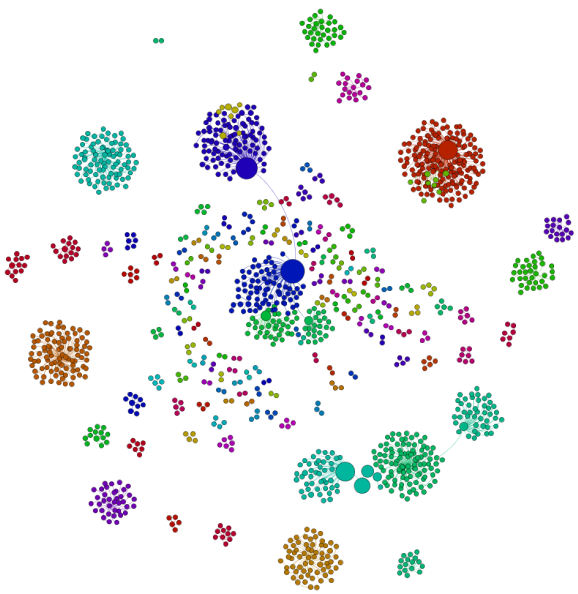

(a) Clustered Users

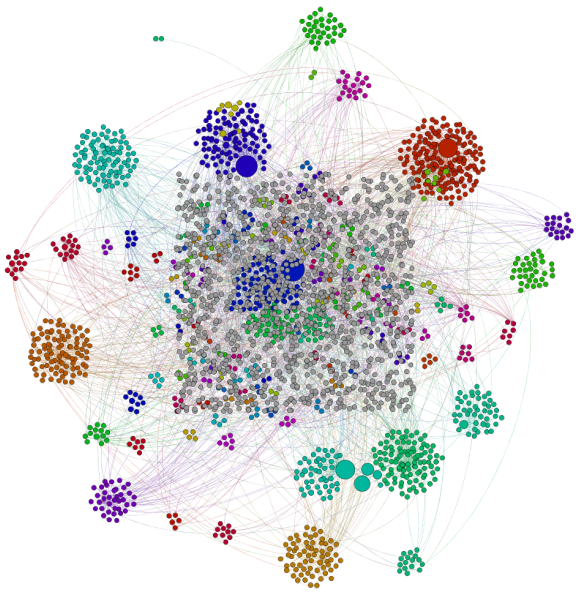

(b) Adding Connections through Comments

Figure 1: Users Connected through Posts and Comments

A delve deeper into this data, running a page rank algorithm in order to weigh the importance of members within the network resulted in a very interesting outcome. This algorithm gives higher importance to those users who have multiple posts directed to them, and as such their posts to other members also carry more weight. Out of the top 5 ranked individuals within the network, two were the Administrator of the NationalField platform, and the CEO of this platform. Whilst the Administrator is not really an

active member, a significant number of posts from within the Impact Hub community were directed to him. The other three, included three important personnel within the Impact Hub network, the Global Managing director, a co-founder of Hub Copenhagen as well as the host of Hub Vienna.

This can be better understood when considering that these three individuals would have been very active in their respective communities, with the Global Managing Director, seemingly interconnecting the central cluster with other clusters. Each of the clusters also revolve around a location, with hosts of each cluster acting as an intermediary bringing people together. In the hub's actual structure, there is a host, whose job is to introduce new members and helping them connect. This role probably led to them welcoming other members in the network, and the new members in the network to go back to the host thanking them for being welcomed in the network one way or another.

Whilst the above network structure portrays very loosely interconnected clusters, using simply posts, introducing comments to the picture adds a totally different dimension as can be seen in Figure 1(b). In Figure 1(b), no ForceAtlas algorithm was used following the one run on Figure 1(a), and the new nodes just overlayed on top of the existing ones. One can observe the edges and nodes which were introduced in the network, representing comments, and users who only commented on other posts. One can notice connections from the outside clusters, also visible in figure 1(a), going from one end to the other. This shows that the relative distance and boundaries that existed in between the clusters no longer hold once users are allowed to comment on each other's posts.

Whilst the reasons for the increased interconnectivity when adding comments to our graph are not explored in detail in this paper there are underlying factors within the network which encourage this activity. First and foremost, unlike other public social networks, every member in the network is able to see all posts made by any user on the network. This allows users to respond to a query, or post to which a user would be interested in. Further research would be required to show whether the new links to outside clusters are linked to the semantic content of the posts, rather than a relationship which might exist outside of the social network.

8 Semantic Social Network Analysis

Having analysed the network structure, we take a look at the extracted semantic entities, and what machines could learn from the underlying network infrastructure. As biographies would be the most user representative these are taken into consideration, looking at the most commonly recurring entities the following are the 10 most popular:

- Sustainability
- Social Entrepreneurship
- Project
- Organisation
- Business
- Social
- Innovation
- Entrepreneur
- Design
- Idea

This after a small discussion with any of the members of the organisation, or even reading a bit on their website makes complete sense. The community is about social entrepreneurship, and sustainability achieved in a social manner, with various entrepreneurs sharing ideas to create new innovations, eventually leading to local businesses. That statement alone, covers over half of the keywords, in the top 10.

Each cluster is represented by a different semantic set of keywords, taking one of the clusters from Figure 1(a), the topics extracted vary slightly. Thus the composition of each cluster, is not only necessarily linked to location, but also to the skills available in the cluster. The top 10 entities from this cluster are:

- Communication
- Social Entrepreneurship
- Organisation
- Education
- Empowerment
- Culture
- Business
- Website
- Millennium
- Experience

One can notice that whilst there is an overlap in between the cluster and the main network, the cluster has keywords which are more specific, representative of topics discussed within the group. Keywords such as Social Entrepreneurship, Business and Organisation are quite generic and thus would be expected to feature all over the network. Semantic Keyword analysis could thus be used to identify key strengths of each cluster, and possible weaknesses by identifying keywords which are missing from these clusters.

9 Evaluation

Social Network Visualisation, can play a key role in understanding the structure of the virtual social network. This can easily help identify weak links within the networks, allowing administrators and moderators to take action and strengthen such links. One such example could be, that you want increased communication between two remote locations, or between two separate working groups.

Semantic entities as shown in the previous section, provide further information on skill and interest distribution within the network. This can be used more effectively to identify skill differences across the network, and better balance the members of an organisation where appropriate. In conjunction with other information showing the success of businesses within each cluster, this would help the network administrators to understand what mixture of skills create a successful enterprise.

The social network visualisation, though deemed effective, as it successfully clustered members across the net-

work was not deemed to be a 100 % success. As one would have expected this visualisation to match the network structure of Impact Hub, which has over 53 Hubs around the globe. However a participation rate of around 50 %, is understood to have had a significant impact on the resulting visualization and analysis. This in itself is an important finding, as it helps the organisation to understand the lack of user activity, and thus be in a position to tackle it.

10 Arising Ethical Issues

When analysing a social network in such manner, one is inherently gathering information about each individual member and making assumptions on items discussed within the network. In particular cases, the semantic algorithms may pick up semantic connotations which are unwanted, or do not make much sense in context. When grouping data, such as in this paper these do not tend to show up however such connotations may be given to individuals where they do not exist.

This possibility of incorrect semantic connotations might be an issue especially when such data could face public entities. In this case the research was for internal purposes, and prior to showing data to other members within the network permission was sought from the related individuals.

11 Future Work

This work is certainly not the end of the line for private online social networks, following the proof of concept presented in this paper several items can be explored in more detail.

- Temporal changes in the private online social networks (do influencers change)
- Semantic composition of successful groups / projects within the network
- Overlaying SNA of an online private network with an organisation's real structure, how these overlap
- Explore weather users are more likely to comment on a post if this matches one of their interests.
- Using Semantic User Profiles to invite members to join particular working groups / clusters.

12 Conclusion

Overall the presented work outlines that in a limited private online social network, one can still conduct both Social Network Analysis and Semantic Social Network Analysis with a degree of success. In an organisation where this research is targeted to a particular purpose this sort of research can be quite useful in identifying both weak and strong points within the organisation. Then conducting a plan to improve the Social Network content delivery in order to increase engagement where required.

References

Abel, F., Gao, Q., Houben, G.-J. and Tao, K. (2011). Semantic Enrichment of Twitter Posts for User Profile Construction on the Social Web. *Lect. Notes Comput. Sci.* 375–389.

Abreu, A. and Camarinha-Matos, L. M. (2011). An Approach to Measure Social Capital in Collaborative Networks. *IFIP Adv. Inf. Commun. Technol.* 29–40.

Asur, S. and Huberman, B. A. (2010). Predicting the Future with Social Media. *2010 IEEE/WIC/ACM Int. Conf. Web Intell. Intell. Agent Technol.*

Fan, L. and Li, B. (2008). VisoLink: A User-Centric Social Relationship Mining. *Rough Sets Knowl. Technol.* 668–675.

Golbeck, J. and Hendler, J. (2004). Accuracy of Metrics for Inferring Trust and Reputation in Semantic Web-Based Social Networks. *Lect. Notes Comput. Sci.* 116–131.

Impact Hub. (2014). What is Impact Hub. [Online]. Available: http://www.impacthub.net/what-is-impact-hub.

Kazienko, P., Michalski, R. and Palus, S. (2011). Social Network Analysis as a Tool for Improving Enterprise Architecture. *Lect. Notes Comput. Sci.* 651–660.

Kumar, K. P. K. and Geethakumari, G. (2014). Analysis of Semantic Attacks in Online Social Networks. *Commun. Comput. Inf. Sci.* 45–56.

Meske, C. and Stieglitz, S. (2013). Adoption and Use of Social Media in Small and Medium-Sized Enterprises. *Lect. Notes Bus. Inf. Process.* 61–75.

Nakatsuji, M., Miyoshi, Y. and Otsuka, Y. (2006). Innovation Detection Based on User-Interest Ontology of Blog Community. *Lect. Notes Comput. Sci.* 515–528.

National Field. (2014). NationalField - Measure Change.

Sahnwaldt, C. (2014). wiki.dbpedia.org - About.

Stankovic, M., Rowe, M. and Laublet, P. (2012). Finding Co-solvers on Twitter, with a Little Help from Linked Data. *Lect. Notes Comput. Sci.* 39–55.

Tao, K., Abel, F., Gao, Q. and Houben, G.-J. (2012). TUMS: Twitter-Based User Modeling Service. *Lect. Notes Comput. Sci.* 269–283.

Teufl, P. and Kraxberger, S. (2011). Extracting Semantic Knowledge from Twitter. *Electron. Particip.* 48–59.

Wang, Q. and Jin, H. (2011). Social Analytics for Personalization in Work Environments. *Lect. Notes Comput. Sci.* 314–326.

Yammer. (2014). Yammer: The Enterprise Social Network. [Online]. Available: https://www.yammer.com/.

Z. C. P. Ltd. (2014). Zoho Connect — Your Social Workspace. [Online]. Available: http://www.zoho.com/connect/.

Zhu, W., Chen, C. and Allen, R. B. (2008). Analyzing the Propagation of Influence and Concept Evolution in Enterprise Social Networks through Centrality and Latent Semantic Analysis. *Adv. Knowl. Discov. Data Min.* 1090–1098.

Xjenza Online - Journal of The Malta Chamber of Scientists
www.xjenza.org
DOI: 10.7423/XJENZA.2014.2.03

Research Article

Uniqueness Typing For A Higher-Order Language

Adrian Francalanza and Melanie Zammit
CS, ICT, University of Malta

Abstract. We investigate type-based analysis for a higher-order channel passing language with strong update, whereby messages of a different kind are communicated over the same channel. In order to reason about such programs, our type system employs the concept of *uniqueness* to be able to assert when it is safe to change the object type a channel. We design a type system based on this concept and prove that our type system is *sound*, meaning that it only accepts programs that do not produce runtime errors.

1 Introduction

Resource usage in settings with limited amounts of resources is an important aspect of computation and one common way how to manage limited resources is through *resource reuse*. In this paper we investigate type-based analysis for resource reuse in concurrent settings; in such settings, the reuse of resources is easy to get wrong because one thread of computation may change the mode of usage of a particular resource while other threads still employ the previous usage mode. In particular, we focus on message-passing programs, such as those written in Go ("The Go Programming Language", n.d.) and Erlang (Armstrong, 2007; Cesarini and Thompson, 2009), where the resources reused are the channels used to transmit the messages on. We carry out our analysis using the pi-calculus(Sangiorgi and Walker, 2003), a standard model for channel-passing computation and, in particular, extend the results obtained in (De Vries et al., 2012) to a higher-order version of the calculus where the values communicated include also the programs themselves.

Consider, as an example, the client-server protocol depicted in Fig. 1. The client sends a program to be executed by the server whereby, for the program to run, it needs to be instantiated with a particular dataset. From the server side, it needs to perform the necessary checks on the code before it runs it whereas the client would ideally not communicate the dataset unless it is certain that the code will be executed (the dataset may be bulky or contain sensitive information).

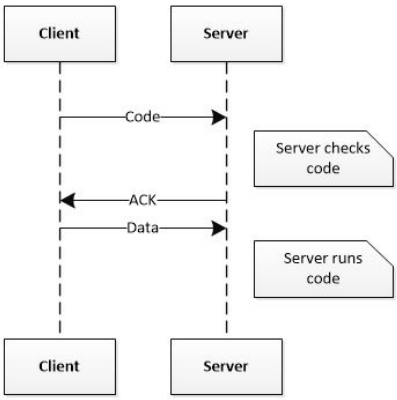

Figure 1: Communication links between a client and a server

Fig. 1 thus describes a two-phase protocol, whereby the client sends the code to the server in the first phase. The server checks the code and acknowledges back if the check is successful and it is prepared to run the code, at which point the client send the data to the server in the second phase of the protocol. Once the server receives the data, it executes the validated code with this data.

A program implementing the protocol of Fig 1 can be expressed as the higher-order pi-calculus parallel composition of a client with a server

$$client \mid server \tag{1}$$

defined as follows:

$$\begin{aligned} server \stackrel{\text{def}}{=}\ & port_1?(x_{code}, x_{inst}, x_{ack}).\\ & \quad \texttt{if}\ check(x_{code})\ \texttt{then}\\ & \quad\ \texttt{run}\ x_{code}.\\ & \quad\ (\texttt{new}\ port_2)(x_{ack}!port_2.port_2?(x_{data}).x_{inst}!x_{data})\\ & \quad \texttt{else nil}\end{aligned}$$

$$\begin{aligned} client \stackrel{\text{def}}{=}\ & (\texttt{new}\ ack, inst)\\ & \quad (port_1!(code, inst, ack) \ \mid\ ack?(x_{port}).x_{port}!data)\end{aligned}$$

$$code \stackrel{\text{def}}{=} \langle inst?(y).P(y)\rangle$$

In (1), the *server* and *client* originally interact only on the port $port_1$. The server inputs three values on this channel,

Correspondence to: Adrian Francalanza (adrian.francalanza@um.edu.mt)

© 2014 Xjenza Online

namely the code to check and run, x_{code}, an acknowledgment channel, x_{inst}, and a channel on which to instantiate the code with, x_{inst}. If the check succeeds, it runs the code and acknowledges back to the *client*, sending it a new channel, $port_2$, on which to initiate the second phase of the protocol. Once it receives the data on $port_2$, it forwards it to the executing code through channel x_{inst}. Dually, the *client* first sends the *code* along with two new channels, *ack* and *inst*, on $port_1$ and as soon as it receives an acknowledgment with the channel for the second phase of the protocol, it sends the *data* on this channel. The code consists of a thunked process, $\langle - \rangle$, that inputs its data on channel *inst* once it is executed, and then continues as P with the data inputted, y.

An alternative server that economises on channels is the one defined below, whereby it *reuses* channel $port_1$ for the second phase of the protocol instead of creating a new channel $port_2$. Note that when $port_1$ is reused, *different* forms of values are communicated on it, namely *data* as opposed to $(code, inst, ack)$. In the literature, this is often referred to as *strong update*(Ahmed et al., 2005).

$$\begin{aligned} srvOpt \stackrel{\text{def}}{=} port_1?(x_{code}, x_{inst}, x_{ack}).& \\ &\texttt{if } check(x_{code}) \texttt{ then} \\ &\quad \texttt{run } x_{code}.x_{ack}!port_1.port_1?(x_{data}).x_{inst}!x_{data} \\ &\quad \texttt{else nil} \end{aligned}$$

When we execute

$$client \mid srvOpt \tag{2}$$

it turns out that we obtain the same behaviour as that of (1). However channel reuse is not always safe and can lead to erroneous executions. For instance, executing

$$client \mid srvOpt \mid client$$

does not have the same behaviour as that of its original counterpart $client \mid server \mid client$; in fact, the former results in a runtime error whereby the second phase of the protocol between one *client* and *srvOpt* is interfered with by a message on $port_1$ from the other *client* with *mismatching communicated values* (this is a direct consequence of the strong update on $port_1$). Alternatively, in the thunked process in *code* is instantiated through $port_1$

$$codeErr \stackrel{\text{def}}{=} \langle port_1?(y).P(y) \rangle$$

the channel reuse in *srvOpt* would also be unsafe and generate a runtime error.

In this paper we develop a type system that statically analyses programs and guarantees that type-checked programs do not generate runtime errors. Our type system accepts correct higher-order programs such as (1), but also programs with safe strong updates such as (2), while rejecting all unsafe programs. § 2 describes our language whereas § 3 presents the uniqueness type system. § 4 presents the main soundness results and § 5 concludes.

2 The Language

Fig. 2 presents the higher-order pi-calculus that will be used. The syntax assumes separate denumerable sets for channel names, $c, d \in \textsc{Chan}$, and variables, $x, y \in \textsc{Var}$; identifiers $i, j \in \textsc{Id} = \textsc{Chan} \cup \textsc{Var}$ range over both channels and variables. The main syntactic class is that of processes $P, Q, R \in \textsc{Proc}$ using values, $u, v \in \textsc{Val}$, consisting of identifiers and thunked processes, $\langle P \rangle$. We sometimes use the shorthand notation $c!v$ to denote $c!v.\texttt{nil}$.

The reduction relation ($\longrightarrow$) is defined as the least relation over closed processes satisfying the rules in Figure 2; it assumes a standard structural equivalence relation (Hennessy, 2007) over processes, $\equiv$, that allows us to abstract over aspects such as the commutativity of parallel composition, $P \mid Q \equiv Q \mid P$ (amongst others). The main rules are rCom, describing communication amongst processes, and rRun, describing the spawning of thunked processes using the command `run`. The remaining rules are standard. In what follows, we use $P \longrightarrow^* Q$ to denote the transitive closure of our reduction relation.

The reduction relation allows us to deduce that

$$client \mid server \longrightarrow^* P(data)$$

and also that

$$client \mid srvOpt \longrightarrow^* P(data)$$

It also allows us to show that, whereas

$$client \mid server \mid client \longrightarrow^* P(data) \mid client$$

is the only possible evaluation, we have the following sequence of reductions for the analogous system that uses the alternative *srvOpt* instead.

$$client \mid srvOpt \mid client \longrightarrow^* \begin{cases} port_1!data \mid \\ (\texttt{new}\, inst)\big(inst?(y).P(y) \mid port_1?(x_{data}).inst!x_{data}\big) \\ \mid client \end{cases}$$

At this point, the input on channel $port_1$ can react with either the output $port_1!data$ (carrying the right format of values) or with the output $port_1!(code, inst, ack)$ from the second client, which carries values of a different (erroneous) format.

We define a predicate on processes to describe the runtime errors we want to rule out; the rules defining this predicate $P \rightarrow_{\text{ERR}}$ are given in Fig. 2. For example, eOut and eIn state that thunked process values $\langle P \rangle$ cannot be used instead of channels to communicate on, whereas eRun states that we cannot use channel values instead of thunked process values when spawning new executions. eIf1 and eIf2 state that comparisons are only allowed on channel values. The remaining rules are the usual contextual rules.

3 Type System

Although there exist numerous type systems for the various variants pi-calculus, they tend to rule out well-behaved

Syntax:

$$
\begin{array}{rcl}
u, v \in \textsc{Val} & ::= & i \mid \langle P \rangle \\
P, Q, R \in \textsc{Proc} & ::= & \texttt{nil} \mid P \mid Q \mid v!u.P \mid v?x.P \mid \texttt{if}\ (v{=}u)\ \texttt{then}\ P\ \texttt{else}\ Q \mid \texttt{run}\ v.P \mid (\texttt{new}\ c)P \\
& \mid & \texttt{rec}\ x.P \mid x
\end{array}
$$

Semantics:

$$
\frac{}{c!v.P \mid c?x.Q \longrightarrow P \mid (Q[v/x])}\ \textsc{rCom}
\qquad
\frac{}{\texttt{run}\ \langle P \rangle.Q \longrightarrow P \mid Q}\ \textsc{rRun}
\qquad
\frac{}{\texttt{rec}\ x.P \longrightarrow P\{|\texttt{rec}\ x.P/x|\}}\ \textsc{rRec}
$$

$$
\frac{}{\texttt{if}\ (c{=}c)\ \texttt{then}\ P\ \texttt{else}\ Q \longrightarrow P}\ \textsc{rThen}
\qquad
\frac{}{\texttt{if}\ (c{=}b)\ \texttt{then}\ P\ \texttt{else}\ Q \longrightarrow Q}\ \textsc{rElse}
$$

$$
\frac{P \equiv P' \qquad P' \longrightarrow Q' \qquad Q' \equiv Q}{P \longrightarrow Q}\ \textsc{rStr}
\qquad
\frac{P \longrightarrow P'}{P \mid Q \longrightarrow P' \mid Q}\ \textsc{rPar}
\qquad
\frac{P \longrightarrow P'}{(\texttt{new}\ c)P \longrightarrow (\texttt{new}\ c)P'}\ \textsc{rRes}
$$

Errors:

$$
\frac{}{\texttt{if}\ (\langle Q \rangle{=}v)\ \texttt{then}\ P_1\ \texttt{else}\ P_2 \rightarrow_{\textsc{err}}}\ \textsc{eIf1}
\qquad
\frac{}{\langle P \rangle!v.Q \rightarrow_{\textsc{err}}}\ \textsc{eOut}
\qquad
\frac{}{\texttt{run}\ c.P \rightarrow_{\textsc{err}}}\ \textsc{eRun}
\qquad
\frac{P \rightarrow_{\textsc{err}}}{(\texttt{new}\ c)P \rightarrow_{\textsc{err}}}\ \textsc{eRes}
$$

$$
\frac{}{\texttt{if}\ (v{=}\langle Q \rangle)\ \texttt{then}\ P_1\ \texttt{else}\ P_2 \rightarrow_{\textsc{err}}}\ \textsc{eIf2}
\qquad
\frac{}{\langle P \rangle?x.Q \rightarrow_{\textsc{err}}}\ \textsc{eIn}
\qquad
\frac{P \rightarrow_{\textsc{err}}}{P \mid Q \rightarrow_{\textsc{err}}}\ \textsc{ePar}
\qquad
\frac{P \equiv Q \qquad Q \rightarrow_{\textsc{err}}}{P \rightarrow_{\textsc{err}}}\ \textsc{eStr}
$$

Figure 2: Higher-Order Pi-Calculus

processes, such as the client-server example with strong updates of (2). Substructural type systems have been proven useful when reasoning about resource management (Pierce, 2004). In particular, De Vries et al. (2012) have defined a sound substructural type system that can reason about channel reuse for the *basic* pi-calculus, whereby code *cannot* be communicated at values. In this work we extend this type system so as to be able to handle resource reuse in higher-order pi-calculus programs.

3.1 Types and Type Environments

Uniqueness is a concept of exclusive access (De Vries et al., 2012), meaning that if a channel has a unique type, then it is guaranteed that only the process typed with that channel type has access to use that channel. Thus, strong update is safe for unique channels. However, even though a channel may not be unique at this instant, it may become unique after n computations. We describe these channels by the channel type attribute, *unique-after-i*. Uniqueness can also be represented as type annotations and reasoned about statically. More precisely, following (De Vries et al., 2012), a channel type has the syntactic form $[C]^a$ and describes two things: C is the *object type* and denotes the values that are allowed to be communicated over the channel; a denotes a type attribute (defined in Fig. 3). Thus, we say that

- An *Affine* channel ($[C]^{\mathbf{1}}$) is a channel with an *access restriction* that limits the channel to only *one* use at most.
- A *Unique-after-n* channel ($[C]^{(\bullet,n)}$) is a channel with an *access guarantee* that the channel will become unique after it is used for n times.
- An *Unrestricted* channel ($[C]^{\omega}$) is a channel with no usage restrictions or guarantees.

We note that unique channel types (De Vries et al., 2012) are in a sense, dual to affine channels (Kobayashi et al., 1999): whereas one yield a guarantee, the other imposes a restriction on usage. However, in order for the guarantees to be sound, we shall need to impose global restrictions on our type analysis (*c.f.* Def. 1) As an example of this, consider two parallel processes, A and B, that are using a channel c exclusively (*i.e.,* channel c is *unique* for process $A \mid B$):

- We would typically type-check one process, say A, with respect to a number, say m, of affine channel types for channel c. This restricts A to use c m times *at most.*
- Dually we would type-check the other process, B , with respect to a unique-after-n channel type for c. At each use, the count is reduced by 1, because this would mean that A used up one of its restrictions. Once 0 is reached, this would mean that A has used up all of its usage permissions, and since access was restricted to the process $A \mid B$, this would mean that B has exclusive access.
- Crucially, however, for the uniqueness guarantee to be sound, we need to require that $m \leq n$; otherwise we would reach 0 while A would still have further usage permissions.

Equipped with this analogy, we present the full type structure and operations for environment manipulation in

Type Structure:

$$
\begin{array}{rcl}
a & ::= & \mathbf{1} \mid \omega \mid (\bullet, n) \\
A, B \in \textsc{bTyp} & ::= & \texttt{int} \mid \texttt{bool} \\
C, D \in \textsc{cTyp} & ::= & B \mid [C]^a \mid \langle L \rangle \\
L, K \in \textsc{pTyp} & ::= & \epsilon \mid i = C, L \\
S, T \in \textsc{Typ} & ::= & C \mid \{L\}
\end{array}
$$

Type Splitting:

$$
\frac{}{B = B \circ B}\ \textsc{pBase} \qquad \frac{}{[C]^\omega = [C]^\omega \circ [C]^\omega}\ \textsc{pUnr} \qquad \frac{}{[C]^{(\bullet,n)} = [C]^{\mathbf{1}} \circ [C]^{(\bullet,n+1)}}\ \textsc{pUnq}
$$

Subtyping:

$$
\frac{}{(\bullet, n) <: (\bullet, n+1)}\ \textsc{sIndx} \qquad \frac{}{(\bullet, i) <: \omega}\ \textsc{sUnq} \qquad \frac{}{\omega <: \mathbf{1}}\ \textsc{sAff} \qquad \frac{a_1 <: a_2}{[C]^{a_1} <: [C]^{a_2}}\ \textsc{sTyp}
$$

Structural Manipulations for Environments:

$$
\frac{}{\Gamma, v : T \ \prec\ \Gamma}\ \textsc{tWeak} \qquad \frac{T_1 <: T_2}{\Gamma, v : T_1 \ \prec\ \Gamma, v : T_2}\ \textsc{tSub} \qquad \frac{}{\Gamma, c : [C_1]^\bullet \ \prec\ \Gamma, c : [C_2]^\bullet}\ \textsc{tRev}
$$

$$
\frac{T = T_1 \circ T_2}{\Gamma, v : T \ \prec\ \Gamma, v : T_1, v : T_2}\ \textsc{tCon} \qquad \frac{T = T_1 \circ T_2}{\Gamma, v : T_1, v : T_2 \ \prec\ \Gamma, v : T}\ \textsc{tJoin}
$$

Figure 3: Type Structure and Operations

our type system, given in Fig.3. We have three classes of types:

- The *base* types ($A, B \in \textsc{bTyp}$) can either be integers (`int`) or boolean values (`bool`).
- The *communicative* types ($C, D \in \textsc{cTyp}$) represent those types that can be sent over a channel, namely base types, channel types and process abstraction types, $\langle L \rangle$ (representing thunked processes).
- The *general* types ($S, T \in type$), made of communicative type and active process types $\{L\}$.

Our type system is substructural(Pierce, 2004), whereby type assumptions, mapping identifiers to types, are used in a controlled manner. We therefore represent our type environments, Γ, as *lists* of type assumptions whereby in particular, we can have duplicate multiple types assigned to an identifier. Type environments are manipulated using the environment structural relation $\Gamma_1 \prec \Gamma_2$ (Fig. 3) which rely on the type splitting $T_1 \circ T_2$ and the subtyping relations $T_1 <: T_2$.

Typing assumptions can be split and re-joined under certain conditions. Active processes, process abstractions and affine channels cannot be split. This way, they can only be used once. However, basic types and unrestricted assumptions can be duplicated, (pBase and pUnr), while $(\bullet, i)$ assumptions can be split into an affine assumption and a $(\bullet, i+1)$ assumption (pUnq), manifesting the duality discussed earlier. Joining is the dual of splitting.

To enhance the expressivity of our type system, we use also a notion of subtyping. When we define a type S of being a subtype of type T ($S <: T$), we mean that we can at any time use the value of type S instead of a value of type T (Pierce, 2002). The rules in Fig. 3 allow us to deduce the following subtyping chain:

$$[C]^\bullet <: [C]^{(\bullet,1)} <: [C]^{(\bullet,2)} <: \ldots <: [C]^\omega <: [C]^{\mathbf{1}}$$

We can there allow an unrestricted channel to be used in place of an affine one (but not vice-versa, as this would break it restriction constraints). As a result of subtyping combined with splitting, we can use a unique-after-n assumption as an unrestricted assumption, and then split it into 2 unrestricted assumptions $(([C]^{(\bullet,n)} <: [C]^\omega) = [C]^\omega \circ [C]^\omega)$. We also can split a unique-after-n assumption into and affine assumption and a unique-after-n+1 assumption, and use the latter instead of an affine assumption $([C]^{(\bullet,n)} = [C]^{\mathbf{1}} \circ ([C]^{(\bullet,n+1)} <: [C]^{\mathbf{1}}))$.

The structural relation for environments ($\prec$) is the least reflexive transitive relation satisfying the rules in Fig. 3. The most obvious rule is weakening (tWeak), which allows extra fresh identifiers to be mapped in the environment and still type-check the process. Splitting (tCon), joining (tJoin) and subtyping (tSub) are other ways of modifying the environment in a safe way. The most important is the rule that allows revision or strong update (tRev). Since a channel is unique, it means that only one process has access to it and therefore, we can change the

type of that channel to allow different types to be communicated over it.

When there is only one type assumption for each identifier in a type environment, we say that the type environment denotes a partial function (from identifiers to types). We define a condition on type environments, consistency, that ensures that multiple type assumptions are not in conflict (this ensures that the guarantees given by unique types are indeed sound, as discussed earlier). In particular, we need to check this also for thunked process types, that may eventually be executed.

Definition 1 (Consistency)**.** A typing environment Γ is consistent if:

1. There exists a partial function Γ' such that $\Gamma' \prec \Gamma$
2. $\Gamma = \Gamma_1, x : \langle \Gamma_2 \rangle$ **implies** Γ_1, Γ_2 is consistent

♦

3.2 The Typing Relation

The typing relation is defined as two separate, mutually dependent relations. One relation is defined over values ($\vdash_v$) and the other is defined over processes ($\vdash_p$). The rules for typing relation over values are given in Fig. 4 whereas those for the typing relation over processes are given in Fig. 5.

$$\frac{}{\Gamma, i : C \vdash_v i : C}\ \textsc{tvId} \qquad \frac{\Gamma_1, \Gamma_2 \vdash_p P}{\Gamma_1 \vdash_v \langle P \rangle : \langle \Gamma_2 \rangle}\ \textsc{tvProc}$$

Figure 4: Value Typing

To type-check an identifier there needs to be a mapping for it in the typing environment (TVID). A new rule (TVPROC) is introduced to type-check process abstractions with respect to some environment ($\Gamma_1 \vdash_v \langle P \rangle : \langle \Gamma_2 \rangle$). In order to do so, we need to ensure that the spawned process, P, type-checks with respect to the existing environment extended with the mappings of the thunked process type, Γ_1, Γ_2.

In Fig. 5, we have three separate rules for typing input processes ($c?x.P$) that differ only in the channel type. If c had no restrictions, (rule TPINW) we can continue to use it in an unrestricted fashion in P . If c had an affine assumption (TPINA), we can no longer use it in the continuation P. Moreover, if it has a unique-after-n assumption (TPINU), we need to account for this one communication and update the guarantee for P accordingly. Therefore, we can now guarantee that c will be unique for process P after $n - 1$ other communications. Apart from updating the channel's assumption, we also need to include the variable's type in the environment. The type will correspond to the type that channel c is allowed to communicate.

Similar reasoning is used to type-check output processes ($c!v.P$). However, we also need different rules for when we communicate an identifier or a process abstraction. When communicating a channel (rules TPOUTIA, TPOUTIW and TPOUTIU), there should be a respective identifier type mapping in the type environment; importantly, the type-checking for the continuation process P can no longer use this type assumption. Once again we will need three separate rules for different channel assumptions.

On the other hand, we cannot use the same logic to type-check higher-order output processes ($c!\langle Q \rangle.P$). This is because the process abstraction is not in the environment. Therefore, we will need to type-check it before sending it to another process. We employ three additional rules for outputting process abstractions. The logic behind channel assumptions is the same as before. However, the process abstraction type is matched to the channel's type by value typing the process (using TVPROC) with respect to an empty environment. By doing so, we are not only making sure that Q is being type-checked, but we are also making sure that it is self-contained (the environment abstracted in its type is enough to type-check it).

The rule for conditionals (TPIF) type checks both possible processes (*i.e.,* P and Q) with respect to the same typing environment as only one of them will be executed. The same environment must also type-check the values we are comparing to channel types. Even though this rule only matches channel names (as is standard in other work in process-calculi), extending the typing rule to more generic boolean conditions is straightforward.

We have two different rules for running a process ($\texttt{run}\, v.Q$). One of them (TPRUN1) covers the case when v is a variable. This rule requires the environment to include a mapping for this variable, with its type corresponding to a process abstraction type. The rest of the environment should be able to type-check the continuation process (Q). The second rule (TPRUN2) covers the case when $v = \langle P \rangle$. This time, we do not have a mapping for the process abstraction in the environment. So we divide the environment in two, part of it type checks the continuation process (Q), and the other part should be used in value typing the thunked process with respect to an empty environment.

In order to type-check a recursive process ($\texttt{rec}\, x.P$) we need to add the recursive variable x to the environment and use it to type-check the continuation processes P. The variable should be an active process type with the same environment used to type-check the original process. Then, when we need to type check a recursion variable, we just need to make sure that the environment contains a map for the variable that corresponds to the rest of the environment. All this is represented in the rules TPREC and TPVAR.

The remaining constructs are standard. `nil` always type-checks, with any environment (TPNIL). The rule for parallel processes (TPPAR) needs to divide the assumptions into two environments, to type-check the parallel processes separately. If both processes need to use the same channel, it is first split using the rules in Fig. 3. The rule for channel name creation (TPRES) introduces new channels with a unique access guarantee. Finally, in TPSTR, if process P type-checks with respect to an environment Γ, it should still type-check after Γ has been restructured using rules in Fig 3.

$$\frac{\Gamma \vdash_p P}{\Gamma, c : [C]^{\mathbf{1}}, j : C \vdash_p c!j.P}\ \textsc{tpOutIA} \qquad \frac{\emptyset \vdash_v \langle Q \rangle : \langle \Gamma_2 \rangle \qquad \Gamma_1 \vdash_p P}{\Gamma_1, c : [\langle \Gamma_2 \rangle]^{\mathbf{1}} \vdash_p c!\langle Q \rangle.P}\ \textsc{tpOutPA}$$

$$\frac{\Gamma, c : [C]^{\omega} \vdash_p P}{\Gamma, c : [C]^{\omega}, j : C \vdash_p c!j.P}\ \textsc{tpOutIW} \qquad \frac{\emptyset \vdash_v \langle Q \rangle : \langle \Gamma_2 \rangle \qquad \Gamma_1, c : [\langle \Gamma_2 \rangle]^{\omega} \vdash_p P}{\Gamma_1, c : [\langle \Gamma_2 \rangle]^{\omega} \vdash_p c!\langle Q \rangle.P}\ \textsc{tpOutPW}$$

$$\frac{\Gamma, c : [C]^{(\bullet, n-1)} \vdash_p P}{\Gamma, c : [C]^{(\bullet, n)}, j : C \vdash_p c!j.P}\ \textsc{tpOutIU} \qquad \frac{\emptyset \vdash_v \langle Q \rangle : \langle \Gamma_2 \rangle \qquad \Gamma_1, c : [\langle \Gamma_2 \rangle]^{(\bullet, n-1)} \vdash_p P}{\Gamma_1, c : [\langle \Gamma_2 \rangle]^{(\bullet, n)} \vdash_p c!\langle Q \rangle.P}\ \textsc{tpOutPU}$$

$$\frac{\Gamma, x : C \vdash_p P}{\Gamma, c : [C]^{\mathbf{1}} \vdash_p c?x.P}\ \textsc{tpInA} \qquad \frac{\Gamma, c : [C]^{\omega}, x : C \vdash_p P}{\Gamma, c : [C]^{\omega} \vdash_p c?x.P}\ \textsc{tpInW} \qquad \frac{\Gamma, c : [C]^{(\bullet, n-1)}, x : C \vdash_p P}{\Gamma, c : [C]^{(\bullet, n)} \vdash_p c?x.P}\ \textsc{tpInU}$$

$$\frac{}{\Gamma \vdash_p \mathtt{nil}}\ \textsc{tpNil} \qquad \frac{\Gamma_1 \vdash_p P}{\Gamma_1, x : \langle \Gamma_2 \rangle \vdash_p \mathtt{run}\, x.P}\ \textsc{tpRun1} \qquad \frac{\Gamma_1 \vdash_p Q \qquad \emptyset \vdash_v \langle P \rangle : \langle \Gamma_2 \rangle}{\Gamma_1, \Gamma_2 \vdash_p \mathtt{run}\, \langle P \rangle.Q}\ \textsc{tpRun2}$$

$$\frac{\Gamma, c : [C]^{\bullet} \vdash_p P}{\Gamma \vdash_p (\mathtt{new}\, c)P}\ \textsc{tpRes} \qquad \frac{\Gamma_1 \vdash_p P \quad \Gamma_2 \vdash_p Q}{\Gamma_1, \Gamma_2 \vdash_p P \mid Q}\ \textsc{tpPar} \qquad \frac{\Gamma, x : \{\Gamma\} \vdash_p P}{\Gamma \vdash_p \mathtt{rec}\, x.P}\ \textsc{tpRec} \qquad \frac{}{\Gamma, x : \{\Gamma\} \vdash_p x}\ \textsc{tpVar}$$

$$\frac{\Gamma \prec \Gamma' \qquad \Gamma' \vdash_p P}{\Gamma \vdash_p P}\ \textsc{tpStr} \qquad \frac{\Gamma \vdash_v v : [C_1]^{a_1} \qquad \Gamma \vdash_v u : [C_2]^{a_2} \qquad \Gamma \vdash_p P \qquad \Gamma \vdash_p Q}{\Gamma \vdash_p \mathtt{if}\ (v = u)\ \mathtt{then}\, P\ \mathtt{else}\, Q}\ \textsc{tpIf}$$

Figure 5: Process Typing

4 Results

We prove soundness for our type system with respect to the errors formalised in Fig. 2. As is standard, we do so by proving Subject Reduction (Thm. 1) and Safety (Thm. 2)

Theorem 1 (Subject Reduction)**.**

if Γ **is consistent and** $\Gamma \vdash_p P$ **and** $P \longrightarrow P'$ **implies there exists** Γ' **such that** Γ' **is consistent and** $\Gamma' \vdash_p P'$

Proof. By rule induction on $\Gamma \vdash_p P$. See (Zammit, 2012) □

Theorem 2 (Type Safety)**.**

$\Gamma \vdash_p P$ **implies** $P \not\longrightarrow_{\text{ERR}}$

Proof. By rule induction on $\Gamma \vdash_p P$. See (Zammit, 2012) □

We are also able to type-check the programs (1) and (2) discussed in the introduction and reject the erroneous programs discussed there. Repeated applications of Thm. 1 ensure that typed programs will remain typed when they compute, whereas Thm. 2 ensures that as long as they type-check, programs never produce an error.

5 Conclusion and Future Work

We have presented a sound type system for reasoning statically about higher-order pi-calculus programs using strong updates. This extended the work in De Vries et al. (2012), which did not consider higher-order communications.

In De Vries et al. (2012) (of which, this work is an immediate extension) the authors give an extensive discussion of related work and type systems. One possible avenue for future work is that of extending our type systems with input/output modalities as in Hennessy (2007), yielding richer notions of channel subtyping. One could also extend uniqueness typing to session types (Honda et al., 1998).

References

Ahmed, A., Fluet, M. and Morrisett, G. (2005). A step-indexed model of substructural state. In *Acm sigplan notices* (Vol. 40, pp. 78–91). ACM.

Armstrong, J. (2007). *Programming erlang.* The Pragmatic Bookshelf.

The Go Programming Language. (nodate). `http://golang.org/`.

Cesarini, F. and Thompson, S. (2009). *Erlang programming.* O'Reilly.

De Vries, E., Francalanza, A. and Hennessy, M. (2012). Uniqueness typing for resource management in message-passing concurrency. *J. Logic. Computation.* 24(3), 531–556.

Hennessy, M. (2007). *A distributed pi-calculus.* Cambridge University Press.

Honda, K., Vasconcelos, V. T. and Kubo, M. (1998). Language primitives and type disciplines for structured communication-based programming. In *Esop* (Vol. 1381, pp. 22–138). LNCS. Springer.

Kobayashi, N., Pierce, B. and Turner, D. (1999). Linearity and the pi-calculus. *ACM Transactions on Programming Languages and Systems (TOPLAS)*. 21(5), 914–947.

Pierce, B. (2002). *Types and programming languages*. MIT press.

Pierce, B. (2004). *Advanced topics in types and programming languages*. MIT press.

Sangiorgi, D. and Walker, D. (2003). *The pi-calculus: a theory of mobile processes*. Cambridge University Press.

Zammit, M. (2012). *A type system for a higher-order language*. University of Malta.

Xjenza Online - Journal of The Malta Chamber of Scientists
www.xjenza.org
DOI: 10.7423/XJENZA.2014.2.04

Research paper

Formal Proofs for Broadcast Algorithms

Mandy Zammit[1] **and Adrian Francalanza**[1]
[1]University of Malta, Faculty of ICT, Department of Computer Science

Abstract. Standard distributed algorithmic solutions to recurring distributed problems are commonly specified and described informally. A proper understanding of these distributed algorithms that clarifies ambiguities requires formal descriptions. However, formalisation tends to yield complex descriptions. We formally study two broadcast algorithms and present an encoding framework using a process descriptive language and formalise these algorithms and their specifications using this framework. Following these new formal encodings we discuss *correctness* proofs for the same algorithms.

Keywords Distributed Algorithms – Broadcast Algorithms – Correctness

1 Introduction

Distributed Systems are decentralised systems made up of *autonomous*, *concurrent*, *interconnected* processes working towards a *common goal* (Tel, 1994; Lynch, 1996). Unlike standalone systems, where if something fails then all else fails, processes in a *distributed system* act as units of failures. This means that distributed systems may undergo *partial-failure* (as opposed to *total system failure*) where the failure of a process in such a system does not imply failure of the whole system.

Distributed problems are known recurring situations which arise when programming distributed systems. Two well known distributed problems are *consensus* (agreement between all processes) and *reliable broadcast* (reliable inter-process communication). *Standard Distributed Algorithms* are algorithmic solutions to these known recurring distributed problems. These distributed algorithms are specified through a number of correctness criteria. Correctness criteria specify the expected (*correct*) behaviour of the distributed algorithm that is being specified. For every distributed problem specification there may be various algorithmic solutions, each aimed to observe the behaviour specified by the correctness criteria.

The current modus operandi of describing distributed algorithms and their specifications is using informal or semi-formal descriptions. Specifications are normally expressed in natural language, whilst distributed algorithms are commonly expressed using some semi-formal pseudo-code, lacking any type of formal semantics (Tel, 1994; Lynch, 1996; Guerraoui and Rodrigues, 2006).

There are a number of reasons as to why the status quo is unsatisfactory. For one, there is a discrepancy between such potentially ambiguous semi-formal descriptions and the implementation of such algorithms (in a machine computable language), which is a large source of erroneous behaviour in the deployment of the system. Another reason why informal descriptions and specifications are deficient is that no formal verification of the algorithms may be done. Formal analysis is essential because such algorithms are very easy to get wrong. Given the concurrent nature of distributed systems, each execution results in a different execution path: if we want to verify that our algorithm observes the behaviour specified by the correctness criteria, then we need to reason on every possible path of execution of the algorithm, something that can only be done through proper formal analysis.

As in Francalanza and Hennessy (2007), Kühnrich and Nestmann (2009), Nestmann et al. (2003) we postulate that it would be desirable to encode both the algorithm and its specification in some formal process description language and then equate their behaviour using some notion of equivalence (as in Equation 1).

$$System = Specification \tag{1}$$

In this paper we focus on Broadcast Algorithms; a small subset of Distributed Algorithms. The rest of the paper is structured as follows; Section 2 describes the Distributed Broadcast problem, and presents two specifications together with an algorithmic solution for each specification. Section 3 presents a *partial-failure* calculus that is able to encode both specification and implementation of these algorithms. Section 4 expresses an encoding framework for broadcast algorithms and their specifications. Section 5 presents an encoded broadcast algorithm using the calculus and encoding framework. Finally section 6 discusses the respective proofs for these broadcast algorithms, and sections 7 and 8 conclude.

Correspondence to: Mandy Zammit (mandy.zammit.08@um.edu.mt)

© 2014 Xjenza Online

2 Distributed Broadcast Problem

Broadcast is used by an entity to disseminate messages to a number of other entities including itself. Broadcast algorithms are a fundamental building block in the programming of distributed systems. There are a number of different broadcast specifications, each differing in the reliability requirements that it guarantees. We explore two different broadcast specifications and two algorithmic solutions; each one aimed at satisfying one of the broadcast specification as expressed in (Guerraoui and Rodrigues, 2006); the algorithms assume perfect failure detectors and are also taken from (Guerraoui and Rodrigues, 2006).

Terminology: ***Broadcast*** is the term used to describe the transition of a message by an entity (broadcaster) to all other entities (including itself) in a given network. This transmitted message is then said to be ***received*** by the other individual entities in the network. However its receipt is only permanently confirmed once it is ***delivered*** to some higher level of abstraction. A ***correct*** process is one which does not to fail during execution, whilst a ***faulty*** process may fail at any point in time during the execution of an algorithm.

2.1 Best-Effort Broadcast

The *Best-Effort* broadcast is a simple broadcast specification with a weak form of reliability, whereby if the broadcaster of a message fails at any point during execution, then no entities are expected to deliver the message. The set of correctness criteria that embody the *best-effort* broadcast specification are:

- ***Validity:*** *(liveness)* For any two processes p_i and p_j. If p_i and p_j are *correct*, then every message broadcast by p_i is eventually delivered by p_j.
- ***No Duplication:*** *(safety)* No message is delivered more than once.
- ***No Creation:*** *(safety)* If a message m is delivered by some process p_j, then m was previously broadcast by some process p_i.

A *liveness* property asserts that some "good" behaviour eventually happens, whereas a *safety* property asserts that nothing wrong should happen during execution.

Algorithm 1 Best Effort Broadcast (adapted from Guerraoui and Rodrigues (2006)

```
1: while ⟨ bebBroadcast — m⟩ do
2:     for p_i ∈ ∏ do trigger ⟨ pp2pSend — p_i, m⟩;
3:     end for
4: end while
5:
6: while ⟨ pp2pDeliver — p_i, m⟩ do
7:     trigger ⟨ bebDeliver — p_i, m⟩;
8: end while
```

Algorithm 1 depicts an algorithmic solution to the *Best-Effort* Specification presented by Guerraoui and Rodrigues (2006). Lines 1 to 4 express the broadcast of a message, whilst lines 6 to 8 describe delivery of a message.

Algorithm 2 (Lazy) Regular Reliable Broadcast (adapted from Guerraoui and Rodrigues (2006))

```
1: while ⟨ Init ⟩ do
2:     delivered := ∅; correct := ∏;
3:     for p_i ∈ ∏ do from[p_i] := ∅;
4:     end for
5: end while
6:
7: while ⟨ rbBroadcast — m⟩ do
8:     trigger ⟨ bebBroadcast — [DATA, self, m] ⟩;
9: end while
10:
11: while ⟨ bebDeliver — p_i, [DATA, s_m, m] ⟩ do
12:     if m ∉ delivered then
13:         delivered := delivered ∪{m};
14:         trigger ⟨ rbDeliver — s_m, m⟩;
15:         from[p_i] := from[p_i] ∪{(s_m, m)};
16:         if p_i ∉ correct then
17:             trigger ⟨ bebBroadcast — [DATA, s_m, m] ⟩;
18:         end if
19:     end if
20: end while
21:
22: while ⟨ crash — p_i ⟩ do
23:     correct := correct \{p_i};
24:     for (s_m, m) ∈ from[p_i] do
25:         trigger ⟨ bebBroadcast — [DATA, s_m, m] ⟩;
26:     end for
27: end while
28:
```

2.2 Regular Reliable Broadcast

The *Regular Reliable* broadcast specification has a stronger form of reliability than the *Best-Effort* broadcast, whereby it requires that, if at least one *correct* process delivers a broadcast message then all other *correct* entities in the network must deliver the same message. This specification shares the same *three* correctness criteria of the *best-effort* broadcast specification, with the addition of a new *liveness* property:

- ***Agreement:*** *(liveness)* If a message m is delivered by some correct process p_i, then m is eventually delivered by every correct process p_j.

Algorithm 2 is an algorithmic solution presented in Guerraoui and Rodrigues (2006) satisfying this specification. Lines 1 to 5 initialise the setting for this algorithm. Broadcast of a message is defined from line 7 to 9, while lines 11 to 15 express delivery of a message, introducing checks for no duplication. Lines 16 to 18 and 22 to 27 re-instantiate a broadcast if the sender of a message is detected to be faulty.

The problem with these algorithmic representations is that they are expressed using some pseudo-code which has no formal semantics. Secondly the main source of complication is the analysis of the interleaving of all the processes, which is not portrayed in these representations. It is also difficult to relate formally the specifications to the actual

code in a formal language. What's more, there exists an implicit problem: we expect that these specifications hold over all possible participants in a broadcast network.

3 A *Partial-Failure* Calculus

The *partial-failure* calculus presented in Francalanza and Hennessy (2007) formalises the characteristics of distributed systems in terms of concurrent process, independently failing locations, inter-process communication and failure detection.

Figure 1 defines the syntax of an extended version of the *partial-failure* calculus. It has two syntactic categories; namely *Processes* and *Systems*. *Processes* may contain nil which is the simplest construct of the language and represents termination. Input ($a?\vec{x}$) and output ($a!\vec{v}$) terms allow vector values $\vec{v}$ to be inputted (when matching the pattern of $\vec{x}$) or outputted on channel a. Processes may be composed of other processes running concurrently ($P \mid Q$). Visibility of channels may be localised to a subset of processes through channel scoping $(\nu\, a)P$. Such scoping disallows any extenral communication interference on channel a. Two processes may preempt each other if they are composed by *choice* ($P + Q$). That is, if a part of P executes first, then any execution from Q is preempted, and vice-versa. Processes may contain a *matching* construct which test for the identity of value vectors $\vec{v_1}$ and $\vec{v_2}$ and proceeds to P or Q accordingly. *Action renaming* $P[^a/_b]$ allows the renaming of (input and output) actions. *Failure-detection* is carried out using the *failure detector* construct ($\mathsf{susp}\ l.P$). This is a guarding construct which tests for the liveness of location l and releases process P once it *correctly* suspects that l has failed. We extend these constructs with processes which may contain the zero construct, which guards process P, releasing it once it detects that no more failures may be induced in the network. This construct is novel to our setting and is only used as a specification construct, i.e., to describe correctness criteria. *Systems* are made up of processes residing at some arbitrary location l ($l|[P|]$). They may also be composed of other systems executing in parallel ($S \mid T$), may contain scoped channels ($(\nu\, a)S$), or renamed channel names ($S[^a/_b]$).

Notations: A series of parallel processes $P_1 \mid \ldots \mid P_n$ is denoted by $\prod_{i=1}^{n} P_i$, whilst a series of choices $P_1 + \cdots + P_n$ is denoted by $\sum_{i=1}^{n} P_i$. We denote the scoping of more than one channel in P by $(\nu\, \tilde{n})P$, where $\tilde{n}$ is the set of channel names that are to be scoped. On the other hand when more than one action renaming is needed on a process, we denote it as $[^{\alpha_1}/_{\beta_1}, \ldots, ^{\alpha_n}/_{\beta_n}]$.

The operational semantics of the language is defined in terms of *configurations* of the form

$$\langle \mathcal{L}, n \rangle \triangleright S$$

where $\langle \mathcal{L}, n \rangle$ represents the distributed network state and S is the distributed system. $\mathcal{L}$ is a *liveset*, which is defined as a set of locations $\{l_1, \ldots, l_n\} \in \textsc{Loc}$ which are alive (Francalanza and Hennessy, 2007). A special type of location, the *immortal location* denoted by $\star$ is assumed to be included in every *liveset* $\mathcal{L}$. On the other hand n represents a bounded number of possible dynamic *location failures* in the network. Intuitively $\langle \mathcal{L}, n \rangle \triangleright\ S$ denotes the system S with its components (or processes) running on locations $\mathcal{L}$, subject to n possible location failures from $\mathcal{L}$. Computation is define by transitions between tuples of configurations as follows

$$\langle \mathcal{L}, n \rangle \triangleright\ S \xrightarrow{\alpha} \langle \mathcal{L}', n' \rangle \triangleright\ S'$$

where α is an action defined as

$$\begin{array}{rcll} \alpha \in \textsc{Act} & ::= & a?\vec{v} & \textit{Input} \\ & \mid & a!\vec{v} & \textit{Output} \\ & \mid & \tau & \textit{Internal} \end{array}$$

Weak actions $\overset{\hat{\alpha}}{\Longrightarrow}$ denote either

$$\xrightarrow{\tau}{}^{*} \xrightarrow{\alpha}{}^{*} \xrightarrow{\tau}{}^{*} \quad if\ \alpha \in \{a?\vec{v},\ a!\vec{v}\}$$

or

$$\xrightarrow{\tau}{}^{*} \quad if\ \alpha = \tau$$

and may also be used to transition between tuples.

The semantic rules of this calculus are given in Figure 1: transitions resulting in an unchanged network have this network omitted from the left tuple. Rule In, Out, and Com describe inter-process communication across a network. We note that we require l, the location where the communication is occurring to be alive. Rule Halt describes the failure of a location whereas, rule Susp describes the detection of a failed location. Rule Zero (a novel addition to the semantics of the calculus) triggers only when no more failures may be induced in the network. The remaining rules are fairly standard (see Francalanza and Hennessy (2007) for further details). The transition semantics of the *partial-failure* calculus induces the usual definition of weak bisimulation equivalence defined as follows

Definition 2 (Weak bisimulation equivalence)**.** Denoted as $\approx$, is the largest relation over configurations such that if $\langle \mathcal{L}_1, n_1 \rangle \triangleright S_1 \approx \langle \mathcal{L}_2, n_2 \rangle \triangleright S_2$ then

- $\langle \mathcal{L}_1, n_1 \rangle \triangleright S_1 \xrightarrow{\alpha} \langle \mathcal{L}'_1, n'_1 \rangle \triangleright S'_1$ implies $\langle \mathcal{L}_2, n_2 \rangle \triangleright S_2 \overset{\hat{\alpha}}{\Longrightarrow} \langle \mathcal{L}'_2, n'_2 \rangle \triangleright S'_2$ such that $\langle \mathcal{L}'_1, n'_1 \rangle \triangleright S'_1 \approx \langle \mathcal{L}'_2, n'_2 \rangle \triangleright S'_2$
- $\langle \mathcal{L}_2, n_2 \rangle \triangleright S_2 \xrightarrow{\alpha} \langle \mathcal{L}'_2, n'_2 \rangle \triangleright S'_2$ implies $\langle \mathcal{L}_1, n_1 \rangle \triangleright S_1 \overset{\hat{\alpha}}{\Longrightarrow} \langle \mathcal{L}'_1, n'_1 \rangle \triangleright S'_1$ such that $\langle \mathcal{L}'_1, n'_1 \rangle \triangleright S'_1 \approx \langle \mathcal{L}'_2, n'_2 \rangle \triangleright S'_2$

♦

4 Encoding Framework using the *Partial-Failure* Calculus

The *Partial-failure* calculus is expressive enough to encode both the broadcast specifications and algorithms in Section 2. We adhere to the following conventions.

4.1 Encoding Algorithms

- ***Independently failing participants*** Participants in broadcast algorithms are autonomous and can fail independently at any given point in time during execution. We encode this characteristic as code running on dedicated locations $l_n|[P_n|]$, where P_n denotes the code of participant n. Location l_n is a unit of failure,

Processes

$P, Q \in \textsc{Proc}$	$::=$	nil	*(Inert)*	$\mid$	$a?\vec{x}.P$	*(Input)*
	$\mid$	$a!\vec{v}$	*(Output)*	$\mid$	$(\nu\, a)P$	*(Channel Scoping)*
	$\mid$	$P \mid Q$	*(Parallel Composition)*	$\mid$	$P + Q$	*(Choice)*
	$\mid$	$\mathsf{if}\ \vec{v_1} = \vec{v_2}\ \mathsf{then}\ P\ \mathsf{else}\ Q$	*(Matching)*	$\mid$	$P[^{\alpha}/_{\beta}]$	*(Rename)*
	$\mid$	$\mathsf{susp}\ l.P$	*(Failure Detector)*	$\mid$	$\mathsf{zero}.P$	*(Zero)*

Systems

$S, T \in \textsc{Sys}$	$::=$	$l\|[P\|]$	*(Located Processes)*	$\mid$	$S \mid T$	*(Parallel Composition)*
	$\mid$	$(\nu\, a)S$	*(Channel Scoping)*	$\mid$	$S[^{\alpha}/_{\beta}]$	*(Rename)*

Transition Rules

Assuming $l \in \mathcal{L}, n \geq 0$

$$\textsc{In}\quad \frac{}{\langle \mathcal{L}, n\rangle \triangleright\ l|[a?(\vec{x}).P|] \xrightarrow{a?\vec{v}} l|[P\{^{\vec{v}}/_{\vec{x}}\}|]}$$

$$\textsc{Out}\quad \frac{}{\langle \mathcal{L}, n\rangle \triangleright\ l|[a!(\vec{v}).\mathsf{nil}|] \xrightarrow{a!\vec{v}} l|[\mathsf{nil}|]}$$

$$\textsc{Susp}\quad \frac{}{\langle \mathcal{L}, n\rangle \triangleright\ l|[\mathsf{susp}\ k.P|] \xrightarrow{\tau} l|[P|]}\quad k \notin \mathcal{L}$$

$$\textsc{Halt}\quad \frac{}{\langle \mathcal{L}, n+1\rangle \triangleright\ S \xrightarrow{\tau} \langle \mathcal{L} \setminus l, n\rangle \triangleright\ S}$$

$$\textsc{Fork}\quad \frac{}{\langle \mathcal{L}, n\rangle \triangleright\ l|[P \mid Q|] \xrightarrow{\tau} l|[P|] \mid l|[Q|]}$$

$$\textsc{New}\quad \frac{}{\langle \mathcal{L}, n\rangle \triangleright\ l|[(\nu\, a)P|] \xrightarrow{\tau} (\nu\, a)l|[P|]}$$

$$\textsc{RenP}\quad \frac{}{\langle \mathcal{L}, n\rangle \triangleright\ l|[(P)\rho|] \xrightarrow{\tau} (l|[P|])\rho}$$

$$\textsc{Eq}\quad \frac{}{\langle \mathcal{L}, n\rangle \triangleright\ l|[\mathsf{if}\ v = v\ \mathsf{then}\ P\ \mathsf{else}\ Q|] \xrightarrow{\tau} l|[P|]}$$

$$\textsc{Neq}\quad \frac{}{\langle \mathcal{L}, n\rangle \triangleright\ l|[\mathsf{if}\ v_1 = v_2\ \mathsf{then}\ P\ \mathsf{else}\ Q|] \xrightarrow{\tau} l|[Q|]}\quad v_1 \neq v_2$$

$$\textsc{Zero}\quad \frac{}{\langle \mathcal{L}, 0\rangle \triangleright l|[\mathrm{zero}.P|] \xrightarrow{\tau} \langle \mathcal{L}, 0\rangle \triangleright l|[P|]}$$

$$\textsc{Sum}\quad \frac{\langle \mathcal{L}, n\rangle \triangleright\ l|[P_i|] \xrightarrow{\alpha} l|[P|]}{\langle \mathcal{L}, n\rangle \triangleright\ l|[\sum_{i \in I} P_i|] \xrightarrow{\alpha} l|[P|]}$$

$$\textsc{Ren}\quad \frac{\langle \mathcal{L}, n\rangle \triangleright\ S \xrightarrow{\alpha} \langle \mathcal{L}, n\rangle \triangleright\ S'}{\langle \mathcal{L}, n\rangle \triangleright\ (S)\rho \xrightarrow{(\alpha)\rho} \langle \mathcal{L}, n\rangle \triangleright\ (S')\rho}\quad \rho = [^{a}/_{b}]$$

$$\textsc{Rest}\quad \frac{\langle \mathcal{L}, n\rangle \triangleright\ S \xrightarrow{\alpha} \langle \mathcal{L}', n'\rangle \triangleright\ S'}{\langle \mathcal{L}, n\rangle \triangleright\ (\nu\, a)S \xrightarrow{\alpha} \langle \mathcal{L}', n'\rangle \triangleright\ (\nu\, a)S'}\quad \textsc{Chan}\alpha \in \mathrm{fc}\,((\nu\, a)S)$$

$$\textsc{Par}\quad \frac{\langle \mathcal{L}, n\rangle \triangleright\ S \xrightarrow{\alpha} \langle \mathcal{L}', n'\rangle \triangleright\ S'}{\langle \mathcal{L}, n\rangle \triangleright\ S \mid T \xrightarrow{\alpha} \langle \mathcal{L}', n'\rangle \triangleright\ S' \mid T}$$

$$\textsc{Com}\quad \frac{\langle \mathcal{L}, n\rangle \triangleright\ S \xrightarrow{a?\vec{v}} S' \qquad \langle \mathcal{L}, n\rangle \triangleright\ T \xrightarrow{a!\vec{v}} T'}{\langle \mathcal{L}, n\rangle \triangleright\ S \mid T \xrightarrow{\tau} S' \mid T'}$$

Figure 1: Partial-Failure Calculus (DPC)

whereby it can be marked as a dead location (by being removed from the liveset $\mathcal{L}$) during execution ceasing execution of code residing on it.

- ***Network initialisation*** An output action on some channel c_n will denote the initialisation of the network, where process P_n would be chosen as the designated broadcaster. c channels are not localised to the network, since initialisation of the network is expected to be triggered from the environment outside the network.
- ***Broadcast*** Broadcast in the algorithms that we study happens over *perfect point-to-point* links. We use the constructs of receiving ($b?x$) and sending ($b!m$) messages over channels to encode perfect point-to-point links. Channels may in general have multiple senders and receivers, but we choose to restrict channels to be used in a *linear* fashion, where only one process may send messages on the channel, and only one other process may receive messages from the same channel. More precisely the channel b_n^m is the channel used by process P_n to send messages to P_m. Dually the channel b_m^n is used by process P_m to send messages to P_n. This linear usage is further ensured by the use of scoping to localise these channels to the network which is using

them. Broadcast is thus encoded as the output of a message over the encoded perfect point-to-point links, discussed previously. Dually the receipt of a broadcasted message is encoded as the input action over the same perfect point-to-point links.

- ***Deliver*** Delivery of a message by some participant P_n will be encoded as the output of the message over some channel d_n which is not scoped. The reason why the channel d_n is not scoped is because delivery of a message is the process of passing the received message to another entity external to the broadcast algorithm.
- ***Failure Detection*** Failure detection is immediately expressed using the suspect ($susp\ l.P$) construct of the *partial-failure* calculus that we use for our encoding.

4.2 Encoding Specifications

In Francalanza and Hennessy (2007), Francalanza and Hennessy propose the decomposition of specification during the encoding process, i.e., instead of encoding all the properties of the specification as one process, they use dedicated *wrapper code* or *testing harnesses* for each correctness criteria of the specification. These dedicated harnesses are able to wrap a system and stop any interaction between foreign entities and the network. A harness will then induce a network broadcast and observe the behaviour of the algorithm whilst determining if its behaviour conforms with the behaviour expected by the correctness criteria which is being tested for. This means that now to verify our algorithms we will have a number of equations (one for each correctness criteria in the specification) as follows

$$(\nu\,\tilde{n})(System \mid Harness_1) \approx SimpleSpecification$$
$$\vdots$$
$$(\nu\,\tilde{n})(System \mid Harness_n) \approx SimpleSpecification$$

The structure of the *SimpleSpecification* will be determined on the type of property which is being tested for. If the criteria being tested for is a *safety* property, the respective simple specification would entail an *inert* (nil) process, whilst if testing for a *liveness* property the simple specification would consists of an output on channel OK. Since a *safety* property asserts that *nothing bad* happens, we construct harnesses which wrap and observe systems, triggering a signal on channel *nok* whenever violations are detected. Stated otherwise, if a *safety* property is satisfied no output on *nok* is generated. Conversely, harnesses wrapping systems and testing for *liveness* properties, output OK signals when the expected behaviour is observed. The following set of characteristics are prevalent to the encoding of testing harnesses.

- ***Reliable code*** It is required that wrapper code testing for a property in a distributed algorithm is reliable, that is, it should never fail unlike the participants in the distributed algorithm. Any wrapper code will thus be located at the *immortal location* $\star$.
- ***Initiators*** A harness commences testing by sending the start message on channel c_i to process P_i, the designated broadcaster. This mimics the initiation of a broadcast from an outside environment and allows the harness to induce the network and test for a specific correctness criteria accordingly.
- ***Testing Mechanism*** The observation of message deliveries is modeled by the input on channels $d_1 \ldots d_n$ where n is the number of participants in the network under test. After consuming these deliveries (produced by participants in the network), each testing harness will execute specific code that acts upon the observed delivery behaviour.

$$\text{RRB}_k^n \triangleq \begin{cases} l_0|[\mathsf{nil}|] & k = 0 \\ (\nu\,\tilde{n})\left(\begin{array}{l} \text{RRB}_{k-1}^n \\ \mid l_k|[P_{\text{BEB}_k^n}[c_k/c'_k,\, d_k/d'_k]|] \\ \mid l_k|[P_{\text{RRB}_k}|] \end{array}\right) & k > 0 \end{cases}$$

$$where \quad 0 \leq k \leq n$$

Best-Effort Broadcast related Processes

$$P_{\text{BEB}_k^n} \triangleq B_{\text{BEB}_k^n} \mid D_{\text{BEB}_k^n}$$
$$B_{\text{BEB}_k^n} \triangleq c_k?\vec{x}.\prod_{j=1}^{n} b_k^j!\vec{x}$$
$$D_{\text{BEB}_k^n} \triangleq \sum_{j=1}^{n} \left(b_j^k?\vec{x}.d_k!\vec{x}\right)$$

Regular Reliable Broadcast related Processes

$$P_{\text{RRB}_k} \triangleq B_{\text{RRB}_k} \mid D_{\text{RRB}_k}$$
$$B_{\text{RRB}_k} \triangleq c_k?\vec{x}.c'_k!(k,\vec{x})$$
$$D_{\text{RRB}_k} \triangleq d'_k?(s,\vec{m}).(d_k!\vec{m} \mid \mathsf{susp}\ l_s.c_k!(s,\vec{m}))$$
$$\tilde{n} = \{b_k^1,\ldots,b_k^k\} \cup \{b_1^k,\ldots,b_k^k\} \cup \{c'_k\} \cup \{d'_k\}$$

Figure 2: Inductive Formal Encoding of (Lazy) Regular Reliable Broadcast

5 Encoding Regular Reliable Broadcast

We present the formal encoding of the regular reliable broadcast algorithm, (which uses the Best Effort Broadcast) and the formal encoding of two *testing harnesses*; one testing for the No Duplication (safety) property and another testing for the Agreement (liveness) property in this same algorithm. The other properties follow the same pattern.

Broadcast specifications quantify over all possible participants in a network, requiring us to provide a proof for *every* instance of participants. We therefore present an inductive formal encoding for the regular reliable broadcast, which will enable us to construct inductive proofs that cover all

$$\textsc{nd}_n^{i,\vec{m}}[-] \triangleq (\nu\,\tilde{n})(\star|[I_i^{\vec{m}} \mid T_n|] \mid [-])$$

where $0 \leq i \leq n$

$$I_i^{\vec{m}} \triangleq \begin{cases} \mathsf{nil} & i = 0 \\ c_i!\vec{m} & i > 0 \end{cases} \qquad (Initiator)$$

$$T_n \triangleq \begin{cases} \mathsf{nil} & n = 0 \\ T_{n-1} \mid T_n^{'} & n > 0 \end{cases} \qquad (Testers)$$

$$T_n^{'} \triangleq d_n?\vec{x}.d_n?\vec{y}.nok!$$

$$\tilde{n} = \{d_1, \ldots, d_n\} \cup \{c_1, \ldots, c_n\}$$

Figure 3: Formal Encoding of No Duplication Harness

$$A_n^{i,\vec{m}}[-] \triangleq (\nu\,\tilde{n})(\star|[I_i^{\vec{m}} \mid T_n \mid T_0^n|] \mid [-])$$

where $0 < i \leq n$

$$I_i^{\vec{m}} \triangleq c_i!\vec{m} \qquad (Initiator)$$

$$T_0^n \triangleq \mathsf{zero}.(OK! + \sum_{j=1}^{n} d_j?\vec{x}.(d_j!\vec{x} \mid ok_0!))$$

$$T_n \triangleq \begin{cases} T_1^{'} & n = 1 \\ T_{n-1}[^{OK}/_{ok_{n-1}}] \mid T_n^{'} & n > 1 \end{cases} \qquad (Testers)$$

$$T_n^{'} \triangleq ok_{n-1}?.((d_n?\vec{x}.OK!) + (\mathsf{susp}\ l_n.OK!))$$

$$\tilde{n} = \{d_1, \ldots, d_n\} \cup \{ok_0, \ldots, ok_{n-1}\} \cup \{c_1, \ldots, c_n\}$$

Figure 4: Formal Encoding of Agreement Harness

cases of participant numbers.

Figure 2 denotes the formal encoding $\textsc{rrb}_k^n$ of the Regular Reliable Broadcast Algorithm (Algorithm 2), whereby $\textsc{rrb}_k^n$ stands for the network of n ultimate participants, but k actual participants yet in the network. Participants are added inductively in this network until k becomes equal to n. Recall from Algorithm 2, that Regular Reliable Broadcast uses the Best-Effort Broadcast, thus Participants in $\textsc{rrb}_k^n$ are made up of Best-Effort related code $P_{\textsc{beb}_k^n}$ and Regular Reliable related code $P_{\textsc{rrb}_k^n}$.

Best-Effort related code $P_{\textsc{beb}_k^n}$ contains broadcast and delivery threads; $B_{\textsc{beb}_k^n}$ and $D_{\textsc{beb}_k^n}$ respectively. The broadcast thread $B_{\textsc{beb}_k^n}$ corresponds to lines 1 to 3 in Algorithm 1 and is only instantiated if there is an input action on the channel c_k. Once instantiated it will broadcast the message to all other entities in the network. The delivery thread $D_{\textsc{beb}_k^n}$ on the other hand corresponds to lines 6 to 8 in Algorithm 1, whereby it allows the receipt of one broadcast message.

Regular Reliable related code $P_{\textsc{rrb}_k^n}$ contain broadcast $B_{\textsc{rrb}_k^n}$ and delivery $D_{\textsc{rrb}_k^n}$ threads as well. The broadcast thread $B_{\textsc{rrb}_k^n}$ corresponds to lines 7 to 9 in Algorithm 2, where once a message is received by some P_i over channel c_i it is forwarded to the *Best-Effort* broadcast underneath. The deliver thread $D_{\textsc{rrb}_k^n}$ corresponds to lines 11 to 20 and 22 to 27 in Algorithm 2, where if a delivery is received from the Best-Effort broadcast underneath (over channel $d_k^{'}$), the delivery thread delivers (over channel d_k) and releases the code which tests for the liveness of the owner of the received message, and starts a new broadcast with the same message if the process is suspected to have failed.

Figure 3 denotes the formal encoding of the No Duplication *testing harness*. This Harness $\textsc{nd}_n^{i,\vec{m}}$ tests for the No Duplication property in the Regular Reliable Broadcast algorithm, and follows the conventions outlined in Section 4. Broadcast initiation is done through process $I_i^{\vec{m}}$, which disseminates a message on channel c_i. The testers in this harness $T_n^{'}$, then wait for a delivery on channel d_n, and trigger a *nok* if a second delivery is observed.

Figure 4 presents the formal encoding of the *testing harness* that tests for the Agreement property in the Regular Reliable broadcast algorithm. The testing harness $A_n^{i,\vec{m}}$ which tests for n processes in a network, induces the broadcast network with message $\vec{m}$ by designating participant P_i as the broadcaster. $I_i^{\vec{m}}$ is the initiation code of the harness which induces the broadcast network by outputting message $\vec{m}$ on channel c_i. T_0^n is the code used to initialise testing. The zero construct is used in this harness definition to restrain testing to commence only when no more failures may be induced in the network. The reason for this is that we need to identify which processes are *correct*, that is, which were guaranteed not to fail during execution. T_0^n then either outputs an OK if no participant had delivered, or if it manages to observe a delivery from any participant, it commences the other testers by outputting an ok_0. Each tester T_n where $n > 0$ then waits for an ok_{n-1}, that is, an ok signal from the Tester $n-1$. When this ok_{n-1} is received, the tester checks if the participant it is testing for P_n is alive, if it is not it promptly outputs on ok_n, but if P_n is still alive then the tester outputs on ok_n only if the participant is ready to deliver the broadcasted message.

6 Stating and Proving Correctness

We have till now presented formal encoding for the informal broadcast specifications and informal algorithmic broadcast implementation discussed in Section 2. This constitutes the main contribution of the paper. Using the Harnesses and Algorithms (formally) defined in section 5, together with the bisimulation equivalence of the *partial-failure* calculus (in which the harnesses and algorithms are expressed), we can formulate our correctness criteria in the

following form:

$$\forall n \;\; Harness(n)[System(n)] \approx SimpleSpec$$

where *SimpleSpec* is nil in the case for safety properties and *OK*! in the case of a liveness property. For instance to verify no duplication we are required to prove

$$\forall n \;\; \mathrm{ND}_n^{i,\vec{m}}[\mathrm{RRB}_n^n] \approx \mathsf{nil}$$

whilst to verify agreement we are required to prove

$$\forall n \;\; A_n^{i,\vec{m}}[\mathrm{RRB}_n^n] \approx OK!$$

These are formal statements with an unambiguous semantics expressed as an equivalence amongst two systems within our calculus. Bisimulation equivalence comes equipped with an elegant (coinductive) proof technique whereby we only need to exhibit a relation that includes the afore mentioned pair and observes the transfer property of definition 2.

However these witness relations can be quite large and unwieldy to construct. Moreover, for each correctness criteria we need to exhibit an infinite number of relations, one for every instance of the broadcast network with a specific number of participants.

Francalanza and Hennessy (2007) propose the decomposition of correctness proofs into two phases; the *failure free* phase (or *basic correctness* phase) and the *correctness preservation* phase (or *fault-tolerance* phase). The first phase tests the algorithm under no failures, and equates its behaviour to a *SimpleSpec*

$$\langle \mathcal{L}, 0\rangle \triangleright (\nu\, \tilde{o})(Sys(n) \mid Harness(n)) \approx SimpleSpec(n)$$

The second phase equates the behaviour of the system under failures to the system in a failure free environment

$$\langle \mathcal{L}, n\rangle \triangleright (\nu\, \tilde{o})(Sys(n) \mid Harness(n))$$
$$\approx$$
$$\langle \mathcal{L}, 0\rangle \triangleright (\nu\, \tilde{o})(Sys(n) \mid Harness(n))$$

We adopt this technique in our Correctness proofs to alleviate the cumbersome witness bisimulations.

Furthermore, in order to address the problem of exhibiting witness bisimulations for every possible number of participants, we can adopt an inductive proof approach, whereby we show that the correctness property holds for the base case (one participant) and then the inductive case ($k + 1$ participants assuming that the property holds for k participants). In (Zammit, 2013) we show how this can be done for a subset of these properties, using a technique called mocking. We however leave the construction of the full proofs for every broadcast property for future work.

7 Related Work

Kühnrich and Nestmann (2009) use a similar process description language but make use of imperfect failure detectors (Chandra and Toueg, 1996) to encode an algorithmic solution to Distributed Consensus. They point out that the technique of decomposing fault-tolerance proofs (Francalanza and Hennessy, 2007) is not quit helpful in the context of imperfect failure detectors. Nestmann et al. in (Nestmann et al., 2003) verify the Distributed Consensus algorithm developed by (Chandra and Toueg, 1996). To encode their algorithm they use a process calculi as well, but opt to represent reachable states in the consensus algorithm as a message matrix. This "global-view matrix-like representation of reachable states" contains history of messages that have been sent until now in the algorithm, and would help in the formal global reasoning about the contribution of processes to individual rounds of the algorithm.

8 Conclusion and Future Work

This paper presents the following contributions:

1. a formal description for the Best-Effort and Reliable Broadcast specification.
2. a formal description of an algorithmic implementation solving Regular Reliable Broadcast.
3. an outline of how to alleviate the burden of proving equivalences presented in Section 6.

As future work we intend to complete the correctness proofs and extend this encoding and proofing technique to other broadcast algorithms with different forms of reliability requirements.

Acknowledgment

The research work disclosed in this publication is partially funded by the Strategic Educational Pathways Scholarship Scheme (Malta). The scholarship is part-financed by the European Union – European Social Fund

References

Chandra, T. D. and Toueg, S. (1996). Unreliable failure detectors for reliable distributed systems. *J. ACM.* 43(2), 225–267.

Francalanza, A. and Hennessy, M. (2007). A fault tolerance bisimulation proof for consesus. In R. D. Nicola (Ed.), *Esop 2007.*

Guerraoui, R. and Rodrigues, L. (2006). *Introduction to reliable distributed programming.* Secaucus, NJ, USA: Springer-Verlag New York, Inc.

Kühnrich, M. and Nestmann, U. (2009). On process-algebraic proof methods for fault tolerant distributed systems. (pp. 198–212). FMOODS '09/FORTE '09. Lisboa, Portugal: Springer-Verlag.

Lynch, N. A. (1996). *Distributed algorithms.* The Morgan Kaufmann Series in Data Management Systems Series. Morgan Kaufmann Publishers.

Nestmann, U., Fuzzati, R. and Merro, M. (2003). Modeling consensus in a process calculus. In *In concur: 14th international conference on concurrency theory. lncs* (pp. 393–407). Springer-Verlag.

Tel, G. (1994). *Introduction to distributed algorithms.* New York, NY, USA: Cambridge University Press.

Zammit, M. (2013). *Inductive basic correctness reasoning in formal fault-tolerance proofs for distributed algorithms* (Master's thesis, University of Malta, Malta).

Xjenza Online - Journal of The Malta Chamber of Scientists
www.xjenza.org
DOI: 10.7423/XJENZA.2014.2.05

Research Article

Monitoring Distributed Systems with Distributed PolyLarva

I. Cassar, C. Colombo, A. Francalanza
University of Malta, Department of Computer Science

Abstract. PolyLarva is a language-agnostic runtime verification tool, which converts a PolyLarvaScript into a monitor for a given system. While an implementation for PolyLarva exists, the language and its compilation have not been formalised. We therefore present a formal implementation-independent model which describes the behaviour of PolyLarvaScript, comprising of the μLarvaScript grammar and of a set of operational semantics. This allows us to prove important properties, such as determinism, and also enables us to reason about ways of re-designing the tool in a more scalable way. We also present a collection of denotational mappings for μLarvaScript converting the constructs of our grammar into constructs of a formal actor-based model, thus providing an Actor semantics for μLarvaScript. We are also able to prove certain correctness properties of the denotational translation such as that the denoted Actors behave in a way which corresponds to the behaviour described by our implementation-independent model. We finally present DistPolyLarva, a prototype implementation of the distributed PolyLarva tool, which implements the new actor-based semantics over a language that can natively handle distribution and concurrency called Erlang.

1 Introduction

Runtime Verification (RV) is a dynamic Bauer et al. (2006), Colombo (2008) verification technique which invokes monitoring procedures at runtime so as to verify that the current execution, of the system being verified, is correct with respect to a given specification. It is therefore important that RV tools should be verified for correctness themselves, thus making users more confident in trusting and relying on such tools for verification. As RV tools weave additional monitoring code into the system being verified, an inevitable runtime overhead is imposed upon the system. Moreover, monitoring demands may quickly increase especially when monitoring distributed systems, as these systems are able to scale up rapidly. Such a drastic increase in monitoring load would impose a negative effect on the monitoring efficiency, thus also affecting the performance of the monitored system. For this reason, various ways are being explored by which this overhead can be minimized Colombo et al. (2012), Francalanza and Seychell (2013). Concurrency and parallelisation provide a way of decreasing these overheads by exploiting tightly-coupled, multi-core architectures. When dealing with high monitoring demands, distributed monitoring may also be a more scalable and feasible alternative for increasing monitoring efficiency as distribution also enables the exploitation of loosely-coupled processing units.

PolyLarva Mizzi (2012), Colombo et al. (2012) is a language agnostic RV compiling tool, which when given an RV specification written in polyLS (short for polyLarvaScript), creates the additional monitoring computation for a given system. polyLS language provides an event-driven monitoring framework by which one can identify and specify a number of monitoring requests, that each monitor can handle, in terms of *Events*. For each monitor, one can also specify a set of monitoring checks and handling procedures in terms of *Conditions* and *Actions*. These three components are then associated with one another in the monitor's list of *rules*.

Example 1.1.

BR1 = ReqFunds(Usr,Sum) / !IsUsrValid(Usr) → WarnUsr();
BR2 = ReqFunds(Usr,Sum) / !EnoughFunds(Sum) → WarnUsr();
BR3 = ReqFunds(Usr,Sum) → TransferFunds(Usr,Sum);

Example 1.1 shows a sample pseudo-script defining three rules all of which are related to the same *ReqFunds* event. Whenever the monitor receives an event *e* from the system, it starts by matching it with the event pattern of the first rule in the sequence, i.e., BR1. If *e* is for example of the form ReqFunds("usr1",9000), it would match the rule's pattern ReqFunds(Usr,Sum) and as a result replace every occurrence of variables Usr by "usr1" and Sum by 9000. Subsequently, when *e* matches the event pattern of BR1, the associated condition !IsUsrValid(Usr) would change into !IsUsrValid("usr1") and evaluate to either true or false. If true, the rule's action WarnUsr() would also execute. Note that once an event matches a rule, it is consumed and it cannot match any further monitoring rules. Otherwise if *e* does not match the event pattern of BR1, or does not satisfy the associated condition, rule BR1 would be ignored and the event is matched with the pattern of BR2.

1.1 Problem Definition

There are several problems with the original PolyLarva Mizzi (2012):

1. PolyLarva was developed using a compiler-driven[1] Colombo et al. (2012) approach, hence no formal language

[1] The aim was to develop an actual compiler implementation.

Correspondence to: I. Cassar (ian.cassar.10@um.edu.mt)

© 2014 Xjenza Online

semantics exist for polyLS. This is not ideal as one would require a thorough understanding of how the PolyLarva compiler is implemented, in order to understand the behaviour of the language constructs. This also makes it hard to understand how the PolyLarva compiler interprets and converts the polyLS constructs into monitoring constructs and even harder to improve it.

2. Since no formal model exists for PolyLarva , there also does not exist any type of formal proof which substantiates the validity and the correctness of the PolyLarva compiler. This makes it hard for users to trust that our RV tool would correctly verify their system, as specified in their compiled script.

3. Due to the shared-state, multi-threaded design of the synthesised monitor, PolyLarva does not provide a foundation by which the compiled monitor could be easily scaled up in order to make use of distributed architectures. A distributed design would introduce more areas that can be explored in order to exploit the advantages of distributed architectures so as to be capable of handling higher monitoring demands.

2 The High-level Model

The main focus of this model is that of providing a formal, implementation-independent description of the runtime behaviour of polyLS. In fact, this model formally describes the behaviour of the most essential constructs of PolyLarva 's polyLS. It consists of the μLarvaScript grammar, derived from the original polyLS language, and from a series of *operational semantics* which provide a formal implementation-independent description of the runtime behaviour of the constructs in our grammar.

The μLarvaScript Grammar presented in Table 3.1 is made from *abstract syntax*, meaning, that the language is treated as if it has already been *parsed* and hence assumed to be syntactically correct. It assumes denumerable sets of values $v \in Val$, variables $x \in Var$, and identifiers $i \in Id = Val \cup Var$, within its other constructs. The *state* of a monitor uses variables to store values collected from system events for further analysis. The grammar also assumes the inclusion of predicate functions, which are used in conditions so as to perform checks on the monitor's state. The entire μLarvaScript grammar is defined below.

Table 3.1 - The μLarvaScript Grammar.

$M \in Mons ::= \langle State, RulesList\rangle \mid \langle State, RulesList\rangle \| Mons$
$d \in RulesList ::= Rule;\ RulesList \mid \varepsilon$
$r \in Rule ::= ((q, c) \mapsto a)$
$n \in EventName \supseteq \{mthdInvoked,\ exThrown,\ mthdRet,\ internal\}$
$s \in State : Var^* ::= \{\ x_0\ ,\ x_1\ , \ldots\}$
$e \in Event ::= EventName(v_0 \in Val \ldots v_k \in Val)$
$q \in Query ::= EventName(i_0 \ldots i_k)$
$b \in Boolean ::= true \mid false$
$c \in Condition ::= Boolean \mid !(Condition) \mid$
$\quad Condition\ \&\&\ Condition \mid p(v_0 \in Val, \ldots, v_k \in Val)$
$a \in Actions : (State \rightarrow State) ::= stop \mid fail \mid noOp \mid a_1, a_2 \mid$
$\quad update(State, Function) \mid load(Mons)$

A monitoring system consists of a collection of concurrent monitors, $M_0 \| M_1$, where each individual monitor, $\langle s, d\rangle$, possesses its own current *local state* "s" and its own *rule list* "d". Monitors are able to process sequences of events "t" which are forwarded to the monitor by the system. The state of a monitor, "s", comprises a set of local variables, $\{x_0, ..., x_n\}$, while a rule list, "d" consists of a sequence of *rules*. Each individual rule, of the form $((q, c) \mapsto a)$, binds an event query "q", and a condition "c", with an action "a". Although an event query, "q", has a very similar structure to an event, "e", the latter describes an actual event which originates from the system being monitored.

Conversely, the former is used to describe a *pattern* which states that the host monitor is able to handle system events which match the pattern denoted by the query. A condition "c", can be a boolean formula or a predicate which performs checks on the monitor's current state and on the values passed as its arguments, so as to yield a boolean result. Similarly, an action "a" is a deterministic function which processes a sequence of operations which can possibly modify the monitor's current state. The monitor supports the following actions: (i) stop – halts the execution of the current monitor; (ii) fail – indicates that the monitored system has violated the property; (iii) nop – the monitor applies a rule but does not carry out an action; (iv) update(S,F) – the monitor takes the current monitor state "S" and a custom action function "F" and applies "$F(S)$", such that F is able to take state S as input and return an updated monitor state; (v) load(M) – a monitor is able to dynamically load another monitor M.

The following example script shows the same rules defined in Example 1.1, written in μLarvaScript syntax. As a shorthand, we refer to an action $update(state, Act(args))$ as $Act(args)$.

Example 3.1.

$\langle\{usr1, funds\},$
$((ReqFunds(Usr, Sum), !IsUsrValid(Usr)) \mapsto WarnUsr());$
$((ReqFunds(Usr, Sum), !EnoughFunds(Sum)) \mapsto WarnUsr());$
$((ReqFunds(Usr, Sum), true) \mapsto TransferFunds(Usr, Sum);\rangle$

2.1 Operational Semantics

The operational semantics for polyLS consists of a group of reduction rules. These rules, defined below, are segmented into high level monitoring rules, denoted by the high-level relation ($\longmapsto$), and into the low-level monitoring rules, denoted by the low-level relation ($\rightarrow$) relation. These rules serve to indicate how a collection of monitors would behave when they receive a system event. In fact, they describe how an event is *ignored* when no monitor in the collection is able to handle the event.

μLarvaScript High-Level Monitoring rules

$$\text{rHLMon1}\ \frac{t \rhd M \rightarrow t' \rhd M'}{t \rhd M \longmapsto t' \rhd M'}$$

$$\text{rHLMon2}\ \frac{e; t \rhd M \not\rightarrow}{e; t \rhd M \longmapsto t \rhd M}$$

μLarvaScript Low-Level Monitoring rules

$$\text{rParMon}\ \frac{t \rhd M_0 \rightarrow t' \rhd M_0'}{t \rhd M_0 \parallel M_1 \rightarrow t' \rhd M_0' \parallel M_1}$$

$$\text{rMonEvtHandling}\ \frac{e, s, d \Downarrow s'}{e; t \rhd \langle s, d\rangle \rightarrow t \rhd \langle s', d\rangle}$$

μLarvaScript Event Consumption rules

$$\text{rConsAx}\ \frac{\text{matches(q,e)}=\sigma \qquad s, c\sigma \Downarrow^c \text{true}}{e, s, ((q,c) \mapsto a); d \ \Downarrow\ a\sigma(s)}$$

$$\text{rConsInd1}\ \frac{\text{matches(q,e)}\neq\sigma \qquad e, s, d \ \Downarrow\ s'}{e, s, ((q,c) \mapsto a); d \ \Downarrow\ s'}$$

$$\text{rConsInd2}\ \frac{\text{matches(q,e)}=\sigma \qquad s, c\sigma \Downarrow^c \text{false} \qquad e, s, d \ \Downarrow\ s'}{e, s, ((q,c) \mapsto a); d \ \Downarrow\ s'}$$

μLarvaScript Condition Evaluation

$$\text{rTru}\ \frac{}{s,\text{true}\ \sigma \Downarrow^c \text{true}} \qquad \text{rFls}\ \frac{}{s,\text{false}\ \sigma \Downarrow^c \text{false}}$$

$$\text{rPred1}\ \frac{p(v_0, \ldots, v_n)(s)}{s, p(x_0, \ldots, x_n)\sigma \Downarrow^c \text{true}}$$

$$\text{rPred2}\ \frac{\neg p(v_0, \ldots, v_n)(s)}{s, p(x_0, \ldots, x_n)\sigma \Downarrow^c \text{false}}$$

$$\text{rNot}\ \frac{s, c\sigma \Downarrow^c b}{(s, !\,c\sigma) \Downarrow^c b_1} \quad \text{where } b_1 = \neg b$$

$$\text{rAnd}\ \frac{s, c_1\sigma \Downarrow^c b_1 \qquad s, c_2\sigma \Downarrow^c b_2}{s, c_1\sigma \ \&\&\ c_2\sigma \ \Downarrow^c b_3}$$

$$\text{where } b_3 = b_1 \wedge b_2$$

The high-level monitoring rules ($\longmapsto$) state that a high-level reduction is only possible if $t \ \triangleright M$ is able to reduce into $t' \ \triangleright M'$ through a series of low-level reductions ($\rightarrow$). However, if a low-level reduction is unable to reduce $e; t \ \triangleright M$ into some other form, then it means that event "e" will be *ignored*, thus reducing $e; t \ \triangleright M$ into $t \ \triangleright M$ where "t" is the tail of "$e; t$" and "M" remained unmodified by the reduction.

rParMon is a low-level inductive rule which determines whether $t \ \triangleright M_0 \| M_1$, consisting of a sequence of events "t" and monitor collection "$M_0 \| M_1$", is capable of reducing into $t' \ \triangleright M_0' \| M_1$, where "$t'$ " is a modified stream of events while "$M_0' \| M_1$" represents a modified monitor collection. It states that such a reduction is only allowed if *there exists* some sub-monitor collection "M_0", which when given the same event stream, "t", reduces it into event stream "t' " and "M_0'", i.e., a modified version of collection "M_0". rMonEvtHandling is an axiom which specifies that a monitor, of the form "$\langle s, d \rangle$" which is provided with a sequence of events "$e; t$", changes its state to "s'". It also specifies that this reduction is allowed if the event "e", together with the current monitor's state "s" and rule list "d", are able to evaluate into the next state "s'" by using the *Event Consumption rules*.

The Event Consumption rules ($\Downarrow$) describe how an individual monitor, consisting of state "s" and rule list "d", reacts and behaves in order to handle the received event "e". In fact they indicate that a *successive* state "s'" is derived once the event has been handled by the monitor and removed from the event stream. Hence, the above rules, describe the operational behaviour by which a μLarvaScript monitor consumes a system event. Particularly, these rules define that a modified state "s'" is only produced when the received system event "e" *matches* a query "q" of one of the monitor's rules, which causes condition "c" to evaluate to true, thus invoking an action "a" which modifies state "s" into some "s'". Note that σ is produced when a query q matches [2] an event e so to provide a mapping between the variables in q and the system values received in e. This mapping is then used by conditions and actions which require information about the system. Furthermore, To evaluate a condition "c", the event consumption rules use the *Condition Evaluation* rules ($\Downarrow^c$) to determine whether the event satisfies or violates the associated condition.

[2] (Cassar, 2013) provides the formal definition for $matches(q, e) = \sigma$.

2.2 The Single Receiver Property

One of the most prominent properties observed in PolyLarva was that no matter how many monitors are specified, only a maximum of *one* monitor ends up receiving and handling an event. For this reason we assume that a *sound monitoring specification* is one which coincides with the Single Receiver Property defined by Definition 3.1. This property is quite essential, especially in a distributed context, so to ensure that two or more monitors are never allowed to handle the same event simultaneously, meaning that *at most only one* monitor is allowed to execute an action whenever a specific event occurs. We therefore base our arguments and evaluation proofs upon this important property, meaning that any guarantees offered by our models, only apply for sound specifications.

Definition 3.1. The Single Receiver Property.

$$t \triangleright M_0 \| M_1 \rightarrow t' \triangleright M' \quad \textit{implies}$$
$$t \triangleright M_0 \rightarrow t' \triangleright M_0' \ \textit{ and } \ t \triangleright M_1 \not\rightarrow$$

3 The Distributed-State Model and its Translation

This model aims to provide a formal description of the behaviour of the μLarvaScript constructs in a way which is closely related to an actual, distributed-state implementation. In fact, this distributed-state model consists in a formal translation from μLarvaScript constructs to constructs of a formal Actor model for Erlang (presented in Sections 3.2 and 3.3) adapted from Francalanza and Seychell (2013). In this way, the meaning of the μLarvaScript constructs is given in terms of a highly scalable Haller and Sommers (2012), distributed state model, which produces a monitoring system capable of handling larger monitoring demands with the same or better performance. This claim is supported by Gustafson's Law Gustafson (1988).

3.1 Concurrency, the Actor Model & Erlang

The Actor Model Gul A. et al. (2001) is a highly scalable paradigm Haller and Sommers (2012) which offers a level of abstraction by which both data and procedures can be encapsulated into a single construct.

Actors differ from objects since actors are also concurrent units of execution, each of which executes independently and asynchronously. This fusion of data abstraction and concurrency relieves the developer from having to recur to the explicit concept of a thread in order to make use of concurrency. Moreover, since Actors communicate through Message Passing Gul A. et al. (2001), the developer does not need to develop explicit synchronization mechanisms to prohibit dangerous concurrent access to the data, shared amongst the communicating threads.

Additionally, message passing between these actors is performed asynchronously Gul A. et al. (2001), which means, that an Actor is able to send a message without having to wait for the

receiver's response. Conversely, the receiver does not need to be listening for incoming messages in order to receive them since the messages are deposited in the Actor's mailbox.

In order for an actor to retrieve the received data, it must issue a receive command to recover a message from its mailbox. An important factor is that message passing in the Actor model normally assumes fairness, that is, any message sent by an actor to another existing actor, is *guaranteed* to eventually be deposited inside the target actor's mailbox. In addition to this merger between data, functions and concurrency, an actor is also assigned a unique and persistent identifier, which is essential to identify the target destination actor of the message being sent. A case in point is Erlang Vermeersch (2009), Armstrong (2007), a programming language which natively implements this model.

Although forms of concurrency are employed in the monitors synthesised by PolyLarva , this is done through multi-threading and shared state communication Mizzi (2012) using explicit locking mechanisms. As these concurrent monitors do not use a distributed state[3], they can only be executed concurrently on the same machine. This implies that unlike a distributed multi-processing design, a multi-threaded monitor side cannot exploit the full processing capabilities of loosely coupled distributed architectures, making it less scalable A and P (2010).

3.2 Actor Calculus for Erlang

The following calculus, adapted from Francalanza and Seychell (2013), denotes a formalized abstract syntax for modeling the behaviour of Erlang programs. The calculus was further restricted so as to only describe the core Erlang constructs which are most relevant to our intents and purposes.

Calculus for Actor Systems:

$$
\begin{array}{rcl}
A, B, C \in \textsc{Actr} & ::= & i[e \triangleleft q] \mid A \parallel B \mid (i)A \\
q, r \in \textsc{MBox} & ::= & \epsilon \mid v : q \\
e, d \in \textsc{Exp} & ::= & v \mid \mathsf{self} \mid e!d \mid \mathsf{rcv}\, g\, \mathsf{end} \mid e(d) \mid \mathsf{spw}\, e \mid \\
 & & \quad x = e, d \mid \mathsf{case}\, e\, \mathsf{of}\, g\, \mathsf{end} \mid \ldots \\
v, u \in \textsc{Val} & ::= & x \mid i \mid a \mid \mu y.\lambda x.e \mid \{v, \ldots, v\} \mid l \mid \mathsf{exit} \mid \ldots \\
l, k \in \textsc{Lst} & ::= & \mathsf{nil} \mid v : l \\
p, o \in \textsc{Pat} & ::= & x \mid i \mid a \mid \{p, \ldots, p\} \mid \mathsf{nil} \mid p : x \mid \ldots \\
g, f \in \textsc{PLst} & ::= & \epsilon \mid p \rightarrow e; g \mid p\ \mathsf{when}\ e \rightarrow e; g
\end{array}
$$

Evaluation Contexts

$$
C \ ::= \quad [-] \mid C!e \mid v!C \mid C(e) \mid v(C) \mid x = C, e \mid \ldots
$$

This calculus uses denumerable sets of variables $x, y, z \in$Var, atoms $a, b \in$Atom, and process identifiers $i, j, k \in$Pid amongst other constructs, so as to describe the execution of an Erlang program in terms of a "*system of actors*" Francalanza and Seychell (2013). A system of actors is composed of a collection of actors executing in parallel, $A \| B$, where each individual actor, $i[e \triangleleft q]$, is uniquely identified by its process identifier i.

Moreover, "e" represents an *expression* which the actor will execute concurrently, with respect to its local mailbox "q" Francalanza and Seychell (2013). An actor's mailbox, is denoted as a list of values[4] "$v : q$", where "v" represents the head of the queue while "q" denotes its tail. Additionally, actor expressions Francalanza and Seychell (2013) usually consist of a sequence of expressions "$x = e, d$", which is expected to reduce down to a value. Moreover, expressions may consist of: (*i*) *sending* messages to other actors through "$e\ !\ d$" (where expression e should reduce to a Pid; (*ii*) referencing to the actor's own process identifier by using self; (*iii*) applying functions to other expressions with "$e(d)$"; (*iv*) branching using the case statement; and (*v*) pattern matching when reading a value from the mailbox through the recv g end construct, where "$g \in$PLst" represents a *guarded / protected list*. Additionally, expressions Francalanza and Seychell (2013) may also define evaluation contexts expressed as "C". An expression defined within a context will be the first to execute entirely. Moreover, values may consist of variables, *recursive functions*[5] $\mu y.\lambda.x.e$, tuples $\{v_1, ..., v_n\}$, lists and other constructs.

3.3 Erlang Reduction Semantics for Actor Systems

The operational semantics in figures 1, 2 and 3 Francalanza and Seychell (2013), provide a formal description of the behaviour of the actor calculus. Moreover, the semantics assume that the actor systems are "*well-formed*" Francalanza and Seychell (2013),ie, every actor is identified by a *unique* process identifier.

$$
\textsc{Com}\ \frac{}{j[C[i!v] \triangleleft q] \parallel i[e \triangleleft q] \ \rightarrow\ j[C[v] \triangleleft q] \parallel i[e \triangleleft q{:}v]}
$$

$$
\textsc{Rd1}\ \frac{\mathrm{mtch}(g, v) = e}{i[C[\mathsf{rcv}\, g\, \mathsf{end}] \triangleleft (v : q)] \ \rightarrow\ i[C[e] \triangleleft q]}
$$

$$
\textsc{Rd2}\ \frac{\mathrm{mtch}(g, v) = \bot \qquad i[C[\mathsf{rcv}\, g\, \mathsf{end}] \triangleleft q]^m \ \rightarrow\ i[C[e] \triangleleft r]^m}{i[C[\mathsf{rcv}\, g\, \mathsf{end}] \triangleleft (v : q)]^m \ \rightarrow\ i[C[e] \triangleleft (v : r)]^m}
$$

Figure 1: Reduction Semantics for Actor Systems - Part 1.

The Com rule, in Figure 1 describes a message passing mechanism by which an actor "$j[C[i!v] \triangleleft q]$" can send a message containing a value "v" and append it at the end of the mailbox of another actor. The recipient actor will only retrieve and be notified about the message, residing in its mailbox, when it issues a recv command. In fact, rules Rd1 and Rd2 can then be used retrieve a message from the actor's mailbox. Rd1 states that a value is retrieved from the mailbox if it matches at least one pattern of some protected list $g \in$PLst, associated with the recv command, thus returning the expression associated with the first matching guarded rule, "$p \rightarrow e$" or "p when $\rightarrow e$". Moreover, rule Rd2 is an inductive rule which allows for an actor to perform a selective receive, meaning that an actor is not restricted to only retrieve the topmost message in the queue, but is allowed to keep on searching in its mailbox, or if necessary keep on waiting for new messages, until it finds a message which matches at least one pattern in the guarded list, associated with the receive function.

The Cs1 rule, in Figure 2, states that a value "v" will only be

[3] "Distributed state" means that each monitor has its own local state and communicate through message passing.

[4] The colon ":" in $v : q$, represents the list constructor operator, ie, value v is added to list q.

[5] The "y" in $\mu y.\lambda.x.e$ denotes a self-referencing variable which is required to perform recursive calls for the function "$\lambda.x.e$".

$$\text{Cs1}\ \frac{\text{mtch}(g, v) = e}{i[C[\mathsf{case}\ v\ \mathsf{of}\ g\ \mathsf{end}]]^m \ \rightarrow\ i[C[e]]^m}$$

$$\text{Slf}\ \frac{}{i[C[\mathsf{self}]] \ \rightarrow\ i[C[i]]}$$

$$\text{App}\ \frac{}{i[C[\mu y.\lambda x.e\,(v)]] \ \rightarrow\ i[C[e\{^{\mu y.\lambda x.e}/_{y}\}\{^{v}/_{x}\}]]}$$

$$\text{Spw}\ \frac{}{i[C[\mathsf{spw}\ e] \triangleleft q] \ \rightarrow\ (j)(i[C[j] \triangleleft q] \parallel j[e \triangleleft \epsilon])}$$

Figure 2: Reduction Semantics for Actor Systems - Part 2.

accepted if it matches a pattern in the associated guarded list "g". For example, consider the following code:

$$\mathsf{case}\ \mathit{Bin}\ \mathsf{of}\ 1 \rightarrow \mathit{ok};\ 0 \rightarrow \mathit{ok};\ _ \rightarrow \mathit{nok}\ \mathsf{end}.$$

This code states that if variable "*Bin*" reduces to 1 or to 0, during execution, then it is accepted and the "*ok*" atom is returned. Otherwise, if it reduces to some other form, "*nok*" is returned, since in Erlang, the "_" pattern refers to a *catch-all* pattern which matches anything. Moreover, the Spw rule is used to describe how new concurrent actor instances can be dynamically created, while the Slf rule dictates that the self statement reduces into the calling Actor's Pid. Moreover,App rule states that when some value "v" is passed as an argument of a recursive function "$\mu y.\lambda x.e$", then all occurrences of the self-referencing variable "y" in expression "e", will be replaced by the entire recursive function. Moreover, all occurrences of argument "x", in function "$\lambda x.e$", will be replaced by the passed value "v".

Moreover, the Ass rule, in Figure 3 below, describes that in an expression sequence "$x = e, d$", when the first expression e is reduced into a value "v", the value obtained can be used by the second expression d. It also states that the obtained value "v" will bind to variable "x", meaning that this variable will store the result obtained after reducing the *entire* expression sequence. The remaining rules are quite self explanatory.

$$\text{Ext}\ \frac{}{i[C[x = \mathsf{exit}, e]] \ \rightarrow\ i[C[\mathsf{exit}]]}$$

$$\text{Ass}\ \frac{v \neq \mathsf{exit}}{i[C[x = v, e]] \ \rightarrow\ i[C[e\{^{v}/_{x}\}]]}$$

$$\text{Par}\ \frac{A \ \rightarrow\ A'}{A \parallel B \ \rightarrow\ A' \parallel B}$$

Figure 3: Reduction Semantics for Actor Systems - Part 3.

3.4 Alternative Semantics for μLarvaScript

The denotations in Figure 4.1 convert μLarvaScript constructs into constructs of the formal Actor model for Erlang Francalanza and Seychell (2013), thus giving Actor semantics to μLarvaScript. Also one must distinguish between the constructs which are declared *within* the denotations and those declared without any denotation. The constructs declared in a denotation are μLarvaScript constructs, for example, *abc* in $[\![abc]\!]^m$ refer to a μLarvaScript construct, while if *abc* is not declared in a denotation, then it is a construct of the Erlang model Francalanza and Seychell (2013).

$[\![t \ \triangleright M]\!]^m$ presents the root denotational function which takes an event stream t and a μLarvaScript monitor specification "M". It then invokes another denotational function $[\![t]\!]^m_{es}$, which creates a coordinating Actor that executes in parallel with the monitoring actors returned by fst($[\![M]\!]^m_{par}$). Moreover, in order for the denotation $[\![t]\!]^m_{es}$ to keep on reducing, it requires a list of process identifiers[6] (Pids) returned by snd($[\![M]\!]^m_{par}$).

The translation $[\![t]\!]^m_{es}$ converts an event stream into a *coordinating actor*, when given a list of Pids. This special Actor is required to interface with the monitored system and to make sure that the synthesized monitor is behaving in accordance with the Single Receiver Property. In fact, $[\![t]\!]^m_{es}$ creates an actor with $[\![t]\!]^m_{mb}$ as its mailbox, meaning that the system events will be delivered to the coordinator's mailbox. The coordinator consists of a recursive function which takes a list of Pids and listens for messages in its mailbox via a recv command. Whenever the coordinator receives the message $\{new, Pid\}$, it signifies that one of the concurrent monitors has issued a $[\![load(M)]\!]^m_a$ action, so as to dynamically create a new concurrent monitor. Hence, the coordinator adds the Pid of the new monitor to its Pid-list and issues a recursive call, to restart listening for other messages.

Fig 4.1 The formal translation.

$$[\![t \ \triangleright M]\!]^m \stackrel{\text{def}}{=} [\![t]\!]^m_{es}(\mathsf{snd}(\ [\![M]\!]^m_{par}\ )) \parallel \mathsf{fst}(\ [\![M]\!]^m_{par}\ )$$

$$\begin{aligned}
[\![t]\!]^m_{es}(\text{PidList}) \stackrel{\text{def}}{=}\ & \mathit{coord}\ [(\mu\, y_{rec}\ \cdot\ \lambda\, X_{lst} \cdot (\\
& \quad \text{recv } \{\text{evt,E}\}: \rightarrow \\
& \qquad \text{bcast}(\{\ \text{E,self()}\ \},\text{X}_{lst}), \\
& \qquad \text{case await(len(X}_{lst}\text{)-1) of} \\
& \qquad\quad 0 \rightarrow y_{rec}(\text{X}_{lst}); \\
& \qquad\quad 1 \rightarrow y_{rec}(\text{X}_{lst}); \\
& \qquad\quad _ \rightarrow \text{error} \\
& \qquad \text{end} \\
& \quad \{\text{new,Pid}\} \rightarrow \\
& \qquad y_{rec}(\text{X}_{lst}\text{:Pid}); \\
& \quad \text{end.)(PidList)} \quad \triangleleft \quad [\![t]\!]^m_{mb}\ ]
\end{aligned}$$

$$[\![M_0 \| M_1]\!]^m_{par} \stackrel{\text{def}}{=} \{\mathsf{fst}(\ [\![M_0]\!]^m_{par}\ ) \parallel \mathsf{fst}(\ [\![M_1]\!]^m_{par}\ )\ ,\ \mathsf{snd}(\ [\![M_0]\!]^m_{par}\ ) : \mathsf{snd}(\ [\![M_1]\!]^m_{par}\ )\}$$

$$[\![\langle s, d\rangle]\!]^m_{par} \stackrel{\text{def}}{=} \{i[(\mu y_{rec} \cdot \lambda X_{state} \cdot X_{new} = \mathsf{recv}([\![d]\!]^m_d\ (X_{state}))\mathsf{end}, y_{rec}(X_{new}).)([\![s]\!]^m_s))) \triangleleft \varepsilon]\ ,\ i\}$$

$$[\![\varepsilon]\!]^m_d \stackrel{\text{def}}{=} \lambda X_{state}\ \cdot\ \{\ \mathsf{Coord}\ ,__\ \} \rightarrow\ \mathsf{Coord}\ !\ \mathsf{nok}, (X_{state});$$

$$[\![r_1\ ;\ d_1]\!]^m_d \stackrel{\text{def}}{=} \lambda X_{state} \cdot [\![r_1]\!]^m_r(X_{state})\ ;\ [\![d_1]\!]^m_d(X_{state})$$

$$\begin{aligned}
[\![((q, c) \mapsto a)]\!]^m_r \stackrel{\text{def}}{=}\ & \lambda X_{state}\ \cdot\ \{\ \mathsf{Coord}, [\![q]\!]^m_q\ \}\ \mathsf{when} \\
& ([\![c]\!]^m_c(X_{state})) \mapsto (\ \mathsf{Coord}\ !\ \mathsf{ok}, [\![a]\!]^m_a(X_{state}))
\end{aligned}$$

$$[\![\{x_0, x_1, \ldots, x_k\}]\!]^m_s \stackrel{\text{def}}{=} [\![x_0]\!]^m_i : [\![x_1]\!]^m_i : \ldots : [\![x_k]\!]^m_i$$

$$[\![\emptyset]\!]^m_s \stackrel{\text{def}}{=} \varepsilon$$

$$[\![n(v_0, \ldots, v_k)]\!]^m_e \stackrel{\text{def}}{=} \{'n'\ ,\ \{[\![v_0]\!]^m_i : [\![v_1]\!]^m_i : \ldots : [\![v_k]\!]^m_i\}\}$$

$$[\![n(i_0, \ldots, i_k)]\!]^m_q \stackrel{\text{def}}{=} \{'n',\ \{[\![i_0]\!]^m_i : [\![i_1]\!]^m_i : \ldots : [\![i_k]\!]^m_i\}\}$$

[6] A Pid uniquely identifies an Actor.

$$[\![true]\!]^m_c \stackrel{\text{def}}{=} \lambda X_{state} \cdot \text{true}$$

$$[\![!\,(C)]\!]^m_c \stackrel{\text{def}}{=} \lambda X_{state} \cdot \text{not } [\![C]\!]^m_c$$

$$[\![C_1 \&\& C_2]\!]^m_c \stackrel{\text{def}}{=} \lambda X_{state} \cdot [\![C_1]\!]^m_c \text{ and } [\![C_2]\!]^m_c$$

$$[\![p(v_0,\ldots,v_k)]\!]^m_c \stackrel{\text{def}}{=} \lambda X_{state} \cdot \lambda v_0,\ldots,v_k \cdot P(\{v_0,\ldots,v_k\}, X_{state})$$

$$[\![stop]\!]^m_a \stackrel{\text{def}}{=} \lambda X_{state} \cdot \text{exit.}$$

$$[\![fail]\!]^m_a \stackrel{\text{def}}{=} \lambda X_{state} \cdot \text{Coord ! error.}$$

$$[\![noOp]\!]^m_a \stackrel{\text{def}}{=} \lambda X_{state} \cdot X_{state}$$

$$[\![update(S,F)]\!]^m_a \stackrel{\text{def}}{=} \lambda F \cdot \lambda S \cdot F(S)$$

$$[\![load(M)]\!]^m_a \stackrel{\text{def}}{=} \lambda X_{state} \cdot (\text{Coord ! } \{new, \text{ spw(fst(} [\![M]\!]^m_{par} \text{)) } \}\ ), X_{state}$$

$$[\![a_0, a_1]\!]^m_a \stackrel{\text{def}}{=} \lambda X_{state} \cdot [\![a_1]\!]^m_a([\![a_0]\!]^m_a(X_{state}))$$

Conversely, when the coordinator reads a system event message, $\{evt, E\}$, it broadcasts the message[7] $e_{msg} \equiv \{\text{self}, E\}$ to all monitors executing concurrently, by using the "*bcast*" function. The coordinator then awaits feedback from the monitors by calling "*await*(*count*)", where "*count*" is initially set to be the length of the coordinator's Pid-list. Moreover, the "*await*" function makes use of a selective receive so as to only retrieve feedback messages, of the form "*ok*" or "*nok*", from all the monitors in its Pid-list. This makes sure that only a maximum of *one* monitor has indeed handled the broadcasted event. In fact it issues an error if more than one monitor handles the event, thus signifying that the Single Receiver Property has been violated by the translated monitoring specification.

$[\![-]\!]^m_{par}$ is a function that converts a μLarvaScript monitor into a meta-level tuple containing a list of monitoring actors together with another list with their Pids. The meta-functions fst and snd are then invoked at compile-time so as to extract the two separate lists from the denoted meta-tuple. Each actor denoted by $[\![\langle s, d\rangle]\!]^m_{par}$ is *always* associated with a unique Pid, "*i*", and is initialized with an empty mailbox "ε" so as to wait for event messages of the form {CoordPid, e}, by issuing a "recv" command so as to listen for messages from the coordinator. This command is followed by $[\![d]\!]^m_d$ which converts a μLarvaScript rule list into an Erlang list of guarded rules. An empty μLarvaScript rule list, is converted by $[\![\varepsilon]\!]^m_d$ into a guarded rule which matches *any* broadcasted event message. This is required since when a message matches its pattern, the monitor sends a rejection feedback to the coordinator by using "*Coord*! *nok*" and leaves the monitor's current state unmodified.

Each μLarvaScript rule, in a non-empty rule list, is translated through $[\![((q,c) \mapsto a)]\!]^m_r$ into an Erlang guarded command. Whenever the guarded rule's tuple query, of the form {Coord,$[\![q]\!]^m_q$}, pattern matches the structure of the received event such that condition $[\![c]\!]^m_c$ returns *true*, the rule sends an "*ok*" feedback message to the coordinator, signifying that the event was handled. It then executes the function denoted by $[\![a]\!]^m_a$ on the monitor's current state, thus generating the next state.

The denotation $[\![-]\!]^m_s$, for the monitor's state, dictates that the monitor's state variables are converted into a list of Erlang variables. The translation $[\![-]\!]^m_e$, states that a μLarvaScript event is translated into an Erlang tuple containing the event name and a *tuple of values* created by the system, while the query denotation, $[\![-]\!]^m_q$, returns an Erlang tuple containing the event name and a *tuple of identifiers*, where each identifier can be either a value or a variable. The condition denotation $[\![-]\!]^m_c$, converts μLarvaScript conditions into Erlang functions which return a boolean value after performing a check on the monitor state passed as its argument. The action denotation $[\![-]\!]^m_a$, translates μLarvaScript actions into Erlang functions which take the monitor's current state and return an updated state accordingly.

[7] Where self refers to the coordinator's Pid and E is the actual system event received.

Example 6.1. This example outlines how a monitor containing only the first rule used in Example 3.1, can be formally translated into Erlang code by applying the denotational functions provided.

$$[\![\langle\{usr1, funds\}, ((ReqFunds(Usr, Sum),\ !IsUsrValid(Usr)) \mapsto WarnUsr()); \rangle]\!]^m$$

$\stackrel{def}{=}$ { ***By applying the root denotation*** $[\![-]\!]^m$}

$$[\![t]\!]^m_{es}(\textsf{snd}(\ [\![\langle\{usr1, funds\}, ((ReqFunds(Usr, Sum),\ !IsUsrValid(Usr)) \mapsto WarnUsr()); \rangle]\!]^m_{par}\ )) \ \|\ \textsf{fst}(\ [\![\langle\{usr1, funds\}, ((ReqFunds(Usr, Sum),\ !IsUsrValid(Usr)) \mapsto WarnUsr()); \rangle]\!]^m_{par}\ )$$

$\stackrel{def}{=}$ { ***Applying*** $[\![-]\!]^m_{par}$ ***, and extracting pidList "[i]" with the*** **snd** ***meta function and the actor expression with*** **fst**. }

$$[\![t]\!]^m_{es}([i]) \ \|\ i[(\mu y_{rec} \cdot \lambda X_{state} \cdot X_{new} = \textsf{recv}(\ [\![((ReqFunds(Usr, Sum), !IsUsrValid(Usr)) \mapsto WarnUsr())]\!]^m_d\ (X_{state}))\textsf{end}, y_{rec}(X_{new}).)([\![\{usr1, funds\}]\!]^m_s))) \triangleleft \varepsilon] \quad \bullet\bullet\bullet$$

$\stackrel{def}{=}$ { ***After applying the necessary denotations*** }

$$[\![t]\!]^m_{es}([i]) \ \|\ i[(\mu y_{rec} \cdot \lambda X_{state} \cdot X_{new} = \textsf{recv}(\lambda X_{state} \cdot \{\textsf{Coord}, \{\text{'ReqFunds'}, Usr, Sum\}\}\ \textsf{when}\ (!IsUsrValid(Usr))\ (X_{state}) \mapsto (Coord!\,ok, (WarnUsr()(X_{state}))); \{\ \textsf{Coord}\ , __\ \} \rightarrow\ \textsf{Coord}\ !\ nok, (X_{state}))\textsf{end}) \triangleleft \varepsilon]$$

$\stackrel{def}{=}$ { ***Applying*** $[\![t]\!]^m_{es}$ ***to create the coordinator***}

$$\begin{aligned}
&\textsf{coord}[(\mu y_{rec} \cdot \lambda X_{lst} \cdot (\textsf{recv}\ \{evt, E\} \\
&\qquad \rightarrow bcast(\{E, self()\}, X_{lst}), \\
&\textsf{case}\ \textsf{await}(len(X_{lst}) - 1)\ \textsf{of}\ 0 \rightarrow y_{rec}(X_{lst}); \\
&\qquad 1 \rightarrow y_{rec}(X_{lst});\ _ \rightarrow \textsf{error end;} \\
&\{new, Pid\} \rightarrow y_{rec}(X_{lst} : Pid)\textsf{end.})([i]) \ \triangleleft\ [\![t]\!]^m_{mb}] \\
&\ \|\quad i[(\mu y_{rec} \cdot \lambda X_{state} \cdot X_{new} = \textsf{recv}(\lambda X_{state} \cdot \\
&\{\textsf{Coord}, \{\text{'ReqFunds'}, Usr, Sum\}\}\ \textsf{when}\ (!IsUsrValid(Usr)) \\
&\quad (X_{state}) \mapsto (Coord!\,ok, (WarnUsr()(X_{state}))); \\
&\{\ \textsf{Coord}\ , __\ \} \rightarrow\ \textsf{Coord}\ !\ nok, (X_{state}))\textsf{end}) \triangleleft \varepsilon]
\end{aligned}$$

4 The DistPolyLarva Prototype

DistPolyLarva ((Cassar, 2013)) is prototype implementation based on our new actor-based design. This prototype seeks to re-implement PolyLarva 's *monitor compiler* in a way which conforms to the denotational translations provided in our distributed-state model. This ensures that any guarantees offered by the formal models would also apply for our prototype compiler.

Also, DistPolyLarva parses a variant of polyLS, called Pseudo-polyLS, into a parse tree which, resembles the μLarvaScript abstract syntax, together with additional parsed constructs. Although our prototype compiler is able to recognize all polyLS keywords and synthesise additional monitoring features, which are not formalized in our models, it only guarantees correct behaviour for specifications which only use constructs from the formalized subset which forms μLarvaScript. The parsed constructs are then converted into Erlang actor expressions in a similar way as in our formal translation. Furthermore, this prototype was developed with the aim to demonstrate that our translation is implementable.

4.1 The Compilation Phases

DistPolyLarva passes a given Pseudo-polyLS specification from four subsequent stages so as to synthesise the required monitoring Erlang code.

Lexical and Parsing Phases: The Lexical phase uses a *regular grammar* which defines a number of patterns that a character sequence, in the given Pseudo-polyLS script, must match in order to be translated into an abstract token. The generated token sequence is passed to the Parsing phase which checks that the structure of the script being compiled, is correct with respect to the production rules defined by the *context free grammar* of our language defined in Table 3.1. If the entire token sequence obeys the rules of the grammar, it is converted into an unambiguous *parse tree* which conforms to the abstract syntax of μLarvaScript. DistPolyLarva's lexer was implemented using a lexer generator called LEEX while its parser was implemented using a parser generator called YECC Ericsson AB (2013).

Semantic Analysis and Code Generation Phase: This phase is essentially an Erlang implementation of our formal denotations in Figure 4.1. It starts by invoking the initial denotational function which inspects the initial node of the parse tree and invokes other denotational functions which inspect the semantics of its child nodes, from left to right. The compiler also checks that any event, condition and action referred by the rules of a specific monitor, is actually declared within the same monitor, so as to preserve scoping. The generated Erlang source modules (.erl) are then written in a directory specified by the user and are compiled into executable Beam files via the Erlang compiler.

5 Evaluation

The high level and distributed-state models were evaluated by proving certain theorems about the runtime behaviour they describe. The guarantees obtained from proving these theorems are also inherited by DistPolyLarva, as this was developed with a close relation to the formal denotational translation. Moreover, the prototype was further evaluated through a series of tests.

5.1 Evaluating the High-level Model

In order to evaluate the behaviour described by this model we proved a theorem which guarantees that any monitoring system, specified in μLarvaScript, will operate deterministically. This property is important since it ensures that whenever any collection of μLarvaScript monitors is in a particular collective state[8], and it receives a specific system event, it will *always* handle the event in the *same* manner, thus transitioning to the same successive collective state. This means that no matter how many times the monitoring system is executed, depending on the current state, it will always handle a specific event in the *same* way, and so transition to *same* consecutive state. Hence, this guarantees that a monitoring system will operate consistently.

Theorem 6.1. μLarvaScript Determinism.
$t \rhd M \longmapsto t' \rhd M' \wedge t \rhd M \longmapsto t'' \rhd M''$ *implies* $t' = t'' \wedge M' \equiv M''$

Specifically, Theorem 6.1 states Cassar (2013) that if M reduces to both $t \rhd M'$ and $t \rhd M''$, by a using *high-level* reduction ($\longmapsto$), then it implies that $t \rhd M'$ and $t \rhd M''$ are *equal* to each other. The proof of this theorem was divided into separate lemmas, each of which were proved accordingly by using various inductive techniques.

5.2 Evaluating the Formal Translation

The evaluation of our denotational semantics consisted in proving Theorem 6.2, which shows that our formal translation is in some sense correct. We showed that the behaviour of *any* actor-based monitoring system, derived using our denotational conversion, *corresponds* to the behaviour described by the high-level model. These proofs not only help to increase the user's confidence but also state that any property proved on our high-level model, such as determinism in Theorem 6.1, would also transitively apply to our synthesised monitoring system. In our proofs we assume that all μLarvaScript specifications observe the Single Receiver Property. This implies that the denotational translation is only guaranteed to provide a correctly-behaving actor implementation when the specification script being translated observes the Single Receiver Property.

Theorem 6.2. Behaviour Correspondence.
Let M be a sound μLarvaScript specification and assume $t \rhd M$ *behaves as* $[\![t \rhd M]\!]^m$ ·

if $t \rhd M \longmapsto {}^*t' \rhd M'$ *and* $[\![t \rhd M]\!]^m \rightarrow^* [\![t' \rhd M']\!]^m$
then $t' \rhd M'$ behaves as $[\![t \rhd M']\!]^m$

Theorem 6.2 was further subdivided and proven using the following correspondence lemmas.

Lemma 6.1. Single-Step Correspondence.
$t \rhd M \longmapsto t' \rhd M'$ *implies* $[\![t \rhd M]\!]^m \rightarrow^* [\![t' \rhd M']\!]^m$

Lemma 6.2. Multi-Step Correspondence.
$t \rhd M \longmapsto {}^*t' \rhd M'$ *implies* $[\![t \rhd M]\!]^m \rightarrow^* [\![t' \rhd M']\!]^m$

Lemma 6.1 guarantees that for *one* high-level reduction, i.e., $t \rhd M \longmapsto t' \rhd M'$, there exists a corresponding translation, $[\![t \rhd M]\!]^m$, which reduces in 0 or more Erlang reduction steps into $[\![t' \rhd M']\!]^m$. The proof for Lemma 6.2 relies on Lemma 6.1 so as to guarantee that for *0 or more* high level reductions, we can find a denotational translation which reduces $[\![t \rhd M]\!]^m$ in 0 or more Erlang steps into $[\![t' \rhd M']\!]^m$.

6 Future Work

As part of our future work we propose to extend our μLarvaScript grammar so as to formalize other polyLS constructs

[8] By "collective state" we refer to the local states of all monitors in the specified monitor collection.

such as timers. This extension requires modifications to our formal models, as well as, additional formal results. The new results would guarantee that the extended high-level model still operates deterministically and that its behaviour still corresponds to the behaviour of an extended version of our distributed-state model. The additional features in our DistPolyLarva compiler could then be properly implemented in a way which guarantees correct operation.

Moreover, as we were more concerned with the mathematical aspect of our designs and since our prototype implementation was only intended to demonstrate our actor-based concept, the DistPolyLarva compiler was rapidly developed. Hence we propose to provide a more thorough implementation based on our prototype and on our formal models. In fact we propose that the code of the prototype should be properly structured so as to be more maintainable in the future. Moreover, the synthesised monitoring code can be further optimized so as to reduce the tool's monitoring overhead as much as possible. Additionally, the finalized compiler should also provide better error reporting and error recovery mechanisms which would further aid users to debug their Pseudo-polyLS specification scripts. We also suggest that the proper implementation should also be tested for efficiency and compared with the original PolyLarva implementation.

7 Conclusion

We have sought to increase the understandability and reliability of PolyLarva with the aim of elevating the user's level of confidence in our RV tool. This was done by providing a high-level operational model which describes the runtime behaviour of the core constructs of polyLS. The evaluation for this model consisted in proving that the model describes a deterministic monitoring behaviour. We also created denotational semantics which convert μLarvaScript specifications into Erlang actor expressions. The evaluation of this model consisted in proving the correctness of the formal translation, which permits that any property proved for the high-level model would also apply for the denoted monitoring Actors. This also helps in increasing the user's level of confidence in our tool. This formal translation was then implemented as the DistPolyLarva prototype compiler which guarantees a correct translation for Pseudo-polyLS specifications which only include constructs that are formalized in μLarvaScript.

References

A, M. K. and P, K. (2010). Distributed computing approaches for scalability and high performance.

Armstrong, J. (2007). *Programming Erlang: Software for a Concurrent World*. Pragmatic Bookshelf.

Bauer, A., Leucker, M. and Schallhart, C. (2006). *Runtime Verification for LTL and TLTL.*

Cassar, I. (2013). *Monitoring Distributed Systems with Distributed PolyLarva.* University of Malta.

Colombo, C. (2008). *Practical Runtime Monitoring with Impact Guarantees of Java Programs with Real-Time Constraints* (Master's thesis, University of Malta).

Colombo, C., Francalanza, A., Mizzi, R. and Pace, G. J. (2012). polyLarva: Runtime Verification with Configurable Resource-Aware Monitoring Boundaries. In *Softw. eng. form. methods - 10th int. conf. sefm 2012* (Vol. 7504, pp. 218–232). Lecture Notes in Computer Science. Springer.

Ericsson AB. (2013). Parse Tools Reference Manual.

Francalanza, A. and Seychell, A. (2013). *Synthesising Correct Concurrent Runtime Monitors in Erlang* (tech. rep. No. CS2013-01). University of Malta.

Gul A., A., Prasannaa, T. and Reza, Z. (2001). *Actors: A Model for Reasoning about Open Distributed Systems*. University of Illinois at Urbana USA.

Gustafson, J. L. (1988). Reevaluating Amdahl's Law. *Commun. ACM*. 31, 532–533.

Haller, P. and Sommers, F. (2012). *Actors in Scala*. USA: Artima Incorporation.

Mizzi, R. (2012). *An Extensible and Configurable Runtime Verification Framework.* (Master's thesis, University of Malta).

Vermeersch, R. (2009, January). Concurrency in Erlang and Scala.

Xjenza Online - Journal of The Malta Chamber of Scientists
www.xjenza.org
DOI: 10.7423/XJENZA.2014.2.06

Research Article

Warpage issues in large area mould embedding technologies

Russell Farrugia[1], Ivan Grech[1], Owen Casha[1], Joseph Micallef[1], Edward Gatt[1], Roseanne Duca[2] and Conrad Cachia[2]
[1]Department of Microelectronics and Nanoelectronics, Malta
[2]ST Microelectronics Malta

Abstract. The need for higher communications speed, heterogeneous integration and further miniaturisation have increased demand in developing new 3D integrated packaging technologies which include wafer-level moulding and chip-to-wafer interconnections. Wafer-level moulding refers to the embedding of multiple chips or heterogeneous systems on the wafer scale. This can be achieved through a relatively new technology consisting of thermal compression moulding of granular or liquid epoxy moulding compounds. Experimental measurements from compression moulding on 8" blank wafers have shown an unexpected tendency to warp into a cylindrical-shape following cooling from the moulding temperature to room temperature. Wafer warpage occurs primarily as a result of a mismatch between the coefficient of thermal expansion of the resin compound and the Si wafer. This paper will delve into possible causes of such asymmetric warpage related to mould, dimensional and material characteristics using finite element (FE) software (ANSYS Mechanical). The FE model of the resin on wafer deposition will be validated against the measurement results and will be used to deduce appropriate guidelines for low warpage wafer encapsulation.

Keywords component – 3D packaging – wafe-level moulding – warpage – epoxy moulding compound

1 Introduction

The demands of high functional electronic devices are indicating a trend towards further miniaturisation and increased performance. In the case of devices for consumer electronic applications, 80 % of the components are passives (do not need electrical power to operate) which constitute 70 % of the product assembly cost in today's mobile phones (Souriau et al., 2005). This has driven the packaging industry to develop advanced 3D packaging solutions in order to achieve trade-offs with dimensional requirements, performance maximization, manufacturability, flexibility and cost. A number of technologies (ex: Embedded Wafer Level Ball Grid Array (eWLB) by Infineon (Meyer et al., 2008) and the Chip in Polymer (CiP) by Fraunhofer IZM, TU Berlin and Wuerth (Boettcher et al., 2008)) have been developed on the basis of the two major packaging trends identified as having low cost potential: large area mould embedding of laterally placed dies and 3D integration of vertically stacked dies. Both concepts may also be combined into a stacked wafer-level System-in-Package coupled with the integration of through mould vias (TMVs) to create the smallest form factor package (Takahashi et al., 2012). Other variations to this process have been reported, for instance the assembly of vertical interconnect elements (VIE) instead of laser drilled via interconnections (Braun et al., 2011). However the back-end processes of these technologies commonly involve wafer-level die embedding using several applicable packaging techniques falling under two categories: moulding and liquid encapsulation such as printing. Moulding techniques which include transfer, film lamination and compression have the advantage of precise dimensional control, however they are expensive. Thermosetting polymers, specifically epoxy moulding compounds (EMCs) are the most widely used moulding materials and their reliability is of crucial importance towards system functionality (Sadeghinia et al., 2012).

One important requirement of any embedding technology is the ability to produce a moulded wafer on which subsequent wafer-level processes can be carried out with ease (Kumar et al., 2009). Consequently warpage resulting from the process-induced residual stresses is of great concern in thin-film packaging (below 1 mm). Room temperature warpage of compression moulded EMC on blank Si wafers has been reported to be significant by Tomita et al. (2012), Takahashi et al. (2012) and Kumar et al. (2009). In this paper the warpage issues concerning wafer-level thermal compression moulding will be discussed whereby a finite element technique used to simulate the cooling of the moulded wafer from the moulding temperature to room temperature will be presented.

Correspondence to: Russell Farrugia (russell.farrugia@um.edu.mt)

© 2014 Xjenza Online

2 Problem overview

Like in any polymer, EMC consists of an amorphous molecular structure which may exist either in a solid/glassy state or a liquid/rubbery state with the glass temperature, T_G defining the transformation between the two states. Moreover the thermosetting properties of EMC signify that molecular structures readily crosslink when heated above T_G through an exothermic reaction known as the curing process with the aid of a catalyst. In order to reduce processing time (the time required for the epoxy to reach the fully cured state and hence maximize its material properties), external heat is supplied during compression moulding to raise the temperature of the moulding compound.

2.1 Compression Moulding

The basic process flow in compression moulding for packaging applications, schematically displayed in Figure 1 can be described as follows (Matsutani, 2009):

1. wafer substrate is supplied face down to the top mould die;
2. a precise amount of the required EMC is prepared before it is inserted into the bottom mould die chase;
3. the substrate is clamped as the mould begins to close while vacuum is applied to remove gases and moisture emitted by the compound;
4. after the mould is completely closed, it is heated to the moulding temperature T_m and kept constant for a specific amount of time to initiate curing of the compound;
5. after curing at T_m is completed the mould is opened to release the moulded substrate allowing it to be cooled in air to room temperature.

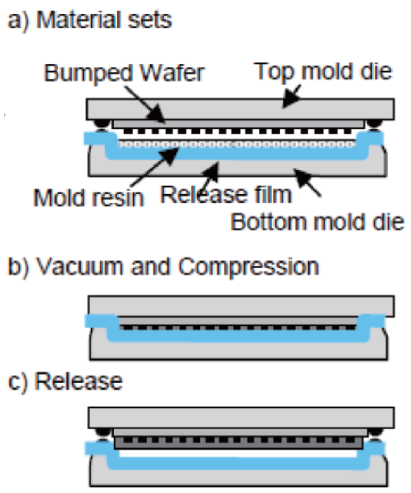

Figure 1: Compression moulding process flow showing (a) the material preparation stage, (b) vacuum, compression and heating stage and (c) final release stage (Tomita et al., 2012).

Compression moulding essentially results in the bonding of two materials having dissimilar thermo-mechanical properties. From the moment that curing is initiated during the mould heating stage, the compound's resistance to deformation starts to increase. Given that the coefficient of thermal expansion of EMC, CTE_{EMC} differs from that of silicon, CTE_{Si}, internal stresses are developed in the moulded wafer during the curing and cooling stages resulting in room temperature warpage. A closed-form mathematical solution of the radius of curvature of the deformation of a bi-material beam under a temperature variation, ΔT, was derived by Timoshenko (Timoshenko, 1925), where the deformation is directly proportional to the beam length, $CTE_{EMC} - CTE_{Si}$, ΔT and inversely proportional to the total moulded wafer thickness. It is additionally dependent on the bending properties and therefore on the characteristic length and Young's modulus.

2.2 Observation of Warpage

Warpage analysis of the moulded Si disc-shaped wafer using analytical calculations is not straight forward. One of the reasons is that the volume change is not constant during the moulding cycle as shown in Figure 2. During the heating stage from room temperature to T_m the compound is largely in the liquid state (above T_G) thus having a linear but relatively high thermal expansion. At the curing stage, the formation of crosslinks results in an isothermal volumetric shrinkage, ϵ_s . During the cooling stage, the thermal shrinkage of the fully cured material is significantly lower than the thermal expansion during heating. However in the case that T_m is higher than T_G, CTE_{EMC} will vary with temperature. A substantial reduction in CTE_{EMC} takes place due to the glassy state transition occurring as the viscoelastic material approaches T_G (see 3).

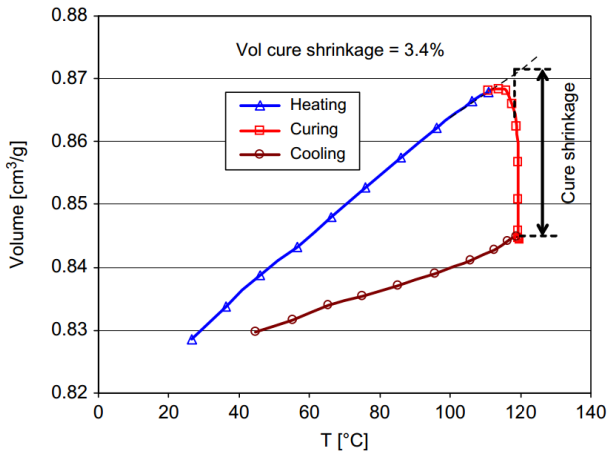

Figure 2: Volume changes during heating (5 °C/min; cooling and shrinkage during isothermal cure of EMC (T_G=120 °C) (Sadeghinia et al., 2012).

The problem of warpage in wafer-level embedding has been recently investigated both experimentally and numerically. Test samples from the back-end process for the stacked TSV- Wafer-level Chip Scale Package (WCSP) platform were presented by Texas Instruments Inc. (Takahashi et al., 2012). Warpage measurements of 8" moulded wafers without stacked chips were found to be as high as 6 mm (EMC thickness: 200 µm, Si thickness: 100 µm). Moreover for all moulded wafers with and without the stacked chips a convex cylindrical-shape deformation

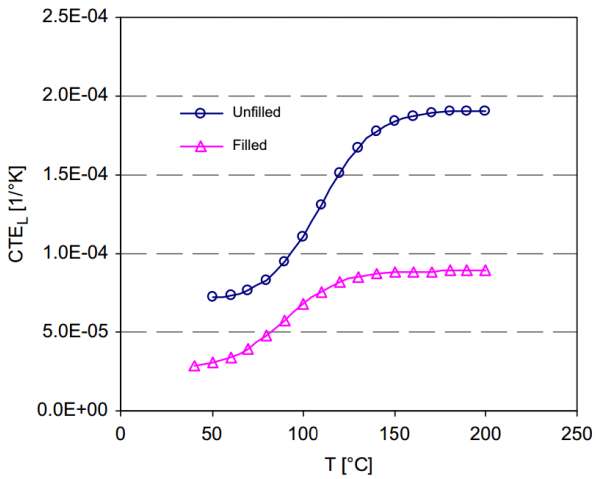

Figure 3: Linear CTE of unfilled and filled EMC vs. temperature ($T_G = 120\,°C$) (Sadeghinia et al., 2012).

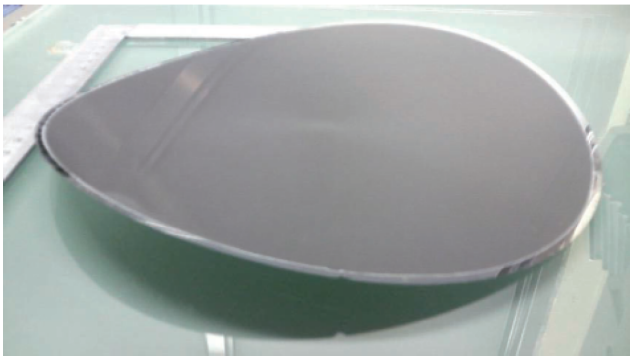

Figure 4: Blank moulded wafer warpage: Si - 100 µm, EMC - 200 µm (Takahashi et al., 2012).

shown in Figure 4 was consistently observed. Warpage was found to increase with an increase in T_G and elastic modulus and a decrease in CTE_{EMC}. Furthermore the effect of post-mould grinding resulted in a deformation increase in accordance with the Timoshenko's analytical formulation.

Similarly Tomita et al. (2012) carried out wafer-level compression moulding whereby the mould thickness uniformity was analysed. This was carried out by measuring the mould deposition thickness at specific radial locations. It was found that a one-directional mould thickness gradient was consistently observed suggesting potential effects due to mould die design and calibration. Other warpage measurements on wafer-level moulding were also carried out by Kumar (Kumar et al., 2009) using infrared interferometry where a warped shape similar to that of Takahashi et al. (2012) was observed. It was also suggested that the thermo-mechanical stresses can be reduced either by adding a low filler content in order to reduce the Young's modulus of the epoxy moulding compound and thus reduce its resistance to deformation or by adding a high filler content to reduce CTE_{EMC} and hence the thermal expansion mismatch within the moulded wafer.

With regards to numerical modelling although the effect of the viscoelastic properties of EMC has been simulated at die level [18], little has been published on the finite element analysis of wafer-level compression moulding. The difficulties in replicating the room temperature deformed shape of the moulded wafer were discussed by Mallik and Stout (2010), Mallik et al. (2014). Due to the fact that the cylindrical-shape is not the only and most likely numerically stable solution, a number of simulation tricks using the ANSYS Mechanical solver were proposed in order to produce a steady and stable cylindrical-shape instead of a bowl-shaped deformation (Mallik and Stout, 2010). Mallik et al. (2014) showed that a good comparison was achieved between the results from FE simulations and measurements for an Al-coated Si wafer.

3 Finite element modelling of Moulded Wafer

Finite element analysis was carried out using the ANSYS mechanical solver within ANSYS Workbench v14 in order to validate measurement results on compression moulded wafers (similar to that depicted in Figure 4) carried out by ST Microelectronics Malta, to test possible causes leading to room temperature warpage and finally to propose improvements which may lead to a reduction in warpage to acceptable production limits.

A static structural simulation was carried out on a model of an 8" (0.2032 m) diameter disc consisting of stacked layers of the epoxy moulding compound and Si. With reference to Figure 4, the EMC layer in the FE model covers the entire wafer while the notch marking the wafer's crystal orientation was assumed to have a negligible effect on the moulded wafer warpage. Both surface and solid modelling approaches were investigated using different element types. In the case of the former a layered shell element (SHELL181) (n.d.) was utilised which enables a layered section to be prescribed to a 2D surface mesh. SHELL181 is typically used for modelling composite shells or sandwich construction and its accuracy is governed by the first-order shear deformation theory (n.d.). Therefore for the layered section function available with ANSYS Mechanical v14, the thicknesses and material type of the respective layers may be inputted in tabular format. The second approach consists of modelling a solid disc using SOLID185 elements whereby the thickness of the EMC and Si layers is prescribed via extrusion.

The following is a description of the properties of the moulding compound and Si wafer prescribed to the previously mentioned models. In the case of EMC the elastic modulus is considered to be isotropic and varies linearly from room temperature to T_m, the rubbery state linear coefficient of thermal expansion ($CTE_{EMC,2}$) is constant above T_G and the glassy state linear coefficient of thermal expansion ($CTE_{EMC,1}$) is constant below T_G. Silicon has anisotropic properties however in the case where thin plates have symmetric boundary conditions, the elastic deformation of such structures can be evaluated using the symmetric biaxial modulus. Therefore the Si properties

for the FE model consist of an isotropic elastic modulus based on the thin film biaxial modulus for a (100) Si wafer: 180 GPa (Hopcroft et al., 2010); together with a constant linear coefficient of thermal expansion. From the experiments, negligible warpage was observed as the moulded wafer is released from the mould die and hence T_m was set as the stress free temperature for both EMC and Si.

The mesh construction is of crucial importance in FE modelling in order to ensure that solution convergence is achieved. A mapped mesh with quadrilateral shaped elements was created for the two previously mentioned modelling approaches. This was carried out by dividing the geometry into 4-edged surfaces/solid bodies to produce an O-mesh displayed in Figure 5. The grid refinement could thus be varied by specifying the number of elements on the body edges. A mesh independence study was also carried out to ensure that the solution does not change with further mesh refinement. For this study only the element dimensions in the x and y-directions were altered, while the element dimension in the z-direction was kept equal to the respective layer thickness.

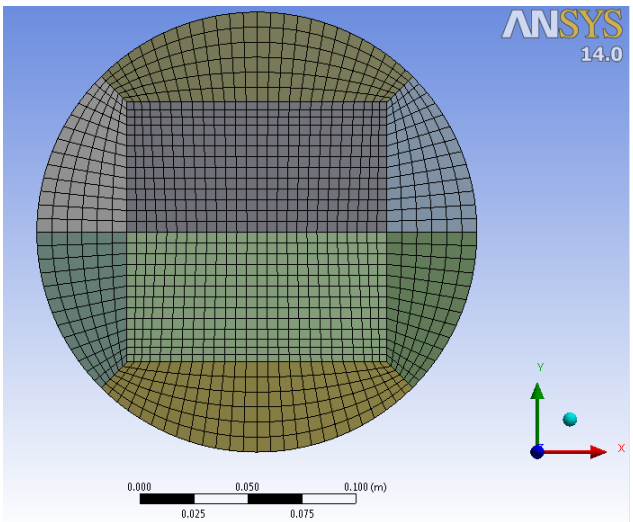

Figure 5: O-mesh with SOLID185 elements

4 Finite element model of moulded wafer: results

The moulded wafer model was initially subjected to a steady state thermal load varying from 175 °C to 25 °C in order to simulate the cooling stage during the mould process. Good agreement was obtained in the resultant out-plane deformation between the surface (using shell elements) and solid models simulated. Preliminary results show that a bowl-shaped warped moulded wafer is obtained when considering isotropic and linear elastic material properties for both EMC and the Si wafer. Additionally simulations carried out by considering silicon's anisotropy in terms of orthotropic material constants resulted in the same warped shape. This implies that in order to generate the cylindrical-shape, anisotropy has to be prescribed either through solver 'tricks' described by Mallik and Stout (2010) whereby 'symmetry-breaking' forces are applied to the moulded wafer during simulated cooling to room temperature which are then removed to obtain the final solution, or by process-related effects observed from the measurements. In fact, the warped shape shown in 6 was obtained by fixing the displacements in all directions of the nodes on the surface of the silicon side along the wafer centre line. It should also be noted that the moulded wafer FE model returns back to the stress-free condition once the displacement constraints are removed at room temperature. Good agreement was obtained between the measurement and numerical results obtained from the 4 moulded wafers listed in Table 1 where the maximum difference between both sets of data was below 5 %.

Compared to the moulded wafer shown in Figure 4, the EMC layer covers the entire wafer in the case of the FE model of Figure 5. A modification to the model whereby the diameter of the EMC layer was reduced by 10 mm showed that the EMC-free wafer edge does not alter the simulation results with and without the displacement constraints applied at the wafer centre-line.

A parametric analysis was carried out in order to evaluate the dependence of warpage on the thickness of the Si wafer and mould cap using the moulding compounds considered in the experimental moulding trials. From these results it can be deduced that the warpage is proportional to the ratio of the mould cap thickness to the wafer thickness as shown in Figure 7. Warpage is also inversely proportional to the total thickness of the moulded wafer (Figure 8) in accordance with the 2D bi-material beam theory by Timoshenko (Timoshenko, 1925). The results also confirm that $(T_m – T_G)$ is significantly important in determining the total thermal contraction during the cooling stage of moulding process. Furthermore a higher elastic modulus for EMC results in increased deformation of the moulded wafer.

The 3D model was also modified in order to simulate the variation in the mould thickness deduced from measurements obtained along the circumference of the moulded wafer. Although initial indications show that the effect of non-planar mould thickness on the warped shape is negligible, further measurements and simulations are required to test this hypothesis.

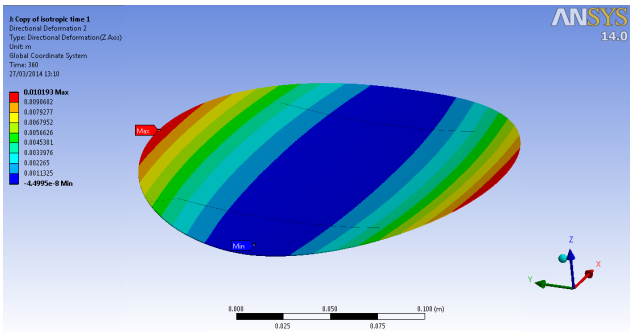

Figure 6: Directional Deformation (Z-Axis) (m) for Moulded Blank Wafer (Si: 375 µm, EMC 200 µm).

Table 1: FE model (using SOLID185 elements) validation against measurement trials.

Wafer thickness	EMC thickness	Mould Temperature	Warpage		% Error
µm	µm	°C	Measurements	FE model	
700	300	175	2	2.091	4.550
375	300	175	9.5	9.847	3.653
375	200	175	6.5	6.803	4.662
280	200	175	11	11.296	2.695

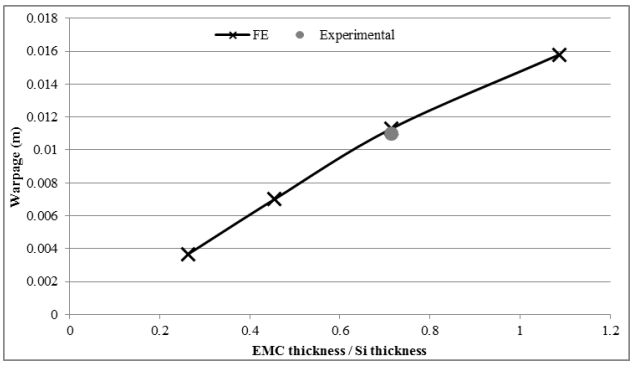

Figure 7: Warpage results against ratio of EMC thickness to Si thickness at $T_m = 175\,°\mathrm{C}$ and total mould thickness of 0.48 mm.

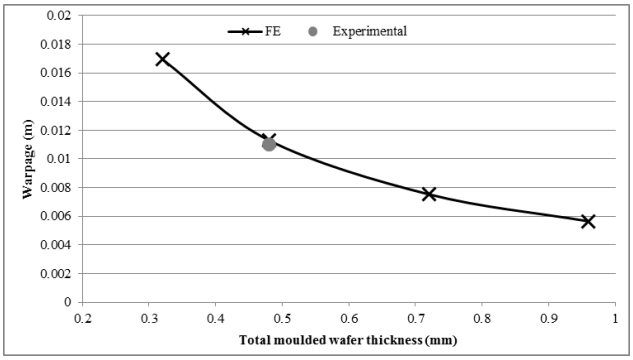

Figure 8: Warpage results against total moulded wafer thickness at $T_m = 175\,°\mathrm{C}$ and ratio of EMC to Si thickness of 0.714.

5 Conclusion

Wafer-level embedded moulding is a relatively new technology with great potential towards the development of low cost 3D integration. However the complex properties of the moulding compound compared to those of the Si wafer result in significant warpage at room temperature hampering the subsequent processing of the embedded dies. Therefore the moulding properties of the EMC need to be fully understood in order to optimise the compression moulding technique. Through finite element simulations and experimental observations, it was deduced that the warpage of wafer-level moulded blank wafers can be reduced by:

- increasing the total thickness of the moulded wafer;
- decreasing the ratio of the mould cap thickness to the wafer thickness;
- reducing the total thermal expansion of the moulding compound from the moulding temperature to room temperature. This can be reduced by choosing a moulding compound with the lowest $(T_m - T_G)$;
- decreasing the elastic modulus of moulding compound.

Apart from optimisation of the EMC material properties and layer thicknesses, other possible techniques can be adapted to this moulding process which may lead to a reduction in the overall warpage. For instance dicing the wafer prior to moulding would highly alleviate the build-up of stress over the entire wafer (Tomita et al., 2012). Moreover reinforcement of the moulding compound by means of glass or carbon fibres would significantly increase the stiffness and hence the resistance to deformation of the mould layer (Kim, 2012). Further work will be carried out to analyse possible causes leading to the warped shaped at room temperature such as non-planarity in the mould cap thickness. This will entail more detailed measurements of the moulded wafer thickness. Simulations will subsequently be carried out on a moulded wafer with embedded dies.

Acknowledgments

This paper is part of my work in LAB4MEMS, an ENIAC Joint Undertaking financed project

References

(nodate). ANSYS® Academic Research, Release 14.0, Help System, Element Reference, Element Library, SHELL181, ANSYS, Inc., 2011.

(nodate). ANSYS® Academic Research, Release 14.0, Help System, Theory Reference, Structures with Material Nonlinearities: Viscoelasticity ANSYS, Inc., 2011.

Boettcher, L., Manessis, D., Ostmann, A., Karaszkiewicz, S. and Reichl, H. (2008). Embedding of Chips for System in Package realization - Technology and Applications. *2008 3rd Int. Microsystems, Packag. Assem. Circuits Technol. Conf.*

Braun, T., Becker, K.-F., Piefke, K., Voges, S., Thomas, T., et al. (2011). 3D stacking approaches for mold embedded packages. In *Microelectron. packag. conf. (empc), 2011 18th eur.* (pp. 1–8). Brighton: IEEE.

Hopcroft, M. A., Nix, W. D. and Kenny, T. W. (2010). What is the Young's Modulus of Silicon? *J. Microelectromechanical Syst.* 19(2), 229–238.

Kim, T. H. (2012). Method of forming wafer level mold using glass fiber and wafer structure formed by the same. Google Patents.

Kumar, A., Dingwei, X., Sekhar, V., Lim, S., Keng, C., et al. (2009). Wafer level embedding technology for 3D wafer level embedded package. In *Electron. compo-*

nents technol. conf. 2009. ectc 2009. 59th (pp. 1289–1296). San Diego, CA: IEEE.

Mallik, A. and Stout, R. (2010). Simulation of warpage of silicon wafersusing ANSYS finite element analysis. In *Imaps, triangle 43rd int. symp.microelectron.* (pp. 486–493).

Mallik, A., Stout, R. and Ackaert, J. (2014). Finite-Element Simulation of Different Kinds of Wafer Warpages: Spherical, Cylindrical, and Saddle. *IEEE Trans. Components, Packag. Manuf. Technol.* 4(2), 240–247.

Matsutani, H. (2009). Compression molding solutions for various high end package and cost savings for standard package applications. In *Microelectron. packag. conf. 2009. empc 2009. eur.* (pp. 1–4). Rimini: IEEE.

Meyer, T., Ofner, G., Bradl, S., Brunnbauer, M. and Hagen, R. (2008). Embedded Wafer Level Ball Grid Array (eWLB). *2008 10th Electron. Packag. Technol. Conf.*

Sadeghinia, M., Jansen, K. M. B. and Ernst, L. J. (2012). Characterization and modeling the thermomechanical cure-dependent properties of epoxy molding compound. *Int. J. Adhes. Adhes.* 32, 82–88.

Souriau, J.-C., Lignier, O., Charrier, M. and Poupon, G. (2005). Wafer level processing of 3D system in package for RF and data application. *Proc. Electron. Components Technol. 2005. ECTC '05.*

Takahashi, Y., Dunne, R., Amagai, M., Koto, Y., Iriguchi, S., et al. (2012). Over Molding Process Development for a Stacked Wafer-level Chip Scale Package with Through Silicon Vias (TSVs). *Trans. Japan Inst. Electron. Packag.* 5(1), 122–131.

Timoshenko, S. (1925). Analysis of bi-metal thermostats. *J. Opt. Soc. Am.* 11(3), 233.

Tomita, Y., Sekihara, Y., Kubota, J., Ichikawa, K. and Sankman, B. (2012). Wafer Level Packaging to Address Future Direct Chip Attach Needs. *Trans. Japan Inst. Electron. Packag.* 5(1), 85–91.

Xjenza Online - Journal of The Malta Chamber of Scientists
www.xjenza.org
DOI: 10.7423/XJENZA.2014.2.07

Meeting Report

Neuropathology and Neuropharmacology of Monoaminergic Systems

Rona R Ramsay[1] and Philippe De Deurwaerdère[2]
[1]Biomedical Sciences Research Centre, University of St Andrews, North Haugh, St Andrews, KY16 9ST, UK.
[2]Institute of Neurodegenerative Diseases, UMR CNRS 5293, 146 rue Léo Saignat, 33076 Bordeaux cedex, France.

Abstract. The third EU COST Action CM1103 "Structure-based drug design for diagnosis and treatment of neurological diseases: dissecting and modulating complex function in the monoaminergic systems of the brain" Annual Conference entitled "Neuropathology and Neuropharmacology of Monoaminergic Systems" was hosted by the University of Bordeaux, France on 8-10 October 2014. The conference, organized by Prof. De Deurwaerdére, was supported by COST (European Cooperation in Science and Technology) and LABEX (LABEX Brain, University of Bordeaux). The program took the form of a three-day meeting, comprising a series of French and international invited talks and breakout sessions designed to identify key gaps in current knowledge and potential future research questions. The aims of this Conference were two-fold: 1. To identify the current state-of-the-art in the understanding of the pathological mechanisms that contribute to different neuropsychiatric disorders, and to what extent, monoamines a multi-target drugs and/or other interventions might prevent these changes. 2. To identify specific areas of research where information is sparse but which are likely to yield data that will impact on future strategies to treat neurodegenerative disorders.

Meeting report

COST Action CM1103 (http://www.cost.eu/domains_actions/cmst/Actions/CM1103) *Structure-Based Drug Design For Diagnosis And Treatment of Neurological Diseases: Dissecting and Modulating Complex Function in the Monoaminergic Systems of the Brain* was established to stimulate an interdisciplinary approach to the task of understanding the molecular basis of neurological and psychiatric disorders. Medicinal chemistry now has many computational tools to aid in the design of novel drugs targeting either one or several proteins. Biological insights are essential to evaluate the efficacy of these novel drugs and to propose also new targets and approaches. Commonalities amongst the brain monoamine neurotransmitters, dopamine (DA), noradrenaline (NA), adrenaline (A) serotonin (5-HT) or histamine, are evident as these systems of neurotransmission are all involved in the pathophysiology of all major neuropsychiatric disorders and brain affections, such as mood disorders, schizophrenia, autism-spectrum disorders, Parkinson's disease (PD), Alzheimer disease, epilepsy, ischemia and dementias. Indeed, the efficacy of numerous medicines against the above-mentioned pathologies has been related at least in part to an action of these chemical drugs on the monoaminergic systems. The collaborative work in the action is a permanent interaction between bottom-up and top-down analyses towards understanding the neuropathology and neuropharmacology of monoaminergic systems. The extended abstracts in these Proceedings are a selection from the contributions to the third annual meeting, held in Bordeaux, of groups actively working towards these goals.

Chemical developments come from existing molecules and their modification either via classical or new ways of synthesis, and computational modeling. Reported at this conference are compounds for single targets such as acetylcholinesterase or aldo-ketoreductase by Magdalena Majekova (Slovak Academy of Sciences, Bratislava), or families of compounds such as benzothiazoles by Kamil Musilek (Kadir Has University, Istanbul) or quinolines by José Marco-Contelles (Consejo Superior de Investigaciones Científicas, Madrid) synthesized and studied with the goal of treating Alzheimer disease, Parkinson's disease or stroke by Mercedes Unzeta (Uni-

Correspondence to: Philippe De Deurwaerdère (deurwaer@u-bordeaux.fr)

© 2014 Xjenza Online

versitat Autonoma de Barcelona). A series of multi-target compounds has been also designed with action on specific pairs (or multiples) of targets. Ligands carefully designed to bind to multiple targets are another accepted strategy in tackling the complex neurodegenerative diseases (Cavalli et al., 2008; Geldenhuys and der Schyf, 2013) but producing the best combinations to explore phenotypic results is not a trivial task (Prati et al., 2014). With large numbers of compounds tested and published in databases, one starting point comes from data-mining existing knowledge. Theoretical prediction of pharmaceutical targets for new compounds is possible using a probabilistic method to build a model of any compound from the ChEMBL dataset. Then, using the circular fingerprint descriptors, a cheminformatic method, developed to explore known off-target interactions of known compounds, was applied to identify which of the new compounds that should bind to the desired targets. This and confirmation of the predicted efficacies are included in this topic.

Reuptake transporters are targets to modulate amine levels in the synaptic cleft, but, unfortunately, crystal structures are not available yet. Nonetheless, homology models of the transporters in conjunction with mutational studies are beginning to define the molecular determinants of binding to these proteins. Structure-based drug design together with good pharmacological data provides the basis for designs combining the features needed for each target into one molecule. These molecular determinants predict quite nicely the behaviour of some compounds (amphetamine, tyramine, cocaine, DA, 5-HT; Yelekci and Connaly, this conference) toward the dopamine transporter in models *in vitro* or *in* vivo (Navailles and De Deurwaerdère, 2011).

Drug design and computational studies are rendered easier by the crystal structures that identify the interaction of the protein with a ligand. Structures for the enzymes that degrade the monoamine neurotransmitters (MAO and COMT) are available for computational exploration of molecular determinants of binding. Inhibition of monoamine oxidases (MAO A and MAO B) by several irreversible inhibitors and a few new, well-tolerated, reversible inhibitors used over the last 30 years, results in increased levels of brain amines (Youdim and Bakhle, 2006). Docking and molecular dynamic studies of the inhibitor in the active site are now standard tools for medicinal chemists aiming to improve inhibitor binding or decide which part of a molecule may be changed without loss of affinity (Samadi et al., 2012). Using structure-based techniques, complete theoretical searches for new lead compounds are also possible (Vilar et al., 2012). Finally, using these models, it is possible to address the selectivity of series of new compounds toward MAO. More recently, the crystal structure of glutamatergic AMPA receptors has been obtained, leading to conceive new series of compounds targeting the GluR1 subunit of the AMPA receptor hopefully as efficiently as antinociceptive compounds as described by Stefania Butini (University of Siena).

Pharmacological evaluation is still a necessary step to determine the accurate efficacy of compounds and to evaluate the selectivity towards other targets. Several MAOI are not selective for MAO and display good affinities for other targets such as lysine-specific demethylases or cytochrome P450 (Binda et al., 2010); Massimo Valoti (University of Siena); Thomas Malcomson (University of St Andrews). Lysine-specific demethylases are involved in epigenetic, cytochrome oxidase are involved in the metabolism of xenobiotics. These other targets together may participate in the behavioural effects of these compounds in animal models and in humans. Indeed, as detailed by Marco Bortolato (University of Kansas) gene deletion of MAOA gives surprising results compared to pharmacological compounds (Finberg, 2014). Apart from the longitudinal and developmental dimensions inherent to gene deletion, Keith Tipton (Trinity College, Dublin) showed that the differences suggest that the biological effects of MAOI do not only result from their interaction with MAO (Finberg, 2014).

Neuropharmacological explorations of the mechanism of action of current drugs are a big challenge in neurobiology in order to identify the targets, ameliorate the phenotype, and limit the side effects. Even if these drugs are currently used in clinic, their mechanism of action is often misunderstood, not only for MAOI. L-DOPA is the gold standard medication in Parkinson's disease but the numerous motor and non-motor side effects occurring after years of treatment lead to conceive other therapeutic strategies and to focus on its mechanism of action (Meissner et al., 2011). Numerous strategies are developed to find new chemical compounds able to stimulate the DA D2 and D3 receptors, the primary mechanism thought to underline the efficacy of L-DOPA. The chemical development of new compounds unmasks new pharmacological concepts and the development of compounds will integrate these new concepts such as biased signaling or heterodimerization of receptors, as detailed by Holger Stark (Heinrich Heine University). Abdelhamid Benazzouz (Université de Bordeaux) emphasized the importance of the deep brain stimulation that also permits to highlight unpredicted targets such as D5 receptors, 5-HT_{2C} receptors in the control of DA neurons (De Deurwaerdère et al., 2013) or to highlight the involvement of 5-HT and NA neurons in the control of dopamine-mediated function (Di Matteo et al., 2008; Navailles, Di Giovanni and De Deurwaerdère, 2014; Navailles, Milan et al., 2014). Finally, Philippe De Deurwaerdère (Université de Bordeaux) presented evi-

Figure 1: Some members of EU COST Action CM1103 "Structure-based drug design for diagnosis and treatment of neurological diseases: dissecting and modulating complex function in the monoaminergic systems of the brain" at the Annual Conference "Neuropathology and Neuropharmacology of Monoaminergic Systems" hosted by the University of Bordeaux, France on 8-10 October 2014.

dence that the chronic use of L-DOPA could affect the activity of MAO enzymes in vivo showing that the different topics developed in the action are interconnected.

Understanding the interactions of neurotransmission systems is an important step for the optimization of therapeutic strategies. The plurality of targets that potentially bind antipsychotics or antiparkinsonian, antidepressant drugs favours the need to develop multi-target compounds. Because neurobiological systems of neurotransmitters establish close relationships (Chesselet, 1984), it is likely that a pharmacological action toward one system will more or less directly affect the other one. This is highlighted perhaps by famous associations and links between some neurotransmitter systems such as the 5-HT/DA interaction (Di Giovanni et al., 2008; Di Matteo et al., 2008), the glutamate/DA interaction (M. Carlsson and A. Carlsson, 1990), the 5-HT/GABA interaction (Soubrié, 2010) and so one. The role of monoamines still remains unresolved even in pathologies such as depression or anxiety where the connection between monoamines and the diseases has been known for years. In epilepsy, although monoamines were thought to control the excitability of hippocampal cells via a lowering influence on depolarizing current, Giuseppe Di Giovanni (University of Malta and Cardiff University), found that 5-HT_{2C} receptors do not modify the electrophysiological responses in the model of maximal dentate activation (MDA) of temporal lobe epilepsy (TLE) while they undergo to a cellular redistribution in the hippocampus of epileptic rats (Orban et al., 2014). Di Giovanni also showed that in the pilocarpine-model of TLE, the activation of the 5-HT_{2C} receptors surprisingly induce a powerful antiepileptic effect, probably mediated by interacting with GABA and glutamate. These findings highlight a strong model-dependence of the 5-HT_{2C} receptor effects which is especially true for TLE epilepsy.

Moreover, the physiopathology of numerous pathologies is still misunderstood. Nela Pivac (Rudjer Boskovic Institute, Zagreb) presented some data concerning the post-traumatic stress disorder, a pathology that probably involves monoamines, but devoid of efficient treatment.

A better understanding of the relationships of chemical systems in the brain relies on the availability of good chemical compounds for research and diagnosis and good models to address the efficacy of compounds and the physiopathology of brain diseases. These models are sometimes classical as those that have been developed in rodents to study numerous neuropsychiatric diseases or less classical as the use of crayfish to study the neurobiological bases of anxiety as underlined by Pascal Fossat (Université de Bordeaux) (Fossat et al., 2014).

Acknowledgments

We thank the numerous contributors, the guest speakers and especially Prof. Giuseppe Di Giovanni for publishing the proceedings of the conference as collection of short communications in Xjenza. We also acknowledge the support by LABEX (LABEX Brain, University of Bordeaux).

References

Binda, C., Valente, S., Romanenghi, M., Pilotto, S., Cirilli, R., et al. (2010). Biochemical, structural, and biological evaluation of tranylcypromine derivatives as inhibitors of histone demethylases LSD1 and LSD2. *J. Am. Chem. Soc.* 132(19), 6827–6833.

Carlsson, M. and Carlsson, A. (1990). Interactions between glutamatergic and monoaminergic systems within the basal ganglia–implications for schizophrenia and Parkinson's disease. *Trends Neurosci.* 13(7), 272–276.

Cavalli, A., Bolognesi, M. L., Minarini, A., Rosini, M., Tumiatti, V., et al. (2008). Multi-target-directed ligands to combat neurodegenerative diseases. *J. Med. Chem.* 51(3), 347–372.

Chesselet, M. F. (1984). Presynaptic regulation of neurotransmitter release in the brain: facts and hypothesis. *Neuroscience.* 12(2), 347–375.

De Deurwaerdère, P., Lagière, M., Bosc, M. and Navailles, S. (2013). Multiple controls exerted by 5-HT2C receptors upon basal ganglia function: from physiology to pathophysiology. *Exp. Brain Res.* 230(4), 477–511.

Di Giovanni, G., Di Matteo, V., Pierucci, M. and Esposito, E. (2008). Serotonin-dopamine interaction: electrophysiological evidence. *Prog. Brain Res.* 172, 45–71.

Di Matteo, V., Di Giovanni, G., Pierucci, M. and Esposito, E. (2008). Serotonin control of central dopaminergic function: focus on in vivo microdialysis studies. *Prog. Brain Res.* 172, 7–44.

Finberg, J. P. M. (2014). Update on the pharmacology of selective inhibitors of MAO-A and MAO-B: focus on modulation of CNS monoamine neurotransmitter release. *Pharmacol. Ther.* 143(2), 133–152.

Fossat, P., Bacqué-Cazenave, J., De Deurwaerdère, P., Delbecque, J.-P. and Cattaert, D. (2014). Comparative behavior. Anxiety-like behavior in crayfish is controlled by serotonin. *Science.* 344(6189), 1293–1297.

Geldenhuys, W. J. and der Schyf, C. J. V. (2013). Designing drugs with multi-target activity: the next step in the treatment of neurodegenerative disorders. *Expert Opin Drug Discov.* 8(2), 115–129.

Meissner, W. G., Frasier, M., Gasser, T., Goetz, C. G., Lozano, A., et al. (2011). Priorities in Parkinson's disease research. *Nat Rev Drug Discov.* 10(5), 377–393.

Navailles, S. and De Deurwaerdère, P. (2011). Presynaptic control of serotonin on striatal dopamine function. *Psychopharmacology.* 213(2-3), 213–242.

Navailles, S., Di Giovanni, G. and De Deurwaerdère, P. (2014). Predicting dopaminergic effects of L-DOPA in the treatment for Parkinson's disease. *CNS Neurosci. Ther.* 20(7), 699–701.

Navailles, S., Milan, L., Khalki, H., Di Giovanni, G., Lagière, M. and De Deurwaerdère, P. (2014). Noradrenergic terminals regulate L-DOPA-derived dopamine extracellular levels in a region-dependent manner in Parkinsonian rats. *CNS Neurosci. Ther.* 20(7), 671–678.

Orban, G., Bombardi, C., Gammazza, A. M., Colangeli, R., Pierucci, M., et al. (2014). Role(s) of the 5-HT2C receptor in the development of maximal dentate activation in the hippocampus of anesthetized rats. *CNS Neurosci Ther.* 20(7), 651–661.

Prati, F., Uliassi, E. and Bolognesi, M. L. (2014). Two diseases, one approach: multitarget drug discovery in Alzheimer's and neglected tropical diseases. *Medchemcomm.* 5(7), 853.

Samadi, A., de los Ríos, C., Bolea, I., Chioua, M., Iriepa, I., et al. (2012). Multipotent MAO and cholinesterase inhibitors for the treatment of Alzheimer's disease: synthesis, pharmacological analysis and molecular modeling of heterocyclic substituted alkyl and cycloalkyl propargyl amine. *Eur. J. Med. Chem.* 52, 251–262.

Soubrié, P. (2010). Reconciling the role of central serotonin neurons in human and animal behavior. *Behav. Brain Sci.* 9(02), 319.

Vilar, S., Ferino, G., Quezada, E., Santana, L. and Friedman, C. (2012). Predicting monoamine oxidase inhibitory activity through ligand-based models. *Curr. Top. Med. Chem.* 12(20), 2258–2274.

Youdim, M. B. H. and Bakhle, Y. S. (2006). Monoamine oxidase: isoforms and inhibitors in Parkinson's disease and depressive illness. *Br. J. Pharmacol.* 147 Suppl, S287–96.

COST ACTION CM1103: Structure-based drug design for diagnosis and treatment of neurological diseases: dissecting and modulating complex function in the monoaminergic systems of the brain

Annual Meeting of the COST ACTION CM1103

Chair: Dr Rona R. Ramsay

Neuropathology and Neuropharmacology of Monoaminergic Systems

Bordeaux

Centre de Génomique Fonctionnelle

October 8-10th 2014

Local organisation
Professor P. De Deurwaerdère, IMN

The subthalamic dopamine D5 receptors in Parkinson's disease

Abdelhamid Benazzouz[*1,2] **and Jonathan Chetrit**[1,2]
[1]Univ. de Bordeaux, Institut des maladies Neurodégénératives, UMR 5293, 33076 Bordeaux, France
[2]CNRS, Institut des maladies Neurodégénératives, UMR 5293, 33076 Bordeaux, France
*abdelhamid.benazzouz@u-bordeaux.fr

Abstract. Parkinson's disease is a neurological disorder characterized by the manifestation of the cardinal motor symptoms, which are attributed to the progressive degeneration of dopaminergic neurons in the substantia nigra pars compacta (SNc). It has been reported that the burst firing is a pathological signature of STN neurons in Parkinson's disease, however, the origin of bursts remains unknown. Here we tested the hypothesis that dopamine D5 receptors, characterized by a high constitutive activity, may contribute to the emergence of burst firing in the STN and therefore in the manifestation of parkinsonian motor deficits. We tested this hypothesis and have shown that application of an inverse agonist inhibits D5 receptors constitutive activity within the STN and reduced burst firing of STN neurons in brain slices. Moreover, itconverted pathological STN burst firing into physiological tonic activity in the 6-OHDA rat model of Parkinson's disease. These results are the first to demonstrate that subthalamic D5 receptors are involved in the pathophysiology of Parkinson's disease and that administering an inverse agonist to these receptors may alleviate motor symptoms.

Keywords Parkinson's disease – Subthalamic nucleus – Dopamine D5 receptors

1 Introduction

Parkinson's disease is a neurological disorder characterized by the manifestation of the cardinal motor symptoms, akinesia, rigidity and tremor at rest. These motor disorders are attributed to the progressive degeneration of dopaminergic neurons in the substantia nigra pars compacta (SNc), which results in dopamine depletion in the striatum and also in extrastriatal nuclei such as the subthalamic nucleus (STN) (Benazzouz et al., 2014). The STN is a basal ganglia structure involved in the control of movement and plays a critical role in the pathophysiology of Parkinson's disease. Previous studies have shown that the tonic regular pattern of STN neurons in a normal situation becomes bursty after dopamine neuron degeneration in animal models (Bergman et al., 1994; Ni et al., 2001) and also in patients with Parkinson's disease (Benazzouz et al., 2002). Lesioning the STN has been shown to reverse the motor deficits induced by MPTP in non-human primates (Bergman et al., 1990). However, the beneficial effect was accompanied by dyskinetic abnormal movements. Nevertheless, to avoid these irreversible side effects, we proposed to replace the lesion by high frequency electrical stimulation of the STN, which dramatically alleviated Parkinsonian-like motor deficits in MPTP-intoxicated monkeys (Benazzouz et al., 1993) and later in patients with advanced stage Parkinson's disease (Limousin et al., 1995). It is now accepted that the burst firing is a pathological signature of STN neurons in Parkinson's disease; however, the origin of bursts and their causal link with motor deficits remain unknown. In our recent study we hypothesized that the constitutive activity of dopamine D5 receptors may be involved in the genesis of burst firing in the STN and consequently in the development of the associated motor deficits.

2 Methods

In vitro and in vivo electrophysiological studies as well as behavioral experiments associated with local infusion of dopamine agents in the STN were performed in the rat.

3 Findings and argument

The STN dopamine D5 receptors, which display a high agonist-independent constitutive activity are able to potentiate burst firing of STN neurons in in vitro rat brain slices (Baufreton et al., 2003). More recently, we have shown that local microinjection of an inverse agonist of D5 receptors reduced burst activity of STN neurons in vitro and transformed the burst firing in the regular tonic activity in vivo. This normalization of firing pattern was associated with the improvement of motor deficits in the 6-OHDA rat model of Parkinson's disease (Chetrit et al., 2013).

4 Conclusion

These results are the first to demonstrate that the constitutive activity of dopamine D5 receptors, located in the STN, are at least in part at the origin of the development of the burst activity and therefore are involved in the pathophysiology of PD. They provide evidence that selective action on this receptor subtype might lead to better-targeted drug therapy for the disease. This opens up new avenues for therapeutic approaches based on specific pharmacological agents.

References

Baufreton, J., Garret, M., Rivera, A., de la Calle, A., Gonon, F., et al. (2003). D5 (not D1) dopamine receptors potentiate burst-firing in neurons of the subthalamic nucleus by modulating an L-type calcium conductance. *J. Neurosci.* 23(3), 816–25.

Benazzouz, A., Breit, S., Koudsie, A., Pollak, P., Krack, P. and Benabid, A.-L. (2002). Intraoperative microrecordings of the subthalamic nucleus in Parkinson's disease. *Mov. Disord.* 17(S3), S145–S149.

Benazzouz, A., Gross, C., Féger, J., Boraud, T. and Bioulac, B. (1993). Reversal of Rigidity and Improvement in Motor Performance by Subthalamic High-frequency Stimulation in MPTP-treated Monkeys. *Eur. J. Neurosci.* 5(4), 382–389.

Benazzouz, A., Mamad, O., Abedi, P., Bouali-Benazzouz, R. and Chetrit, J. (2014). Involvement of dopamine loss in extrastriatal basal ganglia nuclei in the pathophysiology of Parkinson's disease. *Front. Aging Neurosci.* 6.

Bergman, H., Wichmann, T. and DeLong, M. (1990). Reversal of experimental parkinsonism by lesions of the subthalamic nucleus. *Science.* 249(4975), 1436–1438.

Bergman, H., Wichmann, T., Karmon, B. and DeLong, M. R. (1994). The primate subthalamic nucleus. II. Neuronal activity in the MPTP model of parkinsonism. *J. Neurophysiol.* 72(2), 507–20.

Chetrit, J., Taupignon, A., Froux, L., Morin, S., Bouali-Benazzouz, R., et al. (2013). Inhibiting Subthalamic D5 Receptor Constitutive Activity Alleviates Abnormal Electrical Activity and Reverses Motor Impairment in a Rat Model of Parkinson's Disease. *J. Neurosci.* 33(37), 14840–14849.

Limousin, P., Pollak, P., Benazzouz, A., Hoffmann, D., Le Bas, J.-F., et al. (1995). Effect on parkinsonian signs and symptoms of bilateral subthalamic nucleus stimulation. *Lancet.* 345(8942), 91–95.

Ni, Z.-G., Bouali-Benazzouz, R., Gao, D.-M., Benabid, A.-L. and Benazzouz, A. (2001). Time-course of changes in firing rates and firing patterns of subthalamic nucleus neuronal activity after 6-OHDA-induced dopamine depletion in rats. *Brain Res.* 899(1-2), 142–147.

Long Term High Fat Diet Elicits Anxio-Depressive Like Symptoms: Involvement of the Serotonergic system

Zemdegs Juliane[1,2,3]; Quesseveur Gaël[1], Penicaud Luc[2]; Fioramonti Xavier[2]; Guiard Bruno[*1,3]
[1]Centre des Sciences du Goût et de l'Alimentation, CNRS UMR 6265, INRA UMR 1324, Université de Bourgogne, 9E Bvd Jeanne d'Arc, 21000 Dijon, France
[2]Laboratoire « des troubles anxio-dèpressif et neurogenése », EA3544, Faculté de Pharmacie, Université Paris sud 11, 5 rue JB Clément, 92290 Châtenay-Malabry, France
[3]Centre de Recherches sur la Cognition Animale, UMR 5169 CNRS, Bât 4R3, 118 route de Narbonne, 31062 Toulouse, France
*bruno.guiard@univ-tlse3.fr

Abstract. Although epidemiological studies suggest the existence of a bidirectional link between type 2 diabetes (T2D) and major depression, the neurobiological substrates and the mechanisms underlying such comorbidity are still poorly understood. To study the putative relationship between T2D and psychiatric disorders, we validated a metabolic and an emotionality z-score in mice integrating relevant parameters. Interestingly a strong correlation between the intensity of T2D and behavioural anomalies were observed, thereby strengthening the hypothesis that both pathologies are intertwined. The present results also suggest that body weight gain observed in high fat diet (HFD) fed mice is not involved in the anxio-depressive like phenotype. Finally, because the monoaminergic systems plays a pivotal role in major depression, we next asked whether T2D altered the serotonergic neurotransmission in the hippocampus, a brain region involved in emotionality. Remarkably HFD-induced T2D resulted in a significant decrease in hippocampal extracellular 5-HT levels. The latter results are of particular importance because they might predict a resistance of currently available serotonergic antidepressant drugs in animal models of comorbid T2D and depression, but also in patients suffering from both pathologies.

Keywords type 2 diabetes – anxiety – depression – serotonin – behaviour – in vivo intracerebral microdialysis

1 Introduction

Type 2 diabetes (T2D) and depressive disorders are major health concerns, each affecting 350 million people

worldwide. Remarkably, results of recent epidemiological studies strongly support the existence of a bidirectional relationship between both diseases. Indeed, major depression (MD) is associated with a 60 % increased risk of (T2D) (Mezuk et al., 2008) while 10-30 % of T2D individuals suffer from MD (Ali et al., 2008). Although the mechanisms underlying this association are not clearly understood, a recent study showed that a long-term high fat diet (HFD) abolished serotonin (5-HT)-induced activation of the Akt/GSK3β cascade in the DG of the hippocampus (Papazoglou et al., 2014). These results strongly suggested an involvement of the serotonergic system in T2D and depression and make the hippocampus an important region to study such comorbidity.

2 Methods

To study the relationship between T2D and MD, we used HFD-induced T2D. C57BL6J male mice were fed either a standard (STD) or a HFD (hyper-lipidic: 40 % of fat) for 16 weeks and then subjected to a full comprehensive behavioural analysis including tests recapitulating diverse anomalies related to depressive state. An emotionality z-score (Guilloux et al., 2011) was calculated from the performances of mice in paradigms evaluating anxiety, despair and carelessness in the open field (OF), tail suspension (TST) and splash test (ST); respectively. In the same way a metabolic z-score integrating body weight gain, fasting glycaemia and glucose tolerance was calculated in mice in order to establish putative correlations with behavioural impairments. In a second part of this study, anesthetized mice were implanted with microdialysis probes in the ventral hippocampus and the next day (∼ 20 hours after the surgery), dialysate samples were collected every 15 minutes for 2 hours to compare the basal extracellular levels of 5-HT between freely moving animals fed a STD and HF diet.

3 Findings and argument

Our data indicated that mice fed a HFD displayed increased body weight gain relative to control STD animals as shown by their increased body weight gain (11(1) vs 6.0(5) gr; $p < 0.01$), their increased fasting glycaemia (165(17) vs 130(5) ng/dl; $p < 0.05$) and glucose intolerance. Remarkably, this HFD also elicited significant anomalies in mood-related behaviours, such as increased anxiety detected in the open field (time in the center: 109(11) vs 175(20) sec; $p < 0.05$), as well as decreased self-care evaluated in the splash test (time of grooming: 125(15) vs 160(10) sec; $p < 0.05$). In an attempt to correlate the intensity of T2D and anxio-depressive-like symptoms, we therefore established a separate metabolic and emotionality z-score 1. Our analysis showed that the higher the metabolic score, the higher depression severity with a significant correlation between both scores (R^2=0,6). Interestingly, such a correlation persisted when the body weight gain parameter was removed from the metabolic z-score (R^2=0,57).

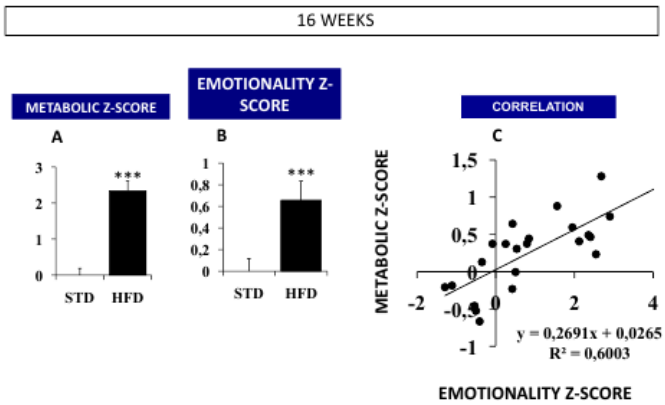

Figure 1: T2D induced anxio-depressive like phenotype. Data are means ± SEM of the "metabolic z-score" (including, body weight gain, fasting glycaemia and glucose tolerance in the oral glucose tolerance test (OGTT) and of the "emotionality z-score" (including animals performances in the OF, TST and ST); respectively. (C) Correlation between metabolic z-score and emotionality z-score.

With respect to the serotonergic neurotransmission, a lower basal extracellular 5-HT levels was detected in the hippocampus of HFD mice compared to STD controls (8.0(9) vs 5.0(3) fmol/samples; $p < 0.05$).

4 Conclusion

These results suggest that metabolic disorders could negatively reverberate on mood and may dampen antidepressant drug response, underlying the necessity to adapt treatment in patients with comorbid diabetes and depression. Further experiments are now required to better understand how T2D alters 5-HT neurotransmission, particularly by evaluating the functional activity of relevant targets such as the 5-HT_{1A} or 5-HT_{1B} autoreceptors or the 5-HT transporter.

References

Ali, M. R., Rasmussen, J. J., Monash, J. B. and Fuller, W. D. (2008). Depression is associated with increased severity of co-morbidities in bariatric surgical candidates. *Surg. Obes. Relat. Dis.* 5(5), 559–64.

Guilloux, J.-P., Seney, M., Edgar, N. and Sibille, E. (2011). Integrated behavioral z-scoring increases the sensitivity and reliability of behavioral phenotyping in mice: Relevance to emotionality and sex. *J. Neurosci. Methods.* 197(1), 21–31.

Mezuk, B., Eaton, W. W., Albrecht, S. and Golden, S. H. (2008). Depression and Type 2 Diabetes Over the

Lifespan: A meta-analysis. *Diabetes Care.* 31(12), 2383–2390.

Papazoglou, I. K., Jean, A., Gertler, A., Taouis, M. and Vacher, C.-M. (2014). Hippocampal GSK3β as a Molecular Link Between Obesity and Depression. *Mol. Neurobiol.* [In Press].

Modelling gene-environment interactions in aggression

Sean C Godar, Laura J Mosher, Marco Bortolato*

Dept. of Pharmacology and Toxicology, University of Kansas, Lawrence (KS)

*bortolato@ku.edu

Abstract. Gene-environment interactions have been shown to play a critical role in the development of aggression and other neuropsychiatric disorders. Several independent studies have highlighted that pathological aggression in males is often linked to the interaction of early-life abuse and/or neglect with allelic variants associated with low activity of monoamine oxidase (MAO) A, the key enzyme for the degradation of brain serotonin and norepinephrine.

To explore the neural underpinnings of the interaction between early stress and low MAO A, we tested the impact of early stress (ES) in MAO A^{Neo} mice, a newly generated line of MAO A hypomorphic mutants. While ES did not significantly affect the aggressive behavior in either MAO A knockout (KO) or wild-type (WT) mice, the same manipulation resulted in a robust enhancement of fighting responses in MAO A^{Neo} mice, to a level comparable with that of MAO A KO counterparts.

These data parallel epidemiological findings on the interaction of low-MAO A allelic variants and early stress in males with respect to the development of antisocial behavior; furthermore, our findings provide a powerful translational platform to investigate the pathophysiology of aggression on a highly isomorphic murine model.

Further studies in our laboratory are beginning to elucidate the neurodevelopmental mechanisms, supporting the interaction of early stress and MAOA genetic variants in reactive aggression and related emotional disturbances.

Support by the National Institute of Health, the EU COST Actions CM1103 as well as the Kansas University Strategic Initiative Grant is acknowledged.

Keywords Monoamine oxidase A – aggression – gene x environment interactions

Modulation of the Glutamatergic System to Novel Potential Therapeutics

Stefania Butini*[1], Simone Brogi[1], Giridhar Kshirsagar[1], Samuele Maramai[1], Anna Maria Aloisi[2], Raminta Venskutonytė[3], Karla Frydenvang[3], Jette S. Kastrup[3], Darryl Pickering[3], Margherita Brindisi[1], Sandra Gemma[1], Giuseppe Campiani[1]

[1]European Research Centre for Drug Discovery and Development, Department of Biotechnology, Chemistry and Pharmacy, University of Siena, Via Aldo Moro 2, 53100 Siena, Italy

[2]Department of Medicine, Surgery and Neuroscience, Policlinico Santa Maria alle Scotte, viale Mario Bracci 16, 53100 Siena, Italy

[3] Department of Drug Design and Pharmacology, Faculty of Health and Medical Sciences, University of Copenhagen, Universitetsparken 2, DK-2100 Copenhagen, Denmark

*butini3@unisi.it

Abstract. Glutamate is the main excitatory neurotransmitter in the CNS, and its actions are mediated by metabotropic and ionotropic receptors (iGluRs, Kainate, AMPA and NMDA receptor subfamilies). The GluK1 subunit of Kainate receptors is predominantly associated in pain pathways. We focused on the development of AMPA/KA selective ligands based on a bicyclic pyrimidinedione scaffold. The selectivity for modulation of the single iGluRs subunits, together with the varying intrinsic activity of the developed ligands, have been extensively examined and correlated to the specific decoration of the core scaffold. The essential contribution given to the design by the recent resolution of the crystal structures of a series of our analogues in complex with the target receptor subunits (GluK1, GluK3 or GluA2), coupled to molecular modeling application, represent a further and determinant support for pursuing our research objective. Preliminarly in vivo data (formalin test) have demonstrated an antinociceptive effect for our potent and selective GluK1 ligands.

Keywords Glutamate receptors – AMPA – Kainate – Pain – X-ray – Molecular modelling

1 Introduction

Glutamate (Glu) plays an important role in neuronal plasticity, neurotoxicity, and in degenerative disorders, its actions are mediated by metabotropic and ionotropic receptors (iGluRs). The excitatory amino acid transporters (EAATs), which are essential for terminating synaptic excitation and for maintaining extracellular L-Glu concentration below toxic levels, represent further key target proteins of the glutamatergic system (Campiani et al., 2003). The iGluRs consist in the Kainate, AMPA and NMDA receptor subfamilies. The GluK1 subunit of the Kainate receptors (KARs) is predominantly associated with pain pathways, as shown in different areas of the CNS, and the use of GluK1 competitive antagonists allowed the demonstration of its involvement in pain signalling (Dolman et al., 2007).

Our research group acquired, over a number of years, strong experience in the selective targeting of either i) transporters (Campiani, De Angelis et al., 2001), and ii) iGluRs (GluA2 or GluK1 selective agonists and antagonists) (Campiani, Morelli et al., 2001; Butini et al., 2008; Venskutonyte et al., 2011).

The development of selective KARs agonist/antagonists may lead to compounds potentially able to treat neuropathic pain. In this frame, we developed AMPA/KA selective ligands based on a bicyclic pyrimidinedione scaffold (Figure 1, (Campiani, Morelli et al., 2001). The selectivity for the modulation of the single iGluRs subunits (Butini et al., 2008; Venskutonyte et al., 2011), together with the varying intrinsic activity of the developed ligands, has been successfully correlated to the particular decoration of the core scaffold. The essential contribution given to the design by the recent resolution of the crystal structures of a series of our analogues in complex with the target receptor subunits (GluK1, GluK3 or GluA2) shed light on the selectivity determinants for our compounds. Molecular modeling studies are in progress to correlate the displacement of key water molecules of the receptor subunit apoforms, for the design of novel, extremely selective ligands. In particular, our focus will be directed on identifying selective GluK3 ligands with respect to the other receptor subtypes in order to promote synaptic plasticity and cognitive processes by fine-tuning KARs.

2 Methods

The application of an array of computer-aided drug design (CADD) tools allowed the identification of potent and selective GluK1 ligands. Moreover, through molecular modeling techniques we further explored the features (steric and electronic components that are indispensable for biological activity) and the shape that the known substrates show when bound to the site of interest.

Standard organic chemistry approaches and ad-hoc developed synthetic methodologies have been exploited for the construction of the selected structural motifs. Automated flash chromatography, HPLC separations

have been performed. Spectroscopic characterization of the compounds was performed with NMR (400, 300 and 200 MHz), MS and tandem MS instruments. X-ray diffraction data for GluA2 LBD and GluK3 LBD were collected at the I911-3 beamline (MAX-Lab, Lund, Sweden).

Two data sets were collected to the following resolutions: 1.0 Å resolution and 1.15 Å resolution for the GluA2 LBD in complex with two derivatives. All the X-ray data was processed using XDS118 and the CCP4 suite of programs. The structures were solved by molecular replacement using PHASER implemented in CCP4.120.

The GluA2 LBD structure in complex with (S)-CPW399 was used as search model for the GluA2 LBD in complex with our compounds. Furthermore, the amino acid residues of GluA2 LBD were built using Autobuild in PHENIX. Ligand coordinates were prepared by using the PRODRG server and fitted into the electron density. Topology and parameter files were obtained by using eLBOW after geometry optimization. After PHENIX refinements structures of the GluA2 complexes were validated in PHENIX as well as using the PDB validation server.

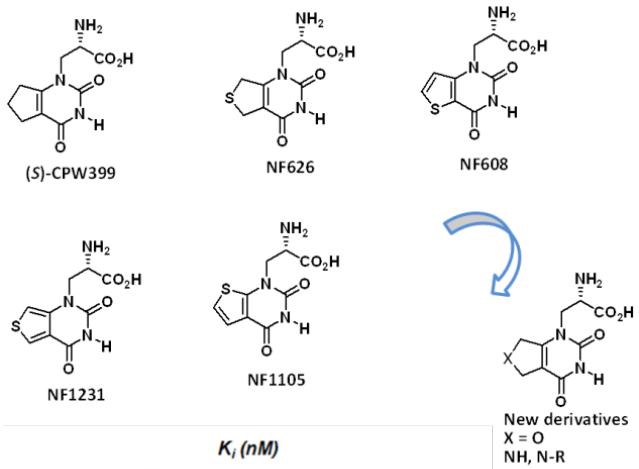

K_i (nM)			
Cmpds	GluA2	GluK1	GluK3
(S)-CPW399	223	44	5,090
NF626	80	5.20	>1,000,000
NF608	112	5.29	>1,000,000
NF1231	465	3.90	1,022
NF1105	503	5.89	4,750

Figure 1: Structure of representative compounds

3 Findings and argument

X-ray crystal structure of NF626 (Figure 1) in complex with GluA2 LBD shows similar binding mode as that of a previously developed ligand (S)-CPW399 (Figure 1). Docking studies in the GluK1 cleft traces out this binding mode. Based on these findings we designed a new series of compounds, bearing different heteroatoms (N or O) as bioisosteric replacement of the sulfur atom (Figure 1). For two of these compounds we were able to get crystal structures at 1.0 Å and 1.15 Å resolution for the GluA2 LBD. The X-ray studies with GluA2 LBD were used for a structure-activity relationship (SAR) analysis. Analysis of superimposed crystal structures of the two compounds and (S)-CPW399 in complexes with GluA2 LBD reveals that the α-amino acid moiety of all three compounds establishes similar contacts with surrounding residues (Pro478, Thr480, Arg485, Ser654 and Glu705) and two water molecules (W1 and W2). Interactions with water molecule W4 (present in two different positions) was observed for one compound; interestingly, this interaction was not found in (S)-CPW399 crystal structure. But the most crucial difference in the X-ray complexes of the new compounds was the conformation of Glu402 which was different form that in the X-ray structure of our lead (S)-CPW399. This may be the relevant feature responsible for the different affinity of these compounds. In addition, the number of water molecules near the GluA2 LBD was quite similar for the analyzed compounds also in comparison with the X-ray structures resolved in complex with the GluK3 LBD (despite the different aminoacidic composition). Taken together all the observed similarities and differences will drive the computational studies needed for rationalizing the recently determined differences in affinity and selectivity of the new compounds.

4 Conclusion

Based on the structure of (*S*)-CPW399 we rationally designed a series of pyrimidynedione-raleted analogues which displayed different potencies and selectivity towards AMPA and KA receptor subtypes. These differences were analyzed by means of computational studies and crystallography. Preliminarly in vivo data (formalin test) have demonstrated an antinociceptive effect for our potent and selective GluK1 ligands.

References

Butini, S., Pickering, D. S., Morelli, E., Coccone, S. S., Trotta, F., et al. (2008). 1 H -Cyclopentapyrimidine-2,4(1 H ,3 H)-dione-Related Ionotropic Glutamate Receptors Ligands. Structure–Activity Relationships and Identification of Potent and Selective iGluR5 Modulators. *J. Med. Chem.* 51(20), 6614–6618.

Campiani, G., De Angelis, M., Armaroli, S., Fattorusso, C., Catalanotti, B., et al. (2001). A Rational Approach to the Design of Selective Substrates and

Potent Nontransportable Inhibitors of the Excitatory Amino Acid Transporter EAAC1 (EAAT3). New Glutamate and Aspartate Analogues as Potential Neuroprotective Agents. *J. Med. Chem.* 44(16), 2507–2510.

Campiani, G., Fattorusso, C., Angelis, M., Catalanotti, B., Butini, S., et al. (2003). Neuronal High-Affinity Sodium-Dependent Glutamate Transporters (EAATs): Targets for the Development of Novel Therapeutics Against Neurodegenerative Diseases. *CPD.* 9(8), 599–625.

Campiani, G., Morelli, E., Nacci, V., Fattorusso, C., Ramunno, A., et al. (2001). Characterization of the 1 H -Cyclopentapyrimidine-2,4(1 H ,3 H)-dione Derivative (S)-CPW399 as a Novel, Potent, and Subtype-Selective AMPA Receptor Full Agonist with Partial Desensitization Properties. *J. Med. Chem.* 44(26), 4501–4504.

Dolman, N. P., More, J. C. A., Alt, A., Knauss, J. L., Pentikäinen, O. T., et al. (2007). Synthesis and Pharmacological Characterization of N 3 -Substituted Willardiine Derivatives: Role of the Substituent at the 5-Position of the Uracil Ring in the Development of Highly Potent and Selective GLU K5 Kainate Receptor Antagonists. *J. Med. Chem.* 50(7), 1558–1570.

Venskutonyte, R., Butini, S., Sanna Coccone, S., Gemma, S., Brindisi, M., et al. (2011). Selective Kainate Receptor (GluK1) Ligands Structurally Based upon 1 H -Cyclopentapyrimidin-2,4(1 H ,3 H)-dione: Synthesis, Molecular Modeling, and Pharmacological and Biostructural Characterization. *J. Med. Chem.* 54(13), 4793–4805.

Synthesis, Pharmacological assessment and Molecular Modeling of Acetylcholinesterase/Butyrylcholinesterase inhibitors: Effect against Amyloid-beta - induced Neurotoxicity

Daniel Silva[1,2], Mourad Chioua[2], Abdelouahid Samadi[2], Paula Agostinho[*3,4], Pedro Garção[3,4], Rocío Lajarín-Cuesta[5], Cristobal de los Ríos[5], Isabel Iriepa[6], Ignacio Moraleda[6], Laura Gonzalez-Lafuente[5], Eduarda Mendes[1], Concepción Pérez[7], María Isabel Rodríguez-Franco[7], José Marco-Contelles[2], and Maria do Carmo Carreiras[1]

[1]iMed.ULisboa, Faculty of Pharmacy, Av. Prof. Gama Pinto, 1649-003 Lisboa, Portugal

[2]Laboratorio de Química Médica (IQOG, CSIC), C/ Juan de la Cierva 3, 28006-Madrid, Spain

[3]Center for Neuroscience and Cell Biology, University of Coimbra, 3004-517 Coimbra, Portugal

[4]Faculty of Medicine, University of Coimbra, 3004-504 Coimbra, Portugal

[5]Instituto Teófilo Hernando, Fundación de Investigación Biomédica, Hospital Universitario de la Princesa, C/ Diego de Léon, 62, 28006-Madrid, Spain.

[6]Departamento de Química Orgánica. Universidad de Alcalá, Ctra. Madrid-Barcelona, Km. 33,6, 28871, Alcalá de Henares, Madrid, Spain.

[7]Instituto de Química Médica (CSIC), C/ Juan de la Cierva 3, 28006-Madrid, Spain.

*pagostinho@fmed.uc

Abstract. The synthesis, molecular modeling, and pharmacological analysis of phenoxyalkylamino-4-phenylnicotinates (**2-7**), phenoxyalkoxybenzylidene-malononitriles (**12-13**), pyridonepezils (14-18), and quinolinodonepezils (**19-21**) are described. Pyridonepezils **14-18** were found to be selective and moderately potent regarding the inhibition of hAChE, whereas quinolinodonepezils **19-21** were found to be poor inhibitors of hAChE. The most potent and selective hAChE inhibitor was ethyl 6-(4-(1-benzylpiperidin-4-yl)butylamino)-5-cyano-2-methyl-4-phenylnicotinate (**18**) [IC50 (hAChE)=0.25(2) µM]. Pyridonepezils 14-18 and quinolinodonepezils **20-21** are more potent selective inhibitors of EeAChE than hAChE. The most potent and selective EeAChE inhibitor was ethyl 6-(2-(1-benzylpiperidin-4-yl)ethylamino)-

5-cyano-2-methyl-4-phenylnicotinate (20-21) [IC50 (EeAChE)=0.0167(2) µM], which exhibits the same inhibitory potency as donepezil against hAChE. Compounds **2**, **7**, **13**, **17**, **18**, **35** and **36** significantly prevented the decrease in cell viability caused by Aβ1-42. All compounds were effective in preventing the enhancement of AChE activity induced by Aβ1-42. Compounds **2-7** caused a significant reduction whereas pyridonepezils **17** and **18**, and compound **16** also showed some activity. The pyrazolo[3,4-b]quinolines **36** and **38** also prevented the upregulation of AChE induced by Aβ1-42. Compounds **2**, **7**, **12**, **13**, **17**, **18** and **36** may act as antagonists of VSCC since they significantly prevented the Ca^{2+} influx evoked by KCl depolarization. Docking studies show that compounds **16** and **18** adopted different orientations and conformations inside the active-site gorges of hAChE and hBuChE. The structural and energetic features of the **16**-AChE and 18-AChE complexes compared to the **16**-BuChE and 18-BuChE complexes account for a higher affinity of the ligand toward AChE. The present data indicate that compounds **2**, **7**, **17**, **18** and **36** may represent attractive multipotent molecules for the potential treatment of Alzheimer's disease.

Keywords Pyridonepezils – Quinolinodonepezils – AChE/BuChE inhibitors – Aβ peptide – Alzheimer's disease.

1 Introduction

Alzheimer's disease (AD) is the most prevalent neurodegenerative disorder (Bertram and Tanzi, 2008). Since the symptoms of AD were associated with an altered cholinergic function, research has focused on the basal forebrain cholinergic system (Wenk, 2003). In the context of our continued interest in the development of new multipotent drugs for the treatment of AD (Leon and Marco-Contelles, 2011) we have started a project targeted to the design and biological analysis of dual AChEIs endowed with additional properties. The syntheses and biological assessment of **pyridonepezils 14-18** (Figure 1), and the **quinolinodonepezils** derivatives **19-21** (Figure 2) are briefly reported.

2 Methods

The syntheses of pyridonepezils **14-17** and quinolinodonepezils **19-21** have been carried out according to the schemes outlined in Figures 1 and 2, respectively (Silva et al., 2013).

Pharmacological assessment involved inhibition of EeAChE/eqBuChE, hAChE/hBuChE (Ellman's protocol) (Ellman et al., 1961), kinetic analysis of AChE inhibition (compounds **16** and **18**) (Silva et al., 2013),

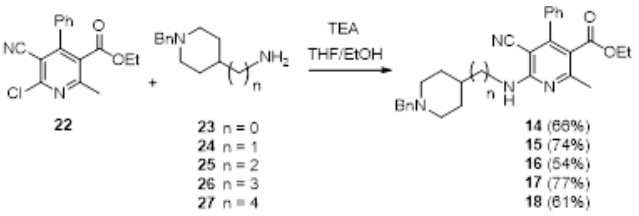

Figure 1: Synthesis of pyridonepezils **14-18** (Silva et al., 2013).

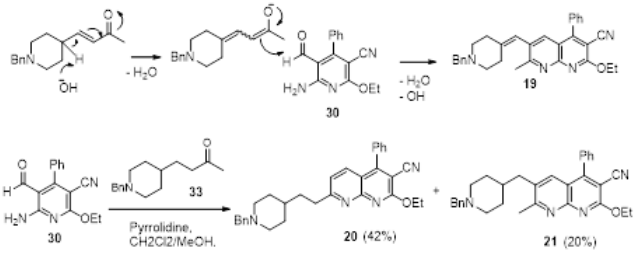

Figure 2: Synthesis of pyridonepezils **19-21** (Silva et al., 2013).

propidium iodide assay (Rosenberry et al., 1999), effect on neuronal viability with MTT (Rosenberry et al., 1999; Lopes et al., 2009), neuroprotection against Aβ-toxicity(Resende et al., 2008), the impact on the enhancement of AChE activity caused by Aβ peptides(Melo et al., 2003), the effect of compounds in intracellular Ca^{2+} homeostasis dysregulation (Demuro et al., 2010), and molecular modelling studies (Silva et al., 2013).

3 Findings and argument

Table 1: Inhibition of EeAChE and eqBuChE by the most potent pyridonepezils (**16-18**)[a]. (Silva et al., 2013)

Compound	Structure	IC_{50} AchE (µM)	IC_{50} BuChE (µM)
Donepezil	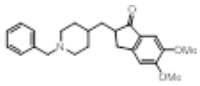	0.0134(9)	0.84(5)
16	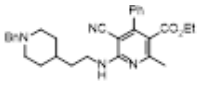	0.0167(7)	0.88(8)
17	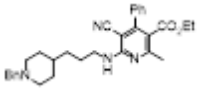	0.019(2)	0.31(5)
18	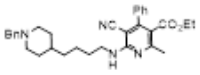	0.030(4)	0.380(18)

[a] Data are expressed as the mean ± SEM of at least three different experiments in quadruplicate.

Pyridonepezils **14-18** were found to be selective regarding the inhibition of *Ee*AChE and hAChE.

Table 2: Inhibition of hAChE/hBuChE by the most potent pyridonepezils (**16-18**)[a].

Compound	Structure	IC_{50} hAchE (µM)	IC_{50} hBuChE (µM)
Donepezil	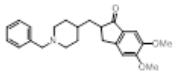	0.016(1)[b]	8.2(2)[c]
16	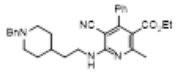	0.31(4)	4.00(50)
17	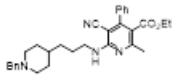	0.320(37)	8.59(60)
18	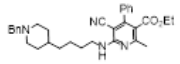	0.25(2)	> 10

[a] Data are expressed as the mean ± SEM of at least three different experiments in quadruplicate;
[b] Notes: Human recombinant AChE
[c] Human serum BuChE (Silva et al., 2013).

IC_{50} values were similar in a few cases (ranging from 0.25 to 4.57 µM. The most potent and selective *Ee*AChE inhibitor was ethyl 6-(2-(1-benzylpiperidin-4-yl)ethylamino)-5-cyano-2-methyl-4-phenylnicotinate (**16**) [IC_{50} (*Ee*AChE)=0.0167(7) µM] (Table 1), which exhibits similar inhibitory potency as donepezil against hAChE (Table 2). The most potent and selective hAChE inhibitor was ethyl 6-(4-(1-benzylpiperidin-4-yl)butylamino)-5-cyano-2-methyl-4-phenylnicotinate (**18**) [IC_{50} (hAChE)=0.25(2) µM] (Table 2). Kinetic analysis of the AChE inhibition by compounds **16** and **18** showed they were non-competitive inhibitors. Cell viability measured as MTT reduction showed that exposure of SH-SY5Y cells during 24 h with 5 µM of the pyridonepezils (**14-18**) did not significantly affect neuronal viability. Moreover, the decrease in cell viability caused by $A\beta_{1-42}$ was significantl prevented by compounds **17** (2.5 µM) and **18** (2.5 µM). In this study $A\beta_{1-42}$ peptide was also examined to enhance AChE activity by about 20 %. All compounds were effective in preventing the enhancement of AChE activity induced by $A\beta_{1-42}$. Pyridonepezils **17** and **18** decreased the activity by 50 % and 30 %, respectively; whereas compound **16** caused a reduction of about 12 %. At 100 µM, compound **18**, which seems to inhibit AChE by a non-competitive mechanism, showed a slight but significant ability to displace propidium iodide 2 µM from the PAS of AChE (12(3) % over control). It was observed that compounds **17** and **18** expressively prevented the Ca^{2+} influx evoked by KCl (50 mM) depolarization, suggesting that this set of compounds can act as antagonists of VSCC. Compounds **16** and **18** were found to adopt different orientations and conformations inside the active-site gorges of hAChE and hBuChE. Compound 16 showed a binding geometry in *Ee*AChE very similar to the one displayed by the compound in hAChE. The structural and energetic features of the ligand-AChE complex compared to the ligand-BuChE complex account for a higher affinity of the ligands toward AChE. For ligands **16** and **18** the energy of the bioactive conformation in BuChE is higher than that in AChE. This energy difference is much higher for compound **18**, which may explain its selectivity.

4 Conclusions

The present data indicate that compounds **17** and **18** are attractive multipotent molecules acting in different key pharmacological targets. Thus, they may accomplish a potential disease-modifying role in the treatment of AD.

References

Bertram, L. and Tanzi, R. E. (2008). Thirty years of Alzheimer's disease genetics: the implications of systematic meta-analyses. *Nat Rev Neurosci.* 9(10), 768–778.

Demuro, A., Parker, I. and Stutzmann, G. E. (2010). Calcium Signaling and Amyloid Toxicity in Alzheimer Disease. *J. Biol. Chem.* 285(17), 12463–12468.

Ellman, G. L., Courtney, K., Andres, V. and Featherstone, R. M. (1961). A new and rapid colorimetric determination of acetylcholinesterase activity. *Biochem. Pharmacol.* 7(2), 88–95.

Leon, R. and Marco-Contelles, J. (2011). A Step Further Towards Multitarget Drugs for Alzheimer and Neuronal Vascular Diseases: Targeting the Cholinergic System, Amyloid-β; Aggregation and Ca2+ Dyshomeostasis. *CMC.* 18(4), 552–576.

Lopes, J. P., Oliveira, C. R. and Agostinho, P. (2009). Cdk5 acts as a mediator of neuronal cell cycle reentry triggered by amyloid-β and prion peptides. *Cell Cycle.* 8(1), 97–104.

Melo, J. B., Agostinho, P. and Oliveira, C. R. (2003). Involvement of oxidative stress in the enhancement of acetylcholinesterase activity induced by amyloid beta-peptide. *Neurosci. Res.* 45(1), 117–127.

Resende, R., Ferreiro, E., Pereira, C. and de Oliveira, C. (2008). Neurotoxic effect of oligomeric and fibrillar species of amyloid-beta peptide 1-42: Involvement of endoplasmic reticulum calcium release in oligomer-induced cell death. *Neuroscience.* 155(3), 725–737.

Rosenberry, T. L., Mallender, W. D., Thomas, P. J. and Szegletes, T. (1999). A steric blockade model for inhibition of acetylcholinesterase by peripheral site

ligands and substrate. *Chem. Biol. Interact.* 119-120, 85–97.

Silva, D., Chioua, M., Samadi, A., Agostinho, P., Garção, P., et al. (2013). Synthesis, Pharmacological Assessment, and Molecular Modeling of Acetylcholinesterase/Butyrylcholinesterase Inhibitors: Effect against Amyloid-β-Induced Neurotoxicity. *ACS Chem. Neurosci.* 4(4), 547–565.

Wenk, G. L. (2003). Neuropathologic changes in Alzheimer's disease. *J. Clin. Psychiatry.* 64 Suppl 9, 7–10.

Chronic L-DOPA alters the activity of monoamine oxidase in vivo

De Deurwaerdère Philippe*[1]; Di Giovanni Giuseppe[2]

[1]Institut des Maladies Neurodégénératives; UMR CNRS 5293; Université Bordeaux; 146 rue Léo Saignat; 33076 Bordeaux, France

[2]Department of Physiology and Biochemistry, Faculty of Medicine and Surgery, University of Malta - Msida, Malta; School of Biosciences, Cardiff University - Cardiff, UK.

*deurwaer@u-bordeaux2.fr

Abstract. We have hypothesed that the function of monoamine oxidase (MAO), normally using three tyrosines to correctly place the substrate in the catalytic site, should be diminished by the substitution of tyrosine by exogenous L-DOPA, the main treatment of Parkinson's disease. We have studied the activity of MAO in vivo after chronic treatment of L-DOPA in naive or hemiparkinsonian rats. To study MAO activity, increasing concentrations of 3-methoxytyramine (3-MT) were applied by reverse intracerebral microdialysis in the striatum and the cortex of rats and the product of 3-MT via MAO,homovanillic acid (HVA) was collected and analyzed using HPLC. We show that the ability of 3-MT to enhance HVA dialysate content in a concentration-dependent fashion was lowered by the chronic treatment with L-DOPA in naïve (50 mg/kg) or 6-hydroxydopamine (6-OHDA) rats (3 or 50 mg/kg). The effect of 3-MT was not affected by peripheral administration of the inhibitor of MAOB F2MPA. The chronic treatment with L-DOPA lowers the function of MAO, presumably MAOA. The research will continue with members of the action CM1103 using appropriate and new pharmacological compounds, namely IMAOA.

Keywords Parkinson's disease – monoamine oxidase – in vivo intracerebral microdialysis – Dopamine and homovanillic acid extracellular levels – 3-methoxytyramine.

1 Introduction

Exogenous L-DOPA in a very efficient medication in Parkinson's disease, but its efficacy is impaired after several years of treatment by numerous side effects including dyskinesia. The presumed role of neo-synthesized DA itself, produced from the decarboxylation of L-DOPA, is not very clear in L-DOPA-induced dyskinesia in both rats and monkeys (Navailles et al., 2011; Porras et al., 2014). This is in part related to the main role of serotonergic neurons in releasing neo-synthesized

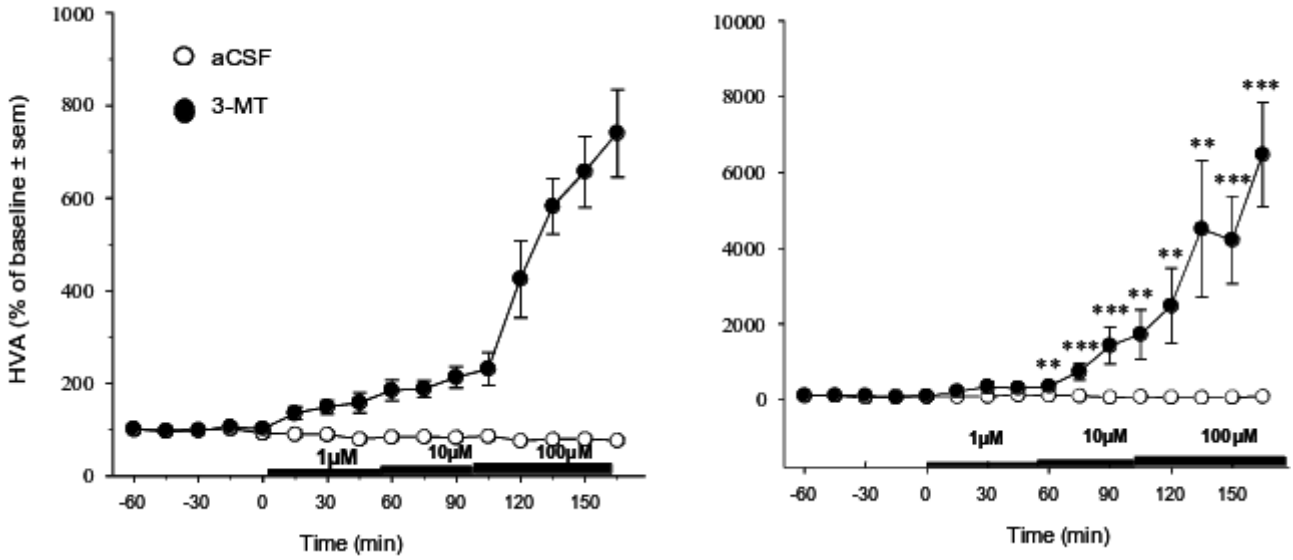

Figure 1: Effect of the local infusion of 1, 10 and 100 µM (each 1-h) 3-MT on the extracellular levels of HVA in the striatum and the prefrontal cortex. Baseline has been calculated from the mean raw data of the 3 fractions preceding the application of 3-HT. * refers to Student's t-test (p< 0.01 or 0.001).

dopamine in the whole brain (Navailles et al., 2011, 2014).This suggests that other mechanisms exist apart from the excessive DA released in L-DOPA-induced dyskinesia. Monoamine oxidase (MAO) A and B are involved in the intracellular catabolism of monoamines. Within the COST action CM1103, several works have been conducted to show that the function of MAO relies on three tyrosines correctly placing the substrate in the catalytic site (Repič et al., 2014). We have postulated here that exogenous L-DOPA would be incorporated in MAO by substituting tyrosine residue (Chan et al., 2012), thereby diminishing the activity of the enzyme in vivo.

2 Methods

To study the activity of MAO in vivo after chronic L-DOPA treatment, we have applied increasing concentrations of 3-methoxytyramine (3-MT), a poorly, biologically active compound that is a substrate of MAO, by reverse intracerebral microdialysis in the striatum and the prefrontal cortex (PFC) of isoflurane-anesthetized rats, simultaneously (Navailles et al., 2013). We have measured dialysate content of homovanillic acid (HVA), the product of 3-MT via MAO, using high pressure liquid chromatography coupled to electrochemical detection (HPLC-EC). The aCSF perfusion (2 µL/min) lasted throughout the whole experiment and dialysate samples were collected every 15 minutes. Each concentration of 3-MT (1, 10 and 100 µM) has subsequently been applied for 1-h. Chronic treatment consisted of daily intraperitoneal administration for 15 days of exogenous L-DOPA methyl ester (free base) at 50 mg/kg in naïve rats and 3 or 50 mg/kg in 6-hydroxydopamine-lesioned (6-OHDA) rats. Stereotaxic coordinates for probe implantation and the experiments, including histological examine, lesion of DA neurons and post-mortem evaluation using HPLC-EC of the extend and the selectivity of the DA lesions performed with 6-OHDA, have been performed according to recently published papers (Navailles et al., 2011, 2013, 2014).

3 Findings and argument

HVA dialysate content in the striatum and the PFC were, respectively: 1630(15) and 8.0(3) pg/30µl. Local infusion of 3-MT enhanced HVA dialysate content in a concentration-dependent manner in both brain regions in naive rats (Figure 1). This effect is maintained in 6-OHDA-lesioned rats in which basal extracellular levels were dropped to 160.0(77) and 3.5(18) pg/30µl, in the striatum and the PFC, respectively. Chronic treatment with exogenous L-DOPA (50 mg/kg) in naïve rats reduced the ability of 3-MT to enhance HVA in the striatum.

In 6-OHDA-lesioned rats, the chronic exposure to L-DOPA at both 3 and 50 mg/kg reduced the ability of 3-MT to produce HVA in both the striatum and the cortex. The rise in HVA extracellular levels was reduced by 70 % in the striatum in both 3 and 50 mg/kg L-DOPA-treated rats but only for the 10 µM concentration of 3-MT ($p < 0.01$, Fisher PLSD after significant

ANOVA). The rise in HVA extracellular levels was reduced by about 80 % in the PFC for the whole concentration response of 3-MT ($p < 0.001$).

MAOB was probably not involved in these effects as the intraperitoneal administration (1 mg/kg) of the selective MAOB inhibitor F2MPA (Di Giovanni et al., 2014), did not alter 3-MT-stimulated HVA production in either naïve or 6-OHDA-lesioned rats.

4 Conclusion

We have built a new in vivo approach for the function of MAO using local application of 3-MT. This allowed us to show that the chronic treatment with L-DOPA lowers the function of MAO, presumably MAOA, in both naive and 6-OHDA rats. These findings are compatible with the incorporation of exogenous L-DOPA into proteins (Chan et al., 2012), though they still do not constitute any proof. The research will continue with appropriate pharmacological tools, namely IMAOA.

References

Chan, S. W., Dunlop, R. A., Rowe, A., Double, K. L. and Rodgers, K. J. (2012). l-DOPA is incorporated into brain proteins of patients treated for Parkinson's disease, inducing toxicity in human neuroblastoma cells in vitro. *Exp. Neurol.* 238(1), 29–37.

Di Giovanni, G., García, I., Colangeli, R., Pierucci, M., Rivadulla, M. L., et al. (2014). N-(furan-2-ylmethyl)-N-methylprop-2-yn-1-amine (F2MPA): A potential cognitive enhancer with MAO inhibitor properties. *CNS Neurosci. Ther.* 20(7), 633–40.

Navailles, S., Bioulac, B., Gross, C. and De Deurwaerdère, P. (2011). Chronic L-DOPA therapy alters central serotonergic function and L-DOPA-induced dopamine release in a region-dependent manner in a rat model of Parkinson's disease. *Neurobiol. Dis.* 41(2), 585–590.

Navailles, S., Lagière, M., Contini, A. and De Deurwaerdère, P. (2013). Multisite Intracerebral Microdialysis to Study the Mechanism of L-DOPA Induced Dopamine and Serotonin Release in the Parkinsonian Brain. *ACS Chem. Neurosci.* 4(5), 680–692.

Navailles, S., Milan, L., Khalki, H., Di Giovanni, G., Lagière, M. and De Deurwaerdère, P. (2014). Noradrenergic terminals regulate L-DOPA-derived dopamine extracellular levels in a region-dependent manner in Parkinsonian rats. *CNS Neurosci. Ther.* 20(7), 671–8.

Porras, G., De Deurwaerdere, P., Li, Q., Marti, M., Morgenstern, R., et al. (2014). L-dopa-induced dyskinesia: beyond an excessive dopamine tone in the striatum. *Sci. Rep.* 4.

Repič, M., Purg, M., Vianello, R. and Mavri, J. (2014). Examining Electrostatic Preorganization in Monoamine Oxidases A and B by Structural Comparison and pKa Calculations. *J. Phys. Chem. B.* 118(16), 4326–4332.

Support the EU COST Actions CM1103 as well as the PEPS-IDEX plan of 2013.

Continuous determination of hROS during microdialysis

Bashkim Misini*[1], Maria Alessandra Colivicchi[2], Wolfhardt Freinbichler[1], Chiara Ballini[2], Wolfgang Linert[1], Keith F. Tipton[3], Laura Della Corte[2]

[1]Institute for Applied Synthetic Chemistry, Vienna University of Technology, Getreidemarkt 9/163-AC, A-1060 Vienna, Austria

[2]Dipartimento di Neuroscienze, Psicologia, Area del Farmaco e Salute del Bambino (NEUROFARBA), Università degli Studi di Firenze, Viale G. Pieraccini 6, 50139 Firenze, Italy

[3]School of Biochemistry and Immunology, Trinity College Dublin, Dublin 2, Ireland

*b_misini@hotmail.com

Abstract. A procedure has been developed for the direct determination of hROS formation by monitoring the conversion of terephthalic acid to the highly fluorescent 2-hydroxy terephthalate by direct flow fluorimetry. The method should allow the rapid assessment of hROS formation evoked by a variety of neurotoxins and other compounds in microdialysis experiments *in vivo*.

Keywords kainate – microdialysis – terephthalic acid – 2-hydroxy terephthalate

1 Introduction

Reactive oxygen species (ROS), which include hydrogen peroxide and superoxide, are more reactive than O_2 itself, but relatively stable and are involved in variety of cell-signaling processes. These may be converted to, the toxic, highly reactive oxygen species (hROS) in the presence of transition metal ions, such as Fe(II). The hROS may exist as free hydroxyl radicals (HO·), as bound ("crypto") radicals or as Fe(IV)−oxo (ferryl) species. Although it is still unclear whether oxidative stress is the primary initiating event, hROS production is considered to play a major role in the cycle of events that results in neurodegeneration (Andersen, 2004).

Direct measurement of hROS is difficult, owing to their very short lifetime and high reactivity. We have previously shown that hROS may be detected by a reaction with terephthalic acid (TA^{2-}) to form the fluorescent product 2-hydroxy terephthalate (OH-TA). The procedure involved inclusion of 250 µM TA^{2-} in the artificial CSF microdialysis perfusing mixture and subsequent determination of OH-TA fluorescence in fractions of the microdialysate, collected at 20 min intervals, with excitation and emission wavelengths set to 340 and 455 nm (Freinbichler et al., 2008). This assay has been shown to be highly sensitive and specific for hROS. Furthermore, TA^{2-} administered during microdialysis appears to be non-toxic and does not interfere with evoked release of the neurotransmitters glutamate, aspartate and taurine. (Freinbichler et al., n.d.). The excitotoxin kainate has been shown to result in the release of each of these transmitters with concomitant hROS formation when administered directly into the striatum through a microdialysis probe (Freinbichler et al., 2008). Although the quantity of extracellular hROS detected appeared to be proportional to the administered kainate concentration, in the range 250-1000 µM, no temporal difference between neurotransmitter and hROS release could be detected.

Although the collection of microdialysate fractions was necessary for amino-acid determination, which involved post-collection reaction with o-phthaldialdehyde followed by separation of the derivatives by hplc before fluorescence detection (Bianchi et al., 1999), such a procedure should not be necessary for hROS determination. The present work was designed to develop a continuous "on-line" procedure that could be used for the direct determination outlining extracellular hROS formation and levels in response to neurotoxic and other stimulants during microdialysis experiments. It was hoped such a 'real-time' procedure might provide a simpler and cheaper alternative with possibly improved time resolution. The apparatus involved the direct passage of the microdialysis effluent through a silica fluorimeter flow cell, with a T-piece splitter allowing a portion to flow into Eppendorf-tube fractions for subsequent neurotransmitter determinations, if required.

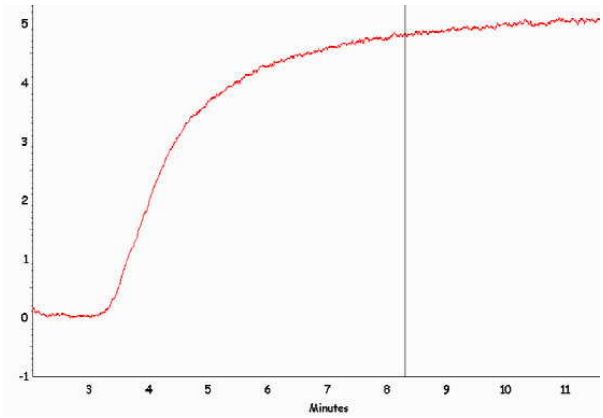

Figure 1: Fluorescence of a standard solution of 100 µM OH-TA applied through the on-line detection system (λ_{ex} 340 nm & (λ_{em} 435 nm).

2 Findings and argument

The response of the system to directly administered OH TA is shown in Figure 1. The fluorescence detected

was proportional to the OHTA concentration. Recovery of OH-TA was estimated to be $> 94\,\%$ and the detection limit was 1.18 nM. Administration of the kainate (1 mM) through the microdialysis probe was shown to evoke the release of taurine with concomitant formation of hROS, validating the suitability of this on-line procedure for hROS determination.

3 Conclusion

Thus, this direct system provides a simple and convenient procedure for assessing extracellular hROS levels evoked by neurotoxins and other compounds in microdialysis experiments *in vivo*.

References

Andersen, J. K. (2004). Oxidative stress in neurodegeneration: cause or consequence? *Nat. Med.* 10(7), S18–S25.

Bianchi, L., Della Corte, L. and Tipton, K. F. (1999). Simultaneous determination of basal and evoked output levels of aspartate, glutamate, taurine and 4-aminobutyric acid during microdialysis and from superfused brain slices. *J. Chromatogr. B Biomed. Sci. Appl.* 723(1-2), 47–59.

Freinbichler, W., Bianchi, L., Colivicchi, M. A., Ballini, C., Tipton, K. F., et al. (nodate). The detection of hydroxyl radicals in vivo. *J. Inorg. Biochem.* 102(5-6), 1329–33.

Freinbichler, W., Colivicchi, M. A., Fattori, M., Ballini, C., Tipton, K. F., et al. (2008). Validation of a robust and sensitive method for detecting hydroxyl radical formation together with evoked neurotransmitter release in brain microdialysis. *J. Neurochem.* 105(3), 738–749.

Support the EU COST Actions Action D34 & CM1103

Serotonin$_{2C}$ receptor stimulation inhibits dopamine transmission in the nucleus accumbens independently of dopamine release: studies with cocaine

Céline Devroye*[1], Adeline Cathala[1], Marlène Maitre[1], Pier Vincenzo Piazza[1], Djoher Nora Abrous[2], Jean-Michel Revest[1], Umberto Spampinato[1].

[1]Inserm, U862, Neurocentre Magendie, Physiopathology of Addiction Group and Université de Bordeaux, Bordeaux, France

[2]Inserm, U862, Neurocentre Magendie, Neurogenesis and Pathophysiology Group and Université de Bordeaux, Bordeaux, France.

*celine.devroye@inserm.fr

1 Introduction

The serotonin$_{2C}$ receptor (5-HT$_{2C}$R), in keeping with its ability to control the mesoaccumbens dopamine (DA) pathway, plays a key role in mediating the behavioral and neurochemical effects of drugs of abuse (Filip et al., 2012). Studies assessing the influence of 5-HT$_{2C}$R agonists on cocaine-induced responses have suggested that 5-HT$_{2C}$Rs can modulate mesoaccumbens DA pathway activity independently of accumbal DA release, by controlling DA transmission in the nucleus accumbens (NAc) (Navailles et al., 2004, 2008).

2 Methods

Combining neurochemical and molecular approaches in male Sprague Dawley rats, we assessed this hypothesis by studying the ability of the 5-HT$_{2C}$R agonist Ro 60-0175 to modulate cocaine-induced changes of mesoaccumbens DA pathway activity, at both pre- and postsynaptic levels. First, we assessed the effect of Ro 60-0175 on cocaine-induced accumbal DA outflow measured by intracerebral microdialysis in freely moving animals. Then, we evaluated possible changes of postsynaptic neuronal activity in the NAc, by assessing the effect of Ro 60-0175 on cocaine-induced changes of c-Fos immunoreactivity and phosphorylation states at threonine 34 and 75 residues of the DA and c-AMP regulated phosphoproteins Mr 32kDa (DARPP-32). The effect of Ro 60-0175 on cocaine-induced DARPP-32 phosphorylation was further studied in animals pretreated with the selective 5-HT$_{2C}$R antagonist SB 242084.

3 Findings and argument

We found that the intraperitoneal (i.p.) administration of 1 mg/kg Ro 60-0175 had no effect on cocaine (15 mg/kg, i.p.)-induced DA outflow in the shell and it increased in the core subregion of the NAc. Also, Ro 60-0175 inhibited cocaine-induced increase in c-Fos immunoreactivity in both subregions of the NAc. Finally, Ro 60-0175 inhibited cocaine-induced phosphorylation of the DA and c-AMP regulated phosphoprotein of Mr 32kDa (DARPP-32) at threonine residues in the NAc core, this effect being reversed by the selective 5-HT2CR antagonist SB 242084 (0.5 mg/kg, i.p.).

4 conclusion

Altogether, these findings demonstrate that 5-HT_{2C}Rs are able to modulate mesoaccumbens DA pathway activity at post-synaptic level, by specifically controlling DA signaling in the NAc core subregion. This interaction, in keeping with the tight relationship between locomotor activity and NAc DA function, could participate in the inhibitory control of cocaine-induced locomotor activity.

References

Filip, M., Spampinato, U., McCreary, A. C. and Przegaliński, E. (2012). Pharmacological and genetic interventions in serotonin (5-HT)2C receptors to alter drug abuse and dependence processes. *Brain Res.* 1476, 132–153.

Navailles, S., De Deurwaerdère, P., Porras, G. and Spampinato, U. (2004). In vivo evidence that 5-HT2C receptor antagonist but not agonist modulates cocaine-induced dopamine outflow in the rat nucleus accumbens and striatum. *Neuropsychopharmacology.* 29(2), 319–26.

Navailles, S., Moison, D., Cunningham, K. A. and Spampinato, U. (2008). Differential regulation of the mesoaccumbens dopamine circuit by serotonin2C receptors in the ventral tegmental area and the nucleus accumbens: an in vivo microdialysis study with cocaine. *Neuropsychopharmacology.* 33(2), 237–46.

Effects of the agonist RO60-0175 and the antagonist SB242084 of 5-HT2C Receptors in the development of Maximal Dentate Activation in the Hippocampus of anesthetized rats

Di Giovanni Giuseppe*[1]; De Deurwaerdère Philippe[2]

[1]Department of Physiology and Biochemistry, Faculty of Medicine and Surgery, University of Malta - Msida, Malta; School of Biosciences, Cardiff University - Cardiff, UK.

[2]Institut des Maladies Neurodégénératives; UMR CNRS 5293; Université Bordeaux; 146 rue Léo Saignat; 33076 Bordeaux, France.

*giuseppe.digiovanni@um.edu.mt

Abstract. Substantial evidence indicates that 5-HT2C receptors are involved in the control of neuronal network excitability and in seizure pathophysiology. Here, we have addressed the relatively unexplored relationship between temporal lobe epilepsy (TLE), the most frequent type of intractable epilepsy, and 5-HT2CRs. In the present study, we investigated this issue using a model of partial complex (limbic) seizures in urethane-anesthetized rat, based on the phenomenon of maximal dentate activation (MDA) using 5-HT2C compounds, electrophysiology, immunohistochemistry and western blotting techniques. The 5-HT2C agonists mCPP (1 mg/kg, i.p.) and lorcaserin (3 mg/kg, i.p.), but not RO60-0175 (1-3 mg/kg i.p.), were antiepileptogenic reducing the MDA response duration. The selective 5-HT2C antagonist SB242084 (2 mg/kg, i.p.) unveiled antiepileptogenic effects of RO60-0175 (3 mg/kg, i.p.) but did not alter those induced by mCPP and lorcaserin. Compared to control rats, electrically stimulated rats showed an increase in glutamic acid decarboxylase levels and a heterogeneous decrease in 5-HT2CR immunoreactivity in different hippocampal areas. In our animal model of TLE, mCPP and lorcaserin were anticonvulsant; likely acting on receptor subtypes other than 5-HT2C. Epileptogenesis induced early adaptive changes and reorganisation in the 5-HT2CR and GABA systems.

Keywords Temporal lobe epilepsy – dentate gyrus – serotonin receptors – memory – depression – serotonergic2C drugs – GABA

1 Introduction

The serotonin (5-hydroxytryptamine; 5-HT) 2C receptor (5-HT2CR) subtype is one of the most studied members of the serotonin receptor family that holds up to 14 subtypes (Di Giovanni et al., 2011; Higgins et al., 2013; De Deurwaerdère et al., 2013; Hoyer et al., 2002). This is not surprising, considering that it is widely expressed within the central nervous system (CNS), and is thought to play a major role in 5-HT regulation of a plethora of behaviours. Despite the importance of the 5-HT2CR, our understanding of its complex signal transduction properties remains incomplete. This is due to its distinctive regulatory properties, such as constitutive activity and RNA-editing in vivo and especially the scarcity of subtype-selective drugs (Di Giovanni et al., 2006; Navailles, Lagière, Guthrie and Deurwaerdère, 2013). Nevertheless, 5-HT2CR has been shown by experimental and clinical observation to represent a possible therapeutic target for the development of drugs for a range of CNS disorders such as schizophrenia, depression, drug abuse, eating disorders and Parkinson's disease to name but a few (Di Giovanni et al., 2011; Crunelli and Di Giovanni, 2014; Navailles, Lagière, Guthrie and Deurwaerdère, 2013; Di Giovanni et al., 2006). Since activation of 5-HT2CRs suppresses neural network hyperexcitability in different brain areas (Jakus and Bagdy, 2011; Isaac, 2005; Crunelli and Di Giovanni, 2014) it might play a similar role in the hippocampus. This hypothesis is corroborated by the high 5-HT2CR mRNA and protein hippocampal expression (Pompeiano et al., 1994; Abramowski et al., 1995) with immunoreactivity for the 5-HT2C receptor, wildly located in the polymorphic cell layer of the dentate gyrus (DG), in the pyramidal cell layer of hippocampus proper (CA1, CA2, and CA3 fields), in the mossy fibers of CA3 and in the subiculum (Li et al., 2004; Clemett et al., 2000). Moreover, 5-HT2C knock out (KO) mice show a selective impairment of DG plasticity in vitro, spatial learning impairment and emergence neophobia (Tecott et al., 1998). Consistently, 5-HT2CR activation decreases theta oscillations (Sörman et al., 2011) implying that 5-HT2CR antagonists might have therapeutic significance in psychiatric or neurological disorders associated with impaired cognitive functions and epilepsy. 5-HT2CR KO mice are extremely susceptible to audiogenic seizures (Brennan et al., 1997), and prone to spontaneous death from seizures (Tecott et al., 1995). Furthermore, an upregulation of 5-HT2CRs with an increase in hippocampal gene expression and inositol triphosphate content and associated depressive mood behavioural changes have recently been shown in pilocarpine-induced temporal lobe epilepsy (TLE) in rats (Krishnakumar et al., 2009).

Despite these compelling data, research on the role of 5-HT2CRs in TLE, the most frequent type of intractable epilepsy, has been relatively scarce and lead to conflicting results (Jakus and Bagdy, 2011; Bagdy et al., 2007).

In the present study, we used a model of partial complex (limbic) seizures based on the phenomenon of maximal dentate activation (MDA) recorded in the DG, induced by repetitive electrical stimulation of the perforant path (PP) in anesthetized rats (Orban et al., 2013; Stringer and Lothman, 1990). To answer the question of a possible involvement of 5-HT2CR in TLE, we evaluated the anticonvulsant properties of a 5-HT2CR agonist RO60-0175 and the selective 5-HT2CR antagonist SB 242084 using the MDA animal model.

2 Methods

2.1 Maximal dentate activation

The induction of the MDA was started when normal DG excitability was revealed, 30 minutes or more following surgery. This was assessed by paired pulse stimulation with two different inter-pulse intervals (i.e. 25 and 150 msec), capable of inducing fast inhibition and excitation, respectively (Orban et al., 2013; Di Giovanni et al., 2014). MDA was characterized electrophysiologically according to published criteria (Stringer et al., 1989; Orban et al., 2013). Stimulus trains of 10 s (pulses of 0.3 ms duration, at 20 Hz) were delivered through the PP electrode at an initial intensity of 100 µA. If MDA was not elicited, the stimulus intensity was increased in 50 µA steps and redelivered every 2.5 minutes until MDA was induced. Threshold was reached at 350(100) µA, and stimulus intensity was further increased by 100 µA. For each stimulus, the duration of MDA, time-to-onset and after discharge (AD) were measured as shown in Figure 1C.

Repeated trains inducing-seizure were delivered every 10 min for 4 h (total of 24 stimulus trains). As shown in Figure 1D, the latency to MDA onset was measured from stimulus onset to the point of PS appearance with half of the maximal amplitude (Orban et al., 2013).

After the AD began to lengthen, either drug or vehicle was administered, after six stimulus train. In the vehicle group, the duration of MDA increases and the time to onset gradually decreases (Stringer and Lothman, 1990; Orban et al., 2013). In order to make comparisons across animals, the measured durations of MDA and time to onset were 'normalized' by subtracting their duration in response to the first stimulus from the duration in response to each subsequent stimulus train. Thus, for individual stimulus trains after the first, a change in duration (or time to onset) was calculated. In this way, data from separate animals were averaged and comparisons across groups of animals were made (Stringer and

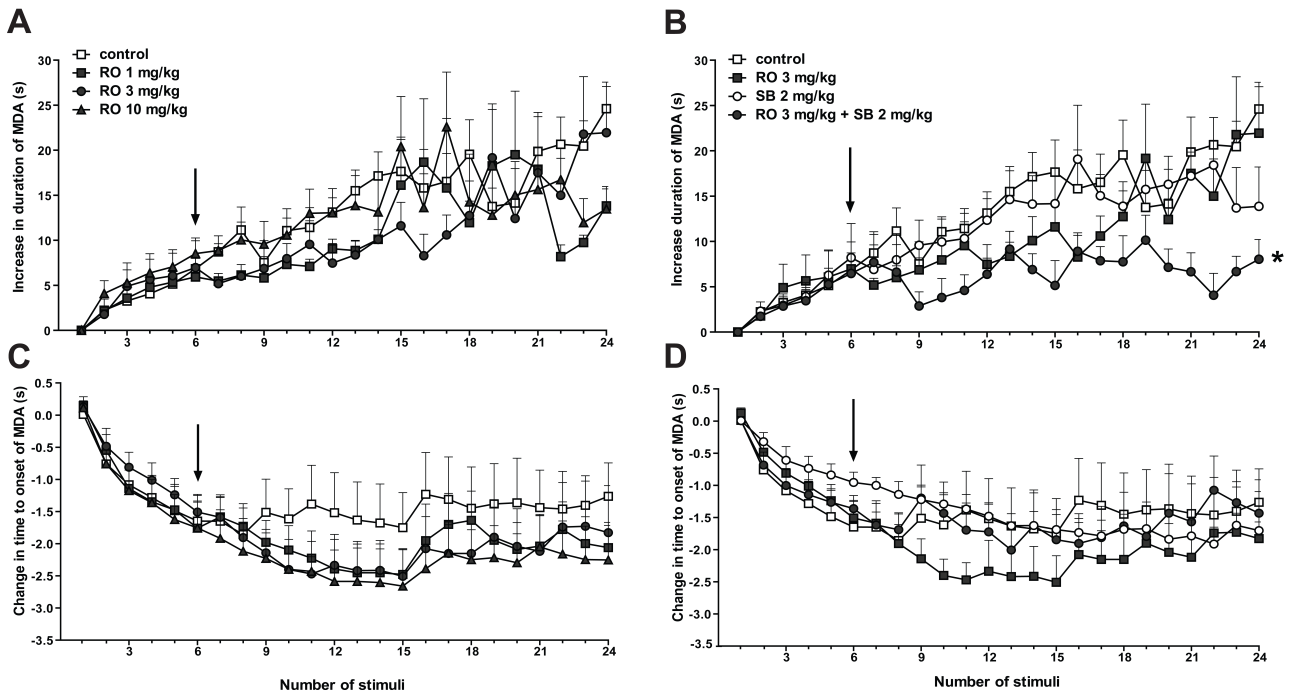

Figure 1: Effect of RO60-0175 (RO) on the parameters of the maximal dentate activation (MDA). The duration and time to onset of MDA were measured for each stimulus train. These values were then normalized, averaged and plotted (± SEM) against stimulus number. Drugs were administered i.p. at the arrows. The open square line indicates the mean values from the vehicle control animals (n = 9). The effect of RO at 1 mg/kg (n = 5, filled squares), 3 mg/kg (n = 7, filled circles) and 10 mg/kg (n = 6, filled triangles) on the increase in duration of MDA (A) and on the change in the time to onset of MDA (C). The effect of SB242084 2 mg/kg alone (n = 5, empty circles) or combined with RO 3 mg/kg (n = 7, filled circles), on the increase in duration of MDA (B) and on the change in the time to onset of MDA (D). One-way ANOVA for repeated measures followed by Fisher's PLSD post-hoc test; * $p < 0.05$. vs vehicle group.

Lothman, 1990; Orban et al., 2013).

3 Findings and argument

3.1 Effect of RO60-0175 on MDA parameters and role of 5-HT2C receptors

Despite a trend toward a decrease after 1 or 3 mg/kg, RO60-0175 did not significantly alter the duration of MDA (Figure 1A). Statistical analysis revealed a significant reduction of the MDA elongation by co-treatment with SB 242084 (2 mg/kg, i.p.) and RO60-0175 (3 mg/kg). However, SB 242084 was without effect by itself (Figure 1B). Despite a trend toward inhibition, RO60-0175 (1, 3, 10 mg/kg n = 6) did not alter the onset of the MDA (Figure 1C). Pre-treatment with the selective 5-HT2C antagonist SB242084 (2 mg/kg, i.p, n = 7), without effect by itself, did not reveal any interaction with 3 mg/kg RO60-0175 on the time to onset of MDA (Figure 1D). Conversely, RO60-0175 (1, 3, 10 mg/kg, n = 6 for each dose), SB242084 (2 mg/kg, n = 7) and co-treatment with 3 mg/kg RO60-0175 and SB242084 did not effected the onset of the MDA (Figure 1C,D).

Effect of RO60-0175 (RO) on the parameters of the maximal dentate activation (MDA). The duration and time to onset of MDA were measured for each stimulus train. These values were then normalized, averaged and plotted (± SEM) against stimulus number. Drugs were administered i.p. at the arrows. The open square line indicates the mean values from the vehicle control animals (n = 9). The effect of RO at 1 mg/kg (n = 5, filled squares), 3 mg/kg (n = 7, filled circles) and 10 mg/kg (n = 6, filled triangles) on the increase in duration of MDA (A) and on the change in the time to onset of MDA (C). The effect of SB242084 2 mg/kg alone (n = 5, empty circles) or combined with RO 3 mg/kg (n = 7, filled circles), on the increase in duration of MDA (B) and on the change in the time to onset of MDA (D). One-way ANOVA for repeated measures followed by Fisher's PLSD post-hoc test; * $p < 0.05$. vs vehicle group.

4 Conclusion

It is interesting to note that that RO60-0175 was devoid of any significant antiepileptic effects over a wide range of doses (1-10 mg/kg). This regimen has

been previously shown to be efficient on various electrophysiological, biochemical and behavioural experiments (Beyeler et al., 2010; Di Matteo et al., 2004; Invernizzi et al., 2007; Navailles, Lagière, Le Moine and De Deurwaerdère, 2013; Di Giovanni et al., 2008; Di Matteo et al., 2008) strongly suggesting that 5-HT2CR stimulation is not involved in the control of MDA elongation. The presence of the 5-HT2C antagonist SB242084 unmasked a decrease in MDA response highlighting the anti-epileptic properties of RO60-0175. The mere involvement of 5-HT2CR in the electrophysiological feature of MDA has been also confirmed on the time to onset of MDA. The latency to onset of MDA can be used as a gauge of seizure threshold (anticonvulsant) and the duration of MDA as a measure of processes that terminate seizure activity in the limbic system and its decrease has been considered to be antiepileptogenic (White, 2002). The anticonvulsant and the antiepileptogenic processes likely involve different mechanisms (Löscher, 2012) and in accordance RO60-0175 did not affect the onset of the MDA.

Overall, these data suggest that MDA does not respond to phasic stimulation of 5-HT2CR. Moreover, our data show also that MDA response is under a poor tonic influence exerted by 5-HT2CR. Indeed, the selective 5-HT2CR antagonist SB242084 (2 mg/kg, i.p.) did not induce any proconvulsant effects seen such as elongation of the MDA and AD in rats or reduction of the MDA latency. Thus, in contrast to the situation reported in 5-HT2C KO mice (Tecott et al., 1995), the lack of a 5-HT2CR tonic control on epilepsy is in agreement with data from generalised epilepsy models (Bagdy et al., 2007). It has been previously reported that SB242084 or the other selective antagonist SB243213 were unable to reduce seizure threshold in adult rodents (Jakus and Bagdy, 2011). Although a constitutive activity of 5-HT2CR could have hardly been unmasked with SB242084 (De Deurwaerdere, 2004), previous data have reported that the prototypical inverse agonist SB206553 did not alter on its own seizure threshold (Upton et al., 1998). Thus, it appears that endogenous 5-HT2CR tone exerts a poor influence on the general activity.

References

Abramowski, D., Rigo, M., Duc, D., Hoyer, D. and Staufenbiel, M. (1995). Localization of the 5-hydroxytryptamine2C receptor protein in human and rat brain using specific antisera. *Neuropharmacology.* 34(12), 1635–1645.

Bagdy, G., Kecskemeti, V., Riba, P. and Jakus, R. (2007). Serotonin and epilepsy. *J. Neurochem.* 100(4), 857–873.

Beyeler, A., Kadiri, N., Navailles, S., Boujema, M. B., Gonon, F., et al. (2010). Stimulation of serotonin2C receptors elicits abnormal oral movements by acting on pathways other than the sensorimotor one in the rat basal ganglia. *Neuroscience.* 169(1), 158–170.

Brennan, T. J., Seeley, W. W., Kilgard, M., Schreiner, C. E. and Tecott, L. H. (1997). Sound-induced seizures in serotonin 5-HT2c receptor mutant mice. *Nat. Genet.* 16(4), 387–390.

Clemett, D. A., Punhani, T., S. Duxon, M., Blackburn, T. P. and Fone, K. C. F. (2000). Immunohistochemical localisation of the 5-HT2C receptor protein in the rat CNS. *Neuropharmacology.* 39(1), 123–132.

Crunelli, V. and Di Giovanni, G. (2014). Monoamine modulation of tonic GABAA inhibition. *Rev. Neurosci.* 25(2).

De Deurwaerdere, P. (2004). Constitutive Activity of the Serotonin2C Receptor Inhibits In Vivo Dopamine Release in the Rat Striatum and Nucleus Accumbens. *J. Neurosci.* 24(13), 3235–3241.

De Deurwaerdère, P., Lagière, M., Bosc, M. and Navailles, S. (2013). Multiple controls exerted by 5-HT2C receptors upon basal ganglia function: from physiology to pathophysiology. *Exp. Brain Res.* 230(4), 477–511.

Di Giovanni, G., Di Matteo, V., Pierucci, M. and Esposito, E. (2008). Serotonin-dopamine interaction: electrophysiological evidence. *Prog. Brain Res.* 172, 45–71.

Di Giovanni, G., Esposito, E. and Di Matteo, V. (Eds.). (2011). *5-HT2C Receptors in the Pathophysiology of CNS Disease.* Totowa, NJ: Humana Press.

Di Giovanni, G., García, I., Colangeli, R., Pierucci, M., Rivadulla, M. L., et al. (2014). N-(furan-2-ylmethyl)-N-methylprop-2-yn-1-amine (F2MPA): A potential cognitive enhancer with MAO inhibitor properties. *CNS Neurosci. Ther.* 20(7), 633–40.

Di Giovanni, G., Matteo, V. D., Pierucci, M., Benigno, A. and Esposito, E. (2006). Central Serotonin2C Receptor: From Physiology to Pathology. *Curr. Top. Med. Chem.* 6(18), 1909–1925.

Di Matteo, V., Di Giovanni, G., Pierucci, M. and Esposito, E. (2008). Serotonin control of central dopaminergic function: focus on in vivo microdialysis studies. *Prog. Brain Res.* 172, 7–44.

Di Matteo, V., Pierucci, M. and Esposito, E. (2004). Selective stimulation of serotonin 2C receptors blocks the enhancement of striatal and accumbal dopamine release induced by nicotine administration. *J. Neurochem.* 89(2), 418–429.

Higgins, G. A., Sellers, E. M. and Fletcher, P. J. (2013). From obesity to substance abuse: therapeutic op-

portunities for 5-HT2C receptor agonists. *Trends Pharmacol. Sci.* 34(10), 560–570.

Hoyer, D., Hannon, J. P. and Martin, G. R. (2002). Molecular, pharmacological and functional diversity of 5-HT receptors. *Pharmacol. Biochem. Behav.* 71(4), 533–554.

Invernizzi, R. W., Pierucci, M., Calcagno, E., Di Giovanni, G., Di Matteo, V., et al. (2007). Selective activation of 5-HT2C receptors stimulates GABAergic function in the rat substantia nigra pars reticulata: A combined in vivo electrophysiological and neurochemical study. *Neuroscience.* 144(4), 1523–1535.

Isaac, M. (2005). Serotonergic 5-HT2C Receptors as a Potential Therapeutic Target for the Design Antiepileptic Drugs. *Curr. Top. Med. Chem.* 5(1), 59–67.

Jakus, R. and Bagdy, G. (2011). The Role of 5-HT2C Receptor in Epilepsy. In G. Di Giovanni, E. Esposito and V. Di Matteo (Eds.), *5-ht2c recept. pathophysiol. cns dis.* Totowa, NJ: Humana Press.

Krishnakumar, A., Nandhu, M. S. and Paulose, C. S. (2009). Upregulation of 5-HT2C receptors in hippocampus of pilocarpine-induced epileptic rats: Antagonism by Bacopa monnieri. *Epilepsy Behav.* 16(2), 225–230.

Li, Q.-H., Nakadate, K., Tanaka-Nakadate, S., Nakatsuka, D., Cui, Y. and Watanabe, Y. (2004). Unique expression patterns of 5-HT2A and 5-HT2C receptors in the rat brain during postnatal development: Western blot and immunohistochemical analyses. *J. Comp. Neurol.* 469(1), 128–40.

Löscher, W. (2012). Strategies for antiepileptogenesis: Antiepileptic drugs versus novel approaches evaluated in post-status epilepticus models of temporal lobe epilepsy. *J. Neurophysiol.* 62(1), 126–135.

Navailles, S., Lagière, M., Guthrie, M. and Deurwaerdère, P. (2013). Serotonin2c Receptor Constitutive Activity: In vivo Direct and Indirect Evidence and Functional Significance. *Cent. Nerv. Syst. Agents Med. Chem.* 13(2), 98–107.

Navailles, S., Lagière, M., Le Moine, C. and De Deurwaerdère, P. (2013). Role of 5-HT2C receptors in the enhancement of c-Fos expression induced by a 5-HT2B/2C inverse agonist and 5-HT2 agonists in the rat basal ganglia. *Exp. Brain Res.* 230(4), 525–535.

Orban, G., Pierucci, M., Benigno, A., Pessia, M., Galati, S., et al. (2013). High dose of 8-OH-DPAT decreases maximal dentate gyrus activation and facilitates granular cell plasticity in vivo. *Exp. Brain Res.* 230(4), 441–451.

Pompeiano, M., Palacios, J. M. and Mengod, G. (1994). Distribution of the serotonin 5-HT2 receptor family mRNAs: comparison between 5-HT2A and 5-HT2C receptors. *Mol. Brain Res.* 23(1-2), 163–178.

Sörman, E., Wang, D., Hajos, M. and Kocsis, B. (2011). Control of hippocampal theta rhythm by serotonin: Role of 5-HT2c receptors. *Neuropharmacology.* 61(3), 489–494.

Stringer, J. L. and Lothman, E. W. (1990). Maximal dentate activation: a tool to screen compounds for activity against limbic seizures. *Epilepsy Res.* 5(3), 169–176.

Stringer, J. L., Williamson, J. M. and Lothman, E. W. (1989). Induction of paroxysmal discharges in the dentate gyrus: frequency dependence and relationship to afterdischarge production. *J. Neurophysiol.* 62(1), 126–35.

Tecott, L. H., Logue, S. F., Wehner, J. M. and Kauer, J. A. (1998). Perturbed dentate gyrus function in serotonin 5-HT2C receptor mutant mice. *Proc. Natl. Acad. Sci.* 95(25), 15026–15031.

Tecott, L. H., Sun, L. M., Akana, S. F., Strack, A. M., Lowenstein, D. H., et al. (1995). Eating disorder and epilepsy in mice lacking 5-HT2C serotonin receptors. *Nature.* 374(6522), 542–546.

Upton, N., Stean, T., Middlemiss, D., Blackburn, T. and Kennett, G. (1998). Studies on the role of 5-HT2C and 5-HT2B receptors in regulating generalised seizure threshold in rodents. *Eur. J. Pharmacol.* 359(1), 33–40.

White, H. S. (2002). Animal models of epileptogenesis. *Neurology.* 59(9, Sup 5), S7–S14.

Neuroinflammation in alzheimer's disease

Dorotea Muck Seler*
Division of Molecular Medicine; Rudjer Boskovic Institute; Bijenicka 54; Hr 10000 Zagreb; Croatia
*seler@irb.hr

Abstract. Alzheimer's disease (AD) is a complex, multifactorial and progressive neurodegenerative disorder. Recent studies suggest that neuroinflammation plays an important role in neurodegenerative processes. Microglia and astrocytes are key brain neuroglial cells that regulate two opposite i.e. protective and harmful effects of inflammation on neurodegeneration. In normal aging and in early stage AD, microglia have a neuroprotective role in which they contribute to the clearance of amyloid-beta (Ab) aggregates and neurofibrillary tangles, and stimulation of anti-inflammatory cytokines. The age-related changes and progressive accumulation of AD specific pathological elements induce chronic activation of microglia in an attempt to remove these pathological structures. Activated microglia release pro-inflammatory cytokines (IL-1, IL-6, TNF-a) and other neurotoxic proteins that further stimulate inflammatory processes and contribute to neuronal dysfunction and neurodegeneration. The studies in a transgenic animal model of AD suggest that astrocytic atrophy and astrogliosis are also associated with development of AD. At the later stages of disease, astrocytes become activated and contribute to the neuroinflammatory component of neurodegeneration. In summary, recent data suggest that neuroinflammatory processes and altered function of the brain innate immune cells represent important risk factor for the development and progression of AD. Targeting neuroinflammation and the immune system might be an attractive new approach in the treatment of AD.

Keywords Alzheimer's disease – inflammation – gliosis – anti-inflammatory compounds – NSAIDs

1 Introduction

Alzheimer's disease (AD) is a complex, multifactorial and progressive neurodegenerative disorder. The main symptoms are progressive decline in cognitive functions (memory, learning and executive functions) due to the progressive loss of neurons in hippocampus, enthorinal cortex and basal forebrain. Although there are several hypotheses that try to explain the development of AD, its etiology is still unclear. The main pathological hallmarks of AD are extracellular senile plaques (accumulation of toxic amyloid-beta peptide; Ab) and neurofibrillary tangles (abnormal hyperphosphorylation of protein tau inside neurons). Recent studies suggest that inflammation and hypertrophy of glial cells (gliosis) play an important role in neurodegenerative processes (Weiner and Frenkel, 2006). Microglia and astrocytes are key brain glial cells that regulate two opposite i.e. protective and harmful effects of inflammation on neurodegeneration.

2 Findings and argument

Microglia are brain innate macrophages/phagocytes that remove and clear fragments of damaged or dead cells (Solito and Sastre, 2012). In normal aging and early stage AD activated microglia have a neuroprotective role in which they contribute to phagocytosis, clearance and degradation of Ab aggregates, neurofibrillary tangles and stimulation of anti-inflammatory cytokines (IL-4, IL-10) release in an attempt to remove these "foreign" structures from the brain.

The age-related changes and progressive accumulation of AD specific pathological elements like insoluble Ab aggregates induces chronic activation of microglia and transformation of neuroprotective microglia to neurotoxic cells. Activated microglia release pro-inflammatory cytokines (IL-1, IL-6, TNF-a) and other neurotoxic proteins that further stimulate inflammatory processes and contribute to neuronal dysfunction and neurodegeneration (Guillot-Sestier and Town, 2013). Recent neuroimaging study (Zimmer et al., 2014) has confirmed the activation of microglia in AD.

Astrocytes are a component of the tripartite synapse that mediates connectivity between neuronal and non-neuronal cells and regulates extracellular homeostasis of ions and neurotransmitters. The perisynaptic astrocytes remove the majority of the excitatory neurotransmitter glutamate from extracellular space and prevent its neurotoxic effect. The studies in a transgenic animal model of AD suggest that astrocytic atrophy and astrogliosis are associated with development of AD. At the later stages of disease, astrocytes become activated and contribute to neurodegeneration (Heneka et al., 2010).

Although cytokines represent the important component of neuroinflammation in AD, the analysis of genotype and allele frequencies of IL-1, IL-6 and TNF-a gene polymorphisms did not show significant difference between patients with AD and healthy controls.

3 Neuroinflammation as a target of treatment

Despite remarkable progress in understanding the molecular mechanisms during development and progression of AD there is no effective medication that can stop

the progress of the disease. New data suggests that components of the inflammatory process could be the new targets for treatment of AD. So far treatment options include anti-inflammatory food ("healthy food") and non-steroidal anti-inflammatory drugs (NSAIDs). Among evaluated natural compounds are gingo biloba extract, resveratrol vitamines and omega3-fatty acids. Although ginko biloba extract prevents formation of Ab fibrils in neuroblastoma cell line in vitro (Luo et al., 2002), its antioxidative, antiamyloidogenic and antiapoptotic effects were not confirmed in longitudinal study in subjects with mild cognitive impairement (Vellas et al., 2012). Epidemiological studies have shown lower incidence of AD in patients with inflammatory diseases (arthritis, rheumatism) and pain that have been long-term treated with NSAIDs. The mechanisms of this protective effect of NSAIDs on cognition is associated with their inhibitory effects on cyclooxygenase (COX) activity and consequently on glial activation. Additionally NSAIDs stimulate non-toxic amyloidogenic pathway of APP metabolism and reduce formation of Ab by inhibition of b- and g-secretase activity (Weggen et al., 2007). Although, NSAIDs may have protective effects, clinical trials did not confirm beneficial effects of NSAIDs in patients with AD. The key point is that NSAIDs most likely modulate activation of microglia and reduce the detrimental effects of inflammation in a very early, preclinical stage of neurodegeneration.

4 Conclusion

In summary, recent data suggests that neuroinflammatory processes and altered function of the brain innate immune cells represent an important etiological risk factor for the development and progression of AD. However it is still unclear if the inflammation is the cause, contributor or secondary event in AD. Targeting neuroinflammation and the immune system might be an attractive new approach in the treatment of AD. Since neuroinflammatory processes start very early and before appearance of AD symptoms, timing is important for the success of an antiinflammatory/preventive treatment with NSAIDs.

References

Guillot-Sestier, M.-V. and Town, T. (2013). Innate Immunity in Alzheimer's Disease: A Complex Affair. *CNSNDDT*. 12(5), 593–607.

Heneka, M. T., Rodríguez, J. J. and Verkhratsky, A. (2010). Neuroglia in neurodegeneration. *Brain Res. Rev.* 63(1-2), 189–211.

Luo, Y., Smith, J. V., Paramasivam, V., Burdick, A., Curry, K. J., et al. (2002). Inhibition of amyloid- aggregation and caspase-3 activation by the Ginkgo biloba extract EGb761. *Proc. Natl. Acad. Sci.* 99(19), 12197–12202.

Solito, E. and Sastre, M. (2012). Microglia Function in Alzheimer's Disease. *Front. Pharmacol.* 3.

Vellas, B., Coley, N., Ousset, P.-J., Berrut, G., Dartigues, J.-F., et al. (2012). Long-term use of standardised ginkgo biloba extract for the prevention of Alzheimer's disease (GuidAge): a randomised placebo-controlled trial. *Lancet Neurol.* 11(10), 851–859.

Weggen, S., Rogers, M. and Eriksen, J. (2007). NSAIDs: small molecules for prevention of Alzheimer's disease or precursors for future drug development? *Trends Pharmacol. Sci.* 28(10), 536–543.

Weiner, H. L. and Frenkel, D. (2006). Immunology and immunotherapy of Alzheimer's disease. *Nat. Rev. Immunol.* 6(5), 404–416.

Zimmer, E., Leuzy, A., Benedet, A., Breitner, J., Gauthier, S. and Rosa-Neto, P. (2014). Tracking neuroinflammation in Alzheimer's disease: the role of positron emission tomography imaging. *J. Neuroinflammation.* 11(1), 120.

Support by COST Actions CM1103.

Combined depletion of Monoamines in Parkinson's disease

Emilie Faggiani[*1,2], **Claire Delaville**[1,2] **and Abdelhamid Benazzouz**[1,2]
[1]Univ. de Bordeaux, Institut des Maladies Neurodégénératives, UMR 5293, 33076 Bordeaux, France.
[2]CNRS, Institut des Maladies Neurodégénératives, UMR 5293, 33076 Bordeaux, France.
*emilie.faggiani@u-bordeaux.fr

Abstract. Parkinson's disease is a neurological disorder characterized by motor and also by non-motor symptoms, which are under-studied and therefore not well supported therapeutically. We investigated the role of combined depletions of dopamine, norepinephrine and serotonin in the manifestation of Parkinsonian-like motor and non-motor deficits in the rat and also their impact on the behavioral effects of deep brain stimulation of the subthalamic nucleus. In a unilateral 6-OHDA rat model of the disease, we show that NA or DA depletion significantly decreased locomotor activity and that anxiety-like states required DA depletion plus the depletion of norepinephrine and serotonin. Anhedonia and "depressive-like" behavior emerged only from the combined depletion of all three monoamines. In the bilateral model, we show that dopamine depletion alone induced locomotor deficits associated with anxiety and mild "depressive-like" behavior and that combined depletions of the three monoamines dramatically exacerbated "depressive-like" behavior. This bilateral model can be considered as a model of advanced stage Parkinson's disease in the rat expressing motor deficits as well as severe mood disorders.

Keywords Parkinson's disease – motor and non-motor symptoms – monoamines – Deep Brain Stimulation.

1 Introduction

Parkinson's disease is characterized by the manifestation of motor symptoms mainly attributed to the degeneration of dopamine neurons in the pars compacta of substantia nigra. Furthermore, despite the focus on motor deficits, Parkinson's disease is also characterized by the manifestation of non-motor symptoms, such as anxiety and depression, for which the mechanisms are still not elucidated. In addition to dopamine cell degeneration, Parkinson's disease is a multi-system disorder characterized also by the loss of norepinephrine neurons of the locus coeruleus (for review, Delaville et al. (2011)) and serotonin cells of the dorsal raphe (Kish, 2003) suggesting that norepinephrine and serotonin depletions are other landmarks of the disease. We focused on the respective role of combined depletions of the monoaminergic systems using the unilateral and also the bilateral 6-OHDA rat model of Parkinson's disease.

2 Methods

We performed selective depletions of dopamine, norepinephrine and serotonin and the behavioral effects of different depletions were investigated using the open field for locomotor activity, the elevated plus maze for anxiety and the forced swim test for "depressive-like" behavior.

3 Findings and argument

One of the main findings is that norepinephrine depletion alone induced severe motor deficits that resembled those reported after 6-OHDA-induced dopamine cell lesion suggesting that norepinephrine, like dopamine, is essential in the control of motor behavior. In the unilateral dopamine depleted animals, the motor deficits were not potentiated by additional depletions of norepinephrine and/or serotonin. However, the manifestation of anxiety and "depressive-like" behavior were due to the combined monoamine depletions (Delaville et al., 2012). In the bilateral rat model, we showed that dopamine depletion alone induced locomotor deficits associated with anxiety and mild "depressive-like" behavior and that combined depletions of the three monoamines dramatically exacerbated "depressive-like" behavior. In addition, we show that deep brain stimulation of the subthalamic nucleus reversed locomotor deficits and anxiety behavior in animals with bilateral dopamine depletion alone. However, the additional depletion of norepinephrine and/or serotonin may interfere with these improvements.

4 Conclusion

Results of these studies highlight the important role played by monoaminergic system depletions in the pathophysiology of Parkinson's disease and propose new rat models with motor and non-motor disabilitiés. They provide evidence that combined depletion of monoamines may alter the efficacy of subthalamic stimulation used in the therapy of the disease.

References

Delaville, C., Chetrit, J., Abdallah, K., Morin, S., Cardoit, L., et al. (2012). Emerging dysfunctions consequent to combined monoaminergic depletions in parkinsonism. *Neurobiol. Dis.* 45(2), 763–773.

Delaville, C., Deurwaerdère, P. D. and Benazzouz, A. (2011). Noradrenaline and Parkinson's Disease. *Front. Syst. Neurosci.* 5.

Kish, S. J. (2003). Biochemistry of Parkinson's disease: is a brain serotonergic deficiency a characteristic of idiopathic Parkinson's disease? *Adv. Neurol.* 91, 39–49.

Vesicular monoamine transporter and the effects of its inhibition in portacaval shunted rats

Wieslawa Agnieszka Fogel*[1], Kimmo Michelsen[2], Pertti Panula[2], Michal Maksymowicz[3], Anna Stasiak[1]

[1]Department of Hormone Biochemistry Medical University of Lodz, Poland

[2]University of Helsinki, Finland

[3]Mossakowski Medical Research Centre Polish Academy of Sciences, Warsaw

*wieslawa.agnieszka.fogel@umed.lodz.pl

Abstract. Large amounts of histamine are formed in the brain and gastric mucosa of portacaval shunted rats. Histamine removal from cytoplasm and sequestration of the amine into storage vesicles within the cell is accomplished by vesicular monoamine transporter VMAT2. To determine whether the brain level of VMAT2 is altered in PCS rats and what the effects of VMAT inhibition are, immunohistochemistry and 3H dihydrotetrabenazine (DTBZ) binding studies were done and in vivo reserpine was administered, respectively. Neither VMAT2 immunofluorescence, nor Kd and V max for VMAT2 differ between PCS and their sham operated control pairs, indicating a high capacity of this transporting system. On the other hand, the depletion of storage vesicles by the blockade of vesicular transporter was much more harmful for PCS rats.

Keywords histamine – portocaval shunt – immunohistochemistry – VMAT2 – reserpine

1 Introduction

Portacaval shunt (PCS) drastically reduces participation of the liver in body metabolism. Among other effects this leads to profound hormonal alterations and intensive skeletal muscle protein breakdown, resulting in a changed blood amino acid profile and concentration with a decrease in branched chain amino acids and an increase in aromatic amino acids. Upon entering the brain, enhanced concentrations of aromatic amino acids, amine neurotransmitter precursors, causes excessive production of dopamine, serotonin and histamine. In the case of the two former, compensatory degradation takes place whereas large amounts of synthesized histamine are deposited in neurons. Increased histamine production also concerns gastric mucosa as well as the brain (Fogel et al., 2001). The vesicular monoamine transporter 2, VMAT2, an H^+-ATPase an-

tiporter, acts to sequester cytosolic histamine in storage vesicles in neurons and endocrine cells (Erickson et al., 1995; Häkanson et al., 1976). In this study two questions were posed; 1) whether there is any modulation in the function of the transporter in the portacavally shunted rat brain and 2) what are the effects of VMAT inhibition (Pollard et al., 1973).

Binding studies with tritiated dihydrotetrabenazine and immunohistochemistry have been applied and reserpine used as a VMAT inhibitor. Results suggest no changes in the VMAT2 function after PCS. On the other hand, in animal treated with reserpine, much richer stores of histamine caused more pronounced injury in PCS rats.

2 Methods

Lewis rats portacavally shunted (end-to-side) according to Lee and Fisher (1961) and sham operated control pairs 2-11 months after surgery were used. Double fluorescent immunohistochemical techniques, employing rabbit-anti-HA (Anti-HA-19C; (Panula et al., 1990) and guinea pig anti VMAT2 (Euro-Diagnostica, Lund, Sweden) were used to disclose the localization and density of VMAT2 and histamine. The binding studies were performed using 3H dihydrotetrabenazine as a VMAT2 ligand (Teng et al., 1998). Reserpine was administered intraperitoneally in a single dose 5 mg/kg, and the rats' consumption and excretion were monitored daily for 1 to 5 days. Tissue samples were collected at autopsy after 1 day or 5 days following the reserpine administration. Both the cerebral cortex and hypothalamus were dissected, frozen in liquid nitrogen and stored at −70 °C until assayed. The stomach was cut open and examined for peptic ulcers. The length of each lesion was measured under 10× magnification and summed per rat. The group mean ±SD was calculated. The gastric mucosa was then scrapped off for histamine estimation (Fogel et al., 2001).

3 Findings and argument

Although histamine in the CNS was increased several fold following PCS, with regard to VMAT 2 no difference in either the distribution pattern or the intensity of immunostaining was noted between shunted and control rat brains. Likewise, there were no changes in DTBZ binding characteristics of the VMAT 2 between PCS rats and sham operated controls. Reserpine treatment evoked long lasting sedation. The rats neither ate nor drank and lost from 13 % (sham) to 17 % (PCS) of their initial body mass over 5 days. In the stomachs of these rats severe ulceration was found at autopsy, which was more extensive and deep in the reserpine-treated shunted rats

4 Conclusion

VMAT 2 capacity is beyond normal demands and may efficiently sequester even such excessive amounts of histamine as produced in hepatic encephalopathy (HE).

Reserpine treatment suggests that the drugs interfering with VMAT may have fatal consequences for HE patients.

References

Erickson, J. D., Eiden, L. E., Schäfer, M. K. H. and Weihe, E. (1995). Reserpine- and tetrabenazine-sensitive transport of 3H-histamine by the neuronal isoform of the vesicular monoamine transporter. *J. Mol. Neurosci.* 6(4), 277–287.

Fogel, W. A., Michelsen, K. A., Panula, P., Sasiak, K. and Andrzejewski, W. (2001). Cerebral and gastric histamine system is altered after portocaval shunt. *J. Physiol. Pharmacol.* 52(4 Pt 1), 657–70.

Häkanson, R., Larsson, L. I., Liedberg, G., Oscarson, J., Sundler, F. and Vang, J. (1976). Effects of antrectomy or porta-caval shunting on the histamine-storing endocrine-like cells in oxyntic mucosa of rat stomach. A fluorescence histochemical, electron microscopic and chemical study. *J. Physiol.* 259(3), 785–800.

Lee, S. H. and Fisher, B. (1961). Portacaval shunt in the rat. *Surgery.* 50, 668–72.

Panula, P., Airaksinen, M. S., Pirvola, U. and Kotilainen, E. (1990). A histamine-containing neuronal system in human brain. *Neuroscience.* 34(1), 127–132.

Pollard, H., Bischoff, S. and Schwartz, J.-C. (1973). Increased synthesis and release of 3H-histamine in rat brain by reserpine. *Eur. J. Pharmacol.* 24(3), 399–401.

Teng, L., Crooks, P. A. and Dwoskin, L. P. (1998). Lobeline displaces [3H]dihydrotetrabenazine binding and releases [3H]dopamine from rat striatal synaptic vesicles: comparison with d-amphetamine. *J. Neurochem.* 71(1), 258–65.

An new animal model of anxiety

Fossat Pascal*
Institut des neurosciences intégratives et cognitives d'aquitaine ; UMR CNRS 5287 ; Université Bordeaux; 146 rue Léo Saignat ; 33076 Bordeaux, France
*pascal.fossat@u-bordeaux.fr

Abstract. We cover, in this extended abstract, our recent work published in Science about anxiety in crayfish (Fossat, 2014). After exposure to stress, crayfish sustainably avoided the aversive illuminated arms of an aquatic plus-maze. This behavior was correlated with a significant increase in brain serotonin but not of dopamine and was abolished by the injection of the benzodiazepine anxiolytic chlordiazepoxide. Serotonin injection into unstressed crayfish induced avoidance; again, this effect was reversed by injection with chlordiazepoxide. Our results demonstrate that crayfish exhibit a form of anxiety similar to that described in vertebrates, suggesting the conservation of several underlying mechanisms during evolution. Analyses of this ancestral behavior in a simple model reveal a new route to understanding anxiety and may alter our conceptions of the emotional status of invertebrates.

Keywords Anxiety – Crayfish – behaviour – Serotonin and Dopamine

1 Introduction

Stress or danger (called stressors) provoke fear and generate immediate responses, such as escape, freezing or aggression. Stress can also lead to anxiety, a more complex state occurring when the stressor is absent or not clearly identified (Belzung and Philippot, 2007; D. C. Blanchard and R. J. Blanchard, 2008; Steimer, 2011). In humans and rodents, anxiety is experienced as an anticipatory fear that facilitates coping with unexpected situations and is revealed by a long-lasting behavioral adaptation intended to minimize threats, even in a different context and without the stressor (Belzung and Philippot, 2007; D. C. Blanchard and R. J. Blanchard, 2008; Steimer, 2011). Anxiety has been intensively studied in humans and rodents (Handley, 1995; López-Muñoz et al., 2011; Walters et al., 1981), but most animals are capable of perceiving danger and exhibit varying degrees of behavioral adaptation to stress (Belzung and Philippot, 2007). Though studies have described fear response after aversive conditioning in Aplysia or pessimistic bias after stress in bees (Walters et al., 1981; Bateson et al., 2011), the characteristics of anxiety have not been fully observed in a single invertebrate model. We show that stressed crayfish (Procambarus clarkii) express context-independent anxiety-like behavior that can be promoted by 5-HT (Fossat et al., 2014).

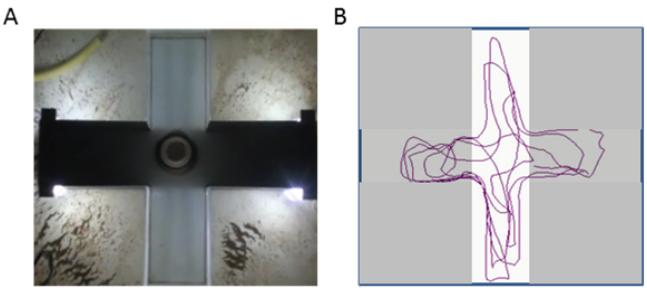

Figure 1: The dark/light plus maze. **A** The maze was cross-shaped with 4 arms (25 cm long and 10 cm wide each) and a middle zone (10×10 cm). 2 arms are illuminated and 2 are dark. **B** Unstressed crayfish spontaneously visit all arms as it is highlighted with a typical crayfish route.

2 Methods

We used adult male crayfish, Procambarus clarkii. Crayfish were first submitted to an aversive stress by means of electric fields generated in a specific tank (see Fossat et al., 2014). Crayfish were then placed in the dark/light plus maze, cross-shaped maze divided in four arms (2 illuminated and 2 darks) (see Figure 1). The spontaneous exploratory behaviour of unstressed and stressed crayfish was recorded for 10 minutes and further analysed with the ethovision XT 8 software (Noldus, NL). We compared the behaviour related to the illuminated arms, namely the % of the total time in light arms, the mean number of entry in light arms, the latency of first in light arms and the retreat ratio (RR). RR is defined as the number of withdrawal towards illuminated arms divided by the total number of attempts. We then measured the brain bioamine levels by HPLC (see Fossat et al., 2014). Finally, we measured the effect of 5-HT injection on the crayfish exploratory behaviour. A quantity of 5 µg/g 5-HT was injected directly within the hemolymph, 15 minutes after behavioural test in the dark/light plus maze.

3 Findings and argument

The stress stimulation significantly modified the spontaneous exploratory behaviour of crayfish. While unstressed crayfish spontaneously explored the whole arms of the maze with a significant preference for the dark arms, stressed crayfish almost never visited the light arms (Figure 2). The consequence of the stress on the exploratory behaviour lasts for 30 minutes and then a normal behaviour is recovered after 1 hour.

We measured the bioamine levels in the crayfish brain and it appears that brain 5-HT is significantly higher

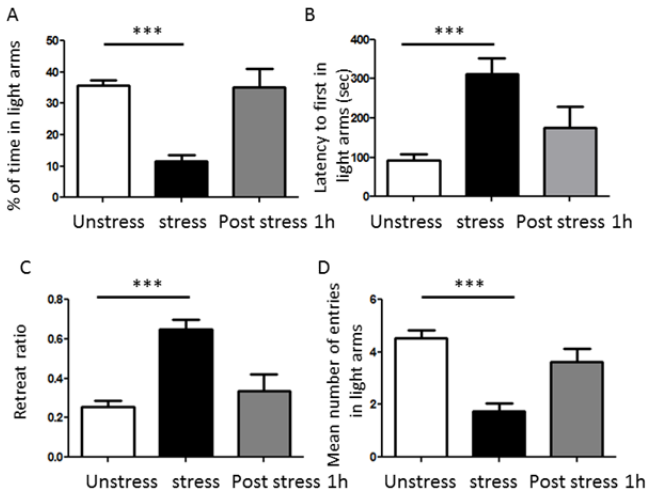

Figure 2: After stress crayfish spent less time in lighr arms, the latency to first entry is significantly increased, the retreat ratio is increased and the mean number of entries in light arm is decreased. All these behavioural changes disappeared 1 hour after stress.

in stressed as compared to unstressed crayfish while dopamine remained unmodified (5-HT: 118(20) pg/mg and 296.2(430) , $p < 0.01$, Mann Whitney and dopamine 50.5(70) pg/mg and 65(11) pg/mg, $p = 0.28$, Mann whitney). Finally, 5HT injections mimick the stressful stimulation and trigger a strong aversion regarding illuminated arms.

4 Conclusion

Taken together, these results suggest that crayfish submitted to an important stress express an apprehension behaviour that limits their exploration of potentially aversive areas (here, the illuminated arms of the dark/light plus maze). This behaviour depends on 5-HT and lasts for minutes after stress and is remarkably similar to the anxiety-like behaviour measured in rodents.

References

Bateson, M., Desire, S., Gartside, S. E. and Wright, G. A. (2011). Agitated honeybees exhibit pessimistic cognitive biases. *Curr. Biol.* 21(12), 1070–3.

Belzung, C. and Philippot, P. (2007). Anxiety from a phylogenetic perspective: is there a qualitative difference between human and animal anxiety? *Neural Plast.* 2007, 59676.

Blanchard, D. C. and Blanchard, R. J. (2008). *Handbook of Anxiety and Fear.* Amsterdam: Academic Press.

Fossat, P., Bacqué-Cazenave, J., De Deurwaerdère, P., Delbecque, J.-P. and Cattaert, D. (2014). Comparative behavior. Anxiety-like behavior in crayfish is controlled by serotonin. *Science.* 344(6189), 1293–7.

Handley, S. L. (1995). 5-Hydroxytryptamine pathways in anxiety and its treatment. *Pharmacol. Ther.* 66(1), 103–148.

López-Muñoz, F., Alamo, C. and García-García, P. (2011). The discovery of chlordiazepoxide and the clinical introduction of benzodiazepines: half a century of anxiolytic drugs. *J. Anxiety Disord.* 25(4), 554–62.

Steimer, T. (2011). Animal models of anxiety disorders in rats and mice: some conceptual issues. *Dialogues Clin. Neurosci.* 13(4), 495–506.

Walters, E., Carew, T. and Kandel, E. (1981). Associative Learning in Aplysia: evidence for conditioned fear in an invertebrate. *Science.* 211(4481), 504–506.

Quinolylnitrones with neuroprotective activity for the treatment of cerebral ischemia

Marco-Contelles José*
Laboratorio de Quimica Médica (Instituto de Química Orgánica General, CSIC Juan de la Cierva, 3; 28006-Madrid (Spain)
*iqoc21@iqog.csic.es

Abstract. We report the synthesis, theoretical calculations, the antioxidant, anti-inflammatory, neuroprotective properties, and the ability to cross the blood-brain barrier (BBB) of (Z)-a-aryl and heteroaryl-N-alkyl nitrones, as potential agents for stroke treatment. The majority of nitrones compete with DMSO for hydroxyl radicals, and most of them are potent lipoxygenase inhibitors. Cell viability-related (MTT assay) studies clearly showed that these nitrones give rise to significant neuroprotection. Particularly, nitrone RP19 which shows potent combined antioxidant and neuroprotective properties, and, therefore, can be considered as new lead compound for further development in specific tests for potential stroke treatment.

Keywords quinolylnitrones – neuroprotection – MTT – cerebral ischemia – RP19

1 Introduction

Cerebral Ischemia (CI) is one of the major causes of death, behind heart diseases and cancer, and is the leading cause of adult disability in developed countries. The large numbers of stroke patients and great economic expenses have imposed a great burden to society. Despite its great social impact, there is a lack of effective therapeutic treatment.

Occlusion of cerebral vessels by blood thrombus is the main cause of CI, which can be hemorrhagic or ischemic, can affect an area (focal ischemia) or whole brain (global ischemia), and can lead to a cascade of damaging biological events, including the release of excitatory amino acid, calcium influx, and neuroinflammation. There is increasing evidence showing that oxidative stress plays a key, major role in CI. This is why we have supported the possibility since the beginning of our project of a therapeutic approach based on antioxidant compounds able to trap reactive oxygenated species, such as hydroxyl radicals, superoxide, peroxinitrite, or peroxide. Thus, an agent that either lyses blood thrombus/inhibits platelet aggregation or scavenges free radicals, or a combination of these two effects, could be useful for the treatment of CI, and the reason for the selection as our target molecules, nitrones, as a well-known organic compounds, which have evolved from classical agents able to trap free radicals to be intensively investigated as neuroprotective drugs for the potential treatment of cerebral ischemia (Floyd et al., 2008).

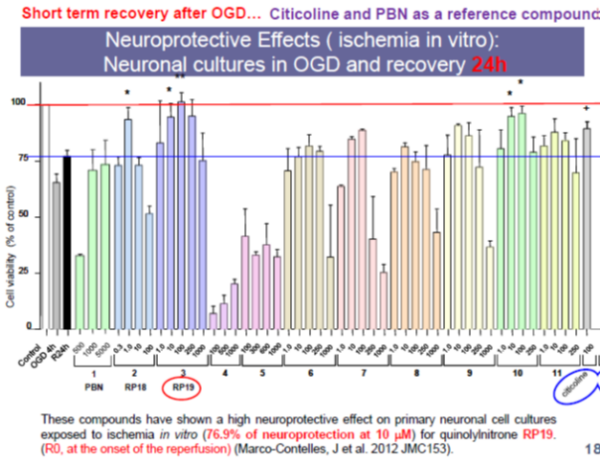

Figure 1: Effect of nitrones on primary neuronal cultures exposed to oxygen-glucose deprivation (OGD). Bar chart showing the percentage of cell viability at 24 h of recovery after 4 h OGD, either untreated (R24h) or treated with different concentrations (µM) of nitrones **12**, 12 (PBN), **16**, **19**, **20**, or citicoline. The value induced by OGD at 4 h is also indicated. Cell viability corresponding to control cells (1.497(50) AU) was considered as 100 %. The values represent the average of three to five independent experiments; error bars representing the SEM. *P < 0.05 versus R24h by Student's t test. Statistical significances below R24h value were not shown.

2 Methods, findings and argument

Cell viability assay by 3-(4,5-dimethylthiazol-2-yl)-2,5-diphenyl tetrazolium bromide (MTT) determination was performed to evaluate the potential neuroprotective effect on nitrones **1-11** against OGD. Exposure of neuronal cultures to 4 h OGD (OGD 4h) induced a significant decrease in cell viability (65.2 %, $p < 0.0001$ versus 100 % control, by one-sample t test), which was partially reversed after 24 h recovery (reperfusion) (R24h, 77.0 %; $p < 0.01$ versus OGD 4h, Student's t test), but without reaching the 24 h control value ($p < 0.0001$ versus 100 % control, one-sample t test) (Figure 1).

Nitrones **1-11** (ranged from 0.1 µM to 1 mM) were added at the beginning of the reperfusion period to evaluate their potential neuroprotective effect. Cytidine-5'-diphosphocholine (citicoline or CDP-choline), a well-known neuroprotective agent, and PBN, described as protective against free radicals, were used as reference compounds to evaluate the neuroprotection on neuronal

cultures. Citicoline was assayed from 1 µM to 1 mM, and we found a neuroprotective effect at 10 and 100 µM (87.4 and 91.5 %, respectively, compared to 100 % control) (Figure 1). PBN did not induce neuroprotective effect in the range of assayed concentration (0.1-10 mM; Figure 2).

The addition of 100-250 µM nitrone 1, 1 µM nitrone 2, or 10-100 µM nitrone 3 (= RP19, Figure 2) and 10, significantly increased cell viability during reperfusion, and returned near control values (100.3-95.7 %, 93.4 %, 94.4-101.2 %, and 94.9-96.1 %, respectively, compared to 100 % control) (Figure 1). The neuroprotection induced by nitrones 1-3 and 10 was compared with citicoline and PBN, these nitrones providing significantly higher neuroprotection than citicoline.

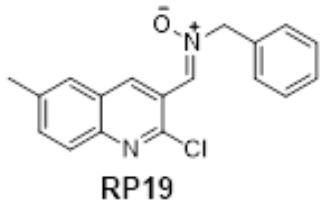

Figure 2: Chemical structure of RP19.

3 Conclusion

Based on these results, we conclude that quinolyl-nitrone RP19 [(Z)-N-((2-chloro-6-methylquinolin-3-yl)methylene)-1-phenylmethanamine oxide] (Chioua et al., 2012; Figure 2) shows high neuroprotective activity, *in vitro* and *in vivo*, and can be considered a promising drug for the potential treatment of CI.

References

Chioua, M., Sucunza, D., Soriano, E., Hadjipavlou-Litina, D., Alcázar, A., et al. (2012). α-Aryl- N -alkyl Nitrones, as Potential Agents for Stroke Treatment: Synthesis, Theoretical Calculations, Antioxidant, Anti-inflammatory, Neuroprotective, and Brain–Blood Barrier Permeability Properties. *J. Med. Chem.* 55(1), 153–168.

Floyd, R. A., Kopke, R. D., Choi, C.-H., Foster, S. B., Doblas, S. and Towner, R. A. (2008). Nitrones as therapeutics. *Free Radic. Biol. Med.* 45(10), 1361–1374.

Aldo-keto reductase inhibitors and their potential in neurodegenerative disorders

Magdalena Majekova*[1]; Milan Stefek[1]; Jana Ballekova[1]; Marta Soltesova Prnova[1]; Pavol Majek[2]; Gerard Esteban[3] and Mercedes Unzeta[3]

[1]Institute of Experimental Pharmacology & Toxicology; Slovak Academy of Sciences; Dubravska 9; Bratislava; Slovakia

[2]Institute of Analytical Chemistry; Faculty of Chemical and Food Technology; STU, Bratislava; Radlinskeho 9; Bratislava, Slovakia

[3]Departament de Bioquimica i Biologia Molecular; Facultat de Medicina; Institut de Neurociencies; Universitat Autonoma de Barcelona; Spain

*magdalena.majekova@savba.sk

Abstract. Aldo-keto reductases belong to the recently indicated targets in neurodegenerative diseases due to the revealed correlation between neurodegenerative and type 2 diabetes mellitus related changes in the brain. As aldose reductase (ALR2) is one of the most promising targets in reducing glucose toxicity, ALR2 inhibitors could represent prospective compounds in developing the multi-target drug leads. We focused on a set of 20 indole derivatives with recently determined inhibition activities towards ALR2 and known selectivity factors as compared with aldehyde reductase (ALR1). We performed a molecular modeling study on the interaction of the indole compounds with monoamine oxidase A and B. The study was based on docking calculation and subsequent full optimization of the complexes. Experimental confirmation of human MAO-A and MAO-B inhibition activities of effective ALR2 inhibitors from the group of indole-1-acetic derivatives (**13** and **20**) is also presented. Compound **20** exhibited prospective properties as a multi-target lead for further design of bifunctional ALR2/MAO inhibitors.

Keywords Alzheimer's disease – type 2 diabetes mellitus – monoamine oxidase – indole-1-acetic acid derivatives – molecular modeling

1 Introduction

The multi-factorial character of neurodegenerative diseases has been commonly accepted as the basis for understanding their mechanisms and also the search for their efficient treatment. Alzheimer's disease and type 2 diabetes mellitus showed many common features (de

la Monte and Wands, 2008) connected mainly with malfunctions in glucose metabolism. They result in elevated sorbitol levels in the brain, mostly derived from glucose flux through the astrocyte polyol pathway (Regenold et al., 2004). After years of extensive study on design, synthesis, in vitro and in vivo testing of ALR2 inhibitors (ARI) (Stefek et al., 2008; Juskova et al., 2011), we performed a systematic search for other positive beneficial properties of ARI in profiling our compounds as multi-target drug leads (MTDLs).

Here we publish the results of in silico screening of 20 indole compounds (Figure 1) for monoamine oxidase inhibition. The compounds were recently tested for their inhibition activities towards ALR2 and ALR1 enzymes (Štefek et al., 2014). Two of the compounds (**13**, **20**) with higher affinities towards ALR2 and good predicted binding energies towards MAO-B were tested also for inhibition of human MAO enzymes. They both showed good MAO-B affinities and compound **20** also possessed considerable MAO-B/MAO-A selectivity.

2 Methods

The optimal conformers of the compounds were obtained by equilibrium conformer systematic search (MMFF94) in the program SPARTAN'08 (Wavefunction, Inc., Irvine, CA, 2009). For modeling the enzyme-ligand interaction, the PDB structure of MAO-A complexed with FAD and harmine was taken from Protein Data Bank (http://www.rcsb.org, structure 2z5x) and for MAO-B the complex with FAD and safinamide (structure 2v5z) was used. The local docking protocol of YASARA (Krieger et al., 2002) was applied. The first ten clusters were then searched for the minimum value of $E_{binding}$ within the optimization protocol em_run.mcr.

Monoamine oxidase activities from recombinant human MAO A and MAO B (Sigma-Aldrich, Madrid, Spain) were measured using the Amplex UltraRed fluorometric coupled method according to the method described by Bautista-Aguilera et al. (2014).

3 Findings and argument

The set of ALR2 inhibitors was divided into three groups: A -with the highest ALR2 inhibition activity ($IC_{50} < 1\,\mu M$); B - compounds with moderate ALR2 activity ($IC_{50} < 10\,\mu M$) and C – compounds with poor ALR2 activity ($IC_{50} > 10\,\mu M$). Compound **13** from the first group showed favorable theoretical prediction of the binding energies towards MAO-A and MAO-B, which was confirmed by experimentation with human enzymes. Compound **20** showed high inhibition of MAO-B with good selectivity towards MAO-A. The group B (**1, 9, 10, 11, 14, 15, 16, 18** and **19**) provided two compounds with promising MAO-A or MAO-B binding energies, namely **9** ($E_{binding} = 315.6\,kJ/mol$) and **10** ($E_{binding} = 322.8\,kJ/mol$).

Table 1: Top: predicted binding energies for interaction with MAO-A and MAO-B for the most efficient ARIs ($IC_{50} < 1\,\mu M$); right side: experimental values of IC_{50} towards human MAO-A and MAO-B.

		$E_{binding}$ (kj/mol)	
	Compound	MAO-A	MAO-B
A	13	326.1	343.7
	17	353.9	271.7
	20	135.7	588.1
		IC_{50}	
	Compound	hMAO-A	hMAO-B
	13	7.1(165)	9.69(199)
	17	n.d.	n.d.
	20	> 800	3.20(57)

Compound **20** provided the attractive interaction with the coenzyme FAD and important residue Ile199 in MAO-B model. This derivative is very similar to the compounds bearing propargyl amine scaffold already established as the potent MAO and cholinesterase inhibitors (Samadi et al., 2012).

4 Conclusion

Of the derivatives studied, 5-(benzyloxy)-1H-indole-1-yl] acetic acid (**20**) has been established to be the most prospective compound for the study and development of multi-target drugs for effective treatment of neurodegenerative diseases. Our next study will focus on further improvement of pharmacodynamic and pharmacokinetic properties of this structural motif.

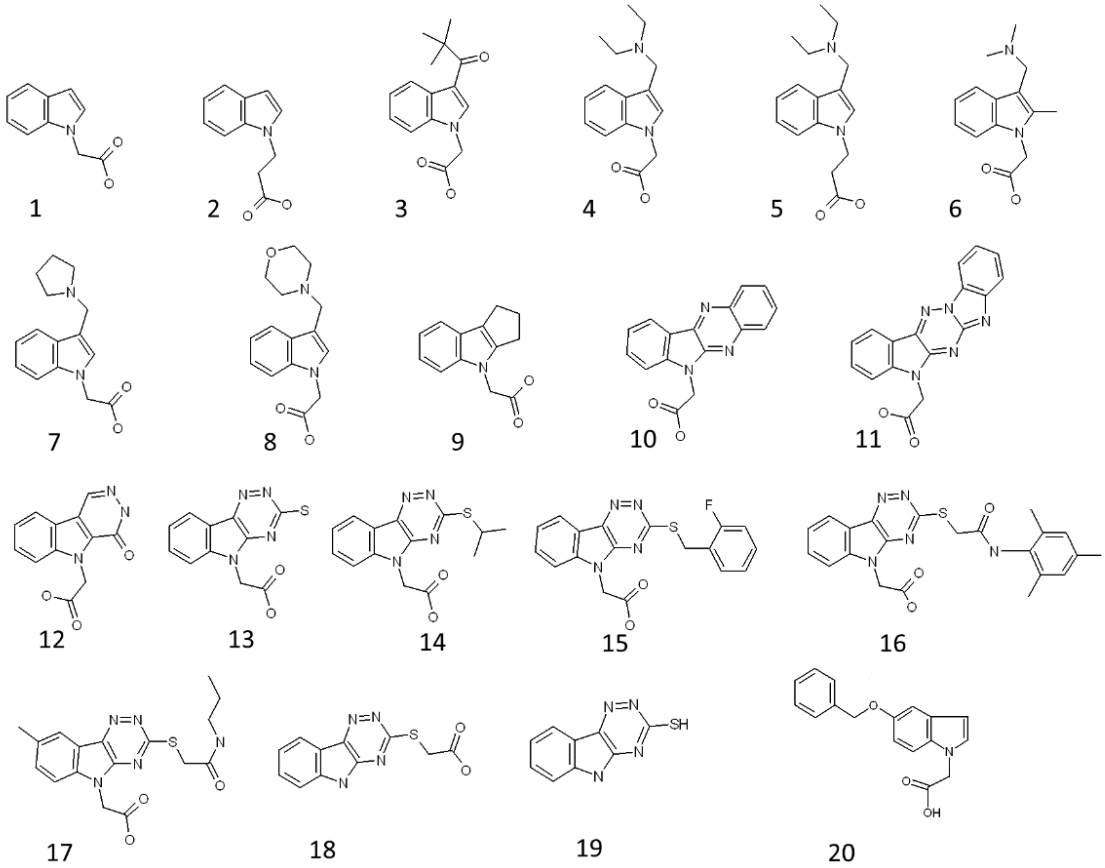

Figure 1: Structure of the indole derivatives

References

Bautista-Aguilera, O. M., Esteban, G., Bolea, I., Nikolic, K., Agbaba, D., et al. (2014). Design, synthesis, pharmacological evaluation, QSAR analysis, molecular modeling and ADMET of novel donepezil–indolyl hybrids as multipotent cholinesterase/monoamine oxidase inhibitors for the potential treatment of Alzheimer's disease. *Eur. J. Med. Chem.* 75, 82–95.

de la Monte, S. M. and Wands, J. R. (2008). Alzheimer's Disease is Type 3 Diabetes–Evidence Reviewed. *J. Diabetes Sci. Technol.* 2(6), 1101–1113.

Juskova, M., Majekova, M., Demopoulos, V. and Stefek, M. (2011). Substituted derivatives of indole acetic acid as aldose reductase inhibitors with antioxidant activity: structure-activity relationship. *Gen. Physiol. Biophys.* 30(4), 342–9.

Krieger, E., Koraimann, G. and Vriend, G. (2002). Increasing the precision of comparative models with YASARA NOVA-a self-parameterizing force field. *Proteins Struct. Funct. Bioinforma.* 47(3), 393–402.

Regenold, W. T., Phatak, P., Kling, M. A. and Hauser, P. (2004). Post-mortem evidence from human brain tissue of disturbed glucose metabolism in mood and psychotic disorders. *Mol. Psychiatry.* 9(8), 731–733.

Samadi, A., de los Ríos, C., Bolea, I., Chioua, M., Iriepa, I., et al. (2012). Multipotent MAO and cholinesterase inhibitors for the treatment of Alzheimer's disease: synthesis, pharmacological analysis and molecular modeling of heterocyclic substituted alkyl and cycloalkyl propargyl amine. *Eur. J. Med. Chem.* 52, 251–62.

Štefek, M., Soltesova Prnova, M., Majekova, M., Rechlin, C., Heine, A. and Klebe, G. (2014). Identification of novel aldose reductase Inhibitors based on carboxymethylated mercapto-triazino-indole scaffold. In *Drug des. med. chem.* Berlin.

Stefek, M., Snirc, V., Djoubissie, P.-O., Majekova, M., Demopoulos, V., et al. (2008). Carboxymethy-

lated pyridoindole antioxidants as aldose reductase inhibitors: Synthesis, activity, partitioning, and molecular modeling. *Bioorg. Med. Chem.* 16(9), 4908–4920.

Pathogenesis and early diagnosis of Alzheimer's disease: involvement of the monoaminergic system

Mirjana Babić*[1], Dubravka Švob Štrac[2], Dorotea Mück-Šeler[2], Nela Pivac[2], Goran Šimić[1]
[1]Department of Neuroscience, Croatian Institute for Brain Research, University of Zagreb School of Medicine, Zagreb, Croatia
[2]Division of Molecular Medicine, RuđerBošković Institute, Zagreb, Croatia
*mbabic@hiim.hr

Abstract. Pathogenesis of Alzheimer's disease (AD) is still not elucidated. There are several different views regarding the occurrence of two main features of AD: amyloid β (Aβ) and tau protein pathology. Generally, it is considered that the increase in the amount of Aβ is an initiating event in AD (particularly in familial cases), while tau protein hyperphosphorylation and aggregation occur as a consequence. On the other hand, based on postmortally analysed brains Braak and Del Tredici documented that intraneuronal tau aggregation precedes diffuse plaque deposition, but Aβ changes occur before increase of tau in cerebrospinal fluid (CSF). Some of the new hypotheses stressed the possibility that the first pathological changes in AD could occur in brainstem nuclei: noradrenergic locus coeruleus (LC), serotonergic dorsal raphe (DRN) and cholinergic nucleus basalis complex. Our recent study summarized all these findings into a unifying hypothesis: long projection fibres from brainstem nuclei release Aβ that could induce neurofibrillary changes within vulnerable cortical glutamatergic pyramidal neurons. The involvement of monoaminergic nuclei in the pathogenesis of AD was further elaborated in an ongoing study showing that exposure to heavy metals (such as inorganic mercury) can lead to AD-like pathology in LC neurons that may spread to neighbouring DRN neurons. Since current biomarkers of AD detect the disease in symptomatic individuals (in whom neurodegeneration is already substantial), novel biomarkers are essential for early AD detection at preclinical stages. Encouraged by the finding of early monoaminergic nuclei degeneration in AD, many investigators tried to assess the diagnostic potential of monoamine metabolites in CSF. However, due to the differences between studies and methodological limitations, these biomarkers have not been proven as diagnostically useful. Although no individual CSF neurotransmitter proved to be specific for AD, usage of more sophisticated techniques could enable the development of several monoamine metabolites profile,

and possibly improve early AD detection (in addition to currently established core biomarkers).

Keywords Alzheimer's disease – pathogenesis – brainstem nuclei – dorsal raphe nucleus – locus coeruleus – early diagnosis – cerebrospinal fluid – monoamine metabolites

1 Involvement of the monoaminergic system in pathogenesis of alzheimer's disease

Two main pathological features of Alzheimer's disease (AD) are senile plaques (composed of amyloid β; Aβ) and neurofibrillary tangles (composed of aggregated tau protein). It is considered that Aβ pathology precedes tau pathology in cerebrospinal fluid (CSF) (Jembrek et al., 2013). However, based on a large series of postmortally analysed brains Braak et al. (2013) showed that intraneuronal tau aggregation precede diffuse Aβ plaque deposition (Braak et al., 2013). New hypotheses emphasize that AD begins concomitantly in the transentorhinal cortex and brainstem nuclei, or even first in the brainstem nuclei (noradrenergic locus coeruleus - LC, serotonergic dorsal raphe – DRN, and cholinergic nucleus basalis complex - NBC) (Grinberg et al., 2009; for review see Šimić et al., 2014). We tried to summarize all of these findings into a unifying hypothesis where long projection fibres from brainstem nuclei release Aβ that could induce neurofibrillary changes within cortical glutamatergic pyramidal neurons (Šimić et al., 2014). As being part of the default mode network, due to their constant activity these glutamatergic pyramidal neurons produce and release more Aβ than elsewhere in the brain (e.g. within the basal ganglia or cerebellum). This leads to an increase in production, oligomerization, and aggregation of Aβ, which initially compromise endosomal-lysosomal processing and mitochondrial metabolism thus activating caspases responsible for tau cleavage, as well as tau hyperphosphorylation, which is presumably caused by the released Aβ oligomers (Šimić et al., 2014). The sequential cleavage of the tau protein leads to the formation of the tau protein fragment from the microtubule-binding repeat region. This fragment may start an autocatalytic process in which there is progressive accumulation of de novo truncated tau oligomers (Wischik et al., 2014). Further fusion of oligomeric tau leads to formation of the core of the paired helical filaments – the main constituent of the neurofibrillary tangles, which have been neuropathologically confirmed to be an early event in AD (in the so-called "pre-tangle" stage). The fragmented tau is also able to propagate between neurons trans-synaptically, ecto- and endosomally, which has recently been confirmed both in vivo and in vitro (de Calignon et al., 2012; Iba et al., 2013; Guo and Lee, 2013). Our previous study supported some of the aforementioned assumptions regarding the early involvement of the monoaminergic systems in the pathogenesis of AD. Namely, noncognitive, behavioral and psychological symptoms of dementia (such as disturbances in mood, emotion, and appetite, deficits in wake–sleep cycle, etc.) have been less considered as clinical criteria for diagnosis of AD. However, the occurrence of these symptoms indeed suggests the involvement of the serotonergic nuclei, which has been confirmed by at least three large retrospective clinical studies (for a review see Šimić et al., 2009. Recent study by Roh et al. (2012) suggested that plaque formation in the brain of transgenic mouse model (APPswe/PS1DE9) of AD causes the disturbance of sleep–wake cycle. Since lesions of the raphe nuclei cause insomnia and are directly associated with the sleep regulation, the pathology of raphe nuclei could be associated with Aβ increase in two ways: through Aβ release from raphe projection axons or through possible sleep deprivation that leads to inadequate clearance of Aβ in AD (a vicious cycle where less sleep is causing more Aβ production; in turn, more Aβ accumulated leading to less sleep) (Roh et al., 2012). Recently, it has been demonstrated that even cognitively normal individuals with biomarker evidence of preclinical AD have worse quality of sleep than control individuals (Ju et al., 2013). Finally, the involvement of monoaminergic nuclei in the pathogenesis of AD was further elaborated in an ongoing study proving that exposure to heavy metals (particularly inorganic mercury) can lead to AD-like pathology in noradrenergic LC neurons, whereas these changes may also spread to neighbouring serotonergic raphe neurons. Since the cause of severe loss of LC neurons in AD is an early event, and these neurons are particularly prone to taking up circulating toxins, in this view it is highly likely that sporadic AD may be a predominantly environmental tauopathy combined with elements of individual genetic susceptibility levels responsible for additional diversity in time of onset, clinical picture and rate of pathological and clinical progression.

2 Monoamine metabolites in early diagnosis of alzheimer's disease

Current biomarkers of AD detect the disease in symptomatic individuals (in whom neurodegeneration is already substantial) (Babić et al., 2013, 2014), so novel biomarkers are essential for early AD detection at preclinical stages. Encouraged by the evidence of early monoaminergic nuclei degeneration in AD, many

investigators tried to assess diagnostic potential of monoamine metabolites in the CSF. The concentrations of monoamine metabolites homovanilic acid (HVA), dihydroxyphenylacetic acid and 5-hydroxyindoleacetic acid (5-HIAA) as well as monoamine synthesis cofactor biopterin were found to be significantly decreased in AD (Kawakatsu et al., 1990; Martignoni et al., 1991; Blennow et al., 1992; Parnetti et al., 1992; Sjögren et al., 1998). AD patients with severe forms of dementia demonstrated the most prominent decrease in the CSF levels of HVA and 5-HIAA, which may reflect a decreased turnover of dopamine and serotonin. However, unaffected (Parnetti et al., 1992; Sheline et al., 1998; Stuerenburg et al., 2004) or elevated (Zubenko et al., 1986; van der Cammen et al., 2006) levels of HVA and 5-HIAA were also reported in AD. Thus, the results of the studies on CSF monoamine metabolites in AD patients have been controversial. In addition to observed changes in the CSF levels of monoamine metabolites, findings of reduced CSF concentrations of neurotransmitters dopamine and serotonin, as well as serotonin precursor 5-hydroxytryptophan suggested a systemic damage of monoaminergic neurons in AD (Volicer et al., 1985). Regarding noradrenergic system, different studies reported increased (Tohgi et al., 1992), decreased (Sjögren et al., 1998) or unchanged (Blennow et al., 1992) levels of noradrenaline and noradrenaline metabolite 3-methoxy-4-hydroxyphenylglycol in CSF of AD patients.

3 Conclusion

In conclusion, due to the differences between studies and methodological limitations, monoamine metabolites have not been proven as diagnostically useful biomarkers for AD. However, although no individual CSF neurotransmitter proved to be specific for AD, usage of more sophisticated techniques could enable the development of several monoamine metabolites profile (Czech et al., 2012), and possibly improve AD detection with currently established (core) biomarkers.

References

Babić, M., Švob Štrac, D., Mück-Šeler, D., Pivac, N., Stanić, G., et al. (2014). Update on the core and developing cerebrospinal fluid biomarkers for Alzheimer disease. *Croat. Med. J.* 55(4), 347–365.

Babić, M., Vogrinc, Ž., Diana, A., Klepac, N., Borovečki, F., et al. (2013). Comparison of two commercial enzyme-linked immunosorbent assays for cerebrospinal fluid measurement of amyloid β1–42 and total tau. *Transl. Neurosci.* 4(2), 234–240.

Blennow, K., Wallin, A., Gottfries, C. G., Lekman, A., Karlsson, I., et al. (1992). Significance of decreased lumbar CSF levels of HVA and 5-HIAA in Alzheimer's disease. *Neurobiol. Aging.* 13(1), 107–113.

Braak, H., Zetterberg, H., Del Tredici, K. and Blennow, K. (2013). Intraneuronal tau aggregation precedes diffuse plaque deposition, but amyloid-β changes occur before increases of tau in cerebrospinal fluid. *Acta. Neuropathol.* 126(5), 631–641.

Czech, C., Berndt, P., Busch, K., Schmitz, O., Wiemer, J., et al. (2012). Metabolite Profiling of Alzheimer's Disease Cerebrospinal Fluid. *PLoS One.* 7(2), e31501.

de Calignon, A., Polydoro, M., Suárez-Calvet, M., William, C., Adamowicz, D. H., et al. (2012). Propagation of Tau Pathology in a Model of Early Alzheimer's Disease. *Neuron.* 73(4), 685–697.

Grinberg, L. T., Rüb, U., Ferretti, R. E. L., Nitrini, R., Farfel, J. M., et al. (2009). The dorsal raphe nucleus shows phospho-tau neurofibrillary changes before the transentorhinal region in Alzheimer's disease. A precocious onset? *Neuropathol. Appl. Neurobiol.* 35(4), 406–416.

Guo, J. L. and Lee, V. M. Y. (2013). Neurofibrillary tangle-like tau pathology induced by synthetic tau fibrils in primary neurons over-expressing mutant tau. *FEBS Lett.* 587(6), 717–723.

Iba, M., Guo, J. L., McBride, J. D., Zhang, B., Trojanowski, J. Q. and Lee, V. M.-. Y. (2013). Synthetic Tau Fibrils Mediate Transmission of Neurofibrillary Tangles in a Transgenic Mouse Model of Alzheimer's-Like Tauopathy. *J. Neurosci.* 33(3), 1024–1037.

Jembrek, M. J., Babić, M., Pivac, N., Hof, P. R. and Šimić, G. (2013). Hyperphosphorylation of tau by GSK-3β in Alzheimer's disease: The interaction of Aβ and sphingolipid mediators as a therapeutic target. *Transl. Neurosci.* 4(4), 466–476.

Ju, Y.-E. S., McLeland, J. S., Toedebusch, C. D., Xiong, C., Fagan, A. M., et al. (2013). Sleep Quality and Preclinical Alzheimer Disease. *JAMA Neurol.* 70(5), 587.

Kawakatsu, S., Morinobu, S., Shinohara, M., Totsuka, S. and Kobashi, K. (1990). Acetylcholinesterase activities and monoamine metabolite levels in the cerebrospinal fluid of patients with alzheimer's disease. *Biol. Psychiatry.* 28(5), 387–400.

Martignoni, E., Bono, G., Blandini, F., Sinforiani, E., Merlo, P. and Nappi, G. (1991). Monoamines and related metabolite levels in the cerebrospinal fluid of patients with dementia of Alzheimer type. Influence of treatment with L-deprenyl. *J. Neural Transm. - Park. Dis. Dement. Sect.* 3(1), 15–25.

Parnetti, L., Gaiti, A., Reboldi, G. P., Santucci, C., Mecocci, P., et al. (1992). CSF monoamine

metabolites in old age dementias. *Mol. Chem. Neuropathol.* 16(1-2), 143–157.

Roh, J. H., Huang, Y., Bero, A. W., Kasten, T., Stewart, F. R., et al. (2012). Disruption of the Sleep-Wake Cycle and Diurnal Fluctuation of β-Amyloid in Mice with Alzheimer's Disease Pathology. *Sci. Transl. Med.* 4(150), 150ra122–150ra122.

Sheline, Y. I., Miller, K., Bardgett, M. E. and Csernansky, J. G. (1998). Higher cerebrospinal fluid MHPG in subjects with dementia of the Alzheimer type. Relationship with cognitive dysfunction. *Am. J. Geriatr. Psychiatry.* 6(2), 155–61.

Šimić, G., Babic, M., Borovecki, F. and Hof, P. R. (2014). Early Failure of the Default-Mode Network and the Pathogenesis of Alzheimer's Disease. *CNS Neurosci. Ther.* n/a–n/a.

Šimić, G., Stanic, G., Mladinov, M., Jovanov-Milosevic, N., Kostovic, I. and Hof, P. R. (2009). Does Alzheimer's disease begin in the brainstem? *Neuropathol. Appl. Neurobiol.* 35(6), 532–554.

Sjögren, M., Minthon, L., Passant, U., Blennow, K. and Wallin, A. (1998). Decreased monoamine metabolites in frontotemporal dementia and Alzheimer's disease. *Neurobiol. Aging.* 19(5), 379–384.

Stuerenburg, H. J., Ganzer, S. and Müller-Thomsen, T. (2004). 5-hydroxyindoleacetic acid and homovanillic acid concentrations in cerebrospinal fluid in patients with Alzheimer's disease, depression and mild cognitive impairment. *Neuroendocrinol. Lett.* 25.

Tohgi, H., Ueno, M., Abe, T., Takahashi, S. and Nozaki, Y. (1992). Concentration of monoamines and their metabolites in the cerebrospinal fluid from patients with senile dementia of the Alzheimer type and vascular dementia of the Binswanger type. *J. Neural Transm. - Park. Dis. Dement. Sect.* 4(1), 69–77.

van der Cammen, T. J. M., Tiemeier, H., Engelhart, M. J. and Fekkes, D. (2006). Abnormal neurotransmitter metabolite levels in Alzheimer patients with a delirium. *Int. J. Geriat. Psychiatry.* 21(9), 838–843.

Volicer, L., Direnfeld, L. K., Langlais, P. J., Freedman, M., Bird, E. D. and Albert, M. L. (1985). Catecholamine Metabolites and Cyclic Nucleotides in Cerebrospinal Fluid in Dementia of Alzheimer Type. *J. Gerontol.* 40(6), 708–713.

Wischik, C. M., Harrington, C. R. and Storey, J. M. D. (2014). Tau-aggregation inhibitor therapy for Alzheimer's disease. *Biochem. Pharmacol.* 88(4), 529–539.

Zubenko, G. S., Marquis, J. K., Volicer, L., Direnfeld, L. K., Langlais, P. J. and Nixon, R. A. (1986). Cerebrospinal fluid levels of angiotensin-converting enzyme, acetylcholinesterase, and dopamine metabolites in dementia associated with Alzheimer's disease and Parkinson's disease: A correlative study. *Biol. Psychiatry.* 21(14), 1365–1381.

Benzothiazoles - Scaffold of interest for CNS targeted drugs

Ondrej Benek[1,2], Lukas Hroch[2,3], Patrick Guest[4], Laura Aitken[4], Ondrej Soukup[3], Kamil Kuca[1,3], Rona Ramsay[4], Frank Gunn-Moore[4] and Kamil Musilek[1,3]

[1] University of Defence, Faculty of Military Health Sciences, Department of Toxicology and Center of Advanced Studies, Trebesska 1575, 500 01 Hradec Kralove, Czech Republic

[2] University Hospital, Biomedical Research Centre, Sokolska 581, 500 05 Hradec Kralove, Czech Republic

[3] Charles University in Prague, Faculty of Pharmacy in Hradec Kralove, Department of Pharmaceutical Chemistry and Drug Control, Heyrovskeho 1203, 500 05 Hradec Kralove, Czech Republic

[4] University of St. Andrews, Medical and Biological Sciences Building, St. Andrews, KY16 9TF Fife, UK

*

Abstract. The novel benzothiazolyl molecules were synthesized and tested on human recombinant ABAD *in vitro*.

Keywords Alzheimer disease – mitochondria – ABAD modulator – synthesis – in vitro.

1 Introduction

Benzothiazole compounds represent heterocyclic systems comprising a benzene ring fused with a thiazole ring containing nitrogen and sulphur in its structure. Besides the presence of a benzothiazole core in naturally occurring molecules, synthesized compounds containing a benzothiazole moiety in their structure proved to be a significant class of potential therapeutics, as they exhibit biological effects such as antitumor, antibacterial, antitubercular, antiviral, anthelmintic, antidiabetic and many others. Apart from the aforementioned peripheral or microbial active sites, benzothiazole analogues are also biologically active compounds in the central nervous system, where some approved drugs containing benzothiazole moiety have already been identified and are used in the treatment of various neurological disorders.

Some benzothiazoles were found to be modulators of Amyloid-binding alcohol dehydrogenase (ABAD). ABAD is to date the most characterized Aβ-binding intracellular protein. Direct interaction of this mitochondrial enzyme with Aβ was confirmed by many different methods. Aβ binding to ABAD triggers a series of events leading to mitochondrial dysfunction characteristic for Alzheimer disease. Thus this interaction may represent a target for treatment strategy against AD (Muirhead et al., 2010).

2 Methods and Findings

The novel series of benzothiazolyl compounds were synthesized with structural modifications. Their purity and entity was checked by $^{1}H/^{13}C$ NMR and HRMS techniques. The activity of prepared compounds was evaluated on human recombinant ABAD (hrABAD) *in vitro*.

The synthesis of novel compounds was established with yields of 30-90 %. The novel compounds exhibited inhibition of hrABAD and some of them showed inhibition ability on low µM or nM scale *in vitro*. Among the prepared compounds, several structural motifs were identified within structure-activity relationship study to play crucial role in hrABAD inhibition (Guest under revision).

3 Conclusion

The inhibitors of hrABAD were successfully prepared and evaluated. The *in vitro* findings showed their ability to inhibit ABAD and thus for further research and development.

References

Muirhead, K. E. A., Borger, E., Aitken, L., Conway, S. J. and Gunn-Moore, F. J. (2010). The consequences of mitochondrial amyloid beta-peptide in Alzheimer's disease. *Biochem. J.* 426(3), 255–70.

Neurobiology and neuropharmacology of PTSD

Nela Pivac*
Rudjer Boskovic Institute; Division of Molecular Medicine; Laboratory for Molecular Neuropsychiatry; Bijenicka 54; POBox 180; HR-10002 Zagreb; Croatia
*npivac@irb.hr

Abstract. This review describes the neurobiology and neuropharmacology of post-traumatic stress disorder (PTSD) and discusses the molecular basis of PTSD. The interaction between various psychosocial, biological, environmental, genetic and epigenetic factors determine vulnerability or resilience to develop PTSD after exposure to a traumatic event. Etiology of PTSD is complex, and still not clear. Since not all subjects exposed to traumatic experience will develop PTSD, it is assumed that vulnerability factors include psychosocial, neuroanatomical, neurotransmitter and neuroendocrine changes. PTSD is frequently comorbid with other psychiatric disorders. The review highlights therapeutic strategies and non-response to current treatment options, and stresses the need for the development of new treatments of PTSD.

Keywords PTSD – genetic variants – neurotransmitter system – comorbidities – therapies

1 Review

Post-traumatic stress disorder (PTSD) is a common, prevalent, severe, disabling and debilitating mental disorder that develops in some, but not all people after exposure to an extreme traumatic event or events. According to the DSM-V criteria, PTSD is a trauma- and stressor-related disorder in which direct exposure to a traumatic experience or witnessing a psychologically stressful event leads to the specific cluster of symptoms: re-experiencing trauma, distressing recollections, dreams, flashbacks; numbing, persistent avoidance of stimuli that might be related or might recall traumatic memories; and hyper-arousal.

Prevalence of lifetime PTSD varies significantly in different countries, from 8 % in US (Kilpatrick et al., 2013), to 18 % in Croatia (Priebe et al., 2010), and to 25 % in Bosnia and Hercegovina (Priebe et al., 2010). The risk of developing PTSD increases if risk factors (female gender, severity, duration and number of traumatic incidents, childhood abuse and neglect, lack of family and social support and existence of previous mental health issues) are present (Zoladz and Diamond, 2013). Half of the exposed victims show acute nature of the disorder but symptoms usually disappear after 3 months. After progression into chronic PTSD, symptoms might reoccur after 12 months to 50 years (Zoladz and Diamond, 2013). The etiology of PTSD is still poorly understood. Since not all subjects exposed to a traumatic event develop PTSD, the extent to which individuals are vulnerable or resilient to trauma depends on a number of factors, primarily trauma related, psychosocial, biological, environmental, genetic and epigenetic factors, and the interaction between them (Domschke, 2012). Heritability ranges from 30-40 % (Almli et al., 2014). Genetic variants in the serotonergic and dopaminergic systems, hypothalamic-pituitary-adrenal (HPA) axis, and other genes related to response to stress and fear are associated with PTSD (Almli et al., 2014). Serotonergic system is involved in the emotional responses and regulation of mood, dopamine has a role in attention, vigilance, sleep and arousal, HPA axis is associated with hyper-responsiveness to stress and emotion dysregulation, brain derived neurotrophic factor (BDNF) and apolipoprotein E are involved in dysregulation of stress, while genes controlling neuropeptide Y and GABA are associated with mechanisms of fear and anxiety. Recently, GWAS studies successfully identified and replicated variants in retinoid-related orphan receptor alpha (RORA) gene as potential genetic risk factors for PTSD, while other risk genes were not replicated, due to the fact that genetic loci contributing to risk of PTSD are numerous and comprised of many rare variants with small effect size, thus most studies are underpowered.

PTSD is frequently comorbid with depressive disorders, substance use disorders, and other anxiety disorders, and these comorbidities complicate the treatment, induce greater psychological distress, significant functional impairment and more frequent inpatient hospitalizations and diminish social functioning (Norman et al., 2012). Treatment strategies in PTSD are focused on reduction or elimination of symptoms, improvement of adaptive functioning, coming back to a safe and trustworthy state, restriction of the generalization of trauma and protection of a patient. Besides psychotherapy and psycho-education, pharmacological treatments that concentrate on the symptom reduction are selective serotonin reuptake inhibitors, anticonvulsants, atypical antipsychotics, alpha adrenergic antagonist, prazosin, and benzodiazepines that are not effective in PTSD symptom improvement but might reduce anxiety and improve sleep (Vieweg et al., 2006; Norman et al., 2012). Patients with PTSD are frequently non-responsive or modestly responsive to current treatment options (Ahearn et al., 2011), and because of the general refractoriness and high rates of comorbidities, there is a high priority for development of novel targeted treatments and interventions.

References

Ahearn, E. P., Juergens, T., Cordes, T., Becker, T. and Krahn, D. (2011). A review of atypical antipsychotic medications for posttraumatic stress disorder. *Int. Clin. Psychopharmacol.* 1.

Almli, L. M., Fani, N., Smith, A. K. and Ressler, K. J. (2014). Genetic approaches to understanding post-traumatic stress disorder. *Int. J. Neuropsychopharmacol.* 17(2), 355–70.

Domschke, K. (2012). Patho-genetics of posttraumatic stress disorder. *Psychiatr. Danub.* 24(3), 267–73.

Kilpatrick, D. G., Resnick, H. S., Milanak, M. E., Miller, M. W., Keyes, K. M. and Friedman, M. J. (2013). National Estimates of Exposure to Traumatic Events and PTSD Prevalence Using DSM-IV and DSM-5 Criteria. *J. Trauma. Stress.* 26(5), 537–547.

Norman, S. B., Myers, U. S., Wilkins, K. C., Goldsmith, A. A., Hristova, V., et al. (2012). Review of biological mechanisms and pharmacological treatments of comorbid PTSD and substance use disorder. *Neuropharmacology.* 62(2), 542–551.

Priebe, S., Bogic, M., Ajdukovic, D., Franciskovic, T., Galeazzi, G. M., et al. (2010). Mental Disorders Following War in the Balkans. *Arch. Gen. Psychiatry.* 67(5), 518.

Vieweg, W. V. R., Julius, D. A., Fernandez, A., Beatty-Brooks, M., Hettema, J. M. and Pandurangi, A. K. (2006). Posttraumatic Stress Disorder: Clinical Features, Pathophysiology, and Treatment. *Am. J. Med.* 119(5), 383–390.

Zoladz, P. R. and Diamond, D. M. (2013). Current status on behavioral and biological markers of PTSD: A search for clarity in a conflicting literature. *Neurosci. Biobehav. Rev.* 37(5), 860–895.

Theoretical and Pharmacological Study of Multitarget Compounds Against Neurological Diseases

Katarina Nikolic*[1], Lazaros Mavridis[2], Oscar M. Bautista-Aguilera[3], José Marco-Contelles[3], Holger Stark[4], Maria do Carmo Carreiras[5], Ilaria Rossi[6], Paola Massarelli[6], Danica Agbaba[1], Rona R. Ramsay[2], and John B. O. Mitchell[2]

[1]Institute of Pharmaceutical Chemistry, Faculty of Pharmacy, University of Belgrade, Belgrade, Serbia.

[2]Biomedical Sciences Research Complex and EaStCHEM School of Chemistry, University of St Andrews, St Andrews, Scotland, KY16 9ST, UK

[3]Laboratorio de Química Médica, Instituto de Química Orgánica General, Consejo Superior de Investigaciones Científicas, C/Juan de la Cierva 3, 28006 Madrid, Spain

[4]Heinrich Heine University, Institute of Pharmaceutical and Medicinal Chemistry, Universitaetsstr. 1, 40225 Duesseldorf, Germany

[5]iMed.UL - Research Institute for Medicines and Pharmaceutical Sciences, Faculty of Pharmacy, University of Lisbon, Avda. Prof. Gama Pinto, 1649-003 Lisbon, Portugal

[6]Dipartimento di Scienze Mediche, Chirurgiche e Neuroscienze, University of Siena, Strada delle Scotte 6, 53100 SIENA, Italy.

*knikolic@pharmacy.bg.ac.rs

Abstract. Multi-target ligands, recently developed in our laboratories, are novel drug candidates able to interact with MAO-A and B; AChE and BuChE; or with HMT and H_3R, as essential drug targets in the treatment of Alzheimer's disease, depression, obsessive disorders, and Parkinson's disease. Using the refined ChEMBL families and our validated cheminformatic approach of the protein target prediction we have identified the pharmaceutical target and off-targets associated with the 134 multipotent compounds able to interact with MAO-A and B; AChE and BuChE; or with HMT and H_3R. High affinities for the top ranked off-targets of the selected ligands were confirmed by *in vitro* testing (5-$HT_{1a}R$, 5-$HT_{2a}R$) and 3D-QSAR(H_3R/D_1R/D_2R/5-$HT_{2a}R$) studies. Multi-target ligands with possible additional beneficial pharmacological activities were selected for further study.

Keywords multi-targeted ligands – circular fingerprints – off-target study – ChE – MAO

1 Introduction

Novel drug design has expanded beyond the one drug-one target theory. Polypharmacology is a new pharmacological concept for the study of drug action which can involve plural targets interacting with multiple targets to address disease in more effective and subtle ways. Therefore, development of multi-targeted ligands as novel drug candidates against neurological diseases was one of the main aims of our recent studies (Juárez-Jiménez et al., 2014; Bautista-Aguilera et al., 2014; Apelt et al., 2002).

2 Methods

Our recently developed PFClust clustering algorithm (Mavridis et al., 2013) was applied to all of the filtered ChEMBL families. A probabilistic method, the Parzen-Rosenblatt kernel density estimation method (Parzen, 1962), was applied to build a predictive model from the ChEMBL dataset. Circular fingerprint descriptors (Glem et al., 2006) were calculated for compounds used in the study and compared by Tanimoto similarity scores. The obtained Tanimoto similarity scores are then transformed into probabilities (pairwise p-values) using kernel (Gaussian) function.

The same cheminformatic methodology was used to create a "predictor" model from the DrugBank database to determine the main pharmacological groups of the examined 134 multi-target ligands (Lowe et al., 2012).

3 Results

For the MAO/ChE inhibitor, compound 71/MBA-VEG8, the cheminformatic method has determined serotonin 5-HT_{1a}R, 5-HT_{2a}R, 5-HT_{2c}R, 5-HT_{5a}R, and D_1R as possible off-targets (Figure 1).

The compound 71/MBA-VEG8 was further examined by the *in vitro* 5-HT_{2a}R and 5-HT_{1a}R binding assay. The binding study has confirmed relatively strong affinity of the 71/MBA-VEG8: Ki(5-HT_{2a}R) = 14.2 nM and Ki(5-HT_{1a}R) = 108 nM for the receptors. High affinities for the top ranked off-targets of the selected ligands were also confirmed by 3D-QSAR(H_3R/D_1R/D_2R/5-HT_{2a}R) studies. The developed workflow, composed of cheminformatic, 3D-QSAR and in vitro studies, represents a reliable methodology that can easily be used in initial phases of drug design process.

4 Conclusions

The identified novel off-targets for the examined ligands were confirmed by *in vitro* 5-HT_{1A} and 5-HT_{2A} receptor binding assay and by 3D-

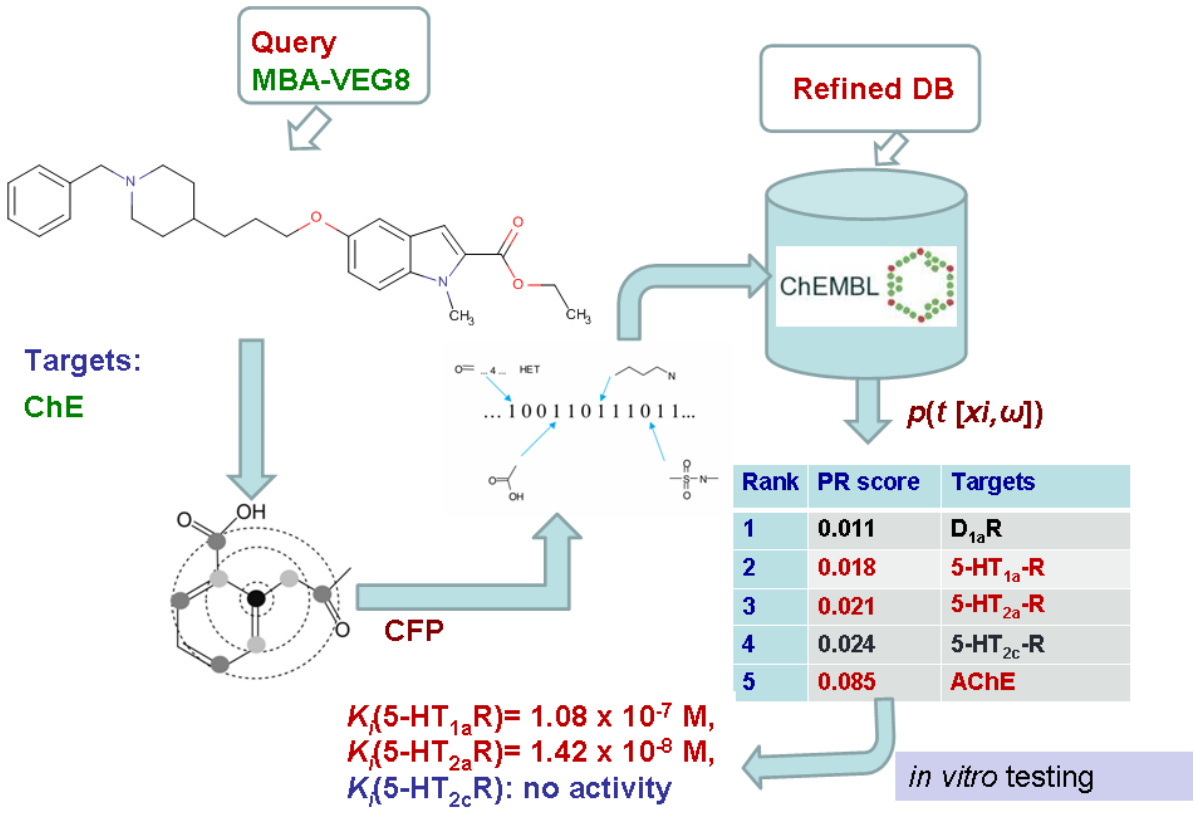

Figure 1: Target for a query compound (71/MBA-VEG8) retrieved from refined ChEMBL dataset.

QSAR($H_3R/D_1R/D_2R/5\text{-}HT_{2a}R$) predictions. Several multi-target ligands were selected for further study, as compounds with possible additional beneficial pharmacological activities.

Acknowledgement

This project has been carried out with the support of WADA. We also acknowledge financial support from the Scottish Universities Life Sciences Alliance (SULSA). OMBA and JMC thenk MINECO (Spain) for a fellowship, and support (SAF2012-33304), respectively. KN and DA acknowledge project supported by the Ministry of Education and Science of the Republic of Serbia, Contract #172033. Further supports by Else Kröner-Fresenius-Stiftung, Translational Research Innovation – Pharma (TRIP), Fraunhofer-Projektgruppe für Translationale Medizin und Pharmakologie (TMP) (to HS) and the European COST Actions BM1007, CM1103 (including STSM 10295 to KN), and CM1207 are also gratefully acknowledged.

References

Apelt, J., Ligneau, X., Pertz, H. H., Arrang, J.-M., Ganellin, C. R., et al. (2002). Development of a New Class of Nonimidazole Histamine H 3 Receptor Ligands with Combined Inhibitory Histamine N- Methyltransferase Activity. *J. Med. Chem.* 45(5), 1128–1141.

Bautista-Aguilera, O. M., Esteban, G., Bolea, I., Nikolic, K., Agbaba, D., et al. (2014). Design, synthesis, pharmacological evaluation, QSAR analysis, molecular modeling and ADMET of novel donepezil–indolyl hybrids as multipotent cholinesterase/monoamine oxidase inhibitors for the potential treatment of Alzheimer's disease. *Eur. J. Med. Chem.* 75, 82–95.

Glem, R. C., Bender, A., Arnby, C. H., Carlsson, L., Boyer, S. and Smith, J. (2006). Circular fingerprints: flexible molecular descriptors with applications from physical chemistry to ADME. *IDrugs.* 9(3), 199–204.

Juárez-Jiménez, J., Mendes, E., Galdeano, C., Martins, C., Silva, D. B., et al. (2014). Exploring the structural basis of the selective inhibition of monoamine oxidase A by dicarbonitrile aminoheterocycles: Role of Asn181 and Ile335 validated by spectroscopic and computational studies. *Biochim. Biophys. Acta - Proteins Proteomics.* 1844(2), 389–397.

Lowe, R., Mussa, H. Y., Nigsch, F., Glen, R. C. and Mitchell, J. B. O. (2012). Predicting the mechanism of phospholipidosis. *J. Cheminf.* 4(1), 2.

Mavridis, L., Nath, N. and Mitchell, J. B. O. (2013). PF-Clust: a novel parameter free clustering algorithm. *BMC Bioinformatics.* 14(1), 213.

Parzen, E. (1962). On Estimation of a Probability Density Function and Mode. *Ann. Math. Stat.* 33(3), 1065–1076.

Cis-cyclopropylamines as mechanism-based inhibitors of monoamine oxidases

Malcomson Thomas[1]; Ganesan A.[*2]; Mangelinckx Sven[3]; Yelekci Kemal[4]; Ramsay Rona R.[1]
[1]Biomedical Sciences Research Complex, University of St Andrews, St Andrews, UK
[2]School of Pharmacy, University of East Anglia, Norwich, UK
[3]Department of Sustainable Organic Chemistry and Technology, Ghent University, Ghent, Belgium
[4]Kadhir Has University, Istanbul, Turkey
[*]A.Ganesan@uea.ac.uk

Abstract. Investigated for the therapy of depression and cancer, cyclopropylamines are known inhibitors of monoamine oxidases (MAO A and MAO B) and lysine-specific demethylases (LSD1). The antidepressant drug, tranylcypromine, which has a *trans* structure, inhibits all three enzymes. We investigated novel primary and secondary cyclopropylamines with an alkoxy group at the 2 position of the cyclopropyl ring, all with the less common *cis* relationship. Theoretical K_i values for both enantiomers were obtained by docking the compounds into MAO A or MAO B using Autodock but revealed very little difference between the enantiomers. Using a mixture of the enantiomers, the reversible inhibition of MAO A gave high IC_{50} values for most compounds. In contrast, the IC_{50} values were sub-micromolar for MAO B. Irreversible binding was similarly selective for MAO B. Spectral changes during the inactivation reaction, the stability of the adduct and its mass were consistent with an adduct to the flavin but rates of inactivation were slower than for tranylcypromine. The best inhibitor was cis-N-benzyl-2-methoxycyclopropylamine, with an IC_{50} of 5 nM for MAO B and 170 nM for MAO A after 30 min preincubation, but no activity on LSD1. This *cis*-cyclopropylamine is over 200-fold more effective than tranylcypromine so could be studied as a lead for selective inhibitors of MAO B that do not inhibit LSD1.

Keywords docking – enantiomers – flavin adduct – mechanism-based inhibitor – tranylcypromine

1 Introduction

Cyclopropylamine is a useful structural scaffold for the design of mechanism-based inhibitors and many structure-activity studies have appeared in the quest for lead compounds for the therapy of depression and cancer. Cyclopropylamines are known inhibitors of monoamine oxidases (MAO), cytochrome P450 (CYP) enzymes, and lysine-specific demethylases (LSD1) (Khan et al., 2013; Binda et al., 2010; Mimasu et al., 2010). The antidepressant drug, tranylcypromine (TCP), is a mechanism-based inactivator of monoamine oxidases (MAO) used in the treatment of depression and also an irreversible inhibitor of LSD1, one of the key demethylase enzymes in epigenetic gene regulation. Contrasting with TCP (a *trans* structure), we have investigated novel cyclopropylamines with the less common *cis* relationship to define their efficacy and selectivity.

2 Methods

Activity for membrane-bound MAO (Sigma-Aldrich, UK) was determined in the coupled Amplex Red assay (Zhou & PanchukVoloshina, 1997). For the reversible inhibition, IC_{50} values in the presence of 2.5xKm substrate concentration (tyramine) with the enzyme added last. The IC_{50} values for the irreversible inactivation were determined from the activity remaining after 30 min of incubation of the enzyme and inhibitor in the presence of 1 mM tyramine. Data were analysed in Graphpad PRISM to give the parameter ±sd from at least 20 points. The adduct was characterised by the spectral and mass change in MAO A (Esteban et al., 2014; Mitchell et al., 2001).

Molecular models of the *cis*-cyclopropylamine inhibitors were built and optimised using ArgusLab 4.0.1 on an Intel i7 HP Laptop, operating Windows 8 Home Premium. MAO A (PDB code: 2Z5X) and MAO B (PDB code: 2V5Z) protein structures were minimised using Accelrys 6.0 adopting a CHARMM force field and simulated annealing. Docking used AutoDock4 (Morris et al., 2009) and Vina coding scripts.

3 Findings and argument

Theoretical K_i values for both enantiomers of seven novel compounds obtained by docking the compounds into MAO A or MAO B using Autodock revealed very little difference between the enantiomers, so all experimental work used the mixture of enantiomers. The computed reversible K_i values ranged from 3 µM to 2 mM with only a 2-fold difference between MAO A and B. In contrast, the experimental IC_{50} values revealed selectivity for MAO B with some of the compounds. The reversible inhibition of MAO A was poor and agreed with the predicted values but the experimental IC_{50} values for MAO B were all low micromolar and as good as or better than the standard drug, tranylcypromine. For the irreversible inhibition, IC_{50} values measured after 30 min pre-incubation of the enzyme and inhibitor are shown in Table 1. The 2-substituted *cis*-analog is less ef-

	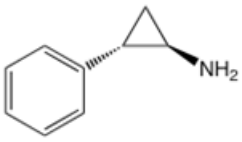	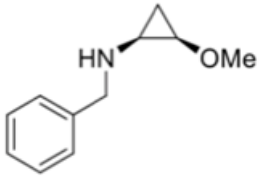
IC_{50} (nM)	tranylcypromine (*trans*)	*cis*-N-Benzyl-2-methoxycyclopropylamine
MAO A	175(68) nM	237(61) nM
MAO B	4.70(5) nM	73.5(49) nM
Selectivity for MAO B	104	3.2

Table 1: Efficacy and selectivity for MAO B for the best *cis*-cyclopropylamine compared to tranylcypromine

fective than tranylcypromine and less selective for MAO B. The slower rate of inactivation of MAO B by the *cis*-compound (0.104(5) min^{-1} compared to 0.263(5) min^{-1} for tranylcypromine) may explain the lower efficacy on MAO B.

The irreversible inactivation was shown to be due to adduct formation by the spectral changes in MAO A, by the stability of the adduct to denaturation in urea and during pronase digestion to release the modified flavin co-factor, and by the mass increase.

4 Conclusion

cis-*N*-Benzyl-2-methoxycyclopropylamine (4) is a new irreversible MAOI with IC_{50} 5 nM for MAO B,170 nM for MAO A, and no activity on LSD1.

References

Binda, C., Valente, S., Romanenghi, M., Pilotto, S., Cirilli, R., et al. (2010). Biochemical, structural, and biological evaluation of tranylcypromine derivatives as inhibitors of histone demethylases LSD1 and LSD2. *J. Am. Chem. Soc.* 132(19), 6827–6833.

Esteban, G., Allan, J., Samadi, A., Mattevi, A., Unzeta, M., et al. (2014). Kinetic and structural analysis of the irreversible inhibition of human monoamine oxidases by ASS234, a multi-target compound designed for use in Alzheimer's disease. *Biochim. Biophys. Acta - Proteins Proteomics.* 1844(6), 1104–1110.

Khan, M. N. A., Suzuki, T. and Miyata, N. (2013). An overview of phenylcyclopropylamine derivatives: biochemical and biological significance and recent developments. *Med. Res. Rev.* 33(4), 873–910.

Mimasu, S., Umezawa, N., Sato, S., Higuchi, T., Umehara, T. and Yokoyama, S. (2010). Structurally Designed trans -2-Phenylcyclopropylamine Derivatives Potently Inhibit Histone Demethylase LSD1/KDM1. *Biochemistry.* 49(30), 6494–6503.

Mitchell, D. J., Nikolic, D., van Breemen, R. B. and Silverman, R. B. (2001). Inactivation of monoamine oxidase B by 1-phenylcyclopropylamine: mass spectral evidence for the flavin adduct. *Bioorg. Med. Chem. Lett.* 11(13), 1757–60.

Morris, G. M., Huey, R., Lindstrom, W., Sanner, M. F., Belew, R. K., et al. (2009). AutoDock4 and AutoDockTools4: Automated docking with selective receptor flexibility. *J. Comput. Chem.* 30(16), 2785–2791.

Evaluation of multiple amine oxidase inhibitory behaviour

Keith F. Tipton*[1], Aldo Olivieri[1], Laura Della Corte[2], Andrew G. McDonald[1]
[1]School of Biochemistry and Immunology Trinity College, Dublin 2, Ireland
[2]Department Neuroscience, Psychology, Drug Area and Child Health, Università degli Studi di Firenze, Firenze, Italy
*ktipton@tcd.ie

Abstract. Amine oxidases will be exposed to a variety of inhibitory compounds, in addition to specific drugs that may be administered for therapeutic purposes. Procedures for analysing the effects of multiple reversible inhibitors are presented in terms of their cumulative effects on enzyme activity.

Keywords inhibition – kinetics xenobiotics – monoamine oxidase – primary-amine oxisase

1 Introduction

The amine oxidases, monoamine oxidase (EC 1.4.3.4; MAO) and primary amine-oxidase (EC 1.4.3.21; SSAO), are sensitive to inhibition by a diverse range of drugs that have been developed for pharmacological and therapeutic uses (Tipton et al., 2011). In some cases it is a metabolite of the administered compound that is inhibitory. In addition a number of dietary components and xenobiotics can inhibit these enzymes (Benedetti Strolin and Tipton, 1999; Olivieri et al., 2011). In some cases, such compounds may actually act as competing substrates for the enzyme and, therefore, can be regarded as competitive inhibitors of the oxidation of the indigenous substrates. The equations describing reaction rates in the presence of two competing substrates are well known (McDonald and Tipton, 2003) and can be expanded to situations involving multiple substrates, each with defined kinetic parameters.

2 Analyses

Any evaluation of the effects of drugs or xenobiotics must take account of the totality if the inhibitory effects arising from all sources. The general equation for the inhibition of an enzyme by multiple reversible inhibitors may be written as:

$$\nu_{1\ldots n} = \frac{V_{\max}}{\frac{K_{\mathrm{m}}}{[S]}\left(1+\frac{[\mathrm{I}]}{K_{\mathrm{i}}}+\frac{[\mathrm{I}_2]}{K_{\mathrm{i}2}}+\frac{[\mathrm{I}_3]}{K_{\mathrm{i}3}}+\ldots\frac{[\mathrm{I}_{\mathrm{n}}]}{K_{\mathrm{in}}}\right)+\left(1+\frac{[\mathrm{I}]}{K'_{\mathrm{i}}}+\frac{[\mathrm{I}_2]}{K'_{\mathrm{i}2}}+\frac{[\mathrm{I}_3]}{K'_{\mathrm{i}3}}+\ldots\frac{[\mathrm{I}_{\mathrm{n}}]}{K'_{\mathrm{in}}}\right)}$$

where $\nu_{1\ldots n}$ is the velocity of the reaction in the presence of n inhibitors that bind to the enzyme in a mutually exclusive fashion, with no enzyme molecule being able to bind more than one of the inhibitors. The substrate concentration is represented by [S] and the inhibitor concentrations by $[\mathrm{I}_1]\ldots[\mathrm{I}_{\mathrm{n}}]$. $V_{\max}$ is the maximum velocity. This equation may be written in condensed form as:

$$\nu_{1\ldots n} = \frac{V_{\max}[\mathrm{S}]}{K_{\mathrm{m}}\left(1+\sum_{[\mathrm{I}]=1}^{\mathrm{n}}\frac{[\mathrm{I}]}{K_i}+[\mathrm{S}]\left(1+\sum_{[\mathrm{I}]=1}^{\mathrm{n}}\frac{[\mathrm{I}]}{K'_i}\right.\right.}$$

or, in dimensionless terms, as

$$\frac{\nu_{1\ldots\mathrm{n}}}{[\mathrm{E}]} = \frac{k_{\mathrm{cat}}}{\alpha\left(1+\beta_1\ldots\beta_{\mathrm{n}}\right)+1\left(\gamma_1\ldots\gamma_{\mathrm{n}}\right)}$$

where [E] is the enzyme concentration, $\alpha\,| = \frac{K_t extm}{[\mathrm{S}]}$, the β values are the respective $\frac{[\mathrm{I}]}{K_{\mathrm{i}}}$ values and γ values are those for $\frac{[\mathrm{I}]}{K'_{\mathrm{I}}}$.

For competitive inhibitors all the K'_{i} values will be equal to infinity so that the equation simplifies to

$$\nu_{1\ldots n} = \frac{V_{\max}}{\frac{K_{\mathrm{m}}}{[S]}\left(1+\frac{[\mathrm{I}_1]}{K_{\mathrm{i}}}+\frac{[\mathrm{I}_2]}{K_{\mathrm{i}2}}+\frac{[\mathrm{I}_3]}{K_{\mathrm{i}3}}+\ldots\frac{[\mathrm{I}_{\mathrm{n}}]}{K_{\mathrm{in}}}\right)}$$

Whereas all the K_{i} values will be infinite for uncompetitive inhibition and both K_{I} and K'_{i} values will be finite for mixed inhibitors.

Clearly, it would be a simple matter to determine the overall effects of reversible inhibitors on the behaviour of an enzyme provided their concentrations and kinetic behaviour and parameters are known. It should also be noted that such effects may affect the rates at which irreversible mechanism-based inhibitors reduce enzyme activity. Unfortunately, such a rigorous analysis requires a great deal of experimental work and a simplified approach has been presented by Chou and Talaly (1977), which is independent of the type of inhibition but relies on the reaction rate at fixed substrate and inhibitor concentrations

$$\nu_{1\ldots\mathrm{n}} = \sum_{[\mathrm{I}]=1}^{\mathrm{n}}\nu_i - \frac{\mathrm{n}-1}{\nu_0}$$

where ν_i is the velocity observed in the presence of each individual inhibitor, and ν_0 is the velocity in the absence of inhibition. However, since the presence of inhibitor(s) is likely to affect the steady-state substrate levels and alterations in the concentrations of one, or more, of the inhibitors may vary with intake, many recalculations could be necessary.

3 Conclusion

The list of dietary components and drugs, which are taken for other purposes, that are known to inhibit one or more of the amine oxidases is quite extensive and include caffeine (MAO & SSAO), imidazolines, used for blood pressure control, (MAO); glucosamine (SSAO); L-lysine (SSAO); the anxiolytic hydroxyzine (MAO & SSAO); components of cigarette smoke (MAO) and products arising from alcohol metabolism (MAO) as well as the methionine arising from creatine metabolism, which acts as a competing SSAO substrate.

Thus a full assessment of the levels of inhibition of these enzymes *in vivo* would necessitate knowledge of an individual's drug and xenobiotic consumption, with consequent tissue levels. Unfortunately, these are generally unavailable.

References

Benedetti Strolin, M. and Tipton, K. F. (1999). Involvement of monooxygenases and amine oxidases in hydroxyl radical generation in vivo. *Neurobiology.* 7(2), 123–34.

Chou, T. C. and Talaly, P. (1977). A simple generalized equation for the analysis of multiple inhibitions of Michaelis-Menten kinetic systems. *J. Biol. Chem.* 252(18), 6438–42.

McDonald, A. and Tipton, K. F. (2003). Kinetics of Catalysed Reactions – Biological. In I. Horváth (Ed.), *Encycl. catal.* (4th ed.). Hoboken, NJ, USA: John Wiley & Sons, Inc.

Olivieri, A., Rico, D., Khiari, Z., Henehan, G., O'Sullivan, J. and Tipton, K. F. (2011). From caffeine to fish waste: amine compounds present in food and drugs and their interactions with primary amine oxidase. *J. Neural. Transm.* 118(7), 1079–1089.

Tipton, K. F., Davey, G. P. and McDonald, A. G. (2011). Kinetic behavior and reversible inhibition of monoamine oxidases—enzymes that many want dead. *Int. Rev. Neurobiol.* 100, 43–64.

Support the EU COST Actions CM1103

Therapeutic approach to cerebrovascular diseases by MTDL containing propargyl moeity and an indole-substituted hydrazine using endothelial hSSAO/VAP-1 expressing cells as an experimental model of cerebral ischemia

***Sun Ping[1], *Solé Montse[1], Esteban Gerard[1], Marco-Contelles José[2], #Unzeta Mercedes*[1]**

[1]Departament de Bioquímica i Biologia Molecular, Institut de Neurociències , Facultat de Medicina, Universitat Autònoma de Barcelona, 08193 Bellaterra, Barcelona, Spain

[2]Laboratorio de Química Médica (IQOG, CSIC), C/ Juan de la Cierva 3, 28006-Madrid, Spain

*Mercedes.Unzeta@uab.es

Abstract. The neurovascular unit, integrated by neurons, microglia and vascular cells maintains the brain homeostasis, but its functionality is altered and contributes to brain pathologies such as Alzheimer's disease (AD) or cerebral ischemia. Vascular adhesion protein 1 (VAP-1) is a pro-inflammatory vascular protein with semicarbazide-sensitive amine oxidase (SSAO) activity. This enzyme is overexpressed in AD cerebrovascular tissue, and elevated in plasma from AD and stroke patients, compromising the cerebrovascular function and therefore the neurovascular unit integrity. We hypothesize that the use of molecules able to interact with different cells types and molecules may enhance the beneficial effects for the treatment of these pathologies. Therefore we have assessed the effect of the indole-substituted hydrazine JL-72 and the MTDL compounds ASS234, DPH-4 and PF 9601N containing a propargyl group in an *in vitro* experimental model of ischemia using human SSAO/VAP-1-expressing endothelial cells. These molecules, with reported neuroprotective properties, also showed a protective effect on this model by SSAO/VAP-1-dependent (DPH-4) or independent (JL-72, ASS234 and PF 9601N) manner. These results suggest a potential use of these compounds for the vascular dysfunction associated to brain diseases and further design of new SSAO/VAP-1 inhibitors might be considered an appropriate therapeutic approach to vascular pathologies.

Keywords cerebral ischemia – Alzheimer's disease – neurovascular unit – MTDL – endothelial hSSAO/VAP-1

1 Introduction

There is increasing evidence that cerebrovascular dysfunction plays a role in cognitive impairment related to Alzheimer's disease (AD). In recent years, the concept of "neurovascular unit" has emerged as a new paradigm for understanding the CNS pathologies, including stroke (Iadecola, 2004). Neurons, glia and vascular cells are closely interrelated and working in concert to maintain the homeostasis of cerebral microenvironment. The development of new agents able to interact with neuronal activity and vascular cells could be an appropriate therapeutic approach for both stroke and AD conditions.

Vascular adhesion protein 1 (VAP-1) is a pro-inflammatory vascular protein that mediates leukocyte recruitment through its semicarbazide-sensitive amine oxidase (SSAO) activity (EC 1.4.3.21) (Jalkanen and Salmi, 2008). This enzyme is over-expressed in human cerebrovascular tissue affected by cerebral amyloid angiopathy (CAA), found in most AD patients (Ferrer et al., 2002) and it is also increased in plasma from severe AD patients (Hernández-Guillamon et al., 2005). Moreover, the soluble form of SSAO/VAP-1 present in plasma predicts the appearance of parenchymal hemorrhages after tissue plasminogen activator treatment in ischemic stroke condition and it is increased in hemorrhagic stroke patients as well (Hernández-Guillamon et al., 2010, 2012). In this concern, the beneficial effect of the indole-substituted hydrazine JL-72 (Esteban et al., 2013) and the multitarget-directed ligands (MTDL) ASS234, DPH-4 and PF 9601N has been already reported in experimental models of Parkinson's disease and AD (Bolea et al., 2013; Wang et al., 2014; Perez and Unzeta, 2003).

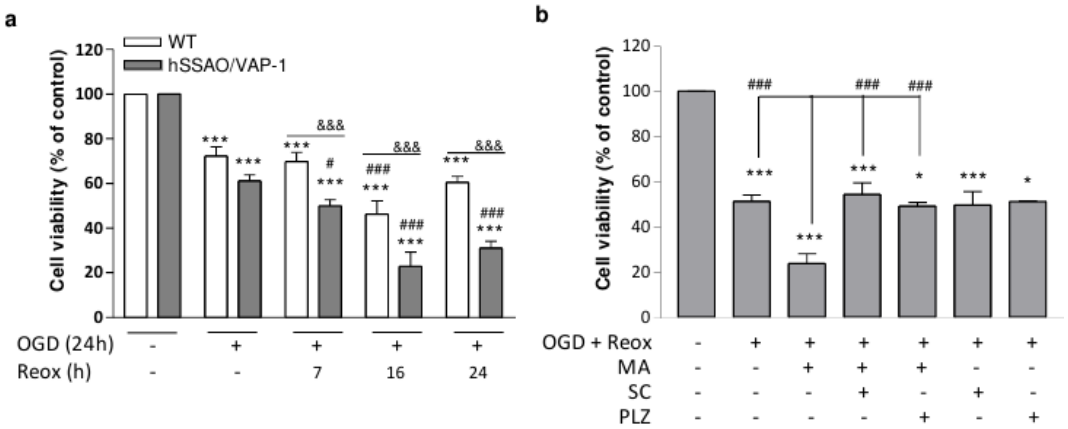

Figure 1: Time-course effect of oxygen and glucose deprivation (OGD) and reoxygenation (Reox) on WT or hSSAO/VAP-1 HUVECs cell viability (a). The effect of methylamine (MA, 1 mM) metabolism by SSAO was analyzed under 24 h OGD with 7 h Reox in SSAO/VAP-1-expressing cells (b). Semicarbazide (Sc, 1 mM) and phenelzine (PLZ, 100 nM) were used as SSAO inhibitors. Cell viability was determined by MTT reduction. Data represent the mean ± SEM of three independent experiments. #, $p < 0.05$; ***,###,&&&, $p < 0.001$ by One-way ANOVA followed by the Newman-Keuls multiple comparison test.

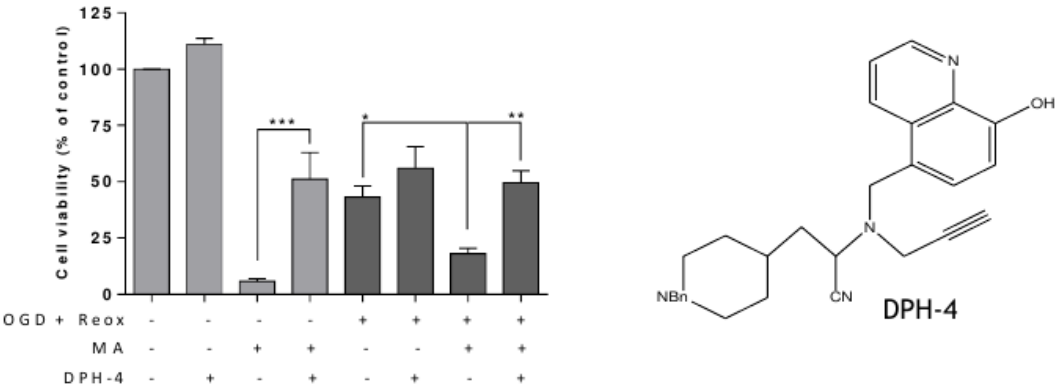

Figure 2: hSSAO/VAP-1 HUVEC cells were subjected to OGD for 24 h and then to reoxygenation for 7 h in the presence of SSAO substrate methylamine (MA, 3 mM) and DPH-4 (1 µM) (left). Controls of the same treatments were performed under normoxia conditions (Norm). Cell viability was determined by the MTT reduction. *, $p < 0.05$; **, $p < 0.01$; ***, $p < 0.001$ by one-way ANOVA and the Newman-Keuls multiple comparison test. Molecular structure of the DPH-4 (right).

2 Methods

Here, the protective effect of these molecules has been assessed in a new *in vitro* experimental model of ischemia developed in our group using human SSAO/VAP-1-transfected endothelial cells (Sun et al., 2014). Cells were subjected to oxygen and glucose deprivation (OGD) for 24 h in the presence of each compound. The cell viability was determined by the MTT reduction assay.

3 Findings and argument

The most suitable OGD and reoxygenation conditions selected were 24 h OGD with 7 h reoxygenation, conditions that rendered a 50 % of cell death analysed by MTT (Figure 1a). When cells were incubated in the presence of methylamine, the specific SSAO/VAP-1 substrate, cell viability decreased significantly, confirming the involvement of the catalytic action of SSAO/VAP-1 in the endothelial cells damage. Furthermore, the cell death was prevented in the presence of semicarbazide or phenelzine (Figure 1b).

The protective effect of molecules JL-72, ASS234, PF 9601-N and DPH-4, were analysed in this experimental model. All of them were found to exhibit distinct inhibitory potencies towards the enzymes SSAO, MAO A, MAO B and AChE/BuChE (data not shown). In each case, a toxicity curve was previously performed in order to use non-toxic concentrations. Partial inhibition of the SSAO activity was only reached with DPH-4. However, a protective effect was observed with all of the molecules when cells were incubated in the presence of methylamine under the experimental ischemic conditions. The compounds JL-72, ASS234 and PF 9601-N, showed 50 % protective effect in an independent SSAO/VAP-1-inhibitory manner, whereas DPH-4 exhibited the highest protection dependent on SSAO/VAP-1 inhibition (Figure 2).

Herein we report for the first time the involvement of SSAO/VAP-1 inhibition on the protective effect of a hydrazine and some propargyl-containing MTDLs on endothelial cells under ischemic conditions.

4 Conclusion

These results suggest a potential use of these compounds for vascular dysfunction associated to CAA-AD or stroke, which may also be applied for the design of new SSAO/VAP-1 inhibitors as an appropriate therapeutic approach to cerebrovascular pathologies.

References

Bolea, I., Gella, A., Monjas, L., Pérez, C., Rodríguez-Franco, M., et al. (2013). Multipotent, Permeable Drug ASS234 Inhibits A Aggregation, Possesses Antioxidant Properties and Protects from A-induced Apoptosis In Vitro. *Curr. Alzheimer Res.* 10(8), 797–808.

Esteban, G., Bolea, I., Sun, P., Solé, M., Samadi, A., et al. (2013). A therapeutic approach to cerebrovascular diseases based on indole substituted hydrazides and hydrazines able to interact with human vascular adhesion protein-1, monoamine oxidases (A and B), AChE and BuChE. *J. Neural Transm.* 120(6), 911–8.

Ferrer, I., Lizcano, J. M., Hernández-Guillamon, M. and Unzeta, M. (2002). Overexpression of semicarbazide sensitive amine oxidase in the cerebral blood vessels in patients with Alzheimer's disease and cerebral autosomal dominant arteriopathy with subcortical infarcts and leukoencephalopathy. *Neurosci. Lett.* 321(1-2), 21–24.

Hernández-Guillamon, M., Esteban, M., Szabo, P., Boada, M. and Unzeta, M. (2005). Human plasma semicarbazide sensitive amine oxidase (SSAO), β-amyloid protein and aging. *Neurosci. Lett.* 384(1-2), 183–187.

Hernández-Guillamon, M., Garcia-Bonilla, L., Sole, M., Sosti, V., Pares, M., et al. (2010). Plasma VAP-1/SSAO Activity Predicts Intracranial Hemorrhages and Adverse Neurological Outcome After Tissue Plasminogen Activator Treatment in Stroke. *Stroke.* 41(7), 1528–1535.

Hernández-Guillamon, M., Solé, M., Delgado, P., García-Bonilla, L., Giralt, D., et al. (2012). VAP-1/SSAO Plasma Activity and Brain Expression in Human Hemorrhagic Stroke. *Cerebrovasc Dis.* 33(1), 55–63.

Iadecola, C. (2004). Neurovascular regulation in the normal brain and in Alzheimer's disease. *Nat. Rev. Neurosci.* 5(5), 347–360.

Jalkanen, S. and Salmi, M. (2008). VAP-1 and CD73, endothelial cell surface enzymes in leukocyte extravasation. *Arterioscler. Thromb. Vasc. Biol.* 28(1), 18–26.

Perez, V. and Unzeta, M. (2003). PF 9601N [N-(2-propynyl)-2-(5-benzyloxy-indolyl) methylamine], a new MAO-B inhibitor, attenuates MPTP-induced depletion of striatal dopamine levels in C57/BL6 mice. *Neurochem. Int.* 42(3), 221–229.

Sun, P., Solé, M. and Unzeta, M. (2014). Involvement of SSAO/VAP-1 in Oxygen-Glucose Deprivation-Mediated Damage Using the Endothelial hSSAO/VAP-1-Expressing Cells as an Experimental Model of Cerebral Ischemia. *Cerebrovasc Dis.* 37(3), 171–180.

Wang, L., Esteban, G., Ojima, M., Bautista-Aguilera, O. M., Inokuchi, T., et al. (2014). Donepezil + propargylamine + 8-hydroxyquinoline hybrids

as new multifunctional metal-chelators, ChE and MAO inhibitors for the potential treatment of Alzheimer's disease. *Eur. J. Med. Chem.* 80, 543–561.

Interaction of novel Monoamino Oxidadese Inhibitor with Cytochrome P450

Veronica Simone[1], Federica Pessina[1], Miriam Durante[1], Maria Frosini[1], Jose Luis Marco Contelles[2], Mercedes Unzeta[3] and Massimo Valoti[*1]

[1]Department of Life Sciences, University of Siena, Via Aldo Moro 2, Siena, Italy

[2]Laboratorio de Quimica Médica Instituto de Química Orgánica General CSIC Juan de la Cierva, 3; 28006-Madrid (Spain)

[3]Departament de Bioquímica i Biología Molecular, Facultat de Medicina, Universitat Autònoma de Barcelona, 08193 Bellaterra, Barcelona, Spain

[*]valoti@unisi.it

Abstract. The effects of monoamine oxidase inhibitors (MAOIs) towards cytochrome P-450 (CYP) dependent activity resulted an important aspect in the therapeutic use of these compounds. Several MAOIs present a propargylamino moiety. This chemical group confers them properties of irreversible inhibitors towards the MAO and could represent a potential molecular site to the formation of suicide substrates toward CYP. In fact CYP metabolism could give rise to the formation of an active electrophil binding site, resulting in an inhibition of CYPs, which could be responsible of a drug-drug interaction when compounds should be administer in a multiple therapy. For these reasons the metabolic features of a series of novel multitarget compounds, characterized by MAO and acethylcoline esterase (AChE) inhibiting properties were studied in human liver microsomes. The kinetic analysis showed that lead compound ASS234, is a poor substrate for human CYPs at variance to those observed in rat liver microsomes.These preliminary in vitro results indicate that ASS234 may have a suitable pharmacokinetic profile.

Keywords Drug Metabolism – Cytochrome P450 – Metabolic stability

1 Introduction

In recent years, attention has been focused on the importance of studies on absorption, distribution, metabolism, excretion and toxicity (ADMET) of drug candidates. The goal of a successful drug discovery program is therefore not only the identification of a new molecule highly active and selective towards a suitable molecular target, but also the early assessment of

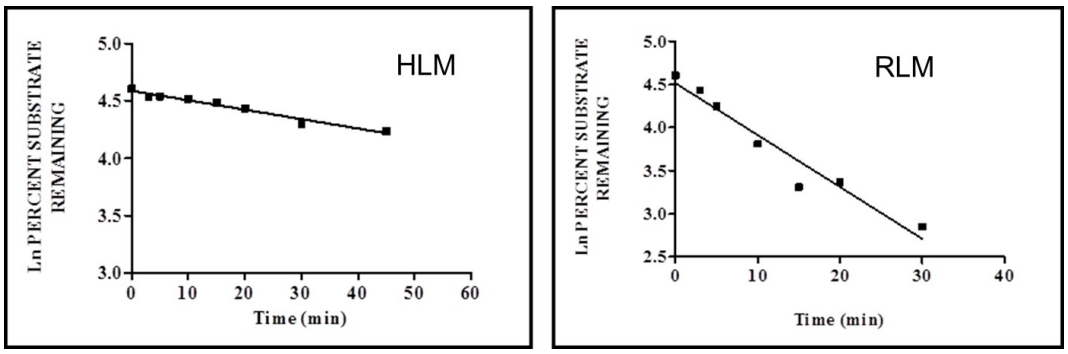

Figure 1: Kinetic parameters for the time-dependent metabolism of ASS234. Results are presented graphically: ln of residual activity as a function of pre-incubation time. Curves were fitted by a straight-line equation for linear regression and r^2 ranged between 0.99 and 0.93. HLM, human liver microsome; RLM, rat liver microsomes.

its ADMET properties, in order to discard those compounds that are unlikely to be successful drug candidates. In this context, cytochrome P450 family (CYP) plays a crucial role both in metabolism and in the toxicity of a drug. CYP enzymes can be inhibited or induced by drugs, resulting in clinically significant drug-drug interactions that can cause unpredictable adverse reactions or therapeutic failures. For these reasons the metabolic features of a series of novel multitarget compounds (Bolea et al., 2011), characterized by MAO and acethylcoline esterase (AChE) inhibiting properties were studied in human and rat liver microsomes.

2 Methods

The incubation mixture (total volume 500 µl) contained the following components (final concentration): TRIS-HCl, pH 7.6 (50 mM), MgCl2 (25 mM), human or rat liver microsomes (0.5 mg protein / ml), NADPH (0.215 mM) and resorufine-derivative probe substrates, such as ETR (2 µM), PTR (10 µM) or BZR (5 µM), and 50 µM novel MOAIs (ASS 50,ASS 64, ASS 92 and ASS 234, see Samadi et al., 2011 according to D'Elia et al., 2009). In a second series of experiments the lead compound ASS234 (5 µM) was incubated of liver microsomal proteins and the reactions were terminated at regular time intervals (0–60 min) by adding a double volume of acetonitrile. Samples were analyzed by HPLC-UV method. The intrinsic clearance (Clintr) was calculated by the following equation

$$\mathrm{Cl_{intr}} = \mathrm{k}(min - 1) \times \frac{[\mathrm{V}]}{[\mathrm{P}]}$$

where k is the rate costant for the depletion of substrate, V is the volume of incubation in µL and P is the amount of microsomal proteins in the incubation medium in mg according to Baranczewski et al. (2006).

3 Findings and argument

All the compounds tested presented a significative inhibition of CYP-dependent metabolism of ETR, (CYP1A family, marker substrate), while the metabolism of other resorufine substrates was unaffected. Moreover, this effect resulted fully reversible and a competitive fashion. In spite the latter experimental evidences the metabolic stability of the lead compound ASS234 was studied.

As reported in figure 1, the plot of the natural logarithm of the percent of the compounds non metabolized versus time was linear, indicating that the substrate depletion by CYPs followed a monoexponential relationship. The calculated rate costant, k, ranged from $0.0083\,\mathrm{min}^{-1}$ up to $0.0602\,\mathrm{min}^{-1}$ for human liver microsomes and rat liver microsomes, respectively. The $\mathrm{Cl_{intr}}$ ranged from 1.7 up to 129.2 (µl min^{-1} mg^{-1}) in human and rat liver, respectively. Furthermore the calculated $t^1/_2$ resulted 7.5 fold greater in human compared rat microsmal preparations, (83 min vs 11 min, respectively).

4 Conclusions

Richmond et al. (2010), classified the chemical compounds based on their Clintr value (expressed as µL min^{-1} mg $\mathrm{protein}^{-1}$), where, in rat, < 9 = very low metabolic turnover; $8 - 50$ = low clearance; $50 - 150$ = moderate clearance; > 150 = high clearance value. These data indicated that the studied compound, AASS 234, possess a double-acting, it presented an high metabolic stability in human, while an high clearance effect was observed in rat. The present results indicate that ASS234 may have a suitable pharmacokinetic profile in human.

References

Baranczewski, P., Stańczak, A., Sundberg, K., Svensson, R., Wallin, A., et al. (2006). Introduction to in vitro estimation of metabolic stability and drug

interactions of new chemical entities in drug discovery and development. *Pharmacol. Rep.* 58(4), 453–72.

Bolea, I., Juárez-Jiménez, J., de los Ríos, C., Chioua, M., Pouplana, R., et al. (2011). Synthesis, Biological Evaluation, and Molecular Modeling of Donepezil and N -[(5-(Benzyloxy)-1-methyl-1 H -indol-2-yl)methyl]- N -methylprop-2-yn-1-amine Hybrids as New Multipotent Cholinesterase/Monoamine Oxidase Inhibitors for the Treatment of Alzheimer. *J. Med. Chem.* 54(24), 8251–8270.

D'Elia, P., De Matteis, F., Dragoni, S., Shah, A., Sgaragli, G. and Valoti, M. (2009). DP7, a novel dihydropyridine multidrug resistance reverter, shows only weak inhibitory activity on human CYP3A enzyme(s). 614(1-3), 7–13.

Richmond, W., Wogan, M., Isbell, J. and Gordon, W. P. (2010). Interstrain differences of in vitro metabolic stability and impact on early drug discovery. *J. Pharm. Sci.* 99(11), 4463–4468.

Samadi, A., Chioua, M., Bolea, I., de Los Ríos, C., Iriepa, I., et al. (2011). Synthesis, biological assessment and molecular modeling of new multipotent MAO and cholinesterase inhibitors as potential drugs for the treatment of Alzheimer's disease. *Eur. J. Med. Chem.* 46(9), 4665–8.

Design of new compounds targeting cancer and CNS diseases

Yagamare Fall*
Departamento de Química Orgánica, Facultad de Química, Universidad de Vigo, 36200, Vigo, Spain
*yagamare@uvigo.es

Abstract. Alzheimer's disease (AD):

One of the strategies being pursued in the search for pharmacological therapies for AD is blockade of tau hyperphosphorylation by selective inhibitors of GSK-3β. Palinurin has emerged as a non-ATP-competitive inhibitor of GSK-3β. We have achieved the first enantioselective total synthesis of palinurin starting from commercially available furaldehyde and (R)-3-hydroxy-2-methylpropionate. The key steps of the synthesis include the use of a chiral pyrrolidine to create the chiral tetronic moiety, and Horner-Wadsworth-Emmonds, Wittig and Wittig-Horner reactions to construct the alkene units.

Vitamin D field:

Next to its classical activities, 1α,25-Dihydroxyvitamin D_3 (**1**, calcitriol) has been shown to inhibit cellular proliferation, to induce cellular differentiation and to have numerous indirect effects on the immune system. However the therapeutical utility of **1** is hampered by the effective doses leading to calcemic side effects and this has stimulated the search for analogues having a relatively weak systemic effect on calcium metabolism while maintaining potent regulatory effects on cell differentiation and proliferation. Among the many new calcitriol analogs, worth mentioning those in which the C-21 methyl group was extended to form a second side-chain giving rise to new class of derivatives, known as Gemini. We developed a novel synthetic methodology for the preparation of Gemini Vitamin D_3 analogs,based on a sigmatropic rearrangement , giving access to a variety of Gemini analogs with potentially interesting biological properties.

Marine toxins:

Polycyclic ethers are the structural basis of many natural products such as the so-called marine ladder toxins, a family of red tide toxins with highly complex unusual molecular architecture, a series of fused cyclic ethers having regular trans-syn-trans stereochemistry. An efficient procedure for preparing enantiopure polycyclic ethers is reported. This method is based on the use of the "furan approach" we developed some years ago in our laboratories and which uses the oxidation of furan by singlet oxygen followed by and intramolecular Michael addition.

Keywords Alzheimer's disease – Vitamin D – Gemini analogs – Marine toxins

Support by the Xunta de Galicia (CN 2012/184) and the EU COST Action CM1103.

Homology modeling of the human dopamine transporter (hdat): the elucidation of the binding site

Kemal Yelekçi*[1], James Connaly[2]
[1]Kadir Has University, Faculty of Engineering and Natural Sciences. Department of Bioinformatics and Genetics. Fatih 34083, Istanbul-Turkey
[2]School of Biochemistry and Immunology, Trinity College Dublin, Ireland
*yelekci@khas.edu.tr

Abstract. The dopamine transporter (DAT) is a sodium-coupled symporter, which is in charge of information transfer in neurons functioning in the nervous system. Disorders such as Parkinson's disease (PD), depression, bipolar disorder, attention deficit hyperactivity disorder (ADHD) and schizophrenia are implicated with the abnormal levels of dopamine. Therapeutics used to treat these diseases as well as many addictive drugs target DAT. Molecular modeling studies have become possible with the availability of the three dimensional (3D) structure of the DAT.

In this study the prospective 3D structures of the human DAT, which is predicted from primary amino acid sequence using homology modeling techniques, were used. We have determined the binding sites and relative binding affinities of several ligands with the predicted structures of DAT. These computationally obtained binding affinities and binding poses, correlate well with the reported experimental values.

Keywords Dopamine transporter (DAT) – homology modeling – docking

1 Introduction

The dopamine transporter (DAT) is a sodium-coupled symporter, which monitors the concentration of dopamine (DA) by re-uptaking the dopamine into presynaptic neurons in the brain (Huang and Zhan, 2007). The transport process of the DAT includes the translocation of the substrate dopamine (DA) and two sodium, one-chloride ions across the cell membrane (Krueger, 1990). The uptake is energetically coupled to transmembrane concentration gradient of Na^+, which is maintained by Na^+K^+ ATPase (Hitri et al., 1994).

Many illnesses such as Parkinson's disease (PD), depression, bipolar disorder, schizophrenia and attention deficit hyperactivity disorder (ADHD) are implicated by the abnormal levels of DA (Vaughan and Foster, 2013). Therapeutics used to treat these diseases as well as many addictive drugs target DAT.

The initial structural study related to DAT was the x-ray crystal structure determination for a bacterial homolog of DAT, which was the bacterial leucine transporter ($LeuT_{Aa}$) from sodium symporter (NSS) family (Yamashita et al., 2005). The early homology modeling study was the folding of rat DAT (rDAT) based on the $LeuT_{Aa}$ as a template (Indarte et al., 2008). Based on both $LeuT_{Aa}$ x-ray chrystal structure and homology modeled rat DAT model, human DAT was folded using homology modeling methods.

2 Methods

The fully automatic model-building program, MODELLER, was utilized in our study. With the aim of satisfying constraints, MODELLER develops a hypothetical target structure based on a familiar template structure. First, these spatial constraints in the form of atom-atom distances and dihedral angles are extracted from the template and transferred into the target protein structure.

The alignment enables us to identify parallel residues between the target and the template. The optimization of the target model continues until a model that best satisfies the spatial constraints is obtained. MODELLER is most commonly used for homology modelling of protein's three-dimensional structure as the program deduces structure by satisfaction of spatial constraints (from Accelrys). The output of MODELLER is a tertiary structure of a protein that satisfies a set of constraints as well as possible (Martí-Renom et al., 2000). MODELLER protocol evaluates protein structure using the Probability Density Function (PDF) energy data and DOPE (Discrete Optimized Protein Energy) scoring function. Using Autodock (Morris et al., 1998) docking program several important model ligands were docked into the biding site of predicted structure of DAT and the binding pose and the relative binding affinities of these ligands were determined.

3 Results and discussion

The availability of three-dimensional structure of the DAT paved the way considerably to understand the binding mechanism of ligands into DAT. Table 1 shows the free energy of bindings (FEB) and inhibition constant values of the selected model compounds, which were docked by Autodock program.

Reported experimental free energy of binding for the DAT-dopamine complex was -7.40 kcal/mol (Dar et al., 2006). The score obtained from our computational study is -6.98 kcal/mol. These two values are quite close confirming that computational value is in good agreement with the experimental values.

Figure 1 shows the 12 trans membrane structure of DAT (ribbon) and dopamine molecule (stick and ball). Figure 2 shows the binding pose and interaction of dopamine substrate with the surrounding amino acid chains of DAT.

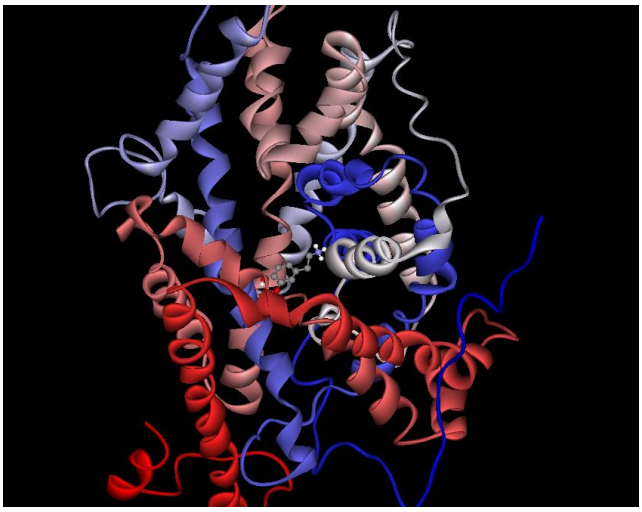

Figure 1: 12 trans membrane helices structure of DAT (ribbon) and dopamine molecule (stick and ball).

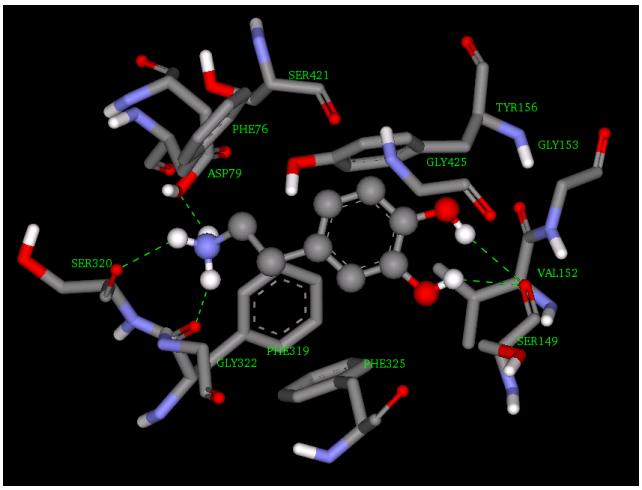

Figure 2: The binding pose and interaction of dopamine substrate with the surrounding amino acid chains of DAT.

Detailed rendering of the figures of hDAT-dopamine complex structure suggests that there is a common binding site for all the ligands buried deep in the transporter channel lined with the residues of PHE76, ASP79, PHE325, LEU322, GLY322, SER320, SER421, SER149, TYR156, VAL152, PHE319, and GLY425.

4 Conclusion

The binding sites and relative binding affinities of several ligands were determined with in the predicted structures of DAT. The computationally obtained binding affinities and binding poses within the predicted DAT

Table 1: Free energy of binding of selected model compounds and their inhibition values.

Compounds	FEB(ΔG) kcal/mol	K_i (mM)
Dopamine	−6.98	7.59
5-Hydroxydopamine	−6.37	21.36
6-Hydroxydopamine	−6.80	10.41
Tyramine	−6.64	13.56
Amphetamine_R	−7.09	6.32
Amphetamine_S	−7.19	5.37
Methamphetamine	−6.46	18.4
5-(2-aminoethyl) -1,3-diol	−6.80	10.42
4-amino-2-hydroxy-benzoate	−4.95	235.3
Cocaine	−7.54	2.88

structure are agreed with their experimental values. The obtained 3D structure of hDAT can be used in the future research studies to design more selective and more potent drug for hDAT.

References

Dar, D. E., Metzger, T. G., Vandenbergh, D. J. and Uhl, G. R. (2006). Dopamine uptake and cocaine binding mechanisms: The involvement of charged amino acids from the transmembrane domains of the human dopamine transporter. *Eur. J. Pharmacol.* 538(1-3), 43–47.

Hitri, A., Hurd, Y. L., Wyatt, R. J. and Deutsch, S. I. (1994). Molecular, Functional and Biochemical Characteristics of the Dopamine Transporter. *Clin. Neuropharmacol.* 17(1), 1–22.

Huang, X. and Zhan, C.-G. (2007). How Dopamine Transporter Interacts with Dopamine: Insights from Molecular Modeling and Simulation. *Biophys. J.* 93(10), 3627–3639.

Indarte, M., Madura, J. D. and Surratt, C. K. (2008). Dopamine transporter comparative molecular modeling and binding site prediction using the LeuT(Aa) leucine transporter as a template. *Proteins.* 70(3), 1033–46.

Krueger, B. K. (1990). Kinetics and Block of Dopamine Uptake in Synaptosomes from Rat Caudate Nucleus. *J Neurochem.* 55(1), 260–267.

Martí-Renom, M. A., Stuart, A. C., Fiser, A., Sánchez, R., Melo, F. and Sali, A. (2000). Comparative protein structure modeling of genes and genomes. *Annu. Rev. Biophys. Biomol. Struct.* 29, 291–325.

Morris, G. M., Goodsell, D. S., Halliday, R. S., Huey, R., Hart, W. E., et al. (1998). Automated docking using a Lamarckian genetic algorithm and an empirical binding free energy function. *J. Comput. Chem.* 19(14), 1639–1662.

Vaughan, R. A. and Foster, J. D. (2013). Mechanisms of dopamine transporter regulation in normal and disease states. *Trends Pharmacol. Sci.* 34(9), 489–496.

Yamashita, A., Singh, S. K., Kawate, T., Jin, Y. and Gouaux, E. (2005). Crystal structure of a bacterial homologue of Na+/Cl–dependent neurotransmitter transporters. *Nature.* 437(7056), 215–223.

Novel thiazole derivatives as dopamine D3 receptor agonists with high selectivity and in vivo activity

Holger Stark*[1], Tim Kottke[2], Eva M. Eichelsbacher[2], Neda Bakthiari[2], Jukka M. Leppanen[2,3], Britta C. Sasse[2], Oliver Saur[2], Michael P. Hill[4], Alan Crossman[4], and Erwan Bézard[4,5]

[1]Institute of Pharmaceutical and Medicinal Chemistry, Heinrich Heine University Duesseldorf, D-40225 Duesseldorf, Germany

[2]Institute of Pharmaceutical Chemistry, Goethe University, Biozentrum, Max-von-Laue-Str. 9, 60438 Frankfurt am Main, Germany

[3]Department of Pharmaceutical Chemistry, University Kuopio, Kuopio, Finland

[4]Motac Neuroscience Ltd., Manchester, United Kingdom

[5]Institut des Maladies Neurodégénératives, UMR CNRS 5293, Université de Bordeaux, Bordeaux, France

*stark@hhu.de

Abstract. L-DOPA is still the gold standard treatment for motor functions with dopamine substitution therapy in patients with Parkinson's disease. Dopamine receptor subtype agonists have great influence on therapeutic options as an ideal dopamine receptor agonist should fulfill the following criteria:

1. a physiological receptor profile with good antiparkinsonian efficacy,
2. a good brain distribution,
3. oral bioavailability,
4. rapid onset,
5. long acting,
6. missing cross reactivity to off-targets and
7. no unwanted side-effects.

Although a small number of non-ergot derivatives are on the market, no single drug available fulfills all the criteria.

In a long-term development program we have changed the 2-aminothiazole motif of pramipexole as a prototypical catechol bioisosteric moiety by removing the aromatic amino functionality as described previously with etrabamine. This derivatisation maintained or improved affinity at dopamine D_3 receptor subtype, maintained agonist properties and simulated binding profile at dopamine D_2-like receptor family.

Depending on the substitution pattern on the core pharmacophore element a series of highly affine and selective agonists have been developed. Selected compounds were screened on unilateral 6-OHDA-lesioned rat model of Parkinsons's disease and further selection on MTPP-treated marmoset model for their antiparkinsonian efficacy in comparison to L-DOPA, apomorphine and ropinerole.

At least two compounds simultaneously fulfilled all the criteria mentioned above and showed high drug potential due to the results of the initial preclinical toxicological screenings. Studies on functional signaling based on [^{35}S]GTP-gamma-S shift and on $ERK_{1/2}$ phosphorylation showed significant differences and a good predictive factor for in vivo activities.

Keywords Parkinson's disease – D2 receptor – D3 receptor – biased signalling

---

Support by the Alexander-von-Humboldt foundation, the EU COST Actions CM1103 and 1207 as well as the DFG INST 208/664-1 FUGG is greatly acknowledged.

Xjenza Online - Journal of The Malta Chamber of Scientists
www.xjenza.org
DOI: 10.7423/XJENZA.2014.2.09

Research Article

Representational Momentum and the Human Face: an empirical note

Ian M. Thornton
Department of Cognitive Science, Faculty of Media and Knowledge Sciences, University of Malta, Msida, MSD 2080, Malta.

Abstract. Recent evidence suggests that observers may anticipate the future emotional state of an actor when viewing dynamic expressions of emotion, consistent with the notion of representational momentum. The current paper presents data that conflicts with these previous studies, finding instead that memory for the final frame of an emotional video tends to be shifted back in the direction of the first frame. While simple methodological issues may explain this difference (e.g., the use of morph sequences in previous studies versus naturalistic expressions here) a more theoretically interesting possibility is also considered. Specifically, recent studies of ensemble representations have shown that observes can rapidly extract the average expression from a display of up to 20 faces. It is suggested that the need to predict versus the need to maintain a stable estimate of the current state often compete when we interact with dynamic stimuli. Our memory for the final expression on an emotional face may be particularly sensitive to task demands and response timing, thus coming to reflect different solutions to this anticipation-averaging conflict depending on the precise experimental scenario.

Keywords Representational Momentum – Dynamic Faces – Ensemble Representations – Anticipation – Averaging – Emotional Expressions

1 Introduction

Representational momentum (RM) refers to a perceptual phenomenon in which observers tend to misremember the stopping point of a dynamic event as being further forward in its direction of motion or change (Freyd and Finke, 1984; Freyd, 1987). In a now classic example, reproduced in Figure 1, three views of a rectangle were presented sequentially so as to imply rotation in the picture plane (Freyd and Finke, 1984). After this inducing sequence, the screen went blank for a brief retention interval and a probe rectangle appeared. Across trials, the probe rectangle was presented either in the true/same orientation as the last inducing image or in positions parametrically varied forward or backward from this orientation. Participants simply indicated whether the presented probe was the same or different relative to the remembered stopping point. As can be seen in Figure 1B, observers were much more likely to endorse probes as being the "same" as the stopping point when those probes were shifted forward in the direction of implied rotation.

Similar "forward shifts" have been reported for a wide range of transformations and a number of mechanisms have been proposed to explain the phenomenon (for review, see Hubbard, 2005). Important in the current context are findings that show that RM is not restricted to simple displays in which a single geometric figure undergoes translation or rotation. Specifically, forward shifts have been found in displays containing multiple elements (Finke and Shyi, 1988; Thornton and Hayes, 2004) and for complex transformations, such as those involving the articulating human form (Graf et al., 2007; Verfaillie and Daems, 2002; Verfaillie et al., 1994). Although there is continued debate about the nature of RM shifts, it is possible that their general role is to help anticipate or predict future states. The goal of the current paper is to comment on recent findings suggesting similar anticipatory processes may occur when we view dynamic faces, possibly helping us to predict the future emotional state of others (Marian and Shimamura, 2013; Palumbo and Jellema, 2013; Uono et al., 2009, 2014; Yoshikawa and Sato, 2008).

Faces are fascinating objects. Although they all share

Correspondence to: Ian M. Thornton (ian.thornton@um.edu.mt)

© 2014 Xjenza Online

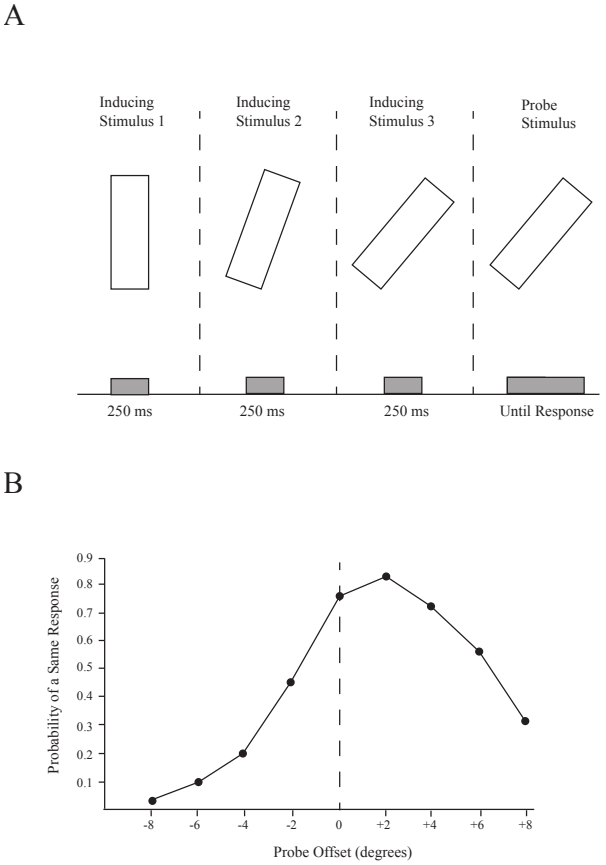

Figure 1: Display and data from Freyd and Finke (1984), redrawn from original. Panel A shows the inducing display and probe items. The three successive views of the rectangle were separated by a blank inter-stimulus interval (ISI) of 250 ms and a retention interval (RI) of 250 ms (all shown as dashed vertical lines). The probe item was either the same as the final inducing item or was varied between −8 and 8 degrees around the true final orientation. The task was to indicate via a key press whether the probe had the same or different orientation. Panel B shows data from 16 participants. It is clear that participants responded "same" more frequently to probes shifted in the direction of motion. Such a shift gave rise to the term "representational momentum".

the same basic configuration – eyes above nose, above mouth – subtle variations in the arrangement of these features make it possible to produce the huge variety of patterns that form the basis of our individual identity. Beyond this variability in configuration, differences in skin texture, 3D shape and, most relevant here, motion, further enhance identity and also make it possible for the face to convey information about race, gender, age, speech and emotion. For a recent, comprehensive review of face research, see Bruce and Young (2012). While the majority of work in face processing literature has employed static, photographic stimuli, the last 20 years has also seen a rapid growth of research into the role of facial motion. Work from my own group, for example, has consistently shown that when we become familiar with a new individual, we use their characteristic facial motion, as well as their facial shape, to encode identity (Knappmeyer et al., 2003; Pilz et al., 2005; Thornton and Kourtzi, 2002). For a general overview of research in this area see (O'Toole et al., 2002; O'Toole and Roark, 2010; Xiao et al., 2014).

Within the context of moving faces, Yoshikawa and Sato asked whether observers would misremember the stopping point of a dynamic face showing emotion (Yoshikawa and Sato, 2008). Using a standard set of photographic stimuli (Ekman and Friesen, 1976), they constructed linear morphs between a neutral face and 6 basic expressions of emotion. On each trial a morph was shown as a brief movie, and stopped at either 80, 90 or 100 % of the peak of the expression. After a brief, blank pause, a probe item appeared and the observer was allowed to adjust the movie frame to find the remembered stopping point. Particularly when movies were played faster than normal and when the true stopping point was around 80 % of the peak of the expression, (Yoshikawa and Sato, 2008) found clear evidence for RM. That is, observers consistently selected a frame that was beyond the actual stopping point of the animation.

The aim of this brief commentary is not to directly question this basic finding. Indeed this RM effect has been replicated several times (Uono et al., 2009, 2014) and patterns consistent with anticipation have also been reported in other labs (Marian and Shimamura, 2013; Palumbo and Jellema, 2013). Rather, the goal here is to raise a note of caution in generalising from these findings and to suggest that when processing dynamic faces, more than one mechanism may be influencing behaviour. The "empirical" part of the title to this paper relates to previously unpublished data from my doctoral dissertation, supervised by Jennifer Freyd at the University of Oregon, that bear directly on the question of RM and faces (Thornton, 1997). The next section provides a brief overview of the methods used to study RM in this thesis and presents some of the findings. In short, over a number of experiments, "backward" rather than "forward" shifts were always obtained. That is, observers typically endorsed probes that were earlier not later in the sequence they had seen. The final section of the paper will relate these findings to previous studies that have shown anticipatory effects, and discuss what factors may account for such different results.

2 Experimental Methods and Results

This section will briefly describe some of the experiments reported in Chapters V-VI of Thornton (1997) as well as some additional control experiments. Figure

2 shows a 20-frame expression sequence typical of those used to explore RM in Thornton (1997). Although having access to the same expressive photographs (Ekman and Friesen, 1976) used in Yoshikawa and Sato (2008), it was decided instead to use naturalistic expressions. An elicitation technique was developed in which volunteers performed a number of tasks, such as recognising sounds, exploring objects by touch, watching comedy footage, all while being filmed. From these filmed sessions, frame sequences of facial expressions, such as smiles, frowns and looks of disgust were extracted to provide both the RM inducing sequences and the probe items. For more details on the elicitation technique and stimuli see Chapter II of Thornton (1997) or Thornton and Kourtzi (2002).

Figure 2: The 20 frame sequence used in Experiments 5 and 7 of Thornton (1997). Numerals refer to frame numbers. To create an inducing sequence, the frames were played sequentially at a rate of 30 fps as an aperture movie with a frame that subtended approximately 3° visual angle. The movie always stopped on frame 10, which is drawn here with a exaggerated border, not shown during the experiment. In Experiment 5, the critical inducing sequence was termed "towards expression" (TE) and involved frames 1-10, so that the expression was played in the normal direction. In Experiment 7, the inducing sequence was termed "towards neutral" (TN) and consisted of frames 20-10, the expression thus unfolding in a reverse direction. In these original experiments, the inducing sequences were also preceded by a longer preview animation in which all frames were shown once in both directions. Thus, for the TE condition the preview consisted of frames 1-20 followed by frames 20-1. The entire movie thus consisted of 50 frames and had a duration of 1500 ms. See text for details on the rationale and possible consequences of this preview design.

During each trial, a sequence of frames was played at normal speed (30 fps) and then stopped abruptly at a given point. Across experimental conditions, the movie could be playing forward (frames 1-10, neutral-to-smile in Figure 3) or in reverse (frames 20-10, smile-to-neutral). Importantly, across conditions the stopping point was always the same (frame 10 in this example). The screen remained blank for a 300 ms retention interval and then a probe item appeared. Figure 3 shows examples of the probe items used for the sequence in Figure 2. The probe item could be identical with the true/same stopping point (Probe 0), or was parametrically varied around that point, one or two steps forward of the stopping point or one or two steps back. Note how, across conditions, the same frames appear as different probe items, depending on the direction of the animation, a point I return to shortly. In all trials, the observer simply had to respond whether the probe was the same or different from the point at which the movie stopped. This is essentially the same experimental design used in Freyd and Finke (1984) and illustrated in Figure 1.

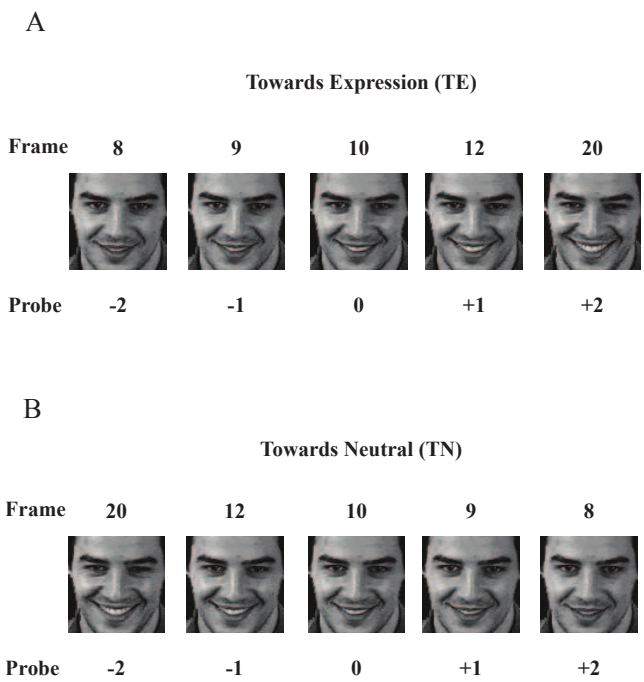

Figure 3: The probe images used in Experiments 5 (Panel A) and 7 (Panel B) of Thornton (1997). The probe always appeared after a 250 ms blank retention interval that followed the inducing sequence. The probe remained visible until participants made a "same" or "different" response using the standard keyboard. Note that the same images appear in both TE and TN conditions, but are assigned different probe positions due to the direction of the inducing sequence. The probe spacing was determined using separate concurrent matching tasks, and attempts to reflect equal perceptual spacing rather than frame spacing per se. For details of the concurrent matching task see Thornton (1997).

As noted in Yoshikawa and Sato (2008), there are a number of issues that need to be addressed when using naturalistic footage, rather than artificial, controlled stimuli to explore RM. The most serious concern is the selection of appropriate probe items. If there is an asymmetry in the amount of change in frames before or af-

ter the true stopping point, then this probe asymmetry, rather than the display dynamics could cause a shift. We tried to control for this in two ways. First, we ran separate concurrent matching experiments to determine the distance in frames that needed to be used in matched pairs of probes in order to achieve equal discriminability (i.e., probes 1/−1 and 2/−2 in Figure 3). See Thornton (1997) for more details on how this matching task was used objectively to measure the amount of perceived change in each probe item. More importantly, by running each inducing sequence in both forward and reverse directions we could disentangle shifts that arose due to the dynamic inducing sequence from those that depended on probe discriminability. For example, with reference to Figure 3, if the slightly more intense smile (frame 12) was harder to discriminate from the stopping point than the less intense smile (frame 8) then this would lead to a forward shift in one condition and a backward shift in the other.

Example results are shown in Figure 4. Panel A shows data from 26 participants who were shown the male sequence in Figure 2. Twelve participants completed the "towards expression" (TE) condition and 14 the "towards neutral" (TN) condition. Each participant completed 100 experimental trials, 20 repetitions at each probe position, presented in a random order. These data were reported as Experiments 5 and 7 in Thornton (1997). Panel B shows data from a within-subjects experiment (N =12) that has the same design, except the same participants completed both TE and TN conditions in separate, counterbalanced blocks. This experiment, which used a female face frowning, was run as a control condition but was not included in the thesis.

There are two important points to note. First, there is no evidence of a forward shift in any of the four conditions. Rather, participants were always more likely to endorse as same a probe that matched an earlier (probe −1) rather than a later (probe 1) point in the sequence. This led to a consistent backward rather than a forward shift. To quantify the overall pattern of responses a weighted mean (WM) was calculated on the distribution of each participant's data. The WM is calculated by multiplying the proportion of 'same' responses at each probe position by that probe's distance from the true/same probe (i.e., 0). The sum of products is then divided by the total number of 'same' responses to yield an appropriately weighted measure of central tendency (Faust, 1990; Gray and Thornton, 2001). All 4 of the conditions in Figure 4 A-B has a weighted mean that is reliably less than zero according to one-sample t-tests (all ps < 0.05). See Table 1 for further details.

The second point to note is that individual probe items do not appear to be influencing the pattern of results. As mentioned above, across the two conditions the exact same image changes its position relative to the true stopping point as a function of the direction of the animation. So, probe 1 in the TE condition (frame 12) becomes probe −1 in the TN condition, for example. If responses depended on asymmetric probe discriminability, the two curves in each panel would be mirror images of each other, rather than following the same basic shape. The fact that the two curves do not completely overlap illustrates the way in which the dynamic context of the inducing sequences affects the interpretation of the same probe images (see also Palumbo and Jellema, 2013). For example, in Figure 4A, it seems likely that the rate of expressive change in the TE sequence (frames 1-10) is greater than in the TN sequence (frames 20-10) leading to different patterns of shifts. The slight difference in duration between the two conditions – the TE sequence actually consists of 10 frames, the TN has 11 frames – could also be a factor, although this seems unlikely as the opposite TE-TN pattern occurs in Figure 4B. These asymmetries, then, seem more likely to reflect idiosyncratic expressive changes, a consequence of using naturalistic expression sequences. Again, however, it is important to stress that none of these shifts show any hint of anticipation.

To further establish that the presence of negative shifts was not an artefact of probe selection, we ran a control condition with linear, schematic faces. Stimuli consisted of an oval face in which two small circles for eyes and a plus sign for the nose were centred and colinear. Three identical lines formed the two eyebrows and the mouth. These lines were expanded and contracted in a linear fashion to convey an impression of surprise. As in previous morph studies (Uono et al., 2009, 2014; Yoshikawa and Sato, 2008) probe items were guaranteed to be equidistant from the true stopping point. The data from the TE condition (reported as Experiment 5 in Thornton, 1997) are shown in Figure 4C. Again, the average weighted mean for this dataset was reliably less than zero.

It should be noted that in all of the experiments reported so far in this paper, the inducing sequence on each trial was preceded by a longer preview animation. Specifically, for the TE condition shown in Figure 2, all frames were played forward (frames 1-20), then backward (frames 20-1) before the final inducing sequence of frames 1-10. This was done to ensure that observers experienced the full range of the expression and had been exposed to probe items both before and after the stopping point. Although such preview animations are not typical of RM studies involving simple rotation or translation, it was felt that the complexity of the non-rigid facial transformations warranted providing additional contextual support. Nevertheless, such context could conceivably have influenced the pattern of shifts in

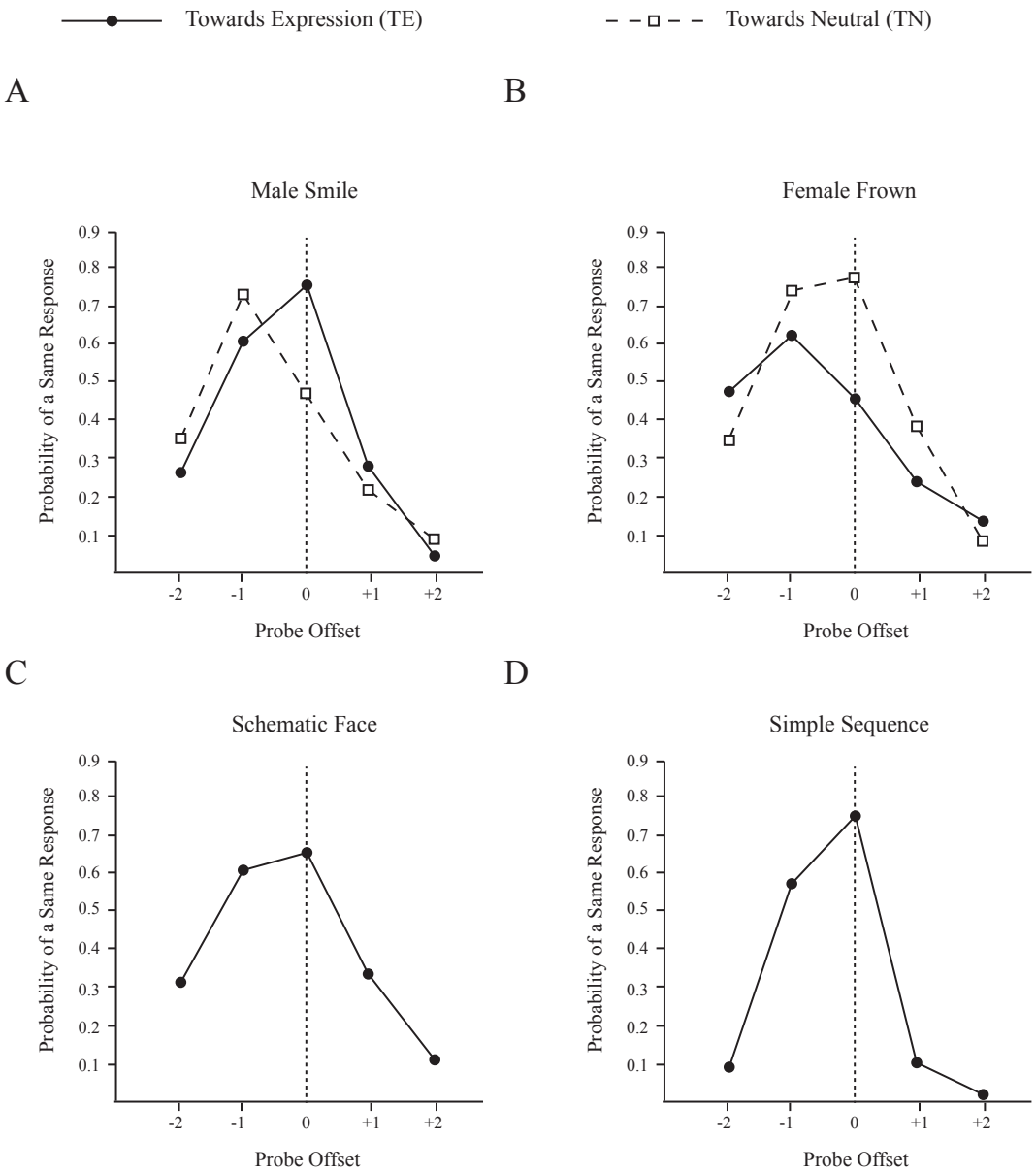

Figure 4: Experimental Results. A) Naturalistic Male Smile. Results from between subject design using data from Experiments 5 (Solid Line) and 7 (Dashed Line) from Thornton (1997). In contrast to the pattern shown in Figure 1B, the peak of the distribution of same responses in both these experiments in shifted backward, giving rise to negative weighted means (see Table 1). B) Naturalistic Female Frown. Results of a within-subjects control experiment using the same experimental design but different facial sequences. C) Schematic Face. Results using a simple, schematic face from Experiment 6, Thornton (1997). D) Simplified Inducing Sequence. Results of a control experiment where the inducing sequence in Figure 2 was simplified to consist only of frames 1-10.

some way. To explore this possibility, a further control experiment was conducted (some years after the thesis) using the same experimental stimuli but with the preview context removed. Figure 4D shows data from this experiment that used an identical design except that a brief, unidirectional expression sequence (frames 1-10 in Figure 2) was used as the inducing display. It is clear, that even without the more complex sequence, there is still a strong negative shift with a weighted mean reliably less than zero.

3 Discussion

The results described above tell a very simple story. Using naturalistic stimuli and a method very similar to that used in classic representational momentum work, there was no evidence for any form of forward, anticipa-

Table 1: Weighted Means (WM) for datasets in Figure 4.

Data Set	Condition	WM	t-value	p-value
Experiment 5 (Figure 4A)	TE	−0.36	$t(11) = 3.8$	$p < 0.01$
Experiment 7 (Figure 4A)	TN	−0.54	$t(13) = 6.7$	$p < 0.001$
Figure 4B	TE	−0.57	$t(11) = 2.9$	$p < 0.05$
Figure 4B	TN	−0.38	$t(11) = 2.8$	$p < 0.05$
Experiment 6 (Figure 4C)	TE	−0.34	$t(11) = 4.7$	$p < 0.001$
Figure 4D	TE	−0.38	$t(11) = 7.6$	$p < 0.001$

tory shift. Rather, and in direct contrast to more recent literature, it seems that observers in these experiments misremembered the facial motion sequence as stopping earlier than was actually shown. How can we explain this different pattern of results and, more importantly, what might it mean for our understanding of face perception in the context of motion?

It remains a possibility that the use of naturalistic stimuli introduced some issues with the probe items that were selected, and this influenced the pattern of results. However, finding the same shifts regardless of whether the inducing sequence was played forward or backward – meaning that the role of individual probe items were also reversed – would seem to argue against this explanation. The use of naturalistic stimuli also means that the movements themselves were more complex and almost certainly less predictable than the linear morphs used in studies that have shown anticipatory effects (Marian and Shimamura, 2013; Palumbo and Jellema, 2013; Uono et al., 2009, 2014; Yoshikawa and Sato, 2008). Again, though, the use of an extended context meant that observers were shown the range of movements possible on each trial, and would quickly have become highly familiar with the facial actions involved. Perhaps more compellingly, the same pattern of negative shifts was observed in Thornton (1997) even when the stimuli consisted of a schematic face where the movements were simple, linear and highly predictable. A more recent study by Courgeon et al. (2010) used an animated virtual character to explore RM shifts. These animations involved more complex movement than a linear morph, but still provided precise control over probe separation. The pattern of results in this study were largely consistent with Thornton (1997), that is, shifts were mainly backward rather than forward.

In terms of methodology, it seems more likely that differences in the task used to assess the shift might be the crucial factor. As reviewed in Hubbard (2005), across the many studies examining RM, there have been two typical methods, one involving probe items, psychophysically equivalent to the method of constant stimuli, and one involving direct response methods, such as positioning a cursor, psychophysically equivalent to the method of adjustment. In the current context, studies that have reported backward shifts (Courgeon et al., 2010; Thornton, 1997) appear to have used the former category of assessment while those reporting forward shifts (Uono et al., 2009, 2014; Yoshikawa and Sato, 2008), the latter. Importantly, at least for translating stimuli, these two methods have previously been shown to yield different results, with assessment by probe items giving rise to smaller shifts than direct pointing methods (Kerzel, 2003a). It would clearly be very interesting to take the same set of facial stimuli and measure performance using these two different methods.

Recently, Jellema and colleagues have argued that top-down "emotional anticipation", rather than low-level visual mechanisms, may explain dynamic distortions when interpreting facial expressions (Jellema et al., 2011; Palumbo and Jellema, 2013). In their work, participants rated the perceived emotion of a neutral image that was preceded by an animation moving from a peak expression towards neutral. For example, following a sequence moving from angry towards neutral, the neutral probe was rated slightly happier, an effect termed a perceptual "over-shoot" bias (Palumbo and Jellema, 2013).

The emotional anticipation explanation suggests that when we view a dynamic face, we may "involuntarily keep track of the emotional state of mind of the actor and implicitly anticipate what the actor's emotional state would be in the immediate future" (Palumbo and Jellema, 2013, p. 10). Interestingly, both "over-shoot" and "under-shoot" effects were observed by Palumbo and Jellema (2013) depending on whether the preceding animation was unidirectional or looped. This further indicates that the precise dynamic context can play an important role in face perception, and may be one factor that explains the negative shifts of Thornton (1997).

Another recent paper, Marian and Shimamura (2013), used a method very similar to Palumbo and Jellema (2013) to explore both contrast effects (i.e. a neutral

face appearing happy after an angry-neutral animation) and momentum effects (i.e. an animation stopping at a 50 % happy face appearing happier). Across several experiments, these authors always found patterns consistent with a forward or "over-shoot" effect, rather than an "under-shoot" or negative shift as found in Thornton (1997). While they note that a single underlying mechanism could account for both contrast and momentum effects, they also point out that the latter seems particularly sensitive to facial context. Specifically, different patterns where found for angry-happy than for sad-happy dimensions and no momentum effect was observed when the stopping point was beyond 75 % maximum. This sensitivity could again help to explain the lack of momentum effects in Thornton (1997), given the use of relatively complex, naturalistic sequences in those experiments.

More generally, it is important to stress again that all of the studies reporting facial anticipation have used the same linear morphing technique to create their stimuli. Indeed, with the exception of Marian and Shimamura (2013), who used the NimStim set of expressions (Tottenham et al., 2009), all of the experiments based their morphs on the same photographs (Ekman and Friesen, 1976). It would certainly be very interesting to establish whether anticipation effects can be observed for a broader class of facial stimuli, particularly containing naturalistic movements rather than linear morphs.

As already mentioned, while morph stimuli may appear subjectively "natural" (Sato and Yoshikawa, 2004), they clearly involve less complex movement than we typically encounter with a face. For example, naturalistic human smiles have specific onset, apex and offset timings, which result in non-linear acceleration/deceleration profiles (Krumhuber and Kappas, 2005; Schmidt et al., 2003). Observers are sensitive to variations in the timing of these components (Edwards, 1998) and may use them to infer the emotional state of an actor (Krumhuber and Kappas, 2005). It is unclear if the absence of such profiles affects the RM task, but it is conceivable that linear inducing sequences and probe items significantly reduce the complexity of anticipation. While the issue of probe selection with naturalistic sequences was certainly not dealt with perfectly in Thornton (1997), the use of either perceptual normalisation or image processing techniques to equate task-relevant differences between probes, should make it possible to move away from strictly linear morphs with some of these designs.

So far, a number of methodological issues have been mentioned to try and account for the appearance of backward shifts in Thornton (1997). Perhaps a more important, or at least more theoretically interesting, question is to ask "why" a backward shift might ever occur? The idea of anticipation, emotional or perceptual, provides a clear rationale for expecting a forward shift: helping an observer predict and respond to what will happen next. Could there also be mechanisms at work that would lead to a backward shift? Would they have any functional significance?

In the broader RM literature, there have been reports of backward shifts in a number of previous papers. For example, backward shifts have been found when target stimuli change their perceived depth (Hubbard, 1996), auditory pitch (Hubbard, 1993a; Johnston and Jones, 2006) or luminance (Brehaut and Tipper, 1996). Similar backward shifts have also been reported in displays with more than one object (Hubbard, 2005, 1993b; Kerzel, 2003b) or tasks involving "bounded" changes, either due to periodic motion or physical barriers of some description (Hubbard and Bharucha, 1988; Verfaillie and D'Ydewalle, 1991). As discussed by Hubbard (2005), these patterns have generally been taken as an indication that factors other than RM are influencing behaviour in a given task. While a number of specific factors have been proposed, most relevant to the current discussion are the ideas of memory averaging and boundary conditions (Hubbard, 2005).

In his review paper, Hubbard (2005) suggested that the patterns described in Thornton (1997) occurred either because the nature of the facial changes were too complex to anticipate or were bounded by the physical limits of facial deformation. While the former point has already been discussed, the latter misses the nature of the sequences used in Thornton (1997). Hubbard states that "there is a clear maximum extent of facial expression, and the observers presumably anticipated a return to a more neutral expression, rather than an increasing intensity of the current expression beyond the maximum biological extent" (Hubbard, 2005, p. 831). However, as can be seen in Figure 2, the endpoint of the inducing sequences were specifically chosen to be away from expression endpoints, and were also presented both towards expression and towards neutral, reducing the likelihood of a simple boundary effect. There is, nevertheless, a more subtle way that performance could have been "bounded". That is, although the facial transformations themselves were continuous, perceptually, a number of factors might differentially weight parts of the sequence. For example, the endpoints might exert some form of anchoring effect (Marian and Shimamura, 2013; Palumbo and Jellema, 2013; Russell and Fehr, 1987), there may be perceptual discontinuities around expression boundaries (de Gelder et al., 1997; Etcoff and Magee, 1992) or the resolution of expression processing may be limited, leading to "perceptual key frames" of some sort. Any of these factors could give rise to "attractor" expressions that might disrupt simple RM ef-

fects. Clearly, these are several possibilities that could be explored in future studies.

Thornton (1997) speculated that some form of memory averaging (Freyd and Johnson, 1987) might be the most likely cause of the observed pattern of backward shifts. An early study by Vicki Bruce and colleagues (Bruce et al., 1991) has shown that over the course of an experiment, participants appeared to extract the average configuration of a set of facial images in which the features had been slightly adjusted, similar to the prototype effects of Posner and Keele (1968). However, the time course of this prototype effect seemed at odds with the supposed trial-by-trial effects of RM.

Over the last decade, however, there has been a growing interest in the idea of rapid ensemble representations (see Alvarez, 2011 for review). That is, there is now a great deal of evidence that the visual system can very quickly (e.g., < 1 second) extract summary representations along a number of dimensions, when presented with complex displays, representations that provide the observer with a precise estimates of central tendency. For example, when briefly shown a spatial array containing 16 dots of various diameters, observers immediately have access to information about the average size (Ariely, 2001). Similar effects have been shown for other basic feature dimensions, such as the mean orientation, motion and brightness of large sets of items (Alvarez, 2011). The general suggestion is that such computations could provide a very efficient means to reduce perceptual bandwidth by providing fairly precise estimates of a set without the need to visually inspect every member.

Importantly in the current context, these averaging mechanisms also seem to be at work when we process faces. Jason Haberman, David Whitney and colleagues, for example, have shown that when observers are presented with an array containing multiple faces, they are able to rapidly extract average emotion and gender (Haberman et al., 2009; Haberman and Whitney, 2007, 2009). Work from other labs has show similar findings for identity (de Fockert and Wolfenstein, 2009) and race (Srismith et al., 2014). Of most relevance here, this averaging process for faces also appears to work over time (Haberman et al., 2009). In this study observers were shown animations containing up to 20 frames from morphed expression sequences. As with the spatial arrays used in previous work (Haberman and Whitney, 2007; Haberman et al., 2009) observers were able to accurately estimate the average expression in these displays. It is important to note that the frames making up the animations in Haberman and Whitney (2009) were presented in a totally random order, not as a coherent expression change. Nevertheless, if ensemble representations do have any functional role to play in the everyday perception of faces, we would clearly expect averages to be computed when normal expression sequences are shown.

Could such estimates of average expression help explain the "backward" shifts observed in Thornton (1997)? Given the directional nature of the inducing sequences used in those experiments, it does appear that the "average" should fall somewhere back along the sequence between the first and final frame. Thus, in contrast to an RM prediction, this might favour some form of backward shift. It seems unlikely that observers in these studies would be directly confusing the true stopping point with the sequence average. Nevertheless, if such an average is automatically computed during the presentation of the inducing sequence, its existence might attract or otherwise bias memory for the final expression, as suggested above in the discussion of RM boundary conditions and averaging.

What is unclear is why averaging should win out over anticipation in these particular studies. An important next step would seem to be to design experiments, preferably using naturalistic sequences, in which we can attempt to measure both effects. My hunch is that the need to predict versus the need to maintain a stable estimate of the current state often compete when we interact with any form of dynamic stimuli. The representations that guide our behaviour in a given situation, the product of this competition, are almost certainly highly context sensitive. Our memory for the final expression on a face, for example, may be particularly sensitive to emotional engagement (Palumbo and Jellema, 2013) and response timing (Freyd, 1987), coming to reflect different solutions to the anticipation-averaging conflict depending on the precise experimental scenario.

References

Alvarez, G. A. (2011). Representing multiple objects as an ensemble enhances visual cognition. *Trends Cogn. Sci.* 15(3), 122–131.

Ariely, D. (2001). Seeing sets: representation by statistical properties. *Psychol Sci.* 12(2), 157–162.

Brehaut, J. C. and Tipper, S. P. (1996). Representational momentum and memory for luminance. *J Exp Psychol Hum Percept Perform.* 22(2), 480–501.

Bruce, V., Doyle, T., Dench, N. and Burton, M. (1991). Remembering facial configurations. *Cognition.* 38(2), 109–144.

Bruce, V. and Young, A. (2012). *Face Perception* (1st ed.). Psychology Press.

Courgeon, M., Amorim, M. A., Giroux, C. and Martin, J. C. (2010). Do users anticipate emotion dynamics in facial expressions of a virtual character. In *Proc. 23rd int. conf. comput. animat. soc. agents (casa 2010).* Saint Malo, France.

de Fockert, J. and Wolfenstein, C. (2009). Rapid extraction of mean identity from sets of faces. *Q J Exp Psychol.* 62(9), 1716–1722.

de Gelder, B., Teunisse, J.-P. and Benson, P. J. (1997). Categorical Perception of Facial Expressions: Categories and their Internal Structure. *Cogn. Emot.* 11(1), 1–23.

Edwards, K. (1998). The Face of Time: Temporal Cues in Facial Expressions of Emotion. *Psychol. Sci.* 9(4), 270–276.

Ekman, P. and Friesen, W. V. (1976). *Pictures of Facial Affect.* Consulting Psychologists Press.

Etcoff, N. L. and Magee, J. J. (1992). Categorical perception of facial expressions. *Cognition.* 44(3), 227–240.

Faust, M. E. (1990). *Representational Momentum: A Dual Process Perspective* (Doctoral dissertation, University of Oregon, Eugene, OR, USA).

Finke, R. A. and Shyi, G. C. (1988). Mental extrapolation and representational momentum for complex implied motions. *J Exp Psychol Learn Mem Cogn.* 14(1), 112–120.

Freyd, J. J. (1987). Dynamic mental representations. *Psychol. Rev.* 94(4), 427–438.

Freyd, J. J. and Finke, R. A. (1984). Representational momentum. *J. Exp. Psychol. Learn. Mem. Cogn.* 10(1), 126–132.

Freyd, J. J. and Johnson, J. Q. (1987). Probing the time course of representational momentum. *J Exp Psychol Learn Mem Cogn.* 13(2), 259–268.

Graf, M., Reitzner, B., Corves, C., Casile, A., Giese, M. and Prinz, W. (2007). Predicting point-light actions in real-time. *Neuroimage.* 36 Suppl 2, T22–32.

Gray, R. and Thornton, I. M. (2001). Exploring the link between time to collision and representational momentum. *Perception.* 30(8), 1007–1022.

Haberman, J., Harp, T. and Whitney, D. (2009). Averaging facial expression over time. *J Vis.* 9(11), 1.1–13.

Haberman, J. and Whitney, D. (2007). Rapid extraction of mean emotion and gender from sets of faces. *Curr. Biol.* 17(17), R751–3.

Haberman, J. and Whitney, D. (2009). Seeing the mean: ensemble coding for sets of faces. *J Exp Psychol Hum Percept Perform.* 35(3), 718–734.

Hubbard, T. L. (1993a). Auditory representational momentum: Musical schemata and modularity. *Bull. Psychon. Soc.* 31(3), 201–204.

Hubbard, T. L. (1993b). The effect of context on visual representational momentum. *Mem Cogn.* 21(1), 103–114.

Hubbard, T. L. (1996). Displacement in depth: representational momentum and boundary extension. *Psychol Res.* 59(1), 33–47.

Hubbard, T. L. (2005). Representational momentum and related displacements in spatial memory: A review of the findings. *Psychon Bull Rev.* 12(5), 822–851.

Hubbard, T. L. and Bharucha, J. J. (1988). Judged displacement in apparent vertical and horizontal motion. *Percept Psychophys.* 44(3), 211–221.

Jellema, T., Pecchinenda, A., Palumbo, L. and Tan, E. G. (2011). Biases in the perception and affective valence of neutral facial expressions induced by the immediate perceptual history. *Vis. cogn.* 19(5), 616–634.

Johnston, H. M. and Jones, M. R. (2006). Higher order pattern structure influences auditory representational momentum. *J Exp Psychol Hum Percept Perform.* 32(1), 2–17.

Kerzel, D. (2003a). Attention maintains mental extrapolation of target position: irrelevant distractors eliminate forward displacement after implied motion. *Cognition.* 88(1), 109–131.

Kerzel, D. (2003b). Mental extrapolation of target position is strongest with weak motion signals and motor responses. *Vis. Res.* 43(25), 2623–2635.

Knappmeyer, B., Thornton, I. M. and Bülthoff, H. H. (2003). The use of facial motion and facial form during the processing of identity. *Vis. Res.* 43(18), 1921–1936.

Krumhuber, E. and Kappas, A. (2005). Moving Smiles: The Role of Dynamic Components for the Perception of the Genuineness of Smiles. *J. Nonverbal Behav.* 29(1), 3–24.

Marian, D. E. and Shimamura, A. P. (2013). Contextual influences on dynamic facial expressions. *Am J Psychol.* 126(1), 53–65.

O'Toole, A. J., Roark, D. A. and Abdi, H. (2002). Recognizing moving faces: A psychological and neural synthesis. *J. Vis.* 2(7), 604–604.

O'Toole, A. J. and Roark, D. (2010). Memory for Moving Faces: The Interplay of Two Recognition Systems. *Dyn. Faces Insights from Exp. Comput.*

Palumbo, L. and Jellema, T. (2013). Beyond face value: does involuntary emotional anticipation shape the perception of dynamic facial expressions? *PLoS One.* 8(2), e56003.

Pilz, K. S., Thornton, I. M. and Bülthoff, H. H. (2005). A search advantage for faces learned in motion. *Exp Brain Res.* 171(4), 436–447.

Posner, M. I. and Keele, S. W. (1968). On the genesis of abstract ideas. *J Exp Psychol.* 77(3), 353–363.

Russell, J. A. and Fehr, B. (1987). Relativity in the perception of emotion in facial expressions. *J. Exp. Psychol. Gen.* 116, 223–237.

Sato, W. and Yoshikawa, S. (2004). Brief Report The dynamic aspects of emotional facial expressions. *Cogn. Emot.* 18(5), 701–710.

Schmidt, K. L., Cohn, J. F. and Tian, Y. (2003). Signal characteristics of spontaneous facial expressions: automatic movement in solitary and social smiles. *Biol Psychol.* 65(1), 49–66.

Srismith, D., Oxner, M., Hayward W, G. and Thornton I, M. (2014). An other-race bias when processing groups of faces. *Perception.* 43.

Thornton, I. M. (1997). *The perception of dynamic human faces* (Doctoral dissertation, University of Oregon, Eugene). Available to download at http://www.ianthornton.com/publications/.

Thornton, I. M. and Hayes, A. (2004). Anticipating action in complex scenes. *Vis. cogn.* 11(2-3), 341–370.

Thornton, I. M. and Kourtzi, Z. (2002). A matching advantage for dynamic human faces. *Perception.* 31(1), 113–132.

Tottenham, N., Tanaka, J. W., Leon, A. C., McCarry, T., Nurse, M., et al. (2009). The NimStim set of facial expressions: judgments from untrained research participants. *Psychiatry Res.* 168(3), 242–249.

Uono, S., Sato, W. and Toichi, M. (2009). Brief Report: Representational Momentum for Dynamic Facial Expressions in Pervasive Developmental Disorder. *J Autism Dev Disord.* 40(3), 371–377.

Uono, S., Sato, W. and Toichi, M. (2014). Reduced representational momentum for subtle dynamic facial expressions in individuals with autism spectrum disorders. *Res. Autism Spectr. Disord.* 8(9), 1090–1099.

Verfaillie, K. and Daems, A. (2002). Representing and anticipating human actions in vision. *Vis. cogn.* 9(1-2), 217–232.

Verfaillie, K. and D'Ydewalle, G. (1991). Representational momentum and event course anticipation in the perception of implied periodical motions. *J Exp Psychol Learn Mem Cogn.* 17(2), 302–313.

Verfaillie, K., Troy, A. D. and Rensbergen, J. V. (1994). Transsaccadic integration of biological motion. *J Exp Psychol Learn Mem Cogn.* 20(3), 649–670.

Xiao, N. G., Perrotta, S., Quinn, P. C., Wang, Z., Sun, Y.-H. P. and Lee, K. (2014). On the facilitative effects of face motion on face recognition and its development. *Front Psychol.* 5, 633.

Yoshikawa, S. and Sato, W. (2008). Dynamic facial expressions of emotion induce representational momentum. *Cogn Affect Behav Neurosci.* 8(1), 25–31.

Xjenza Online - Journal of The Malta Chamber of Scientists
www.xjenza.org

News Article

2014 Science in the House with Members of Parliament

David Magri
Department of Chemistry, University of Malta

2014 Science in the House with Members of Parliament

Scientists and researchers met on Thursday 25th September with Members of Parliament in the Committee Room at the Presidential Palace in Valletta for Science in the House. A poster exhibition consisting of 13 posters representative of various research disciplines studied at the University of Malta. The event was inaugurated under the auspices of the Office of the Speaker at the House of Representatives, The Grand Master's Palace, Valletta.

The researchers were met by the Deputy Speaker, The Hon. Censu Galea, in the presence of Project Coordinator for Science in the City and Acting Chair of the Malta Chamber of Scientists Prof. Alex Felice, University of Malta Rector Prof. Juanito Camilleri and Government Whip and MP Carmelo Abela. A common theme among the speakers was the importance of science and technology investment to the growth of a knowledge-based economy. A highlight of the discussion, stimulated by a poster with the text "Today's Science, Tomorrow's Jobs" and the University Research Trust slogan "Brighter thinking, broader future", was the importance of the national government in investing up to 3 % of GDP for science and technology research by 2020.

Following the opening speeches, the Deputy Speaker and other speakers viewed the poster one-by-one, while interacting with the scientists and research students. Each poster gave a brief outline of the importance of the research and how the research impacts everyday lives. The exhibition provides a unique opportunity for Members of Parliament and researchers to discuss national science policy in an informal setting. The posters were left on display in the Committee Room in the Palace in Valletta during the 4th October Notte Bianca Arts and Culture Festival, and subsequently left on display for a week in the corridor of the Palace for the parliamentarians to view at their leisure.

Figure 1: The speakers at the opening of Science in the House. From left to right are: MP Carmelo Abela, Deputy Speaker The Hon Censu Galea, Science in the City Coordinator and Acting Chair of the Malta Chamber of Scientists Prof. Alex Felice, and the University of Malta Rector Prof. Juanito Camilleri.

2014 Science in the House Poster Titles and Researchers

1. Genetically Modified Fruit Flies
   Untangling the Mysteries of Motor Neuron Disease
   Ruben Cauchi, Michelle Briffa and Rebecca Borg
2. What a Drug is this Aspirin?
   Aspirin and Cancer Cells
   Rena Balzan and Gianluca Farrugia
3. Building Telescopes
   Solving Problems in Modern Astrophysics
   Kristian Zarb Adami, Jackson Said and members of the Institute of Space Sciences and Astronomy
4. Recreating the Big Bang

© 2014 Xjenza Online

Understanding the Secrets of the Universe
Nicholas Sammut, Gianluca Valentino, Nicholas Aquilina, Marja Grech, Adrian Grima, Pierluigi Mollicone, Marija Cauchi, Miryea Borg

5. Got a Great Idea?
   Let's Make It Work
   Takeoff -Anton Bartolo, Martina Pace and Monique Chambers
6. Decontamination Technologies
   Improving the Quality of Fresh Foods
   Vasilis Valdramidis, David Millan Sango, Daniela Abela and Anna McElhatton
7. Where are the Fishes Staying?
   Linking Seafloor Marine Life to Essential Fish Habitats
   Patrick Schembri, Julian Evans, Leanne Bonnici, Juan Jose Bonello and Kimberly Terribile
8. Life Bank for the Future
   The Malta BioBank and Genome Research
   Alex Felice, Joanna Vella and others
9. Treating Neurological Disorders
   Endocannabinoids in the Treatment of Epilepsy
   Giuseppe di Giovanni, Roberto Colangeli, Massimo Pierucci, Gergely Orban, Kenneth Scerri, Stefania Butini and Roberto Di Maio
10. Sustainable Tourism in the Mediterranean Region
    A Case Study of Malta and Sardinia
    Rita Cannas and Nadia Theuma
11. Control of Human Haemoglobin Gene Expression
    New Treatments for Blood Disorders
    Alex Felice, Joseph Borg, Godfrey Grech, Christian Scerri and Sjaak Philipsen
12. Information Processing with Molecules
    Engineering Molecules with Sense and Logic
    David Magri, Maria Cardona and Kyle Paterson
13. Auxetic Patterns in Surgery
    Improving Meshing Designs for Skin Grafting
    Joseph Grima, Ruben Gatt, Daphne Attard, Joseph Briffa, Aaron Casha, Jeffrey Dalli,Luke Mizzi and Keith Azzopardi

Xjenza Online - Journal of The Malta Chamber of Scientists
www.xjenza.org

News Article

In memory of Prof. Giuseppe Amato (1944-2004)

Giuseppe Crescimanno

Held by Prof. Giuseppe Crescimanno on November 25th 2014 at the Department of Experimental Biomedicine and Clinical Neurosciences University of Palermo, Italy.

Prof. Giuseppe Amato, full Professor of Human Physiology at the University of Palermo died ten years ago, after a life spent in high level research activities, and after several years of teaching and in the governance of various university institutions.

He had attended the Institute of Human Physiology of Palermo University, directed by Prof. Vittorio Zagami, since 1966. During this time, he learnt the basis of experimental neurophysiology, working in the laboratory directed by Prof. Vittorio La Grutta.

In 1971, he was appointed Ordinary Assistant and in 1973 he received the first university temporary lectureship at the Faculty of Mathematical, Physical and Natural Sciences.

His first research revealed an inhibitory activity of the caudate nucleus on the auditory primary area in the cat, and on the complex relationships between pulvinar and suprasilvian cortex.

In 1976, he won a NATO Grant that allowed him to attend the Institute of Neurophysiology and Psychology of C.N.R.S in Marseille directed by Prof. Jacques Paillard. During this intensive period of work he collaborated with Prof. Paillard and Prof. Jean Massion studying the physiology of voluntary movement. After the NATO Grant, to conclude his research, he won a grant from the European Science Foundation for the European Training Program in Brain and Behavior Research. Among his principal findings, arising from the researches in Marseille, we remember the role of the internal segment of the globus pallidus and of the putamen on the beginning and execution of a voluntary oriented movement in the baboon.

When he returned to Palermo, his research concerned the inhibitory control exerted by the striatum on the amigdaloid paroxysmal activity.

In 1980, Prof. Amato became Full Professor in Human Physiology. At 36 years old, he was one of the youngest winners of a competition for full professor in Human Physiology in Italy. At that time his research concerned the role of the dopaminergic system in the control of aggressive behaviour and the influence of the claustrum on PTNs activity, in the cat.

During the following years, Prof. Amato was elected Sanitary Director of the University Policlinic "Paolo Giaccone", Dean of the School of Medicine, and Head of the Experimental Medicine Department. Despite his involvement in very important institutional activities, his interest in research was never archived.

He was an exceptional scientist and an unmatched teacher for many generations of students. For me, he was a generous friend and a stimulating colleague to whom still goes my gratitude and real affection.

Giuseppe Crescimanno, Palermo, Italy
25.11.2014

© 2014 Xjenza Online

Xjenza Online - Journal of The Malta Chamber of Scientists
www.xjenza.org
DOI: 10.7423/XJENZA.2014.2.10

Research Article

Viscosity of liquid Ga_xNi_{100-x} alloys

Andriy Yakymovych[1] **and Stepan Mudry**[2]
[1]University of Vienna, Department of Inorganic Chemistry (Materials Chemistry), Währinger str. 42, 1090 Vienna, Austria
[2]Ivan Franko National University Lviv, Department of Metal Physics, Kyrylo and Mephodiy str. 8, 79005 Lviv, Ukraine

Abstract. We studied the viscous properties of molten Ga_xNi_{100-x} alloys in the concentration region between two peritectic points ($77 < x < 94$). The measurements of the viscosity coefficient were carried out using an oscillating crucible method. Temperature dependence of viscosity revealed anomalous behavior in the vicinity of the melting point, particularly for the $Ga_{80}Ni_20$ melt. This feature was analyzed, taking into account the formation of clusters. We show that the formation of chemically ordered clusters is the main reason for the atypical behavior of the dependence of viscosity on temperature and concentration. The obtained results are in agreement with structural parameters obtained from X-ray diffraction.

Keywords liquid alloys – viscosity – cluster formation – chemical bonding in liquid alloys

1 Introduction

Binary Ga-Ni is a component of higher-order systems widely used in industry. For example Co-Ni-Ga and Ni-Mn-Ga can be used as shape memory materials (Chumlyakov et al., 2004). Moreover, the phase diagram of Ga-Ni consists of only a few chemical compounds. Such compounds retain their chemical ordering in a liquid state and influence the atomic distribution of molten alloys of similar concentrations (Massalsky, 1990). Understanding the behavior of physical properties is important for many technological processes, thus driving the investigation of structure-sensitive properties.

In particular, the viscous properties of liquid Ga_xNi_{100-x} alloys rich in Ga are of special interest. These alloys are thought to be sensitive to an applied magnetic field, because it is thought that they contain Ni-based magnetic clusters. Simultaneously, it is still unclear whether melts of peritectic concentration are related to the structure of molten alloys of similar concentration.

1.1 Experimental Details

The samples were prepared from nickel and gallium with a purity of 99.99 % and 99.999 %, respectively. Their dynamic viscosity was investigated using an oscillating cup viscometer (Mudry et al., 2008). The temperature was measured and controlled using a WRe-5/20 thermocouple placed below the sample. Our aim was to measure the parameters of rotational oscillations. Viscosity was calculated according to the relationship between the logarithmic decrement, the time period and viscosity by means of the modified Roscoe equation (Vollmann and Riedel, 1996). The accuracy of the obtained viscosity values was higher than 5 %.

We carried out diffraction studies using a high-temperature X-ray diffractometer (Plevachuk et al., 2009). Cu-K_α radiation monochromatized by a LiF single crystal as a monochromator with Bragg-Brentano focusing geometry was used. The scattered intensities were recorded with an angular step of 0.05° within the region of the principal peak and 0.5° for the remaining values of the scattering angle. Intensity curves were corrected for polarization and incoherent scattering (Cromer and Waber, 1965) and were subsequently normalized to electron units by the Krogh-Moe method (Krogh-Moe, 1956). The structure factors $S(k)$ were calculated on the basis of the obtained intensity curves.

Correspondence to: A. Yakymovych (yakymovych@online.ua)

© 2014 Xjenza Online

2 Results and discussion

The temperature dependence of the dynamic viscosity of the melts under investigation showed differing (Arrhenius or non-Arrhenius) behavior, dependent on the alloy composition (Figure 1). Particularly, for the molten $Ga_{94}Ni_6$ alloy, the viscosity increased with a decrease in temperature according to the Arrhenius law:

$$\eta = A \exp^{(\frac{E}{RT})} \quad (1)$$

where η is the viscosity coefficient of the liquid; A is a constant; E is the activation energy of viscous flow; R is the universal gas constant; T is the temperature. The values of parameters A and E are given in 1.

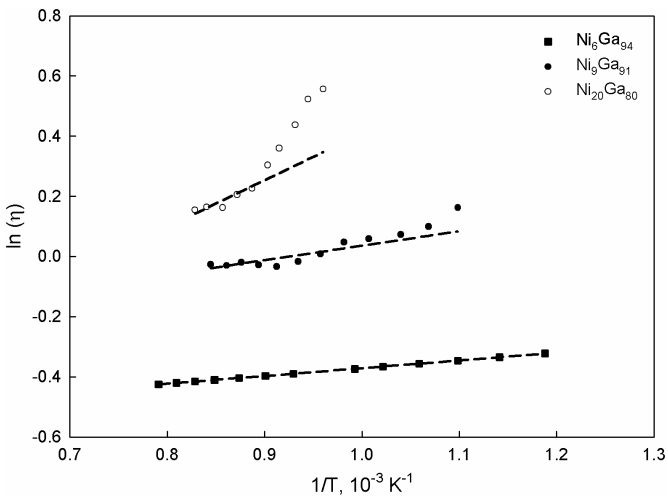

Figure 1: The temperature dependence of viscosity for liquid $Ni_{100-x}Ga_x$ alloys.

Experimental data of the viscosity versus temperature can be used to calculate the activation energy of viscous flow E by fitting into the Arrhenius-type equation, given by equation 1.

As seen in Table 1, a small addition of Ni to Ga (6 at. %) decreases the activation energy, while higher contents of Ni causes a drastic increase of the activation energy. The viscosity isotherm, together with the dependence of the activation energy of viscous flow on the content of Ni is presented in Figure 2. For alloys with 6 at. % nickel, the viscosity coincides with that of liquid Ga. Following the addition of nickel, the viscosity coefficient increased. In contrast to viscosity, the activation energy increased when nickel content was 20 at. %.

The data indicates that the energy of activation assumed higher values at temperatures close to the melting point. Taking into account these data, as well as the dependence of viscosity on temperature and concentration, we conclude that the addition of Ni atoms significantly affects the viscous properties of melts enriched with Ga.

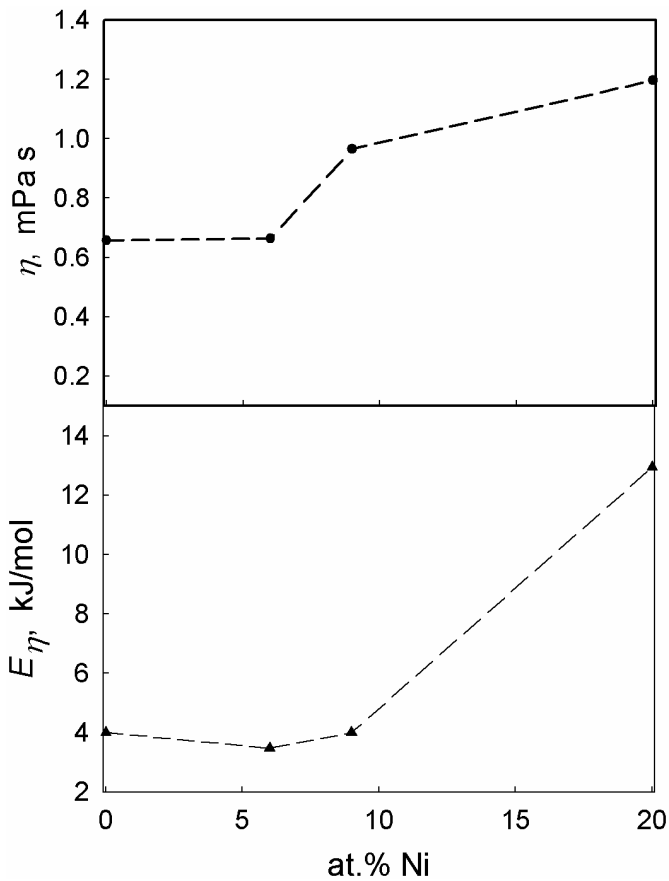

Figure 2: Isothermal viscosity (upper figure) and activation energy (bottom figure) for liquid Ga_xNi_{100-x} alloys at 1173 K.

The obtained results suggest that Ni atoms diluted in Ga are randomly distributed and preferentially surround themselves with neighbours unlike them. With an increase in Ni content, the interaction of unlike atoms becomes stronger, which results in an increase in viscosity and in the energy of activation. When the concentration of Ni reaches 20 at. %, such interaction is even stronger and promotes the formation of chemically ordered structural units (clusters). Thus, we were able to identify two major factors responsible for an increase in both the viscosity and the energy of activation, i.e. the preferred interaction of unlike atoms that result in the formation of chemically ordered clusters and an increase in the size of such clusters.

Naturally, such changes in the interatomic interaction must be related to structural features in the liquid state. Therefore, we also carried out diffraction studies of these liquid alloys. The structure factors $S(k)$ revealed a profile atypical for metallic melts Figure 3. All curves were different from the $S(k)$ for liquid Ga. Although the content of Ga prevailed in this alloy, the structure factors were significantly different from those

Table 1: Activation energies for Ga-enriched melts.

Alloy composition (at.%)	A (mPa s)	E (kJ mol^{-1})	Source
Ga	0.44	4.00	(Battezzati and Greer, 1989)
$Ga_{94}Ni_6$	0.53	2.14	this work
$Ga_{91}Ni_9$	0.64	4.00	this work
$Ga_{80}Ni_{20}$	0.32	12.94	this work

of Ga. A wide principal peak can be interpreted as a sum of submaxima corresponding to structural units with atomic distribution, the structure of which was similar to that of Ga and Ni, respectively. The profile of the principal peak changes significantly upon the addition of Ni atoms. This profile corresponded to the diffraction peaks of Ga_4Ni, Ga_3Ni_2 and GaNi formed due to peritectic reactions. It is possible that molten alloys enriched with Ga rearrange their atomic distribution upon cooling in order to form clusters whose structure would be similar to that of the above-mentioned chemical compounds.

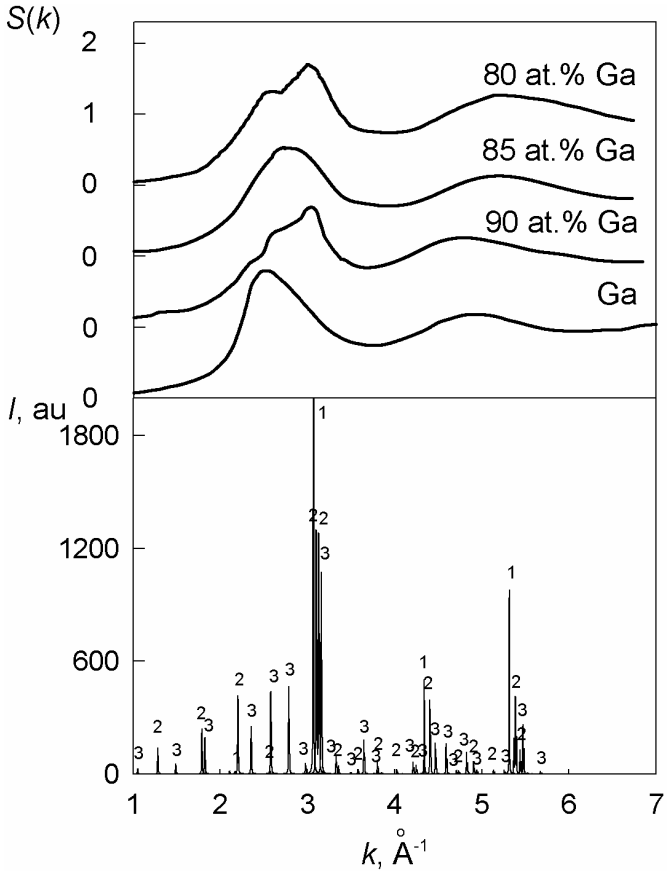

Figure 3: Structural factors for Ga-Ni liquid alloys (upper figure) compared with diffraction patterns for intermetallic phases of GaNi (1), Ga_3Ni_2 (2) and Ga_4Ni (3) (bottom figure).

Taking into account these features, we assume that a certain fraction of Ni atoms form chemically ordered clusters with a structure similar to that of Ni. These clusters are randomly distributed in the matrix of Ga. The fraction of clusters increases with an increase in the content of Ni. This assumption is in accordance with the results of viscosity measurements.

3 Conclusions

The changes of the viscosity coefficient with temperature and concentration for Ga-enriched molten Ga_xNi_{100-x} alloys revealed the existence of inhomogeneous structure, characterized by the presence of a Ga-based matrix and Ga_nNi_m clusters with a wide range of compositions. The viscosity data are in agreement with the results of X-ray diffraction, which also confirm the trend to chemical ordering in the liquid state for Ga-enriched alloys of the Ni-Ga binary system.

References

Battezzati, L. and Greer, A. (1989). The viscosity of liquid metals and alloys. *Acta Metall.* 37, 1791–1802.

Chumlyakov, Y. I., Kireeva, I., Karaman, I., Panchenko, E., Zakharova, E., et al. (2004). Orientational dependence of shape memory effects and superelasticity in CoNiGa, NiMnGa, CoNiAl, FeNiCoTi and TiNi single crystals. *Russ. Phys.* 47(9), 893–914.

Cromer, D. and Waber, J. (1965). Scattering factors computed from relativistic Dirac-Slater wave functions. *Acta Cryst.* 18, 104–109.

Krogh-Moe, J. (1956). A method for converting experimental X-ray intensities to an absolute scale. *Acta Cryst.* 9, 951–953.

Massalsky, T. (1990). *Binary Alloy Phase Diagrams* (2nd). ASM, Materials Park, OH.

Mudry, S., Sklyarchuk, V. and Yakymovych, A. (2008). Influence of doping with Ni on viscosity of liquid Al. *J. Phys. Stud.* 12(1), 1601–1605.

Plevachuk, Y., Sklyarchuk, V., Yakymovych, A. and Shtablavyi, I. (2009). Methods and facilitirs for thermodynamical and structure investigations of liquid metallic alloys. In *Proceedings of the 6th in-*

ternational conference on electromagnetic processing of materials (epm 2009) (pp. 415–418).

Vollmann, J. and Riedel, D. (1996). The viscosity of liquid Bi-Ga Alloys. *J. Phys.: Condens. Matter.* 8(34), 6175–6184.

Xjenza Online - Journal of The Malta Chamber of Scientists
www.xjenza.org
DOI: 10.7423/XJENZA.2014.2.11

Research Article

A Fruitful fly forward: The role of the fly in drug discovery for neurodegeneration

Michelle Briffa[1], Neville Vassallo and Ruben J. Cauchi[1]
[1]Department of Physiology and Biochemistry, University of Malta, Msida, Malta GC

Abstract. Neurodegenerative diseases such as Alzheimer's disease (AD), Parkinson's disease (PD) and Huntington's disease (HD) are increasing in prevalence and the need for novel disease-modifying therapies is critical. Identifying compounds that modify disease progression has been a struggle - mainly due to the insufficient knowledge regarding the underlying pathophysiological mechanisms of these diseases. Traditional high-throughput screening *in vitro* have previously identified positive hits. However, subsequent validation experiments *in vivo*, rendered them ineffective and/or toxic. *Drosophila* models of neurodegenerative disease can be effectively exploited in drug screens for the identification of compounds and target disease mechanisms. This review sheds light on how *Drosophila* models of neurodegeneration can aid the therapeutic discovery process through the use of chemical and genetic suppressor/enhancer screens and other existing techniques. Integrating *Drosophila* models of neurodegeneration to the drug discovery process holds great promise for the enhanced rate of therapeutic-modifying compound discovery.

Keywords Drosophila – fruit fly – drug discovery – neurodegeneration – Alzheimer's disease – Parkinson's disease – Huntington's disease.

1 Introduction

Drug discovery is the process by which new candidate compounds and molecules that have a therapeutic effect on disease symptoms are discovered. Traditionally, the process of drug discovery begins with identifying a disease-causing protein, followed by a screening of a large library of known chemical compounds in order to identify drugs that ameliorate or alter the function of the disease-causing proteins. Subsequently, compounds are optimized and then testedin animal models (Pandey and Nichols, 2011). The traditional high-throughput screening (HTS) approach has been the source of many documented successes, ranging from identifying therapeutic compounds to cell functions and pathological pathways (Giacomotto and Ségalat, 2010). However, despite the numerous triumphs brought about by HTS, the past couple of year shave seen a slow-down in the development of new therapeutic drugs, due to a variety of reasons, mainly the positive hits generated by initial screening are being rendered invalid when tested in animal models and therapeutically ineffective when tested on humans; furthermore, the method depends on predetermined targets and therefore, does not leave space for new target discovery (Giacomotto and Ségalat, 2010; Lindsay, 2003).

Lately, there has been an increased interest in target discovery. The identification of novel targets and early validation techniques will help reduce subsequent failure rates of positive hits,and address the problems being faced by the pharmaceutical companies (Lindsay, 2003). The limited predictive value of HTS for clinical outcome can be overcame with the use of animal models for a primary drug screening platform (Pandey and Nichols, 2011).

Drosophila melanogaster is one such organism that is gaining momentum as a valid screening tool for the drug discovery process (Lieschke and Currie, 2007). *Drosophila* has been used since the 20th century and provides the advantage of combing genetic acquiescence and a rapid lifecycle. In addition, culture conditions are compatible with large-scale screening and their use permits high-throughput screening in a whole animal context which is not dependent on a predetermined tar-

Correspondence to: M. Briffa (michelle.briffa@um.edu.mt)

© 2014 Xjenza Online

get (Giacomotto and Ségalat, 2010). Another advantageous aspect to keep in mind is that key biological features are conserved from the flies to humans, including a highly structured brain, elaborate neuromuscular junctions, and underlying mechanisms of synaptic transmission. This context provides a good foundation for developing an appropriate model for human disease characterising the pathological phenotype (Lenz et al., 2013). Screening for novel drugs in *Drosophila* enables the selection of high-quality hits that display keys features such as transdermal availability, metabolic stability and low toxicity (Pandey and Nichols, 2011). This in turn reduces the expenses spent on primary screening and filters the quality of positive hits for secondary screening.

2 Why The Fly?

2.1 Brief history of the fly

Drosophila is an old player in the biomedical field with a rich history spanning over 100 years. Fruit flies have been indirectly associated with medical progress and drug discovery for many years, mainly through genetic, biochemical and disease pathology-related discoveries (Ségalat, 2007). Indeed, Nobel prizes have been awarded to people for their pioneering research in flies, starting with Thomas Hunt Morgan for the role of chromosomes in heredity (1933), Hermann Muller for the production of mutations by x-rays (1946), Edward B. Lewis, Christiane Nusslein-Volhard and Eric F. Wieschaus for genetic control of early structural development (1995) and finally Jules Hoffman for the discoveries around innate and adaptive immunity (2011).

In the modern era, *Drosophila* was amongst first complex organisms to have its entire genome sequenced (Adams et al., 2000). A couple of years later when the human genome was sequenced, the observed homologies between the two genomes was recognised and this strengthened its role as a model to understand disease processes (Pandey and Nichols, 2011). Recently, their use as direct HTS tools gained momentum mainly due to their unique life cycle, form, function and experimental manipulation (Rand, 2010).

2.2 Basic biology of the fly

Flies are reared in small vials on a simple solid food medium of cornmeal, yeast and agar. At the optimum temperature of 25 °C their generation time is 10-11 days from egg to adult (Rand, 2010). The fly has a very rapid lifecycle which is comprised of four distinct stages: embryo, larva, pupa and adult. Each stage presents a unique opportunity to assess the susceptibility to the nervous system to xenobiotics (Rand, 2010). The embryo stage lasts around 24 hours at 25 °C and during this time neurogenesis and differentiation give rise to a fully functioning nervous system, capable of sensory and motor behaviours characteristic to the larva (Rand, 2010). In fact, the embryo is typically used in developmental studies examining pattern formation, cell fate determination, organ formation, neuronal development and axon guidance (Pandey and Nichols, 2011). The larval stage lasts over 4 days and is characterised by a period of growth that results in a 10-fold increase in body size (Truman and Bate, 1988). The larva is used to study physiological processes and simple behaviours like foraging (Pandey and Nichols, 2011). The following 5-6 days of pupal metamorphosis is characterised by tissue reorganisation and the fusing together of the adult structures from the precursor imaginal disc tissues. At the same time, the central and periphery nervous system neurons undergo pruning and regrowth while newly born adult neurons migrate to their final position and extend their synapses to their targets (Williams and Truman, 2004). The emerged adult fly is a complex organism capable of showing behaviours like flight, chemo-, photo- and geo-taxis, foraging and mating (Rand, 2010). The brain of the adult fly has more than 100,000 neurons that form discreet circuits and mediate complex behaviours including circadian rhythms, sleep, learning and memory, courtship, feeding, aggression, grooming, and flight navigation (Pandey and Nichols, 2011) (Figure 1).

2.3 Genetic Workhorse

Drosophila has been primary regarded as a model for the study of genetics. The first genetic principles of chromosomal heredity and mutagenesis, were primary discovered using the fly (Rubin and Lewis, 2000). The large polytene chromosomes served as a template for gene mapping and the mutagenesis screens rapidly advanced the knowledge of gene function. The fly has a relatively simple genetic make-up of four chromosomes encoding roughly 13,600 genes (half the number found in humans) (Adams et al., 2000). More than 95 % of its genetic content is on three of its four chromosomes, with the first being the sex chromosome and the other three being the autosomes (Rand, 2010). The sequence identification of genes brought about by the emergence of molecular cloning and recombinant DNA technology, opened doors to functional analysis of transgenes *in vivo* (Rand, 2010). The method of creating transgenic flies through transposable element transformation, opened the door to manipulating the expression of endogenous or exogenous genes over the course of development and provided a means of integrating foreign DNA into the chromosome (Duffy, 2002). Variations in the method has led to the creation of the "workhorse" of fly transgenic models, the Gal4-UAS gene expression

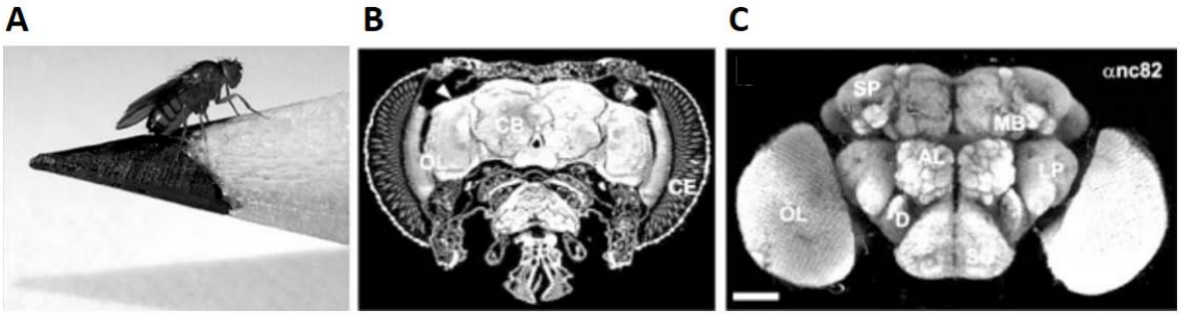

Figure 1: Drosophila as a model organism.(a) The arthropod Drosophila fits on a pencil tip and can be easily kept in the laboratory. Their anatomy displays characteristic features that can be used as phenotypes to study neurodegeneration and as endpoints in high-throughput screening. (b) Confocal image of a cross-section through the adult Drosophila head; auto-immunofluorescence visualises the ommatidia of the compound eye (CE), the optic lobe (OL) and the central brain (CB). The cell bodies (arrowheads) are topologically separated from axonal extensions which make up the neuropil. (c) Confocal image of a whole mount adult brain immunolabelled with anti-nc82 which recognises the Bruchpilot protein that is specifically enriched in active zones of synaptic terminals. This allows the visualisation of cortical areas in the fly brain, including optic lobes (OL), antennal lobes (AL), superior protocerebrum (SP), lateral protocerebrum (LP), mushroom bodies (MB), deuterocerebrum (D), and subesophageal ganglion (SG) (adapted from Hirth (2010)).

system (Duffy, 2002). This bipartite approach keeps the yeast transcription factor Gal4 and the Upstream Activating Sequence (UAS) promoter (which holds the transgene) to which Gal4 binds, on different parental strains. When the two strains are mated, the progeny expresses the transgene in the specific tissues defined by the Gal4 driver (Pandey and Nichols, 2011). Other modifications and enhancers further refined tissue specificity as well as temporal expression specificity (McGuire et al., 2004). This methodology has been crucial in creating "humanized" versions of the flies that express disease genes that invoke neuropathology mimicking human disease in the fly (Bilen and Bonini, 2005; Cauchi and van den Heuvel, 2006).

3 Modelling Neurodegeneration in the Fly

The genetic advantages and tools that come with the use of *Drosophila* make it very easy to rapidly generate models of human disease, which can be used for therapeutic target discovery. The generation of *Drosophila* models that express human genes is a popular approach for studying neurodegenerative diseases. Fly models for neurodegenerative diseases have been generated, studied and used for many years. Neurodegenerative diseases are considered to be predominately diseases that occur at an older age, implying that processes that are altered due to aging may contribute to their pathogenesis (Newman et al., 2011). They are characterised by the misfolding, aggregation and deposition of normal or abnormal proteins that become aberrant (Newman et al., 2011). Many late-onset neurodegenerative diseases are generally associated with the formation of intracellular aggregates of toxic proteins (Taylor et al., 2002). The common hypothesis is that neurodegenerative diseases come about when the production of neurotoxic proteins exceeds the cell's capacity for clearing them or when they evade autophagic clearance altogether (Pandey and Nichols, 2011).

3.1 Parkinson's disease

PD is a progressive, disabling, heterogeneous neurodegenerative disorder that clinically presents with motor and non-motor features (Henchcliffe et al., 2011). PD is characterized by loss of dopaminergic neurons in the substantia nigra and formation of filamentous intraneuronal inclusions (Lewy bodies [LBs]) (Feany and Bender, 2000). The major components of LBs are amyloid fibrils of the protein α-synuclein (Spillantini et al., 1998). Mutations in the α-synuclein gene (SNCA) are associated with familial PD and have an increased aggregation propensity *in vitro* (Conway et al., 2000; Greenbaum et al., 2005). Overexpression of human α-synuclein in different model systems, have provided a pathologically true model of PD. In several of these models, the rate of fibril and inclusion body formation does not correlate with neurotoxicity (Chen and Feany, 2005; Volles and Lansbury, 2007). This lack of correlation formed the basis for the hypothesis that small oligomers, but not fibrils, are the most toxic species of α-synuclein (Lashuel and Lansbury, 2006). One great advantage of using *Drosophila* to model PD is their ability to reprise some of the key neuropathological characteristics of PD. Transgenic flies show age-dependent, progressive degeneration of dopamine neurons, inclusion-like formation, progressive locomotor deficits and a decrease in lifespan (Muqit and Feany, 2002).

3.2 Alzheimer's disease

Alzheimer's disease is the most prevalent form of senile dementia in humans, with its manifestation being age-dependent and its incidence in the general population expected to rise from 6 % to 30 % over the next 65 years (Puglielli et al., 2003). AD is diagnosed by the presence of neuritic plaques, composed mainly of Aβ peptides and neurofibrillary tangles composed of tau protein (Finelli et al., 2004). There is evidence that the β-amyloid peptides are central to the pathogenesis of AD (Crowther et al., 2006). These peptides are generated by β- and ɣ-secretase cleavage of amyloid precursor protein (APP) to yield peptides of either 40 or 42 amino acids ($A\beta_{1-40}$ or $A\beta_{1-42}$) (Crowther et al., 2006). Recently, studies have shown that monomeric peptides are not toxic but that oligomeric peptides gain toxicity that is subsequently lost when mature fibres are formed (Lashuel and Lansbury, 2006). In order to understand the pathway of neurodegeneration in AD, a faithful animal model is required. Current mouse models have successfully recapitulated AD-like phenotypes (Crowther et al., 2006; Hsiao et al., 1996). Despite this, mouse models are laborious to characterize and develop. *Drosophila* models of AD drive the expression of the Aβ peptides in temporal and tissue specific manner. Several fly models of AD have been made, including ones expressing Arctic Aβ peptides (E693G; an aggressive mutation for the AD model) and show progressive neurodegeneration, amyloid deposits, reduction in lifespan and locomotor dysfunction (Crowther et al., 2006; Sofola et al., 2010; Iijima et al., 2004; Finelli et al., 2004).

3.3 Huntington's Disease

A large and diverse group of neurodegenerative diseases are characterised by the abnormal function of long tracks on tri-nucleotide repeats. The repeats can be of two kinds; part of the protein-coding sequences which result in the production of long stretch of polyglutamine-containing (polyQ) peptides or in non-coding sequences (Konsolaki, 2013). Huntington's disease (HD) is associated with expanded polyQ repeats in the gene Huntington within exon 1. Translated stretches of polyglutamines disrupt cellular processes including nucleolar stress, the functions of miR34 (its disruption is linked to the occurrences of some types of cancer), autophagic processes involved in the immune system and the Akt/GSK3b pathway (involved in cellular growth) (Konsolaki, 2013). In addition, a form of mutant Huntington may interfere with specific components of transcriptional machinery in early stages of HD (Cui et al., 2006).

Mutant Huntington is expressed ubiquitously but selective cell loss is observed in the brain (Vonsattel and DiFiglia, 1998). In clinical settings, HD is characterised by involuntary movements and psychiatric disturbances (Vonsattel and DiFiglia, 1998). Due to the fact, that polyglutamine diseases are brought about by single-gene defects (e.g. Huntington gene in HD), *Drosophila* models are commonly used to study this neurodegenerative disease. Pathological hallmarks of HD, such as intracellular and cytoplasmic aggregates of expanded Huntington are present in Drosophila models of HD (Pandey and Nichols, 2011). *Drosophila* models can be generated through the expression of truncated wild-type and mutant forms of Huntington, however, it has been noted that increased polyQ expression leads to increased severity of degeneration, age-dependent degeneration and repeat length-dependent protein aggregation in *Drosophila* models (Spada and Taylor, 2010). These models have provided a platform to demonstrate that human disease genes can yield parallel neurodegenerative effects in *Drosophila* models (Pandey and Nichols, 2011).

4 Drug Discovery Takes Flight

4.1 Drug delivery

The mode of drug or compound delivery is an important aspect to take into consideration when performing drug discovery screens (Figure 2). Exposure of the compound to the cells or organs of interest in flies can take a variety of forms depending on the developmental stage of the fly. For embryos, drugs can be administered via maternal feeding, injection or *in vitro* incubation (Rand, 2010). Due to the unknown metabolic and delivery characteristics of the embryo, maternal feeding requires the determination of the experimental dosage (Rand, 2010). Embryo injection methods have recently been optimized for use in high-throughput screens using an automated system based on microelectromechanical systems injectors, which allows successful mass-injections of *Drosophila* embryos (Zappe et al., 2006). Chemical exposure through *in vitro* incubation of fly embryos has been effective, however, one limitation of this system is the permeabilization of the vitelline membrane of the *Drosophila* egg chamber (Rand, 2010). For larva and adult flies, drugs can be supplied through dosages in food media (Peng et al., 2009). For longer exposures, the drug can be mixed in the solid media and the larva can be reared on it; when shorter exposure to the drug is required, the compound can be diluted and mixed in a yeast paste (Pandey and Nichols, 2011). Drugs (e.g. cocaine) have also been successfully delivered to both larva and adult flies through injection methods (Dimitrijevic et al., 2004). The routes for drug administration in adult flies are numerous. Drugs can be presented as vapour or aerosols in a controlled environment (Moore et al., 1998; Parr et al., 2001), in the solid media (Peng

et al., 2009), from a drug-saturated filter paper (Nichols et al., 2002), dropped directly onto the exposed nerve cord of decapitated flies (Torres and Horowitz, 1998), or injected directly into the fly abdomen (Dzitoyeva et al., 2003). The route of administration is also dependent on the taste of the drug being administered: if the drug has a poignant smell the flies might not eat it. If ingesting the drug is the route of administration chosen, then it might be necessary to introduce the drug to the fly through a rewarding substrate (e.g. yeast, sucrose or banana) (Pandey and Nichols, 2011).

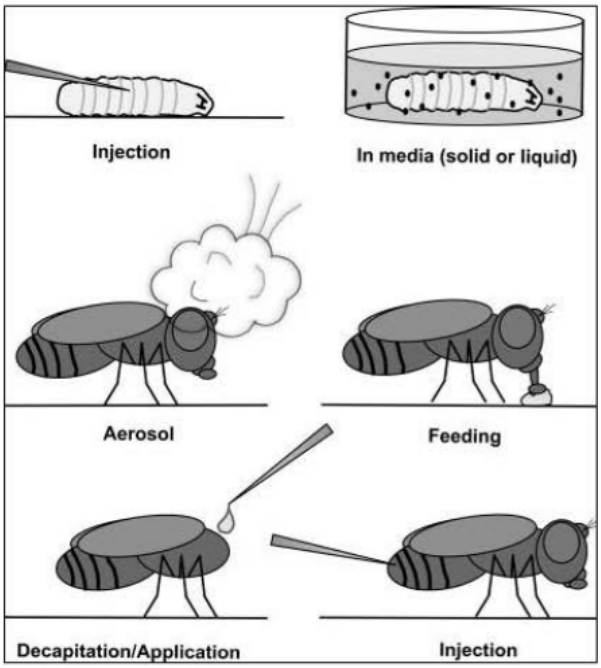

Figure 2: Routes for drug administration for drug delivery in *Drosophila*. For larva (top), drug can be directly injected or drug can be mixed with media. Media can be either solid or liquid with 2 % yeast paste to encourage feeding behaviour. Adults can have drug delivered as an aerosol or gas, as a mixture with food substrate, as a direct application to exposed nerve cord, or as an injection. Drug administration through feeding generally has the highest throughput (Pandey and Nichols, 2011).

Feeding assays can also be performed in order to determine whether the presence of a drug is influencing food intake. One such assay is based on measuring the feeding frequency by observing the proboscis-extension. This method can then be validated by short-term measurements of food dye intake (Wong et al., 2009). When administering drugs, it is important to keep in mind that female flies feed more frequently than males and therefore, their food intake is higher, a consideration that is especially important for drug delivery. Flies feed more often when housed in larger groups, and their feeding times vary on the time of the day (Wong et al., 2009). There are also different strategies to be considered when feeding drugs to adult flies. Firstly, the flies will generally consume a large amount of food if previously starved for up to 18 hours. This strategy allows for the observation of the acute effects of the drugs, however, there is a significant amount of dosage variability of the ingested drug and is relatively low-throughput. Secondly, maintaining flies on drug/food for longer than 24 hours allows for steady-state levels to be achieved before testing. This method allows high-throughput administration of the drug across large populations, however, the possibility of adaptive mechanisms (such as down-regulation of target genes) to prolonged exposure may occur. When interpreting the data, it is important to keep in mind that if the flies are removed from the drug-supplemented food before being subjected to tests, the rate of drug elimination may need to be accounted for (Pandey and Nichols, 2011).

Once the method of administration has been chosen, the next issue to tackle is the compound concentration that will be delivered to the flies. A key consideration to take into account are the potential differences in the pharmacokinetics and pharmacodynamics of compounds and small molecules. These molecules can produce significant discrepancies in drug levels, tissue distribution profiles and toxicity, between mammals and flies (Pandey and Nichols, 2011). Since the target is not always known and the treatment is usually delivered through food media, it is difficult to predict the range of doses that need to administered in order to avoid a low ineffective concentration, or a high toxic one (Giacomotto and Ségalat, 2010). A conceivable approach would be to test compounds at several concentrations and log dilutions, established by existing data and the chemical properties of the compound. Physiologically effective concentrations can vary from 0.01 to 100 mM in the food media, although the commonly used concentrations are within the range of 1 to 10 mM (Pandey and Nichols, 2011; Giacomotto and Ségalat, 2010). The best approach is to start with high concentrations of the compounds in the medium, since this will ensure that a lot of the compounds will display a toxic effect on the flies and they could be further re-tested at a lower concentration (Giacomotto and Ségalat, 2010). Despite this, pilot studies have also been done using three different log dilutions of 1 mM, 10 mM and 100 mM in order to ensure the efficacy of a given assay and that drugs are being ingested.

4.2 The screening process

Once the drug has been delivered to the fly, the next step is to screen the flies in an attempt to find hits showing an activity or an affinity on a selected target or in a disease model (Spring, 2005). This usually involves an alternation of the pathogenic phenotype that could

be directly attributed to the administered drug. Traditional HTS involves massive parallel analysis of the effects of molecules from a large library of compounds based on *in vitro* cell culture, biochemical assays or receptor binding assays (Pandey and Nichols, 2011) (Figure 3). This approach has contributed to the discovery of therapeutically effective compounds, identification of cellular pathways and pathophysiological mechanisms. Its ultimate goal is to discover and explain relationships between chemical structures and biological activities (Giacomotto and Ségalat, 2010). Despite the varied documented successes, this approach has three major limitations. Firstly, it provides a biased approach dependent on the existence of detectable targets (Lindsay, 2003). Secondly, most disease mechanisms cannot be reproduced *in vitro* due to a difference in the complexity between cells and multicellular organisms (Giacomotto and Ségalat, 2010). Thirdly, most of the positive hits generated by the initial screening, fail to reproduce the results once tested in organisms such as rodents. The latter is due to a number of difficulties resulting from poor absorption, solubility, distribution, metabolism, excretion and toxicity characteristics, which result in a waste of funds and efforts and a dead-end for most hits (Bleicher et al., 2003). One such example is that of a recent screen of 184,880 novel compounds on Huntington's disease (HD) aggregates which led to the identification of positive hits, including a number of benzothiazoles that inhibited polyglutamine-mediated aggregation of toxic and misfolded proteins (Heiser et al., 2002). In a cell culture model of aggregation, all the primary hits were found to be toxic to cells, and in an animal model of HD, none of the compounds were therapeutically effective (Hockly et al., 2006). The advantages of integrating the fly in the primary screening process include; cost-effectiveness and high-quality positive hits to streamline the pool of candidates, before moving on to secondary screening on expensive mammalian-based models (Pandey and Nichols, 2011).

Drug discovery studies from models of disease can be done in two approaches: the disease model can be used in the chemical enhancer/suppressor drug screens or the model can be used to further understand the pathological processes of the disease and in turn, highlight potential therapeutic targets. Chemical enhancer/suppressor (or candidate drug delivery) can be unbiased and they consist in testing chemical libraries for their ability to reverse the disease phenotype (Newman et al., 2011). For this purpose, mutant strains of *Drosophila* which mimic human disease and have clear and easy readouts of phenotypic modulation, are an attractive package for medium to high-throughput drug screening (Giacomotto and Ségalat, 2010) (Figure 3). An example of such a screen is that reported by Zhang et al. (2005), in which primary screening of a 16,000 compound library that was done in a yeast model of HD, identified 4 compounds capable of preventing polyQ aggregation and toxicity. A cell-based assay and a *Drosophila* rough eye phenotype HD model, were then used to test the anti-aggregation properties of these 4 compounds. One of them, C2-8 was found to suppress the rough eye phenotype and polyQ inclusion formation, atrophy and motor impairment in a rodent model (Chopra et al., 2007). Several biased candidate drug studies have been undertaken in *Drosophila* models of neurodegeneration in which, compounds were used to interfere with protein misfolding (Fujikake et al., 2008), aggregation (Apostol et al., 2003), clearance (Sarkar et al., 2008) and neuronal dysfunction (Steffan and Thompson, 2003) (Table 1).

Drosophila models of neurodegeneration can be used in two ways to study the underlying pathological characteristics of a disease: unbiased genetic screens can be used to identify novel players, or genetic/pharmacological manipulation of proteins or pathways implicated in the disease can shed light on the downstream consequences (Newman et al., 2011). In traditional forward genetic screens, randomly mutagenized flies are screened for disturbances of a pre-defined phenotype or process. The mutagenized flies can be produced by a chemical mutagen (e.g. ethylnitrosourea) or mediated mutagenesis through transposon elements (e.g. P-element and piggyBac) (Lindsay, 2003; Lenz et al., 2013). Models of disease can be used in this genetic enhancer/suppressor screen by expressing the disease gene with a random mutant gene, which may or may not interact and modify the phenotype (Newman et al., 2011). One such screen involved using transgenic flies with the Aβ pathology expressed in the eye, crossed against 1,963 mutant fly stocks. This screen identified 23 modifiers of the rough eye phenotype including proteins in the secretory pathway, cholesterol homeostasis pathway, and proteins involved in chromatin structure and function (Cao et al., 2008). This unbiased screen identified some pathways and proteins previously implicated in the disease pathology, but more importantly, it helped shed light on some new participants of the disease process which can now be targeted for therapeutic interventions. Strategic expression or pharmacological manipulation of implicated proteins or pathways, can help with validating hypotheses about pathogenic mechanisms (Newman et al., 2011). The 'Tau microtubule' hypothesis is one of the proposed theories to explain the pathological Tau processes underlying AD. *In vitro* cell-based screens produced convincing evidence to support this theory, however, there was no such evidence *in vivo* (Cowan et al., 2010). All aspects of this hypothesis were tested in one *in vivo* experimental paradigm

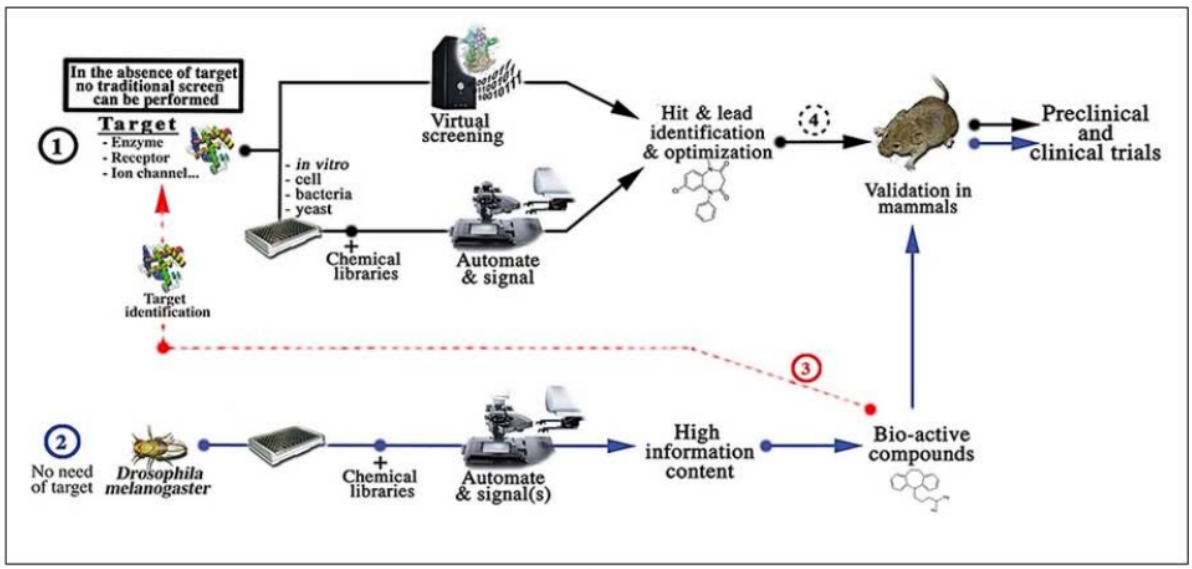

Figure 3: High-throughput screening using Animal Models for Drug Discovery.(1, black lines) A schematic view of the different stages which came upon a drug discovery process based on traditional HTS. In the absence of target or in complex mechanism the HTS can hardly be set up. (2, blue line) An alternative approach is utilising phenotypic chemical screens with small animal models like Drosophila. (3, red line) Identification of hits in these models may reveals new molecular mechanisms and targets. The target could be further used in traditional HTS. (4), Drosophila may also bridge the gap between traditional high-throughput screening and validation in mammalian models (adapted from Giacomotto and Ségalat (2010)).

Table 1: Overview of *Drosophila* Models of Neurodegeneration and their successes in Drug Discovery. **β-Amyloid**, Beta Amyloid; **HD**, Huntington's Disease; **HSP**, Heat shock protein; **REP**, Rough eye phenotype.

Disease	Genes Involved	Phenotypes	Drug Discovery/Target Discovery	Positive Hits/Targets involved	References
Alzheimer's Disease (AD)	B-Amyloid Protein	Eye degeneration, accumulation of amyloid plaques, vacuolation of brain, reduced lifespan and locomotor defects.	1963 mutant fly stock tested in Aβ42 *Drosophila* model with REP modifications. 23 modifiers were identified.	Proteins involved in: • Secretory pathway • Cholesterol homeostasis • Regulators of chromatin	(Cao et al. 2008)
	Tau	Eye degeneration, disruption of the microtublular network at presynaptic never terminals, axonal degeneration, neuromuscular junctions morphological defects	Mutant tau flies with a library of 1250 mutants and identified 30 lines involved in REP modification.	Proteins included: • 4 cytoskeletal • 3 molecular chaperones • Cysteine string protein • 2 members of the HSP40 co-chaperone family	(Blard et al. 2007)
Parkinson's Disease (PD)	α- Synculein	Age-dependent loss of dopaminergic neurons ad progressive climbing defects.	Mutant flies overexpressing α- Synculein were fed with: • Geldanamycin (enhancer of Hsp70 expression and modulator of stress response) • Ubiquitin • Cathepsin D • Nicotinamide • Polyphenols	• Geldanamycin, ubiquitin and cathepsins D suppresses α-Synculein toxicity. • Nicotinamide suppresses α-Syn toxicity through improvement of oxidative mitochondrial dysfunction.	(Auluck and Bonini 2002, Lee et al. 2009) (Cullen et al. 2009) (Jia, et al., 2008) (Long et al. 2009)
	Parkin and Pink	Dopaminergic neuron loss, age-dependent motor deficits, reduced lifespan, locomotor defects, male sterility and mitochondrial pathology	Parkin and Pink1-deficient flies were treated with: • Vitamin E • Rapamycin	• Vitamin E offered neuroprotection against degeneration. • Rapamycin suppressed parkin and pink1 related phenotypes.	(Wang, et al., 2006) (Tain, et al., 2009)
Huntington's Disease (HD)		Axonal transport defect, lethality, neurodegeneration, behaviour and electrophysiological defects	Library of 16,000 compounds (Chembridge, San Diego, CA) in primary screens using yeast, PC12 cells and mouse hippocampal slice. Secondary screen was performed on fly models of HD.	C2-8	(Meriin et al. 2002) (Apostol et al. 2003, Zhang et al. 2005)

using a *Drosophila* model of tauopathies (Mudher et al., 2004). *Drosophila* models of neurodegeneration play an important role in drug discovery design as they provide a vital step for the primary screening of drugs in whole organisms (for examples refer to Table 1).

4.3 Measurable endpoints

Another crucial step which has a profound impact upon the quality of the information produced from the screening process, is the output measurements or endpoints (Giacomotto and Ségalat, 2010) (Table 2). The requirement of HTS makes choosing endpoints a bal-

ance between the complexity of the measurable outcome (e.g. behavioural phenotype, changes in morphology or molecular composition), and the simplicity in detection and quantification (Rand, 2010). As automated animal screening is not always possible, identifying and quantifying endpoints usually depends on laborious observations and manual scoring (Evanko, 2006). *Drosophila* screens vary depending on the assay and the degree to which it can be mechanised (Pandey and Nichols, 2011). The higher throughput assay depends on the scoring of visible phenotypes, dead/alive, or a visible marker. One of the highest throughput quantitative strategies involves measuring the fluorescent markers in embryos by flow cytometry (Pulak, 2006). Viability or lethality in both larval and pupal stages has proven to be a very effective high-throughput endpoint in toxicology screening in *Drosophila* (Christie et al., 1985), together with measurement of fluorescent markers (e.g. green fluorescent protein [GFP]-tagged genes). Medium throughput endpoints which involve manual scoring techniques include observation of overt morphological development (Tögel et al., 2013), or indication of a rough eye phenotype (Pandey and Nichols, 2011). The latter techniques, despite being medium throughput endpoints are still able to screen thousands of drugs per week. Neurodegenerative disorders often result in locomotion or behavioural defects such as circadian activity, which produce quantifiable measures of neurodegeneration. Lower throughput behavioural assays, such as learning, memory and social interaction assays (including measuring aggression and courtship), require time to train the flies and produce a throughput of 25 to 50 drugs per week (Scott et al., 2002). Lower throughput assays are mostly used for validation of leads and target determination and include assays which require a more detailed analysis of the fly using biochemical techniques such as affinity chromatography coupled to mass spectrometry, microarray technologies, and genome-wide RNA interference (RNAi) screening or metaboprofiling studies (Sleno and Emili, 2008; Lindsay, 2003). The challenge that lies ahead with improving the screening process involves optimising the sensitivity of quantifiable endpoints for pathway-specific screening.

5 Considerations and Limitations

Whole-animal screening is a new and useful tool in the drug discovery processes. Despite this, animal models do come with their limitations. The profitability of an animal model of disease lies in its ability to manifest the relevant disease phenotype, together with the similarity of the underlying pathological changes, to human disease. Recent analyses point to the conservation of approximately 77 % of human disease genes in *Drosophila* (Reiter et al., 2001). Despite this, nearly all diseases are multifactorial and involve a variety of interactions from different genes and complexes, hence, the consequential ramifications is the failure of animal models to replicate the human disease gene network (Venter et al., 2001).

An additional limitation to keep in mind is the fact that *Drosophila* are surrounded by a thick cuticle that serves as a physical barrier to the penetration of molecules (Ségalat, 2007). Compounds penetrate through the animal's epidermis by both ingestion and diffusion (Kaletta and Hengartner, 2006). As a result, the concentration of a given compound within the animal is never accurately known and it varies, depending on the chemical properties of the compounds. Consequently, it is close to impossible to determine if a negative result is due to poor penetration, docking problems or a true absence of biological activity in the model; on the other hand, positive results can only be qualitatively interpreted (Ségalat, 2007). In an unbiased screen, the target is not known; since the treatment is delivered through the media, it is difficult to predict the range of doses which have to be tested. To avoid missing hits, a feasible approach may be to test compounds at several concentrations, starting with a high concentration and then retesting with lower ones (Giacomotto and Ségalat, 2010; Pandey and Nichols, 2011).

The anatomical and molecular differences between small model organisms and humans with respect to the metabolism of compounds, may result in the exclusion of a significant fraction of positive hits (Giacomotto and Ségalat, 2010). One such example is the anatomical differences between insects and vertebrates in relation to the blood brain barrier (BBB). The *Drosophila* humoral/central nervous system (CNS) is protected from the open circulatory system through a thin layer of glial-deprived epithelial cells (Stork et al., 2008). This makes the BBB in *Drosophila* much simpler than that of vertebrates, hence resulting in differences between humans and flies with regards to drug delivery to the brain tissues. The question, 'how well is the translation from fly to human?' still remains due to, pharmacokinetics and pharmacodynamics of small molecules as well as species-specific metabolic issues. Some drugs may be toxic in flies but not in human and vice versa. This can be due to a difference in metabolism of the drugs across species. In addition, the biochemical and physiological differences may lead to significant discrepancies in drug levels and tissue distribution profiles between mammal and fly (Pandey and Nichols, 2011). Despite this, the animal models are likely to reflect a comparative toxicity to mammals, which would substantiate future parallel studies in other invertebrate and vertebrate models (Rand, 2010).

Table 2: Throughput endpoints in *Drosophila melanogaster* models. (adapted from Pandey and Nichols (2011)).

High Throughput	Medium Throughput	Low Throughput	References
Lethality	Olfactory	Locomotor defect	(Pandey and Nichols, 2011)
Body Size	Overt morphological development	Body wall contraction	(Rand, 2010)
Necrotic Patches	Rough Eye Phenotype (Retinal degeneration)	Body wall muscle	(Pulak, 2006)
Viability	Negative Geotaxis Assay	Response to pain	(Christie et al., 1985)
Lethality	Circadian activity – sleep, arousal & rest behaviour	Phototaxis	(Tögel et al., 2013)
Visible & Fluorescent Markers	Body weight	Rotorod Test (Sleno and Emili, 2008)	
Flow cytometry	Fecundity	Electrophysiology	(Scott et al., 2002)
Visible phenotypes	Aggression	Prepulse inhibition	(Lindsay, 2003)
Lifespan Assay (dead/alive)	Wing expansion behaviour	Courtship behaviour	
Flight ability		Feeding behaviour	
Stress test		Learning and memory behaviour	
Anaesthesia Response		Seizure behaviour	
		Visual discrimination	
		Social interaction assay	
		Aggressive behaviour	
		Biochemical techniques (i.e. affinity chromatography, mass spectrometry, micro-arrays genome wide RNAi screening & metaboprofiling)	

When using *Drosophila* to model neurodegenerative diseases that are common in old age, several challenges can be encountered. Despite the fact that *Drosophila* is readily used to address questions about tissue-specific functional decline and genetic perturbations on ageing, the techniques used including lifespan and locomotor analysis can also be fraught with pitfalls if not carefully applied (He and Jasper, 2014). Some of the suggestions to keep in mind when modelling ageing in *Drosophila* include: careful control of genetic backgrounds due to the heterosis effect, which generally results in a longer lifespan in outcrossed animals; proper maintenance of source cultures with defined larval densities to avoid infection; synchronised populations with controlled mating status in order to have same-aged flies; gender differences which account for asymmetric inheritance of mitochondrial genomes, hormonal and metabolic differences, and maternal effects (Tower and Arbeitman, 2009); diet consisting of a standardized amount of yeast and hydration in food (Ja et al., 2009); control of temperature, humidity and circadian light exposure, which can all have an effect on the ageing process in the flies (He and Jasper, 2014).

6 Conclusion

Animal models are increasingly being incorporated into drug discovery screens. Due to their small size, they provide a more efficient alternative to *in vitro* screens as they fulfil the requirements of large-scale screens, whilst providing a system in which the physiological context is preserved. Despite this, *Drosophila* models have some limitations when it comes to HTS and therefore, they are only fully exploited when they are integrated in a mixed approach for drug discovery. For example, a combination of unbiased enhancer/suppressor screens (used to identify the novel targets), together with subsequent validation using candidate genetic or pharmacological tools, has been previously used in AD *Drosophila* models (Cao et al., 2008). Another example is the use of pharmacological agents in order to identify suspected cellular processes affected by the administered compounds, followed by genetic validation of the candidate players (Mudher et al., 2004; Pallos et al., 2008). In conclusion, *Drosophila* models of neurodegeneration hold a lot of promise as they provide not only a way of modelling the disease mechanism at a subcellular level, but they also allow for the study of pathological mechanisms through behavioural consequences. This information can be easily used for the design of disease-modifying therapeutic drug discovery that can be potentially applied to treat human conditions. Furthermore, the integration of *Drosophila* models in the drug discovery process allows for the selection of potential therapeutic models with an improved safety profile earlier in the drug discovery process, resulting in less funds and time being wasted on false positive hits. All in all, the future should see the incorporation of *Drosophila* in drug discovery strategies increasing drastically, especially within the areas of neurodegenerative diseases.

Acknowledgements

Drug discovery research at the Department of Physiology and Biochemistry of the University of Malta, is supported by the Malta Council for Science & Technology through the National Research & Innovation Programme 2012 (R&I-2012-066).

References

Adams, M. D., Celniker, S. E., Holt, R. A., Evans, C. A., Gocayne, J. D., et al. (2000). The genome sequence of Drosophila melanogaster. *Science.* 287(5461), 2185–95.

Apostol, B. L., Kazantsev, A., Raffioni, S., Illes, K., Pallos, J., et al. (2003). A cell-based assay for aggregation inhibitors as therapeutics of polyglutamine-repeat disease and validation in Drosophila. *Proc. Natl. Acad. Sci. U. S. A.* 100(10), 5950–5.

Bilen, J. and Bonini, N. M. (2005). Drosophila as a model for human neurodegenerative disease. *Annu. Rev. Genet.* 39, 153–171.

Bleicher, K. H., Böhm, H.-J., Müller, K. and Alanine, A. I. (2003). Hit and lead generation: beyond high-throughput screening. *Nat Rev Drug Discov.* 2(5), 369–378.

Cao, W., Song, H.-J., Gangi, T., Kelkar, A., Antani, I., et al. (2008). Identification of novel genes that modify phenotypes induced by Alzheimer's beta-amyloid overexpression in Drosophila. *Genetics.* 178(3), 1457–1471.

Cauchi, R. J. and van den Heuvel, M. (2006). The fly as a model for neurodegenerative diseases: is it worth the jump? *Neurodegener Dis.* 3(6), 338–356.

Chen, L. and Feany, M. B. (2005). Alpha-synuclein phosphorylation controls neurotoxicity and inclusion formation in a Drosophila model of Parkinson disease. *Nat. Neurosci.* 8(5), 657–663.

Chopra, V., Fox, J. H., Lieberman, G., Dorsey, K., Matson, W., et al. (2007). A small-molecule therapeutic lead for Huntington's disease: preclinical pharmacology and efficacy of C2-8 in the R6/2 transgenic mouse. *Proc. Natl. Acad. Sci. U.S.A.* 104(42), 16685–16689.

Christie, N. T., Williams, M. W. and Jacobson, K. B. (1985). Genetic and physiological parameters associated with cadmium toxicity in Drosophila melanogaster. *Biochem. Genet.* 23(7-8), 571–583.

Conway, K. A., Lee, S. J., Rochet, J. C., Ding, T. T., Williamson, R. E. and Lansbury, P. T. (2000). Acceleration of oligomerization, not fibrillization, is a shared property of both alpha-synuclein mutations linked to early-onset Parkinson's disease: implications for pathogenesis and therapy. *Proc. Natl. Acad. Sci. U.S.A.* 97(2), 571–576.

Cowan, C. M., Chee, F., Shepherd, D. and Mudher, A. (2010). Disruption of neuronal function by soluble hyperphosphorylated tau in a Drosophila model of tauopathy. *Biochem. Soc. Trans.* 38(2), 564–570.

Crowther, D. C., Page, R., Chandraratna, D. and Lomas, D. A. (2006). A Drosophila model of Alzheimer's disease. *Meth. Enzym.* 412, 234–255.

Cui, L., Jeong, H., Borovecki, F., Parkhurst, C. N., Tanese, N. and Krainc, D. (2006). Transcriptional repression of PGC-1alpha by mutant huntingtin leads to mitochondrial dysfunction and neurodegeneration. *Cell.* 127(1), 59–69.

Dimitrijevic, N., Dzitoyeva, S. and Manev, H. (2004). An automated assay of the behavioral effects of cocaine injections in adult Drosophila. *J. Neurosci. Meth.* 137(2), 181–184.

Duffy, J. B. (2002). GAL4 system in Drosophila: a fly geneticist's Swiss army knife. *Genesis.* 34(1-2), 1–15.

Dzitoyeva, S., Dimitrijevic, N. and Manev, H. (2003). Gamma-aminobutyric acid B receptor 1 mediates behavior-impairing actions of alcohol in Drosophila: adult RNA interference and pharmacological evidence. *Proc. Natl. Acad. Sci. U.S.A.* 100(9), 5485–5490.

Evanko, D. (2006). In praise of manual high-throughput screening. *Nat. Methods.* 3(9), 662–663.

Feany, M. B. and Bender, W. W. (2000). A Drosophila model of Parkinson's disease. *Nature.* 404(6776), 394–398.

Finelli, A., Kelkar, A., Song, H.-J., Yang, H. and Konsolaki, M. (2004). A model for studying Alzheimer's Abeta42-induced toxicity in Drosophila melanogaster. *Mol. Cell. Neurosci.* 26(3), 365–375.

Fujikake, N., Nagai, Y., Popiel, H. A., Okamoto, Y., Yamaguchi, M. and Toda, T. (2008). Heat shock transcription factor 1-activating compounds suppress polyglutamine-induced neurodegeneration through induction of multiple molecular chaperones. *J. Biol. Chem.* 283(38), 26188–26197.

Giacomotto, J. and Ségalat, L. (2010). High-throughput screening and small animal models, where are we? *Br. J. Pharmacol.* 160(2), 204–16.

Greenbaum, E. A., Graves, C. L., Mishizen-Eberz, A. J., Lupoli, M. A., Lynch, D. R., et al. (2005). The E46K mutation in alpha-synuclein increases amyloid fibril formation. *J. Biol. Chem.* 280(9), 7800–7807.

He, Y. and Jasper, H. (2014). Studying aging in Drosophila. *Methods.* 68(1), 129–133.

Heiser, V., Engemann, S., Bröcker, W., Dunkel, I., Boeddrich, A., et al. (2002). Identification of benzothiazoles as potential polyglutamine aggregation in-

hibitors of Huntington's disease by using an automated filter retardation assay. *Proc. Natl. Acad. Sci. U.S.A.* 99 Suppl 4, 16400–16406.

Henchcliffe, C., Dodel, R. and Beal, M. F. (2011). Biomarkers of Parkinson's disease and Dementia with Lewy bodies. *Prog. Neurobiol.* 95(4), 601–613.

Hirth, F. (2010). Drosophila melanogaster in the Study of Human Neurodegeneration. *CNS Neurol. Disord. - Drug Targets.* 9(4), 504–523.

Hockly, E., Tse, J., Barker, A. L., Moolman, D. L., Beunard, J.-L., et al. (2006). Evaluation of the benzothiazole aggregation inhibitors riluzole and PGL-135 as therapeutics for Huntington's disease. *Neurobiol. Dis.* 21(1), 228–236.

Hsiao, K., Chapman, P., Nilsen, S., Eckman, C., Harigaya, Y., et al. (1996). Correlative memory deficits, Abeta elevation, and amyloid plaques in transgenic mice. *Science (80-.).* 274(5284), 99–102.

Iijima, K., Liu, H.-P., Chiang, A.-S., Hearn, S. A., Konsolaki, M. and Zhong, Y. (2004). Dissecting the pathological effects of human Abeta40 and Abeta42 in Drosophila: a potential model for Alzheimer's disease. *Proc. Natl. Acad. Sci. U.S.A.* 101(17), 6623–6628.

Ja, W. W., Carvalho, G. B., Zid, B. M., Mak, E. M., Brummel, T. and Benzer, S. (2009). Water- and nutrient-dependent effects of dietary restriction on Drosophila lifespan. *Proc. Natl. Acad. Sci. U.S.A.* 106(44), 18633–18637.

Kaletta, T. and Hengartner, M. O. (2006). Finding function in novel targets: C. elegans as a model organism. *Nat Rev Drug Discov.* 5(5), 387–398.

Konsolaki, M. (2013). Fruitful research: drug target discovery for neurodegenerative diseases in Drosophila. *Expert Opin Drug Discov.* 8(12), 1503–1513.

Lashuel, H. A. and Lansbury, P. T. (2006). Are amyloid diseases caused by protein aggregates that mimic bacterial pore-forming toxins? *Q. Rev. Biophys.* 39(2), 167–201.

Lenz, S., Karsten, P., Schulz, J. B. and Voigt, A. (2013). Drosophila as a screening tool to study human neurodegenerative diseases. *J. Neurochem.* 127(4), 453–460.

Lieschke, G. J. and Currie, P. D. (2007). Animal models of human disease: zebrafish swim into view. *Nat. Rev. Genet.* 8(5), 353–367.

Lindsay, M. A. (2003). Target discovery. *Nat. Rev. Drug Discov.* 2(10), 831–8.

McGuire, S. E., Roman, G. and Davis, R. L. (2004). Gene expression systems in Drosophila: a synthesis of time and space. *Trends Genet.* 20(8), 384–391.

Moore, M. S., DeZazzo, J., Luk, A. Y., Tully, T., Singh, C. M. and Heberlein, U. (1998). Ethanol intoxication in Drosophila: Genetic and pharmacological evidence for regulation by the cAMP signaling pathway. *Cell.* 93(6), 997–1007.

Mudher, A., Shepherd, D., Newman, T. A., Mildren, P., Jukes, J. P., et al. (2004). GSK-3beta inhibition reverses axonal transport defects and behavioural phenotypes in Drosophila. *Mol. Psychiatry.* 9(5), 522–530.

Muqit, M. M. K. and Feany, M. B. (2002). Modelling neurodegenerative diseases in Drosophila: a fruitful approach? *Nat. Rev. Neurosci.* 3(3), 237–43.

Newman, T., Sinadinos, C., Johnston, A., Sealey, M. and Mudher, A. (2011). Using Drosophila models of neurodegenerative diseases for drug discovery. *Expert Opin Drug Discov.* 6(2), 129–140.

Nichols, C. D., Ronesi, J., Pratt, W. and Sanders-Bush, E. (2002). Hallucinogens and Drosophila: linking serotonin receptor activation to behavior. *Neuroscience.* 115(3), 979–984.

Pallos, J., Bodai, L., Lukacsovich, T., Purcell, J. M., Steffan, J. S., et al. (2008). Inhibition of specific HDACs and sirtuins suppresses pathogenesis in a Drosophila model of Huntington's disease. *Hum. Mol. Genet.* 17(23), 3767–3775.

Pandey, U. B. and Nichols, C. D. (2011). Human disease models in Drosophila melanogaster and the role of the fly in therapeutic drug discovery. *Pharmacol. Rev.* 63(2), 411–436.

Parr, J., Large, A., Wang, X., Fowler, S. C., Ratzlaff, K. L. and Ruden, D. M. (2001). The inebriactometer: a device for measuring the locomotor activity of Drosophila exposed to ethanol vapor. *J. Neurosci. Methods.* 107(1-2), 93–99.

Peng, C., Chan, H. Y. E., Li, Y. M., Huang, Y. and Chen, Z. Y. (2009). Black tea theaflavins extend the lifespan of fruit flies. *Exp. Gerontol.* 44(12), 773–783.

Puglielli, L., Tanzi, R. E. and Kovacs, D. M. (2003). Alzheimer's disease: the cholesterol connection. *Nat. Neurosci.* 6(4), 345–351.

Pulak, R. (2006). Techniques for analysis, sorting, and dispensing of C. elegans on the COPAS flow-sorting system. *Methods Mol. Biol.* 351, 275–286.

Rand, M. D. (2010). Drosophotoxicology: the growing potential for Drosophila in neurotoxicology. *Neurotoxicol Teratol.* 32(1), 74–83.

Reiter, L. T., Potocki, L., Chien, S., Gribskov, M. and Bier, E. (2001). A systematic analysis of human disease-associated gene sequences in Drosophila melanogaster. *Genome Res.* 11(6), 1114–1125.

Rubin, G. M. and Lewis, E. B. (2000). A brief history of Drosophila's contributions to genome research. *Science.* 287(5461), 2216–2218.

Sarkar, S., Krishna, G., Imarisio, S., Saiki, S., O'Kane, C. J. and Rubinsztein, D. C. (2008). A rational mechanism for combination treatment of Huntington's disease using lithium and rapamycin. *Hum. Mol. Genet.* 17(2), 170–178.

Scott, R., Bourtchuladze, R., Gossweiler, S., Dubnau, J. and Tully, T. (2002). CREB and the discovery of cognitive enhancers. *J. Mol. Neurosci.* 19(1-2), 171–177.

Ségalat, L. (2007). Invertebrate animal models of diseases as screening tools in drug discovery. *ACS Chem. Biol.* 2(4), 231–6.

Sleno, L. and Emili, A. (2008). Proteomic methods for drug target discovery. *Curr Opin Chem Biol.* 12(1), 46–54.

Sofola, O., Kerr, F., Rogers, I., Killick, R., Augustin, H., et al. (2010). Inhibition of GSK-3 ameliorates Abeta pathology in an adult-onset Drosophila model of Alzheimer's disease. *PLoS Genet.* 6(9), e1001087.

Spada, A. R. L. and Taylor, J. P. (2010). Repeat expansion disease: progress and puzzles in disease pathogenesis. *Nat. Rev. Genet.* 11(4), 247–258.

Spillantini, M. G., Crowther, R. A., Jakes, R., Hasegawa, M. and Goedert, M. (1998). alpha-Synuclein in filamentous inclusions of Lewy bodies from Parkinson's disease and dementia with lewy bodies. *Proc. Natl. Acad. Sci. U.S.A.* 95(11), 6469–6473.

Spring, D. R. (2005). Chemical genetics to chemical genomics: small molecules offer big insights. *Chem Soc Rev.* 34(6), 472–482.

Steffan, J. S. and Thompson, L. M. (2003). Targeting aggregation in the development of therapeutics for the treatment of Huntington's disease and other polyglutamine repeat diseases. *Expert Opin. Ther. Targets.* 7(2), 201–213.

Stork, T., Engelen, D., Krudewig, A., Silies, M., Bainton, R. J. and Klämbt, C. (2008). Organization and function of the blood-brain barrier in Drosophila. *J. Neurosci.* 28(3), 587–597.

Taylor, J. P., Hardy, J. and Fischbeck, K. H. (2002). Toxic proteins in neurodegenerative disease. *Science.* 296(5575), 1991–1995.

Tögel, M., Pass, G. and Paululat, A. (2013). In vivo imaging of Drosophila wing heart development during pupal stages. *Int. J. Dev. Biol.* 57(1), 13–24.

Torres, G. and Horowitz, J. M. (1998). Activating properties of cocaine and cocaethylene in a behavioral preparation of Drosophila melanogaster. *Synapse.* 29(2), 148–161.

Tower, J. and Arbeitman, M. (2009). The genetics of gender and life span. *J. Biol.* 8(4), 38.

Truman, J. W. and Bate, M. (1988). Spatial and temporal patterns of neurogenesis in the central nervous system of Drosophila melanogaster. *Dev. Biol.* 125(1), 145–157.

Venter, J. C., Adams, M. D., Myers, E. W., Li, P. W., Mural, R. J., et al. (2001). The sequence of the human genome. *Science.* 291(5507), 1304–1351.

Volles, M. J. and Lansbury, P. T. (2007). Relationships between the sequence of alpha-synuclein and its membrane affinity, fibrillization propensity, and yeast toxicity. *J. Mol. Biol.* 366(5), 1510–1522.

Vonsattel, J. P. and DiFiglia, M. (1998). Huntington Disease. *J. Neuropathol. Exp. Neurol.* 57(5).

Williams, D. W. and Truman, J. W. (2004). Mechanisms of dendritic elaboration of sensory neurons in Drosophila: insights from in vivo time lapse. *J. Neurosci.* 24(7), 1541–1550.

Wong, R., Piper, M. D. W., Wertheim, B. and Partridge, L. (2009). Quantification of food intake in Drosophila. *PLoS One.* 4(6), e6063.

Zappe, S., Fish, M., Scott, M. P. and Solgaard, O. (2006). Automated MEMS-based Drosophila embryo injection system for high-throughput RNAi screens. *Lab Chip.* 6(8), 1012–1019.

Zhang, X., Smith, D. L., Meriin, A. B., Engemann, S., Russel, D. E., et al. (2005). A potent small molecule inhibits polyglutamine aggregation in Huntington's disease neurons and suppresses neurodegeneration in vivo. *Proc. Natl. Acad. Sci. U.S.A.* 102(3), 892–897.

Xjenza Online - Journal of The Malta Chamber of Scientists
www.xjenza.org
DOI: 10.7423/XJENZA.2014.2.12

Research Article

Select polyphenols protect mitochondria against amyloid aggregates in Alzheimer and Parkinson diseases

Mario Caruana[1] **& Neville Vassallo**[1]
[1]Dept. of Physiology & Biochemistry, University of Malta, Msida, Malta

Abstract. Alzheimer and Parkinson diseases are age-related neurodegenerative disorders in which formation of amyloid aggregates by amyloid-beta (Abeta) and α-synuclein (αS) proteins, respectively, are recognised critical events that occur early in the disease process. These aggregates cause disruption of mitochondrial function in neurons, initiating a pathophysiological cascade leading to bio-energetic collapse and ultimately neuronal cell death. The detailed mechanisms are, however, largely unknown. In vitro studies in our laboratory aimed to, (i) investigate destabilisation of mitochondrial phospholipid membranes by these amyloid aggregates and, (ii) explore the protective effect of select polyphenolic compounds on mitochondria. Exposure of mitochondria, isolated from human neuroblastoma SH-SY5Y cells, to amyloid aggregates induced a strong and dose-dependent release of cytochrome *c*, reflecting damage to the outer and/or inner mitochondrial membranes. Importantly, targeting of aggregates to mitochondria was shown to be dependent upon cardiolipin, a mitochondria-specific phospholipid known to play a critical role in launching apoptosis. Moreover, the ability of amyloid aggregates to damage mitochondrial membranes was confirmed using a liposome permeabilisation assay. Finally, we found that the polyphenol compounds morin, rosmarinic acid, epigallocatechingallate and black tea extract were potent mito-protectants, and may thus delay the onset of neurodegenerative diseases.

Keywords Alzheimer's disease – Parkinson's disease – amyloid-beta – α-synuclein – mitochondrial membrane – permeabilisation – cardiolipin – polyphenols.

1 Introduction

Alzheimer's disease (AD) and Parkinson's disease (PD) are incurable neurodegenerative disorders that are generally prevalent in the elderly population. Epidemiological studies in humans, as well as molecular studies in toxin-induced and genetic animal models of AD and PD show that mitochondrial dysfunction is a defect occurring early in the pathogenesis of both diseases (Büeler, 2009). Mounting evidence indicates that mitochondrial abnormalities triggered by small, soluble prefibrillar aggregates (termed oligomers) are early occurrences, preceding neurological pathology and clinical symptoms characteristic of both AD and PD. Perforation of mitochondrial membranes leads to the release of pro-apoptotic proteins such as cytochrome c (Cyto *c*) into the cellular cytosol, triggering neuronal apoptosis (Lin et al., 2009). In addition, epidemiological studies have associated nutrition components, such as polyphenols, to lower incidence of such neurodegenerative diseases, though the molecular basis for their protective effect is not known (de Lau and Breteler, 2006).

The aim of this paper is to describe *in vitro* studies that have been carried out in our laboratory which determine: (i) the effects of specific amyloid-beta (Abeta) and α-synuclein (αS) oligomeric aggregates on synthetic and cellular mitochondrial membranes, and (ii) identify mitochondrial-protective polyphenolic compounds. The first part of the report provides a background on the pathophysiological effects of such oligomeric proteins on mitochondria, followed by a brief description of the accomplished experiments.

Correspondence to: Neville Vassallo (neville.vassallo@um.edu.mt)

© 2014 Xjenza Online

2 An overview of mitochondrial dysfunction in AD and PD

Mitochondria are organelles enclosed by a double membrane and are essential for cell viability. They are partitioned into four main compartments: the outer mitochondrial membrane (OMM), inter-membrane space (IMS), inner mitochondrial membrane (IMM) and matrix (Bogaerts et al., 2008). These organelles possess important functions within the cell, such as generation of adenosine triphosphate (ATP) during oxidative phosphorylation (Hausmann et al., 2008), homeostatic control of cytosolic calcium and iron concentration (Feissner et al., 2009), iron-sulfur (Fe/S) cluster and heme biogenesis (Lill and Mühlenhoff, 2005; Rouault and Tong, 2005) and also contribute to programmed cell death (Garrido and Kroemer, 2004). The critical role of a mitochondrial-specific phospholipid, cardiolipin (CL) in the apoptotic process has been extensively reported (Bradley et al., 2011; Korytowski et al., 2011). Cardiolipin is essentially an IMM phospholipid, since it is only present in minute quantities in the OMM, possibly through inner-to-outer mitochondrial membrane contact sites (de Kroon et al., 1997; Gonzalvez and Gottlieb, 2007). This phospholipid is critical for the optimal function of numerous enzymes that are involved in mitochondrial energy metabolism. Moreover, the formation of OMM openings required for the release of pro-apoptotic proteins such as Cyto *c* into the cytosol, was dependent on the presence of CL (Kuwana et al., 2002). While it is clear that some type of opening develops in the OMM during death signalling to allow exit of apoptogenic proteins from the IMS, the molecular nature and regulation of this pore remain unclear (Smith et al., 2005; Cheng et al., 2010).

2.1 Parkinson's disease

PD is distinguished from other forms of parkinsonism by the presence of Lewy bodies (LBs) and Lewy neurites (LNs), which are juxtanuclear and neuritic ubiquitinated protein aggregates composed predominantly of the synaptic protein αS (Shults, 2006). Cumulative evidence now suggests that the abnormal aggregation of this neuronal protein is critically involved in the pathogenesis of PD. The presence of mitochondrial dysfunction is noteworthy given the evidence already implicating mitochondrial toxins in the pathogenesis of PD (Camilleri and Vassallo, 2014). Sporadic forms of PD are attributed to environmental contaminants; substances like rotenone and 1-methyl-4-phenyl-1,2,3,6-tetrahydropyridine (MPTP) inhibit complex I and also promote Cyto *c* release from the IMS (Perier et al., 2005; Banerjee et al., 2010). αS has been shown to interfere at various intracellular sites, including vesicle membranes (Iwai et al., 1995), mitochondria (Hsu et al., 2000), the cell death pathway (da Costa et al., 2006), the proteasome (Tanaka et al., 2001), and the Golgi apparatus (Gosavi et al., 2002). Although subcellular αS is largely cytosolic, a fraction of it was shown to be present in, or associated with, mitochondria (Nakamura et al., 2008). Devi and colleagues demonstrated import of αS into mitochondria and there it is shown to be predominantly associated with the IMM. This membrane association is due to the presence of a mitochondrial targeting signal and is dependent upon mitochondrial membrane potential, ATP levels and the oxidation of mitochondrial proteins (Devi et al., 2008; Parihar et al., 2008). Of interest is the fact that subcellular distribution of αS was found to be uneven between different brain regions, with higher levels of mitochondrial αS in the hippocampus, striatum and substantia nigra (Zhang et al., 2008).

A number of experimental studies suggest that αS may be closely linked to mitochondrial dysfunction and oxidative stress. An increase in the amount of αS binding with mitochondria was shown to be due to over-expression of αS in cell cultures (Shavali et al., 2008; Cole et al., 2008). Studies in yeast cells have demonstrated that abrogation of mitochondrial DNA prevented αS-induced reactive oxygen species (ROS) formation and apoptosis, implying that mitochondria are necessary in mediating the toxicity of αS (Büttner et al., 2008). Moreover, over-expression of A53T mutant αS was shown to induce Cyto *c* release and activation of downstream caspases in rat PC12 cells, resulting in apoptosis (Smith et al., 2005). Furthermore, association of αS to mitochondria in cells was also related to oxidation of mitochondrial proteins and elevated levels of calcium and nitric oxide (Parihar et al., 2008). The amount of αS associated with mitochondria seems to correlate with mitochondrial dysfunction.

Mitochondrial defects were also observed in numerous transgenic mouse models over-expressing wild-type (WT) or mutant αS. Some examples comprise selective oxidation of metabolic proteins related to mitochondria (Poon et al., 2005), evidence of mitochondrial pathology after treatment with MPTP (Song et al., 2004), deterioration of mitochondria containing αS including decreased complex IV activity and mitochondrial DNA damage (Martin et al., 2006). Worthy of note is the fact that some of the reported mitochondrial alterations due to expression of WT or A53T αS in mice were observed early in the disease process (Abou-Sleiman et al., 2006). These animal models suggest that αS may have a physiological role in mitochondria, and that the mitochondrial defects may be the result of a toxic gain-of-function due to over-expressed or mutated αS present in mitochondria (Büeler, 2009). In contrast, mice lacking αS expression also show mitochondrial dysfunction that is

manifested by altered plasma membrane lipid composition and reduced performance of the electron transport mitochondrial complex I and III activity (Ellis et al., 2005). As both the lack and overexpression of αS have adverse effects on neuronal mitochondria, the physiological equilibrium seems to be of pivotal importance.

2.2 Alzheimer's disease

AD is characterised by neuronal degeneration in the presence of extracellular plaque deposits of Abeta peptides in specific brain regions and intraneuronal, neurofibrillary tangles (NFTs) related to the hyperphosphorylation of the Tau protein in affected neurons (Murphy and LeVine, 2010). Mitochondria may be a common early target of both Abeta and Tau in AD. Gotz and coworkers reported an independent and synergistic action of both peptides on mitochondria leading to bioenergetic defects and increased oxidative stress in a triple transgenic mouse model exhibiting both pathological features of the disease (Eckert et al., 2010). The progressive mitochondrial accumulation of Abeta has been observed in the AD brain. Image analysis revealed accumulation of Abeta in 40 % and 70 % of mitochondria in the temporal lobe and hippocampus respectively, compared to 5 % and 14 % in non-AD brains (Chen and Yan, 2010). Abnormal mitochondrial gene expression, mitochondrial accumulation of Abeta and Abeta–dependent mitochondrial dysfunction were detected in AD transgenic mice from as early as 2-4 months of age, before the occurrence of cognitive difficulties (Reddy et al., 2004; Hauptmann et al., 2009; Du et al., 2010). In addition, mitochondrial dysfunction was observed to occur regardless of the genetic mutation involved, and lead to specific metabolic changes which could be used as biomarkers for the early diagnosis of AD (Trushina et al., 2012). These findings highlight the early and important involvement of mitochondria in the disease. Abeta-induced mito-toxicity is associated with decreased ATP production (Blass et al., 2002), increased ROS levels and oxidative stress (Rodrigues et al., 2001; Felice et al., 2007), disturbances of Ca^{2+} homeostasis (Sanz-Blasco et al., 2008), and destabilisation of mitochondrial membranes, amongst others. Nevertheless, the exact pathway and sequence through which these events occur remains unclear (Canevari et al., 2004).

To summarise, evidence suggests that mitochondrial dysfunction and intrinsic mitochondrial-mediated apoptosis play a key role in molecular cell death pathways of AD and PD (Northington et al., 2005; Martin, 2010). Several mechanisms of Abeta and αS-induced neurotoxicity have been proposed. Loss of normal cellular homeostasis and damage to cellular organelles such as mitochondria may indicate a unifying toxic cause: membrane permeation. Research reports support the hypothesis that Abeta and αS oligomers share a common mechanism of toxicity. Indeed, a common conformation unique to soluble oligomers has been identified (Glabe and Kayed, 2006), which specifically lead to permeabilisation of lipid bilayers regardless of protein sequence (Kayed et al., 2004). The importance of oligomer-induced mitochondrial impairments lies with their early and direct involvement in the pathogenesis of PD and AD (Cha et al., 2012; Trushina et al., 2012). Thus, drugs or natural compounds with the potential to adjust mitochondrial dynamics, function and biogenesis may help in attenuating the onset of both AD and PD.

3 Polyphenols as mito-protectants in vitro

Substantial evidence from the reviewed literature suggests that mitochondria are one of the main intracellular compartments linking the processes between the aggregation of Abeta and αS and final dopaminergic neuronal degeneration. Several natural polyphenolic compounds have been demonstrated to specifically and efficiently hinder the aggregation process of αS (Caruana et al., 2011). In our lab, we have also demonstrated the inhibitory effect of selected polyphenols and extracts on membrane damage, induced by αS and Abeta oligomers (Gauci et al., 2011; Caruana et al., 2012). On the basis of these results, we have extended our studies to investigate the destabilisation of synthetic and isolated mitochondrial phospholipid membranes by amyloid aggregates. The ultimate goal here was to establish whether mitochondrial membranes could be protected against amyloid-induced dysfunction by these promising groups of bioactive small-molecule compounds and extracts.

3.1 Amyloid aggregate-induced mito-toxicity

The first part of the study investigated the direct toxicity of Abeta and WT/mutant αS (A53T, A30P) aggregates on synthetic mitochondrial membranes. Liposome systems mimicking mitochondrial membranes have been used successfully in ascertaining the membrane permeabilising abilities of amyloid proteins (Epand et al., 2002; Kuwana et al., 2002; van Meer et al., 2008; Williams et al., 2010). The four types of synthetic lipid vesicle membranes used here mimic mitochondrial outer and inner membrane composition, as well as that of the neuronal plasma membrane for comparison (Table 1).

Assessment of vesicle permeabilisation by aggregated Abeta and WT/mutant αS was performed using fluorescence-based methods on such mitochondrial-like model systems. Essentially, the amyloid proteins were able to directly perforate the artificial mitochondrial membranes. We further noted that this effect was highly

Table 1: Phospholipid composition of IM-, OM- and L-type liposome membranes. OM-type liposomes - characteristic of mitochondrial membranes; IM-type liposomes - characteristicof inner mitochondrial membranes; L-type liposomes - characteristic of mitochondrial membranes but lacking cardiolipin.

Phospholipid	% composition		
	IM-type	OM-type	L-type
L-α-phosphatidylcholine (PC)	38	46.5	50.1
L-α-phosphatidylethanolamine (PE)	24	28.4	30.6
L-α-phosphatidylinositol (PI)	16	8.9	9.6
L-α-phosphatidylserine (PS)	4	8.9	9.6
Cardiolipin (CL)	18	7.3	-

dependent upon the presence of specific low-molecular-weight oligomeric species. In a further series of liposomal studies we discovered that mitochondria-specific lipid CL particularly enhanced permeabilisation by αS and Abeta (Chicco and Sparagna, 2007; Cole et al., 2008; Camilleri et al., 2013). Therefore it can be inferred from our experiments that IM-type membranes (rich in CL) are especially susceptible to Abeta and αS toxicity. Indeed, IM-membranes contain twice as much CL as OM-liposomes, whilst L-type liposomes (which lack CL) were the least damaged by the protein aggregates. Accordingly, it was suggested that mitochondria-localised αS is predominantly associated with the inner membrane in dopaminergic neuronal cell cultures and PD brains (Devi and Anandatheerthavarada, 2010). This supports recent data stating that oligomeric αS target disruption of lipid vesicles having negatively charged membranes and that CL is essential for the interaction between WT and A30P αS with large unilamellar vesicles whose composition is similar to that of the IMM (van Rooijen et al., 2009; Zigoneanu et al., 2012). In addition, it was reported that CL was the phospholipid found to most strongly stimulate Abeta aggregation (CL > PI > PS > PC = PE) (Chauhan et al., 2000) and that affinity of αS to CL possibly drives mitochondrial fission by αS oligomers, but not monomers (Nakamura et al., 2011). It is thus highly plausible that exclusive properties of the mitochondria-specific CL (see review by Szeto, 2014) provide a platform for rapid and enhanced membrane destabilisation by amyloid aggregates. These results indicate a pivotal pathway of neuronal apoptosis induction and intriguingly suggest a common toxic mechanism for the three aggregation-prone peptides.

An important endeavour of the study was to extrapolate the findings from the liposome permeabilisation assays to the membranes of respiring mitochondria isolated from a neuronal cell line. Interaction of aggregated Abeta and αS with the mitochondrial membrane lead to its disruption and release of the respiratory protein Cyto *c*, hence initiating mitochondrial-driven cell death pathways in neurons. For this purpose, a protocol was first established for isolation of fresh intact mitochondria from the SH-SY5Y human neuronal cell line. Subsequently, the isolated mitochondria were exposed to the proteins in question in order to determine whether this would damage the outer and/or inner mitochondrial membranes, specifically by inducing Cyto *c* release (CCR) from IMS. This was determined by means of a quantitative enzyme-linked immunosorbent assay. We reported that aggregated, but not monomeric, Abeta and WT/mutant αS disrupted the mitochondrial membrane leading to CCR. Taken together, the various *in vitro* neuronal models may indicate that amyloid misfolding is naturally paralleled to mitochondrial apoptosis and may contribute to neurodegeneration.

3.2 Polyphenols inhibit cytochrome *c* release from mitochondria

Polyphenolic compounds are naturally-present constituents of a wide variety of fruits, vegetables, food products and beverages derived from plants such as olive oil, tea, and red wine (Stevenson and Hurst, 2007). They are characterised by a polyphenol structure (Figure 1), which generally consists of two aromatic rings (2-phenyl-1,4-benzopyrone), each containing at least one hydroxyl group, which are connected via a three-carbon bridge and become part of a six-member heterocyclic ring (Beecher, 2003; Porat et al., 2006; D'Archivio et al., 2007). In the current literature, very few studies have to date examined the protective effect of polyphenols on amyloid-induced mitochondrial dysfunction. For instance, the flavone baicalein reduced the MMP-lowering effect of (E34K) mutant αS in whole cells (Jiang et al., 2010) and grape fruit extract protected mitochondria in a Drosophila model of PD (Long et al., 2009). Thus, it was relevant to investigate whether small-molecule polyphenols are able to suppress CCR from the IMS and therefore act as mito-protectants.

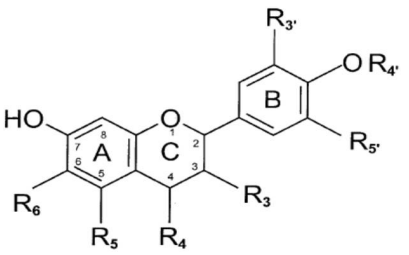

Figure 1: General structure and numbering pattern for common food polyphenols (adapted from (Beecher, 2003)). This figure shows the general structure and numbering pattern for common polyphenolic compounds. For most food flavonoids, R4′=H, R5=OH and R6=H. Individual flavonoids within each subclass are characterised by unique functional groups at R3, R3′, and R5′.

The relative efficacy of small-molecule compounds on preventing CCR from mitochondria was also determined by means of a quantitative enzyme-linked immunosorbent assay. The results demonstrated that the mitochondrial membrane can indeed be protected against αS/Abeta-induced disruption by a group of polyphenolic compounds, specifically by suppressing CCR. Seven polyphenolic compounds (apigenin, baicalein, epigallocatechin-gallate [ECGC], morin, nordihydroguaiaretic acid [NDGA] and rosmarinic acid [RA]) and black tea extract [BTE] were able to significantly limit CCR induced by aggregated WT/mutant αS and Abeta (Camilleri et al., 2013). It was encouraging to note that these compounds also featured as the top six compounds in the liposome permeabilisation assay. Hence, such experiments show that polyphenols constitute a major class of compounds that can indeed protect mitochondrial damage from αS and Abeta oligomeric assemblies at the membrane. Data emerging from our laboratory provides support to studies exploring the therapeutic potential of inhibitors of apoptosis proteins (IAPs) by raising the threshold of CCR required for commitment to apoptosis (Clayton et al., 2005).

4 Conclusion

It is increasingly evident that misfolded and aggregated disease proteins are not simply neuropathologic markers of neurodegenerative disorders but, instead, almost certainly contribute to disease pathogenesis. Our research was driven by the fact that formation of amyloid aggregates and mitochondria-induced apoptosis of neurons are critical events in the pathophysiology of these neurodegenerative diseases. Most importantly, mitochondrial dysfunction precedes neurological pathology and clinical symptoms characteristic of AD and PD.

Liposomal studies and CCR assays on isolated neuronal mitochondria in our laboratory clearly showed that specific proteins involved in AD and PD are able to permeate mitochondrial membranes and this ability is markedly dependent on aggregation conditions. Release of Cyto *c* suggests major disruption of mitochondrial membranes and is probably enough to induce neuronal apoptosis. An important finding underscored by liposomal studies is the prominent contribution of CL to both αS and Abeta-induced mitochondrial permeabilisation, accounting for the selective disruption of mitochondrial-like membranes as opposed to cellular-like membranes, and thus suggesting a common underlying mechanism of toxicity. Screening of a select group of small drug molecules and extract yielded potential mitoprotective agents with shared structural characteristics against toxicity induced by Abeta and αS aggregates. The *in vitro* assays performed in our studies are thus valid tools for the identification of potential therapeutic agents for subsequent *in vitro* analysis, hopefully arresting AD/PD at an early stage. In such debilitating maladies where no cure is available, increasing prevalence and high economic burden urgently necessitate disease-modifying treatment.

Acknowledgements

We are grateful to the Malta Council for Science and Technology (R&I-2008–068 and R&I-2012-06, to N.V.), the University of Malta (PHBRP06 and MDSIN08-21, to N.V) and the Malta Government Scholarship Scheme (to M.C.) for funding our research.

References

Abou-Sleiman, P. M., Muqit, M. M. K. and Wood, N. W. (2006). Expanding insights of mitochondrial dysfunction in Parkinson's disease. *Nat. Rev. Neurosci.* 7(3), 207–219.

Banerjee, K., Sinha, M., Pham, C. L. L., Jana, S., Chanda, D., et al. (2010). Alpha-synuclein induced membrane depolarization and loss of phosphorylation capacity of isolated rat brain mitochondria: implications in Parkinson's disease. *FEBS Lett.* 584(8), 1571–1576.

Beecher, G. R. (2003). Overview of dietary flavonoids: nomenclature, occurrence and intake. *J. Nutr.* 133(10), 3248S–3254S.

Blass, J. P., Gibson, G. E. and Hoyer, S. (2002). The role of the metabolic lesion in Alzheimer's disease. *J. Alzheimers Dis.* 4(3), 225–232.

Bogaerts, V., Theuns, J. and van Broeckhoven, C. (2008). Genetic findings in Parkinson's disease and translation into treatment: a leading role for mitochondria? *Genes Brain Behav.* 7(2), 129–151.

Bradley, J. M., Silkstone, G., Wilson, M. T., Cheesman, M. R. and Butt, J. N. (2011). Probing a complex of cytochrome c and cardiolipin by magnetic circular dichroism spectroscopy: implications for the initial

events in apoptosis. *J. Am. Chem. Soc.* 133(49), 19676–19679.

Büeler, H. (2009). Impaired mitochondrial dynamics and function in the pathogenesis of Parkinson's disease. *Exp. Neurol.* 218(2), 235–246.

Büttner, S., Bitto, A., Ring, J., Augsten, M., Zabrocki, P., et al. (2008). Functional mitochondria are required for alpha-synuclein toxicity in aging yeast. *J. Biol. Chem.* 283(12), 7554–7560.

Camilleri, A. and Vassallo, N. (2014). The centrality of mitochondria in the pathogenesis and treatment of Parkinson's disease. *CNS Neurosci Ther.* 20(7), 591–602.

Camilleri, A., Zarb, C., Caruana, M., Ostermeier, U., Ghio, S., et al. (2013). Mitochondrial membrane permeabilisation by amyloid aggregates and protection by polyphenols. *Biochim. Biophys. Acta.* 1828(11), 2532–2543.

Canevari, L., Abramov, A. Y. and Duchen, M. R. (2004). Toxicity of amyloid beta peptide: tales of calcium, mitochondria, and oxidative stress. *Neurochem. Res.* 29(3), 637–650.

Caruana, M., Högen, T., Levin, J., Hillmer, A., Giese, A. and Vassallo, N. (2011). Inhibition and disaggregation of α-synuclein oligomers by natural polyphenolic compounds. *FEBS Lett.* 585(8), 1113–1120.

Caruana, M., Neuner, J., Högen, T., Schmidt, F., Kamp, F., et al. (2012). Polyphenolic compounds are novel protective agents against lipid membrane damage by α-synuclein aggregates in vitro. *Biochim. Biophys. Acta.* 1818(11), 2502–2510.

Cha, M.-Y., Han, S.-H., Son, S. M., Hong, H.-S., Choi, Y.-J., et al. (2012). Mitochondria-specific accumulation of amyloid β induces mitochondrial dysfunction leading to apoptotic cell death. *PLoS ONE.* 7(4), e34929.

Chauhan, A., Ray, I. and Chauhan, V. P. (2000). Interaction of amyloid beta-protein with anionic phospholipids: possible involvement of Lys28 and C-terminus aliphatic amino acids. *Neurochem. Res.* 25(3), 423–429.

Chen, J. X. and Yan, S. S. (2010). Role of mitochondrial amyloid-beta in Alzheimer's disease. *J. Alzheimers Dis.* 20 Suppl 2, S569–78.

Cheng, A., Hou, Y. and Mattson, M. P. (2010). Mitochondria and neuroplasticity. *ASN neuro.* 2(5), e00045.

Chicco, A. J. and Sparagna, G. C. (2007). Role of cardiolipin alterations in mitochondrial dysfunction and disease. *Am. J. Physiol., Cell Physiol.* 292(1), C33–44.

Clayton, R., Clark, J. B. and Sharpe, M. (2005). Cytochrome c release from rat brain mitochondria is proportional to the mitochondrial functional deficit: implications for apoptosis and neurodegenerative disease. *J. Neurochem.* 92(4), 840–849.

Cole, N. B., Dieuliis, D., Leo, P., Mitchell, D. C. and Nussbaum, R. L. (2008). Mitochondrial translocation of alpha-synuclein is promoted by intracellular acidification. *Exp. Cell Res.* 314(10), 2076–2089.

da Costa, C. A., Dunys, J., Brau, F., Wilk, S., Cappai, R. and Checler, F. (2006). 6-Hydroxydopamine but not 1-methyl-4-phenylpyridinium abolishes alpha-synuclein anti-apoptotic phenotype by inhibiting its proteasomal degradation and by promoting its aggregation. *J. Biol. Chem.* 281(14), 9824–9831.

D'Archivio, M., Filesi, C., Benedetto, R. D., Gargiulo, R., Giovannini, C. and Masella, R. (2007). Polyphenols, dietary sources and bioavailability. *Ann. Ist. Super. Sanita.* 43(4), 348–361.

de Kroon, A. I., Dolis, D., Mayer, A., Lill, R. and de Kruijff, B. (1997). Phospholipid composition of highly purified mitochondrial outer membranes of rat liver and Neurospora crassa. Is cardiolipin present in the mitochondrial outer membrane? *Biochim. Biophys. Acta.* 1325(1), 108–116.

de Lau, L. M. L. and Breteler, M. M. B. (2006). Epidemiology of Parkinson's disease. *Lancet Neurol.* 5(6), 525–535.

Devi, L. and Anandatheerthavarada, H. K. (2010). Mitochondrial trafficking of APP and alpha synuclein: Relevance to mitochondrial dysfunction in Alzheimer's and Parkinson's diseases. *Biochim. Biophys. Acta.* 1802(1), 11–19.

Devi, L., Raghavendran, V., Prabhu, B. M., Avadhani, N. G. and Anandatheerthavarada, H. K. (2008). Mitochondrial import and accumulation of alpha-synuclein impair complex I in human dopaminergic neuronal cultures and Parkinson disease brain. *J. Biol. Chem.* 283(14), 9089–9100.

Du, H., Guo, L., Yan, S., Sosunov, A. A., McKhann, G. M. and Yan, S. S. (2010). Early deficits in synaptic mitochondria in an Alzheimer's disease mouse model. *Proceedings of the National Academy of Sciences of the United States of America.* 107(43), 18670–5.

Eckert, A., Schulz, K. L., Rhein, V. and Götz, J. (2010). Convergence of amyloid-beta and tau pathologies on mitochondria in vivo. *Mol. Neurobiol.* 41(2-3), 107–114.

Ellis, C. E., Murphy, E. J., Mitchell, D. C., Golovko, M. Y., Scaglia, F., et al. (2005). Mitochondrial lipid abnormality and electron transport chain impairment in mice lacking alpha-synuclein. *Mol. Cell. Biol.* 25(22), 10190–10201.

Epand, R. F., Martinou, J.-C., Montessuit, S., Epand, R. M. and Yip, C. M. (2002). Direct evidence for membrane pore formation by the apoptotic protein Bax. *Biochem. Biophys. Res. Commun.* 298(5), 744–749.

Feissner, R. F., Skalska, J., Gaum, W. E. and Sheu, S.-S. (2009). Crosstalk signaling between mitochondrial Ca^{2+} and ROS. *Front Biosci (Landmark Ed).* 14, 1197–1218.

Felice, F. G. D., Velasco, P. T., Lambert, M. P., Viola, K., Fernandez, S. J., et al. (2007). Abeta oligomers induce neuronal oxidative stress through an N-methyl-D-aspartate receptor-dependent mechanism that is blocked by the Alzheimer drug memantine. *J. Biol. Chem.* 282(15), 11590–11601.

Garrido, C. and Kroemer, G. (2004). Life's smile, death's grin: vital functions of apoptosis-executing proteins. *Curr. Opin. Cell Biol.* 16(6), 639–646.

Gauci, A. J., Caruana, M., Giese, A., Scerri, C. and Vassallo, N. (2011). Identification of polyphenolic compounds and black tea extract as potent inhibitors of lipid membrane destabilization by $A\beta_{42}$ aggregates. *J. Alzheimers Dis.* 27(4), 767–779.

Glabe, C. G. and Kayed, R. (2006). Common structure and toxic function of amyloid oligomers implies a common mechanism of pathogenesis. *Neurology.* 66(2 Suppl 1), S74–8.

Gonzalvez, F. and Gottlieb, E. (2007). Cardiolipin: setting the beat of apoptosis. *Apoptosis.* 12(5), 877–885.

Gosavi, N., Lee, H.-J., Lee, J. S., Patel, S. and Lee, S.-J. (2002). Golgi fragmentation occurs in the cells with prefibrillar alpha-synuclein aggregates and precedes the formation of fibrillar inclusion. *J. Biol. Chem.* 277(50), 48984–48992.

Hauptmann, S., Scherping, I., Dröse, S., Brandt, U., Schulz, K. L., et al. (2009). Mitochondrial dysfunction: an early event in Alzheimer pathology accumulates with age in AD transgenic mice. *Neurobiol. Aging.* 30(10), 1574–1586.

Hausmann, A., Samans, B., Lill, R. and Mühlenhoff, U. (2008). Cellular and mitochondrial remodeling upon defects in iron-sulfur protein biogenesis. *J. Biol. Chem.* 283(13), 8318–8330.

Hsu, L. J., Sagara, Y., Arroyo, A., Rockenstein, E., Sisk, A., et al. (2000). Alpha-synuclein promotes mitochondrial deficit and oxidative stress. *Am. J. Pathol.* 157(2), 401–410.

Iwai, A., Masliah, E., Yoshimoto, M., Ge, N., Flanagan, L., et al. (1995). The precursor protein of non-A beta component of Alzheimer's disease amyloid is a presynaptic protein of the central nervous system. *Neuron.* 14(2), 467–475.

Jiang, M., Porat-Shliom, Y., Pei, Z., Cheng, Y., Xiang, L., et al. (2010). Baicalein reduces E46K alpha-synuclein aggregation in vitro and protects cells against E46K alpha-synuclein toxicity in cell models of familiar Parkinsonism. *J. Neurochem.* 114(2), 419–429.

Kayed, R., Sokolov, Y., Edmonds, B., McIntire, T. M., Milton, S. C., et al. (2004). Permeabilization of lipid bilayers is a common conformation-dependent activity of soluble amyloid oligomers in protein misfolding diseases. *J. Biol. Chem.* 279(45), 46363–46366.

Korytowski, W., Basova, L. V., Pilat, A., Kernstock, R. M. and Girotti, A. W. (2011). Permeabilization of the mitochondrial outer membrane by Bax/truncated Bid (tBid) proteins as sensitized by cardiolipin hydroperoxide translocation: mechanistic implications for the intrinsic pathway of oxidative apoptosis. *J. Biol. Chem.* 286(30), 26334–26343.

Kuwana, T., Mackey, M. R., Perkins, G., Ellisman, M. H., Latterich, M., et al. (2002). Bid, Bax, and lipids cooperate to form supramolecular openings in the outer mitochondrial membrane. *Cell.* 111(3), 331–342.

Lill, R. and Mühlenhoff, U. (2005). Iron-sulfur-protein biogenesis in eukaryotes. *Trends Biochem. Sci.* 30(3), 133–141.

Lin, T.-K., Liou, C.-W., Chen, S.-D., Chuang, Y.-C., Tiao, M.-M., et al. (2009). Mitochondrial dysfunction and biogenesis in the pathogenesis of Parkinson's disease. *Chang Gung Med J.* 32(6), 589–599.

Long, J., Gao, H., Sun, L., Liu, J. and Zhao-Wilson, X. (2009). Grape extract protects mitochondria from oxidative damage and improves locomotor dysfunction and extends lifespan in a Drosophila Parkinson's disease model. *Rejuvenation Res.* 12(5), 321–331.

Martin, L. J. (2010). The mitochondrial permeability transition pore: a molecular target for amyotrophic lateral sclerosis therapy. *Biochim. Biophys. Acta.* 1802(1), 186–197.

Martin, L. J., Pan, Y., Price, A. C., Sterling, W., Copeland, N. G., et al. (2006). Parkinson's disease alpha-synuclein transgenic mice develop neuronal mitochondrial degeneration and cell death. *J. Neurosci.* 26(1), 41–50.

Murphy, M. P. and LeVine, H. (2010). Alzheimer's disease and the amyloid-beta peptide. *J. Alzheimers Dis.* 19(1), 311–323.

Nakamura, K., Nemani, V. M., Azarbal, F., Skibinski, G., Levy, J. M., et al. (2011). Direct membrane association drives mitochondrial fission by

the Parkinson disease-associated protein alpha-synuclein. *J. Biol. Chem.* 286(23), 20710–20726.

Nakamura, K., Nemani, V. M., Wallender, E. K., Kaehlcke, K., Ott, M. and Edwards, R. H. (2008). Optical reporters for the conformation of alpha-synuclein reveal a specific interaction with mitochondria. *J. Neurosci.* 28(47), 12305–12317.

Northington, F. J., Graham, E. M. and Martin, L. J. (2005). Apoptosis in perinatal hypoxic-ischemic brain injury: how important is it and should it be inhibited? *Brain Res. Brain Res. Rev.* 50(2), 244–257.

Parihar, M. S., Parihar, A., Fujita, M., Hashimoto, M. and Ghafourifar, P. (2008). Mitochondrial association of alpha-synuclein causes oxidative stress. *Cell. Mol. Life Sci.* 65(7-8), 1272–1284.

Perier, C., Tieu, K., Guégan, C., Caspersen, C., Jackson-Lewis, V., et al. (2005). Complex I deficiency primes Bax-dependent neuronal apoptosis through mitochondrial oxidative damage. *Proc. Natl. Acad. Sci. U.S.A.* 102(52), 19126–19131.

Poon, H. F., Frasier, M., Shreve, N., Calabrese, V., Wolozin, B. and Butterfield, D. A. (2005). Mitochondrial associated metabolic proteins are selectively oxidized in A30P alpha-synuclein transgenic mice–a model of familial Parkinson's disease. *Neurobiol. Dis.* 18(3), 492–498.

Porat, Y., Abramowitz, A. and Gazit, E. (2006). Inhibition of amyloid fibril formation by polyphenols: structural similarity and aromatic interactions as a common inhibition mechanism. *Chem Biol Drug Des.* 67(1), 27–37.

Reddy, P. H., McWeeney, S., Park, B. S., Manczak, M., Gutala, R. V., et al. (2004). Gene expression profiles of transcripts in amyloid precursor protein transgenic mice: up-regulation of mitochondrial metabolism and apoptotic genes is an early cellular change in Alzheimer's disease. *Hum. Mol. Genet.* 13(12), 1225–1240.

Rodrigues, C. M., Solá, S., Brito, M. A., Brondino, C. D., Brites, D. and Moura, J. J. (2001). Amyloid beta-peptide disrupts mitochondrial membrane lipid and protein structure: protective role of tauroursodeoxycholate. *Biochem. Biophys. Res. Commun.* 281(2), 468–474.

Rouault, T. A. and Tong, W.-H. (2005). Iron-sulphur cluster biogenesis and mitochondrial iron homeostasis. *Nat. Rev. Mol. Cell Biol.* 6(4), 345–351.

Sanz-Blasco, S., Valero, R. A., Rodríguez-Crespo, I., Villalobos, C. and Núñez, L. (2008). Mitochondrial Ca2+ overload underlies Abeta oligomers neurotoxicity providing an unexpected mechanism of neuroprotection by NSAIDs. *PLoS ONE.* 3(7), e2718.

Shavali, S., Brown-Borg, H. M., Ebadi, M. and Porter, J. (2008). Mitochondrial localization of alpha-synuclein protein in alpha-synuclein overexpressing cells. *Neurosci. Lett.* 439(2), 125–128.

Shults, C. W. (2006). Lewy bodies. *Proceedings of the National Academy of Sciences of the United States of America.* 103(6), 1661–8.

Smith, W. W., Jiang, H., Pei, Z., Tanaka, Y., Morita, H., et al. (2005). Endoplasmic reticulum stress and mitochondrial cell death pathways mediate A53T mutant alpha-synuclein-induced toxicity. *Hum. Mol. Genet.* 14(24), 3801–3811.

Song, D. D., Shults, C. W., Sisk, A., Rockenstein, E. and Masliah, E. (2004). Enhanced substantia nigra mitochondrial pathology in human alpha-synuclein transgenic mice after treatment with MPTP. *Exp. Neurol.* 186(2), 158–172.

Stevenson, D. E. and Hurst, R. D. (2007). Polyphenolic phytochemicals–just antioxidants or much more? *Cell. Mol. Life Sci.* 64(22), 2900–2916.

Szeto, H. H. (2014). First-in-class cardiolipin-protective compound as a therapeutic agent to restore mitochondrial bioenergetics. *Br. J. Pharmacol.* 171(8), 2029–2050.

Tanaka, Y., Engelender, S., Igarashi, S., Rao, R. K., Wanner, T., et al. (2001). Inducible expression of mutant alpha-synuclein decreases proteasome activity and increases sensitivity to mitochondria-dependent apoptosis. *Hum. Mol. Genet.* 10(9), 919–926.

Trushina, E., Nemutlu, E., Zhang, S., Christensen, T., Camp, J., et al. (2012). Defects in mitochondrial dynamics and metabolomic signatures of evolving energetic stress in mouse models of familial Alzheimer's disease. *PLoS ONE.* 7(2), e32737.

van Meer, G., Voelker, D. R. and Feigenson, G. W. (2008). Membrane lipids: where they are and how they behave. *Nat. Rev. Mol. Cell Biol.* 9(2), 112–124.

van Rooijen, B. D., Claessens, M. M. A. E. and Subramaniam, V. (2009). Lipid bilayer disruption by oligomeric alpha-synuclein depends on bilayer charge and accessibility of the hydrophobic core. *Biochim. Biophys. Acta.* 1788(6), 1271–1278.

Williams, T. L., Day, I. J. and Serpell, L. C. (2010). The effect of Alzheimer's Aβ aggregation state on the permeation of biomimetic lipid vesicles. *Langmuir.* 26(22), 17260–17268.

Zhang, L., Zhang, C., Zhu, Y., Cai, Q., Chan, P., et al. (2008). Semi-quantitative analysis of alpha-synuclein in subcellular pools of rat brain neurons: an immunogold electron microscopic study using a C-terminal specific monoclonal antibody. *Brain Res.* 1244, 40–52.

Zigoneanu, I. G., Yang, Y. J., Krois, A. S., Haque, E. and Pielak, G. J. (2012). Interaction of α-synuclein with vesicles that mimic mitochondrial membranes. *Biochim. Biophys. Acta.* 1818(3), 512–519.

Xjenza Online - Journal of The Malta Chamber of Scientists
www.xjenza.org
DOI: 10.7423/XJENZA.2014.2.13

Research Article

A 10 year review of the number of bovine dairy holdings and the dairy bovine population on the Maltese Islands

Mauro Buttigieg[1], Matteo Gianesella[1] and Andrew James[2]
[1]Dipartimento di Medicina Animale, Produzioni e Salute (MAPS), Università degli Studi di Padova, Viale dell'Università 16, 35020 Legnaro, Padova, Italy.
[2]Veterinary Epidemiology & Economics Research Unit, School of Agriculture, Policy and Development, University of Reading, Earley Gate, P.O. Box 237 Reading RG6 6AR United Kingdom.

Abstract. The process of identification and registration of bovines and bovine holdings on the Maltese Islands has been computerised since 2002, with the introduction of the National Livestock Database of Malta. This is a computerised and centralised system which has made collection, management and analysis of data possible. The aims of this paper were to study in detail ten year trends in the number of bovine dairy holdings together with the bovine population on these holdings and to compare these trends with those reported in other European countries. Six trends related to the number of bovine dairy holdings and their bovine population were analysed in the study. The general trends showed that there was a significant decrease in the number of dairy holdings, in the bovine population and in the number of female bovines greater than 2 years of age during the study period. The average herd size and the average number of females greater than 2 years of age on the dairy holdings showed no statistically significant changes. On the other hand, a significant increase in the ratio of female to male bovines was registered on these holdings.

Keywords National Livestock Database – number of bovine dairy holdings – bovine population – Maltese Islands

1 Introduction

The data collection with regards to the number of dairy holdings and the number of bovines takes place regularly in every European country. This is necessary amongst other things to allow for the monitoring of various parameters such as production, animal welfare and food safety.

Jongeneel et al. (2011) report that the number of dairy holdings in the European Union has been gradually declining from the year 2000. Furthermore, Nowicki et al. (2009) reported that this trend was expected to continue.

The objectives of this paper were to study in detail the ten year trends in the number of dairy bovine holdings together with the population of bovines on these holdings and to compare these trends with those reported in other European countries. Three methods were used in the study to collect three datasets which were then analysed statistically.

The period of study was from the 1st January 2003, a year before Malta's accession to the European Union (EU) on the 1st of May 2004 (Government of Malta, 2003), to the 31st December 2012.

The study involved retrieval of data from the National Livestock Database (NLD) which is a computerised, centralised system set up in 2002, with the aim to facilitate the recording, management and analysis of livestock data.

The NLD is managed by the Veterinary and Phytosanitary Regulation Department (VPRD) within the Ministry for Sustainable Development, the Environment and Climate Change. This database was recognised as being fully operational by the European Union as stated by Commission Decision 2004/588/EC of the 3rd June 2004 (European Commission, 2004). Furthermore, by means of Commission Decision 2005/415/EC (European Commission, 2005), Malta was authorised to make use

Correspondence to: Mauro Buttigieg (maurobut@go.net.mt)

© 2014 Xjenza Online

of the NLD and replace surveys of bovine livestock as required by Directive 93/24/EC (European Commission, 1993).

All bovine herds are obliged by Maltese law to be registered with the VPRD. Two important laws in this regard are Subsidiary Legislation 437.78 published as Legal Notice 292 of 2005 (Government of Malta, 2005b) and Subsidiary Legislation 437.84 published as Legal Notice 311 of 2005 (Government of Malta, 2005a).

The obligation of identification and registration of each bovine together with the collection of all the data in one national computerised system has made it possible to collect and analyse data regarding all registered bovines on holdings present on the islands of Malta and Gozo at any point in time.

2 Materials and Methods

2.1 Study design

A retrospective longitudinal study was conducted on the entire population of dairy herds present on the islands of Malta and Gozo registered in the NLD. No bovines were registered on the island of Comino during the study period. Six trends related to the number of dairy holdings and the dairy bovine population were analysed.

Bovine holdings on the Maltese Islands fall into two categories. These are the dairy holdings and the non-dairy holdings. The dairy holdings are licensed to produce and sell their milk to a dairy processing plant and their main objective is the production of fresh milk.

The non-dairy holdings are those bovine holdings which are not licensed to produce and sell milk and their main activity is the fattening of bovines for slaughter. These latter holdings are relatively small, family run and mostly managed on a part-time basis. The mean number of active non-dairy holdings per year throughout the 10 year period under study as calculated by Method 2 described below was 206.40 (SD = 21.82) in Malta and 13.70 (SD = 4.06) in Gozo. The holdings in Malta had a mean bovine population of 8.50 (SD = 0.91) and those in Gozo had a mean of 4.67 bovines (SD = 0.70). The non-dairy holdings in Malta contained 14.57 % (SD = 2.50) of the total bovine population of Malta, whereas the holdings in Gozo contained only 1.09 % (SD = 0.17) of the total bovine population of Gozo.

Due to the dynamic nature of the livestock population on holdings, different results can be obtained depending on what is considered as being an active holding. As a result, three methods were used in this study:

Method 1 (M1): Using this method, an active bovine holding was taken as being a holding on which at least one bovine was registered at the reference date of the 1st December of each year of the study.

Method 2 (M2): This method considers an active holding as one on which at least an average of one bovine is registered on the holding throughout the year. This method takes into account the average population on the holding per year, starting from the 1st January to the 31st December of each year. The calculation of the average population is in principle the average of the number of animals present for each day in the period. For computational efficiency, the database locates all the animals that were present at any time during the period. It then calculates the number of days that each animal was present during the period (animal-days). The total number of animal-days is then divided by the number of days in the year to obtain the average population per year on any particular holding.

Method 3 (M3): Using this method, a holding was considered as being active when at least one female bovine older than 2 years of age (F>2y) was present on the holding on the 1st December of each year of the study. In this case it is assumed that dairy holdings having F>2y are still involved in milk production since nearly all of these bovines would be milk producing cows. This consideration was made since a number of dairy holdings winding down their activities would still have a number of bovines on the holding, such as young heifers and male calves or bulls, but in actual fact they would not be actively involved in milk production. This is especially so since during the period 2007 to 2012 an eradication programme for enzootic bovine leucosis (EBL) was underway (Government of Malta, 2009). The fact that at least one F>2y is present on a holding licensed as being a dairy holding assumes that it contains dairy cows and therefore is still involved in milk production.

The 1st December of each year was chosen as the reference date in order to follow the guidelines of the National Statistics Office (NSO) of Malta which uses the 1st December as its reference date when compiling the yearly cattle census as per Commission Regulation (EC) 1165/2008 (European Commission, 2008a) and Commission Regulation (EC) 1166/2008 (European Commission, 2008b).

2.2 Statistical Analyses

The data collected from the NLD was transferred to Excel files where data verification and validation was carried out. In all cases data from 2003 to 2012 were used in the statistical analyses. However during the verification process, the data fields concerning the number of F>2y of age for the year 2003, were not considered to be sufficiently accurate. This is due to the fact that when inputting data for animals born prior to 2003 in the database, the date of birth had to be transposed from pre-existing paper records which at times had in-

complete or inaccurate data. As a result, data for 2003 were omitted when analysing trends regarding F>2y of age.

The data used in the statistical analyses was then transferred to SPSS version 21, a statistical package that permitted descriptive statistics, correlation analysis and analysis of variance to be carried out.

3 Results and Discussion

3.1 The trend in the number of dairy holdings on the Maltese Islands

The trend in the total number of dairy holdings per year on the Maltese Islands during the period 2003 to 2012, calculated by the three methods described, is shown by the line diagram in Figure 1.

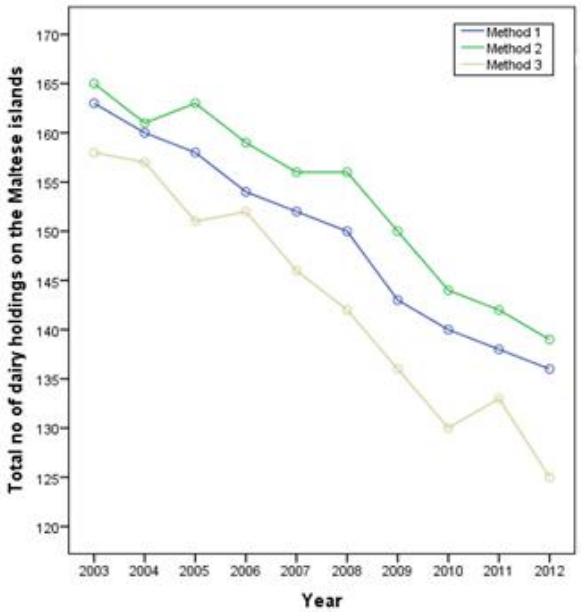

Figure 1: Line diagram showing the total number of dairy holdings on the Maltese Islands per year from 2003 to 2012 calculated by the three methods described.

All three methods show a decrease in the total number of dairy holdings on the Maltese Islands from maximum peaks in 2003 of 163, 165 and 158 holdings to minimum numbers in 2012 of 136, 139 and 125 holdings for methods 1, 2 and 3 respectively. This gives a decrease in the number of dairy holdings during the study period of 16.56 % when using M1, 15.76 % when using M2 and 20.89 % when using M3. This decrease, although less pronounced, is similar to trends registered in EU-27 member states. These include all member states excluding Croatia which joined the European Union on the 1st of July 2013. The total number of holdings with dairy cows in the EU-27 member states fell by 32 % from 2007 to 2010. The decrease amounts to 47 % if values for 2003 and 2010 are compared (Marquer, 2013).

The biggest difference in the number of holdings is obtained when using M3. This method is more appropriate for calculating the actual number of active dairy holdings producing milk from their herds since it is only dairy holdings having at least one F>2y of age which are taken into consideration. M1 gives a mean number of dairy holdings of 149.40 (SD = 9.65) which is higher than 143.00 (SD = 11.63) obtained when using M3. This is due to the fact that the former would include some holdings which were closing down their activity during the 10 year period and had no F>2y of age present on the holding but still had some male or younger female bovines. When using M2, the mean number of holdings was 153.50 (SD = 9.23). The mean is even higher in this method since the yearly average would take a longer time to fall below the cut-off point of at least one bovine present on the holding.

Very strong negative correlations ranging from r= −0.913 to r= −0.992 (n = 10) are present between the total number of dairy holdings and the year, when analysed separately on both islands and as a total number of holdings in Malta plus Gozo. This applies to the three methods used and in all cases the correlations have a significance of $p<0.0005$. This implies that there has been a statistically significant decrease in the number of dairy holdings from 2003 to 2012 in both Malta and Gozo.

The mean number of dairy holdings in Malta during the study period was significantly higher than in Gozo. This varied from 105.70 (SD = 7.03) calculated when using M1, 109.00 (SD = 6.46) calculated using M2 and 100.10 (SD = 8.40) as calculated using M3. The mean number of holdings in Gozo calculated by M1 was 43.70 (SD = 2.71). When calculated using M2 and M3 the values were 44.50 (SD = 2.92) and 42.90 (SD = 3.25) respectively.

The yearly percentage of dairy holdings present in Malta compared to Gozo calculated using the three methods was 70.74 % (SD = 0.40) for M1, 71.02 % (SD = 0.51) for M2 and 69.99 % (SD = 0.25) for M3. This percentage does not show great variations during the 10 year period under study denoting that the percentage distribution of dairy holdings in Malta and Gozo was relatively stable from 2003 to 2012.

3.2 The trend in the total number of bovines on dairy holdings

The trend in the total number of bovines on dairy holdings on the Maltese Islands is shown in Figure 2

The data analysed is from year 2004 to 2012 since data concerning the number of F>2y of age for year 2003 were not deemed to be sufficiently reliable and were removed from the analysis. A small decrease in the total number

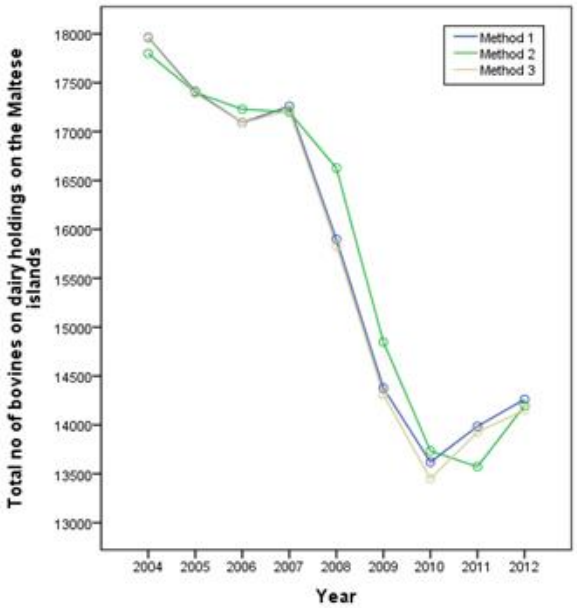

Figure 2: Line diagram showing the total number of bovines on dairy holdings on the Maltese Islands from 2004 to 2012 calculated by the three methods described.

of bovines on dairy holdings on the Maltese Islands was registered from 2004 to 2007 using the three methods. The decrease was of 3.92 % when calculated using M1, 3.37 % using M2 and 4.12 % using M3. A sharp decrease in the bovine population then follows till 2010 and this is again demonstrated by all three methods. The decrease from 2007 to 2010 is of 21.08 % for M1, 20.15 % for M2 and 21.88 % for M3. An increase of 4.71 % and 5.23 % is then present from 2010 to 2012 as calculated using M1 and M3 respectively, whereas M2 shows a further slight decrease of 1.19 % till 2011 with an increase of 4.60 % from 2011 to 2012.

The overall decrease in the total number of bovines on dairy holdings on the Maltese Islands from 2004 to 2012 is of 20.61 %, 20.25 %, and 21.18 % as calculated using methods 1, 2 and 3 respectively.

The mean number of bovines on all dairy holdings on the Maltese Islands from 2004 to 2012, as calculated when using M1 was 15,763.00 (SD = 1,714.12). M2 gave a value of 15,845.56 (SD = 1,729.97) and M3 15,702.33 (SD = 1,758.47).

Very strong negative correlations of r= −0.930, −0.930 and −0.929 (n = 9) are present between the total number of bovines on dairy holdings and the year calculated using methods 1, 2 and 3 respectively. These correlations are highly significant at a value of $p<0.0005$ denoting that there has been a significant decrease in the total number of bovines on dairy holdings on the Maltese Islands during the study period.

Statistically significant strong negative correlations ($p<0.05$) ranging from −0.764 to −0.944 are also present when the bovine populations on dairy holdings on both islands are analysed separately showing that the decrease in the total number of bovines is present on both islands.

The bovine population on the dairy holdings in Malta is significantly larger than in Gozo. The mean number of bovines on all dairy holdings in Malta from 2004 to 2012, as calculated using M1 was 10,153.00 (SD = 1,265.76). M2 gave a value of 10,219.44 (SD = 1,298.12) and M3 10,107.00 (SD = 1,297.41). The values for Gozo were 5,610.00 (SD = 503.70) for M1, 5,626.11 (SD = 501.62) for M2 and 5,595.33 (SD = 513.77) for M3.

When the percentages of the number of bovines on dairy holdings in Malta relative to Gozo are analysed, the values show that 64.32 % (SD = 1.44), 64.40 % (SD = 1.64) and 64.27 % (SD = 1.45) of bovines, as calculated using methods 1, 2 and 3 respectively, are present on dairy holdings in Malta relative to Gozo. Only M2 shows a significant correlation with r = −0.692, n = 9, $p< 0.05$ between the percentage bovine population and the year under review. The fact that a significant correlation, which is not very strong, was obtained in only one of the methods implies that the percentage distribution of bovines on dairy holdings in Malta relative to Gozo was relatively stable during the study period.

3.3 The trend in the number of female bovines over 2 years of age on dairy holdings

The trend in the number of F>2y of age on dairy holdings on the Maltese Islands was analysed since this data reflects the potential milk production on this type of holding. Method 3 was used in the analysis of this parameter. The trend for the period 2004 to 2012 is shown by the line diagram in Figure 3.

The number of F>2y of age on dairy holdings in Malta shows a decrease from 5,725 bovines in 2004 to 4,419 in 2012. This represents a decrease of 22.81 %. The mean number of F>2y of age in Malta for the same period was 4,897.00 (SD = 461.63).

In Gozo, the number of F>2y of age increases slightly from 2,493 in 2004 to 2,811 in 2007. A slight decrease then follows to reach 2,331 in 2012. From 2004 to 2012 the number of F>2y of age on dairy holdings in Gozo decreased by only 6.50 %. The mean number of F>2y of age in Gozo was 2,570.33 (SD = 175.80).

If the total number of F>2y of age on both islands is taken into consideration, a decrease of 17.86 % from 8,218 in 2004 to 6,750 in 2012 can be seen. The mean number of F>2y of age on the Maltese Islands was 7,467.33 (SD = 563.73).

This trend is very similar to the trend in the number of dairy cows on holdings in the European Union.

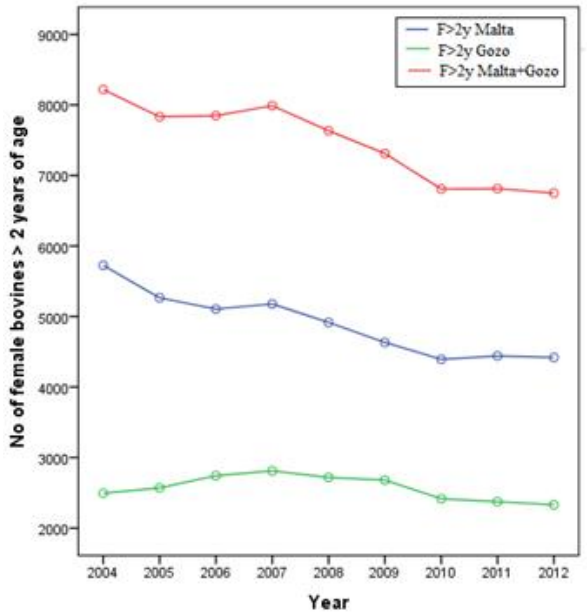

Figure 3: Line diagram showing the number of female bovines greater than 2 years of age on dairy holdings in Malta, Gozo and Malta + Gozo from 2004 to 2012.

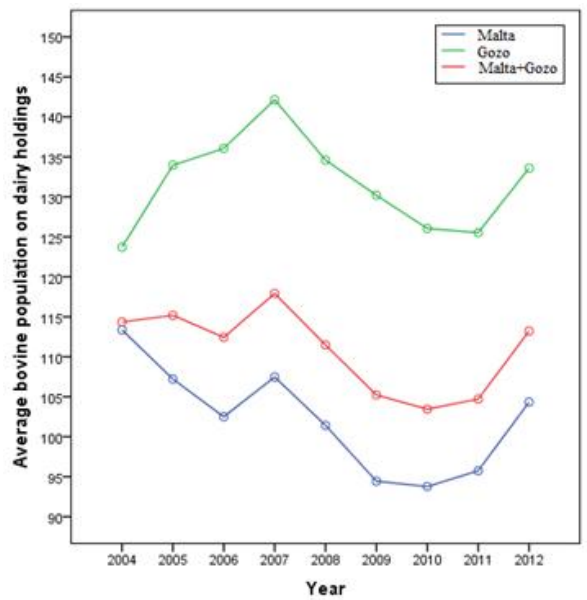

Figure 4: Line diagram showing the average bovine population (average herd size) on dairy holdings in Malta, Gozo and Malta + Gozo from 2004 to 2012.

(Marquer, 2013) reports a decrease of 20 % in the number of dairy cows on the specialist dairying holdings in the EU-27 countries from 2007 to 2010. Specialist holdings are defined as deriving at least two thirds of their output from the dairy activity (Marquer, 2013).

A statistically significant, strong negative correlation is present between the number of F>2y of age in Malta and the period under study ($r = -0.956$, $n = 9$, $p < 0.0005$) showing that the number of F>2y of age in Malta decreased significantly during the study period. However, no significant correlation is present between the number of F>2y of age and the period under study in Gozo. This implies that their number in Gozo has remained relatively unchanged during the study period. When the trend for both islands is analysed together we obtained a statistically significant, strong negative correlation with $r = -0.946$, $n = 9$ and $p < 0.0005$.

The number of dairy cows in the EU stood at 22.9 million in 2011. Whilst Germany had the highest proportion of dairy cows, at 18.3 % within the EU-27 countries (Marquer, 2013), the Maltese Islands with a dairy cow population of 6,813 in 2011, had the smallest proportion at 0.03 %.

3.4 The trend in the average bovine population (average herd size) on dairy holdings

This trend was included in the study to determine if the average herd size on dairy holdings on both islands was increasing to make up for the decreasing number of holdings. The trend is shown by the line diagram in Figure 4. In this instance data obtained by Method 3 was used in the analysis.

The average herd size on dairy holdings on the Maltese Islands was relatively stable from 2004 to 2006. This was mainly due to a decrease in the average herd size on dairy holdings in Malta from 113.37 in 2004 to 102.50 in 2006 and an increase in Gozo from 123.70 in 2004 to 136.07 in 2006. In 2007 an increase was registered in both Malta (107.47) and Gozo (142.14). In Malta the average population reached its minimum of 93.77 in 2010 whilst in Gozo a minimum of 125.53 was reached in 2011. An increase was then registered in both islands in 2012 with values reaching 104.33 in Malta and 133.58 in Gozo. The decrease on both islands from 2007 to 2010 was mainly due to the ongoing EBL eradication programme.

No statistically significant correlation is present between the average bovine population and the year in Malta and Gozo ($r = -0.589$, $n = 9$, $p = 0.095$) or in Gozo alone ($r = -0.137$, $n = 9$, $p = 0.726$). A statistically significant, weak negative correlation is present between the average bovine population on dairy holdings in Malta and the period under study ($r = -0.692$, $n = 9$, $p = 0.039$). This implies that the average herd size on dairy holdings on both islands, although showing some fluctuations during the study period, remained relatively constant.

A statistically significant difference is present between the average herd size on dairy holdings in Malta and Gozo as determined by one-way ANOVA ($F\ (2,24) =$

58.42, $p < 0.0005$). A Tukey post-hoc test shows that the average herd size on dairy holdings as calculated using M3 in Malta is statistically significantly lower (102.25 ± 6.67, $p < 0.0005$) than the average herd size on dairy holdings in Gozo (131.76 ± 5.93) for the period 2004 to 2012.

3.5 The trend in the average number of F>2y of age on dairy holdings

Apart from analysing the average herd size on dairy holdings, the trend in the average number of F>2y of age on these holdings on the Maltese Islands was also studied. This was considered important since any changes in this data group are very likely to affect the milk producing potential of the dairy holdings. The trend in the average number of F>2y of age on dairy holdings is shown in Figure 5.

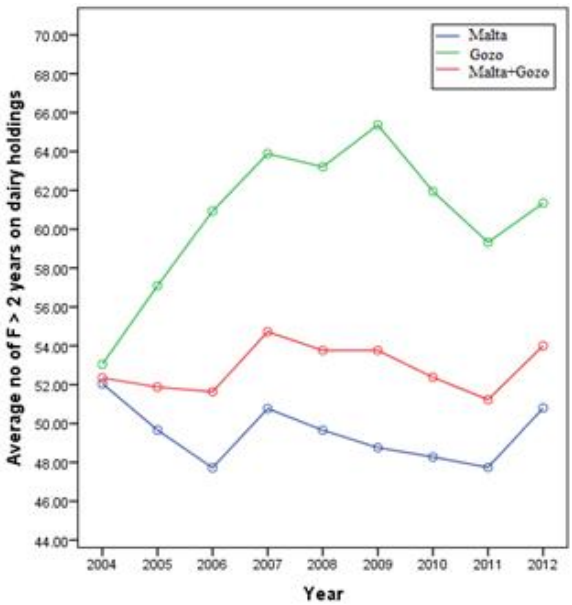

Figure 5: Line diagram showing the average number of female bovines greater than two years of age on dairy holdings in Malta, Gozo and Malta + Gozo from 2004 to 2012.

The trend on dairy holdings in Malta is quite different to that in Gozo. The trend in Malta is relatively stable throughout the period 2004 to 2012 with a mean of 49.49 (SD = 1.51). In Gozo, the average number of F>2y increases from a minimum value of 53.04 in 2004 to a maximum of 65.37 in 2009. The average then decreases till 2011 to increase to 61.34 in 2012. The trend for the two islands together follows closely the trend shown for Malta.

For the period under study, no statistically significant correlation was present between the average number of F>2y on dairy holdings and the year in Malta ($r = -0.354$, $n = 9$, $p = 0.350$), Gozo ($r = 0.525$, $n = 9$, $p = 0.146$), or on both islands taken together ($r = 0.194$, $n = 9$, $p = 0.617$). This implies that the average number of F>2y of age on both islands was relatively constant during the study period. This is in contrast to the trend in the EU-27 countries where the average number of dairy cows per holding has been reported to have increased (Marquer, 2013).

A statistically significant difference is present between the average number of F>2y on dairy holdings in Malta and Gozo from 2004 to 2012 as determined by one-way ANOVA ($F(2,24) = 49.48$, $p < 0.0005$). A Dunnett T3 post-hoc test shows that the average number of F>2y on dairy holdings in Malta is statistically significantly lower (49.49 ± 1.51, $p < 0.0005$) than the average on dairy holdings in Gozo (60.68 ± 3.77). The average number of F>2y on dairy holdings in Malta and Gozo (52.86 ± 1.23) lies in between these two values. If we assume that female bovines over two years of age on Maltese dairy holdings are in fact dairy cows, than this average is higher than the average of around 28 dairy cows on EU-27 specialist dairying holdings where a maximum of 141 dairy cows per holding was reported in Denmark and a minimum of 3 cows per holding was reported in Romania (Marquer, 2013).

3.6 The trend in the ratio of female to male bovines on dairy holdings

The mean number of female bovines on the Maltese Islands during the period 2004 to 2012 calculated using M3 was 12,567.89 (SD = 1,039.70) whereas the mean number of male bovines was 3,134.44 (SD = 730.22).

The ratio of female to male bovines on dairy holdings in both Malta and Gozo was relatively stable from 2004 to 2007. In Malta an increase in the ratio followed from 3.71 in 2007 to 5.75 in 2011. The ratio decreased slightly to 5.19 in 2012. In Gozo a marked increase was present from 2.93 in 2007 to 4.29 in 2009 and then the ratio remained relatively stable at 3.99 in 2012 (Figure 6).

The increase in both cases is due to a proportionally larger decrease in the number of males on the holdings. This was possibly due to the slaughtering trends during the EBL eradication campaign.

Statistically significant, strong positive correlations are present between the ratio of female to male bovines and the year in Malta ($r = 0.879$, $n = 9$, $p < 0.05$), Gozo ($r = 0.856$, $n = 9$, $p < 0.05$), and Malta and Gozo ($r = 0.884$, $n = 9$, $p < 0.05$).

A statistically significant difference is present between the female to male bovine ratios on dairy holdings in Malta and Gozo calculated using M3 over the period 2004 to 2012 as determined by one-way ANOVA ($F(2,24) = 5.01$, $p < 0.05$). A Tukey post-hoc test shows that the female to male bovine ratio on holdings in Malta is statistically significantly higher (4.55 ± 0.78,

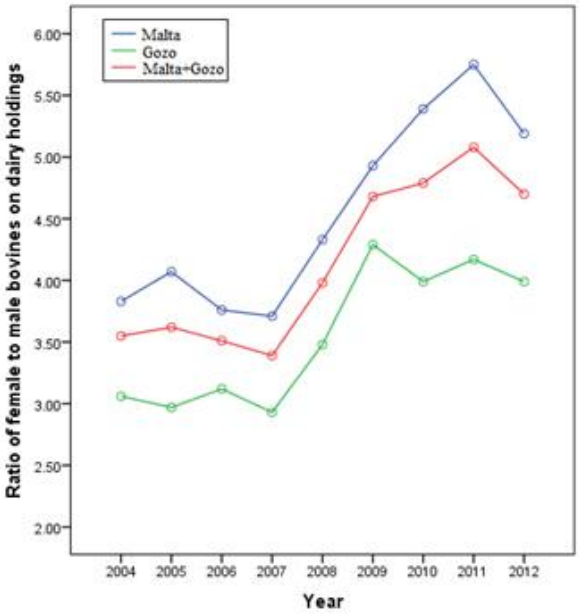

Figure 6: Line diagram showing the change in ratio between the number of female to male bovines on dairy holdings in Malta, Gozo and Malta + Gozo from 2004 to 2012.

$p < 0.05$) than the ratio on dairy holdings in Gozo (3.56 ± 0.56). This difference might be due to the fact that the number of non-dairy bovine holdings in Gozo and their average herd size are considerably lower than those in Malta. As a result dairy holdings in Gozo tend to keep more male bovines up to slaughtering age rather than selling them to non-dairy holdings at an early age as happens in Malta.

4 Conclusions

This study has described and analysed six trends with regard to dairy holdings and their bovine population on the Maltese Islands from 2003, a year before Malta's accession to the European Union to 2012. The general trends on the Maltese Islands show that there was a significant decrease in the number of dairy holdings, in the total bovine population and in the number of F>2y of age during the study period. The number of dairy holdings and the total bovine population decreased by approximately 17.74 % and 20.68 % respectively, depending on the method used for their calculation. The total number of F>2y on dairy holdings on the islands decreased by 17.86 % from 2004 to 2012. On the other hand, the average herd size and the average number of F>2y on the dairy holdings on the Maltese Islands showed no statistically significant changes. A significant increase in the ratio of female to male bovines from 3.55 to 4.70 was registered on these holdings. The fact that the average herd size and the average number of F>2y of age on the holdings showed no significant changes implies that the bovine population on the holdings during the study period was relatively stable.

Acknowledgments

The authors wish to thank the Veterinary and Phytosanitary Regulation Department of Malta and in particular the staff at the Identification and Registration Section, for their help in data collection from the National Livestock Database. We also wish to thank Prof. Liberato Camilleri from the Faculty of Science, University of Malta for reviewing the statistics used in this paper.

References

European Commission. (1993). Council Directive 93/24/EEC of 1 June 1993 on the statistical surveys to be carried out on bovine animal production. *OJ.* L 149/5.

European Commission. (2004). Commission Decision of 3 June 2004 recognising the fully operational character of the Maltese database for bovine animals. *OJ.* L 257/8.

European Commission. (2005). Commission Decision 2005/415/EC of the 1 of June 2005 authorising Malta to make use of the system established by Title I of Regulation (EC) No 1760/2000 of the European Parliament and of the Council to replace surveys of bovine livestock. *OJ.* L141/30.

European Commission. (2008a). Regulation (EC) No 1165/2008 of the European Parliament and of the Council of 19 November 2008 concerning livestock and meat statistics and repealing Council Directives 93/23/EEC, 93/24/EEC and 93/25/EEC. *OJ.* L321/1.

European Commission. (2008b). Regulation (EC) No 1166/2008 of the European Parliament and of the Council of 19 November 2008 on farm structure surveys and the survey on agriculture production methods and repealing Council Regulation (EEC) 571/88. *OJ.* L 321/14.

Government of Malta. (2003). *Comprehensive monitoring report on Malta's preparation for membership.* Government of Malta.

Government of Malta. (2005a). Bovine Animals (Identification and Registration) and Beef Labelling Rules. Retrieved May 25, 2013, from http://www.justiceservices.gov.mt/DownloadDocument.aspx?app=lom&itemid=11020&l=1. Subsidiary Legislation 437.84.

Government of Malta. (2005b). Identification and Registration of Animals Rules. Retrieved May 25, 2013, from http://www.justiceservices.gov.mt/DownloadDocument.aspx?app=lom&itemid=11014&l=1. Subsidiary Legislation 437.78.

Government of Malta. (2009). Measures for the Eradication of Brucellosis, Tuberculosis and Leucosis in Cattle Rules. Retrieved January 22, 2014, from http://www.justiceservices.gov.mt/DownloadDocument.aspx?app=lom&itemid=11022&l=1. Subsidiary Legislation 437.86.

Jongeneel, R., Burrell, A. and Kavallari, A. (2011). *Evaluation of CAP measures applied to the dairy sector.* European Commission.

Marquer, P. (2013). *Milk and dairy production statistics.* Eurostat.

Nowicki, P., Goba, V., Knierim, A., van Meijl, H., Banse, M., et al. (2009). *Scenar 2020 - II - Update of Analysis of Prospects in the Scenar 2020 Study.* European Commission, Directorate-General Agriculture and Rural Developmen.

Xjenza Online - Journal of The Malta Chamber of Scientists
www.xjenza.org
DOI: 10.7423/XJENZA.2014.2.14

Review Article

Measuring β-cell function *in vivo* to understand the pathophysiology of type 2 diabetes

Luca P. Farrugia, Adrian Vella MD
Endocrine Research Unit, Division of Endocrinology, Diabetes & Metabolism, Mayo Clinic College of Medicine, 200 1st Street SW, Joseph 5-194, Rochester, MN, USA

Abstract. Diabetes arises when insulin secretion is inadequate for the prevailing metabolic conditions. As such appropriate measurement of β-cell function is necessary for a better understanding of the pathophysiology of prediabetes and diabetes. Unfortunately this is not a straightforward process and requires utilization of mathematical modelling to best appreciate its complexities. This is because insulin concentrations in the plasma represent a balance between the processes of secretion, hepatic extraction and clearance. In isolation such simple measures reveal very little about β-cell function. Moreover, since insulin lowers glucose accounting for the effect of the former on the latter it is a key part of understanding insulin action. The development of the minimal model has allowed simultaneous measurement of the dynamic relationship between insulin secretion and insulin action and produces a quantitative number – the Disposition Index – which quantifies β-cell function. At present this remains the best functional measure of islet health, however, it may not capture other phenotypes such as β-cell senescence or the effect of incretin hormones on β-cell function. Future ongoing development and interaction with other technologies, such as functional imaging, should enhance the contribution of this functional testing to the prevention, treatment and understanding of type 2 diabetes.

Keywords Insulin Secretion – Insulin Action – Incretin Effect – Glucagon-Like Peptide-1 – Minimal Model

1 Introduction

Diabetes is defined by the presence of elevated fasting and postprandial glucose concentrations, and, indeed, currently a fasting glucose of ≥126 mg/dL would qualify a patient as having diabetes. A fasting glucose (≤100 mg/dL) is considered to be normal, and the range in between these two parameters characterizes an intermediate, often transitory, state referred to as prediabetes. It is well recognized that individuals with a higher fasting glucose, have a higher risk of transitioning to diabetes. For example, in a population from Olmsted County, if fasting glucose is ≥110 mg/dL, but ≤126 mg/dL over 10 years, the risk is 40 % (i.e., 40 % of that particular population will transition to diabetes) (Dinneen et al., 1998). This may strike one as being a particularly high number, but conversely, 60 % of people in the range of fasting glucose never actually transition to diabetes. In essence, if you look at the people whose fasting glucose is ≤100 mg/dL, 10 % of those at 10 years would have transitioned to diabetes, again implying that fasting glucose by itself may not necessarily be the best marker for diabetes risk and also demonstrating that there is significant heterogeneity of diabetes risk at a given fasting glucose level. The factors driving the transition to diabetes are at present not well characterized.

2 Pathophysiology of Diabetes: Defects in Insulin Secretion and Action

As already mentioned, diabetes is characterized by a fasting glucose which is elevated after a meal challenge. Glucose rises to higher concentrations and stays elevated for a lot longer than it does in normal non-diabetic in-

Correspondence to: Adrian Vella MD (vella.adrian@mayo.edu)

© 2014 Xjenza Online

dividuals. This elevation in glucose over time is what leads to diabetes complications. Why does this arise? It arises because fasting insulin concentrations are inappropriate for the prevailing degree of glycaemia. Also, in response to a meal challenge, insulin concentrations rise to a lower peak and take a long time getting to that peak compared to the ten-fold elevation in insulin concentrations that occurs within about 30-45 minutes of meal ingestion in non-diabetic individuals. In addition to delayed and defective insulin secretion, people with type 2 diabetes inappropriately suppress glucagon in response to meal ingestion. In fact, a paradoxical rise in glucagon is often present, in contrast to glucagon suppression observed in the first two hours after meal ingestion that is seen in non-diabetic individuals. This further exacerbates postprandial hyperglycemia (Butler and Rizza, 1991).

Diabetes is also characterized by defects in insulin action (i.e. the ability of insulin to suppress endogenous production of glucose and to stimulate the peripheral uptake of glucose in insulin-sensitive tissues is impaired when compared to non-diabetic individuals). How important is the interaction of defects in insulin secretion with defects in insulin action? To address this question, when people with varying degrees of insulin action are studied, worsening defects in insulin secretion cause far greater rises in glucose concentration than either defect alone, with such effects most marked in people with type 2 diabetes. For example, Basu et al. (1996) studied three groups of people with varying grades of insulin resistance (i.e. one group comprised insulin-sensitive, lean, non-diabetic individuals. Another group comprised insulin-resistant people with type 2 diabetes, and in a third intermediate group were obese non-diabetic individuals who had milder degrees of insulin resistance). These individuals were studied on two occasions in the presence of a pancreatic clamp with somatostatin to inhibit endogenous insulin secretion and with glucagon-growth hormone replacement at basal concentrations. Subjects then received a 'diabetic' insulin profile (i.e. a decrease in delayed insulin infusion which mimicked postprandial response of insulin seen in diabetic individuals) versus a normal non-diabetic insulin profile. In all subjects, infusion of a 'diabetic' insulin profile in comparison to the 'non-diabetic' profile resulted in higher glucose concentrations, but the effect was most marked in the more insulin-resistant individuals. This implies that, in reality, if insulin action is sufficient, defects in insulin secretion can be compensated for. However, with varying degrees of insulin resistance, the hyperglycemia that occurs in response to a diabetic insulin profile increases (Basu et al., 1996).

These observations, in a sense, dispute the previous prevailing theory of predisposition to diabetes, which hypothesized that people secrete insulin increasingly in response to increasing degrees of insulin resistance. However, there comes a time when the beta cells collectively cannot sustain this increased rate of insulin secretion and hyperglycemia develops (DeFronzo, 1988). This theory has also been called the Starling's curve of the pancreas, taking its cue from the Starling curve as it applies to the heart where increasing degrees of preload increase contractility of the myocardium up to the point of cardiac failure. In practice, this is unlikely to occur, because across populations of individuals with prediabetes, it seems that with worsening degrees of hyperglycemia insulin secretion and action both decline concurrently, rather than insulin secretion increasing, as insulin action decreases and then suddenly failing (Sathananthan et al., 2012)

3 Measuring Insulin Secretion *in vivo*

The original proposition of a Starling Curve of the pancreas is likely flawed because it is based on population cross-sectional data with no longitudinal follow-up. In addition, most of the calculations used to quantify insulin secretion in response to a standardized meal challenge used qualitative peripheral insulin concentrations. It is important to remember that insulin concentrations alone do not necessarily reflect insulin secretion. The insulin concentrations that appear in the peripheral circulation have already gone through hepatic extraction and therefore do not necessarily reflect the concentrations of insulin appearing in the portal circulation as a result of insulin secretion. Thus the insulin concentrations peripherally represent the net sum of two processes–insulin secretion and hepatic extraction (Rossell et al., 1983). Therefore, for quantitative measures of insulin secretion, current state-of-the art measurements utilize C-peptide which is secreted in a 1:1 molar ratio with insulin. The problem with this approach is that while insulin has a half-life of $\sim$ 5 minutes in the circulation, C-peptide has a half-life of $\sim$ 35 minutes and tends to accumulate over time. Therefore to calculate insulin secretion rates, insulin secretion needs to be deconvoluted from the C-peptide concentrations using known rates of clearance for C-peptide (Cobelli et al., 2014).

The other observation to consider is that insulin secretion in response to a physiologic or supraphysiologic challenge arises from two distinct compartments. This phenomenon was first observed in isolated islets and then subsequently in perfused pancreata, where it was clear that exposure to glucose acutely results in a rapid upstroke in insulin concentrations, which is then rapidly followed by a second upstroke which is more sustained than the first, but whose amplitude is lower. These are

collectively referred to as the first and second phases of insulin secretion. The first phase of insulin secretion represents a pool of insulin that is already present in granules during fasting and is released immediately in response to hyperglycemia. In contrast, the second phase of insulin secretion likely represents the synthesis and secretion of insulin in response to sustained hyperglycemia. This phenomenon has subsequently been shown in rodents, primates and in humans in response to intravenous glucose challenges. However, this biphasic pattern of insulin secretion is actually not observed in response to oral glucose challenges, likely because of the effects of hepatic extraction, the magnitude of which differs in response to the first and second phase of insulin secretion (Nesher and Cerasi, 2002).

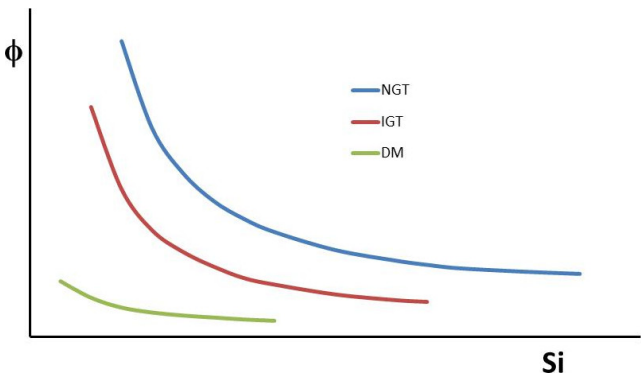

Figure 1: The nature of the hyperbolic relationship between β-cell responsivity (Φ) and Insulin action (S_i) depending on the glucose tolerance status of an individual. NGT = Normal Glucose Tolerance, IGT = Impaired Glucose Tolerance, DM = Diabetes Mellitus.

4 The Minimal Model

Reproducible, optimal, and quantitative measures of insulin secretion require some form of modeling which takes into account the fact that insulin is secreted into a remote compartment (i.e. the portal vein which is not accessible for peripheral sampling) and that between its appearance in the portal vein and its appearance in the systemic circulation there is a time lag to account for the distribution of insulin across various tissues and compartments. This is required because sampling in the peripheral circulation does not necessarily represent what is occurring at that time in the portal circulation in response to a given challenge. The current minimal model assumes that the sample pool of insulin differs slightly but significantly from the actively circulating pool of insulin and, again, this differs from the pool of insulin which is actually released. The minimal model also takes into account the delay (otherwise known as time, T) between the first and second phase of insulin secretion which represents the time to stimulate insulin synthesis in response to a given stimulus (Breda et al., 2001, 2002; Man et al., 2002).

The other consideration when measuring insulin secretion is to take into account the fact that insulin secretion occurs in the context of the prevailing insulin action. Just as it is unreasonable to talk about power in engineering terms without taking into account the amount of weight the said power needs to move, the same applies for beta cell function, and in such circumstances, insulin secretion should be expressed as a function of the prevailing insulin action. The resulting disposition index is currently considered the gold-standard measure of β-cell function. The disposition index tends to decrease across the spectrum of prediabetes, and the lower the disposition index, the likelier the risk of developing diabetes in the subsequent decade (Cobelli et al., 2014; Xiang et al., 2014).

Insulin secretion is related to insulin action via a hyperbolic relationship so that when glucose tolerance is maintained, even small decreases in insulin action are associated with a very significant increase in insulin secretion in an effort to maintain euglycaemia provided beta cell function is intact. The hyperbolic curve, which describes this relationship, will shift to the left as the beta cell fails and an individual becomes diabetic. Experimentally this paradigm has been proven in multiple situations, either by using pharmacotherapy or lifestyle intervention to improve insulin action with a commensurate offloading in insulin secretion or conversely making individuals acutely insulin resistant using various interventions such as free fatty acid elevation or niacin to increase insulin secretion, assuming euglycaemia is maintained in such circumstances (Bergman, 1989; Bergman et al., 2002).

The concept of the disposition index has been criticized more recently because of the realization that some individuals may not actually be able to respond by increasing insulin secretion in the presence of very significant changes in insulin action, and therefore, a hyperbolic relationship may not always exist. Indeed, efforts are now underway to perhaps better characterize the nature of the relationship between secretion and action in a given individual. How this relationship progresses over time, and whether genetic predisposition or disease itself actually accounts for a lot of these changes is, at present, uncertain (Ferrannini and Mari, 2004).

Another important reason for using an oral challenge over an intravenous glucose challenge to measure beta cell function is because it incorporates the incretin contribution to insulin secretion (Campioni et al., 2007).

5 What is the incretin effect?

It has long been known by physiologists that for a given glucose load administered intrajejunally as op-

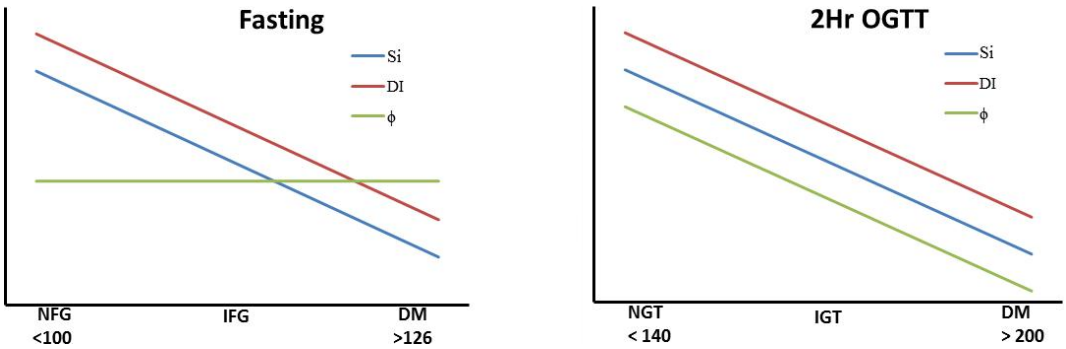

Figure 2: The relationship between β-cell responsivity (Φ) and Insulin action (S_i) and Disposition Index (DI) across the spectrum of impaired fasting glucose (left panel) and across the spectrum of impaired glucose tolerance (right panel). NFG = Normal Fasting Glucose, NGT = Normal Glucose Tolerance, IGT = Impaired Glucose Tolerance, DM = Diabetes Mellitus.

posed to intravenously, despite lower glucose concentrations, insulin secretion is far higher. Because of this, the existence of a gut hormone that stimulates insulin secretion and glucose disposal was hypothesized. The observed effect has been termed the 'incretin effect' because of its effect in assimilating an oral challenge (Mcintyre et al., 1964). The subsequent observation that several segments of the intestine stained for glucagon and the realization that this was confined to enteroendocrine cells helped propel the discovery of Glucagon-like Peptide-1 (GLP-1). The intestine is characterized by cellular heterogeneity and a distinct population of cells, characterized as APUD cells (since they take up amine precursors and decarboxylate them) that actively secrete multiple gut hormones. The glucagon-staining cells today are called L cells, and in actual fact, the immunoreactivity for glucagon arises not because they contain glucagon but because they contain a fragment of proglucagon, GLP-1. GLP-1 arises from transcription and translation of the glucagon gene to produce proglucagon but, whereas in the alpha-cell prohormone convertase 2 converts proglucagon to glucagon, in the L-cells of the gut prohomone convertase 1 converts proglucagon to GLP-1. Another product of proglucagon is glucagon-like peptide-2 (GLP-2). GLP-2 is actually a growth factor for intestinal epithelial cells and has no effect on insulin secretion or glucose metabolism. A larger fragment of proglucagon, oxyntomodulin, has effects on appetite, but its effects are probably not very significant in normal physiologic circumstances (Holst et al., 1994; Holst and Orskov, 2001). Nevertheless, GLP-1 has excited the interest of endocrinologists because it is a powerful insulin secretagogue and it stimulates insulin secretion in a glucose-dependent manner (i.e. insulin secretion will not be stimulated if glucose concentrations are within normal limits and at fasting concentrations). Unfortunately, GLP-1 has a very short half-life in the circulation. Therefore, if GLP-1 is to have therapeutic effect in people with diabetes, it will need to be infused on a continuous basis, given that its half-life is on the order of 1-2 minutes. GLP-1 activity depends on the integrity of the two end-terminal amino acids, loss of which inactivates GLP-1. An alternative is to inhibit the main enzyme responsible for its degradation. This enzyme is dipeptidyl-peptidase 4 and, indeed, dipeptidyl peptidase 4 inhibitors form a new class of glucose-lowering agents used to treat diabetes (Drucker and Nauck, 2006).

The third alternative is to use another analog of GLP-1 capable of stimulating the seven transmembrane helix GLP-1 receptor, yet resistant to the degradative effects of DPP-4. Such analogs are often called GLP-1 receptor agonists and, again, have been shown to have significant therapeutic viability in the treatment of diabetes.

There are significant differences between these two classes of agents which help to inform some of the underlying physiology that predisposes to diabetes. DPP-4 inhibitors raise endogenous GLP-1 concentrations, and in fact, active concentrations of GLP-1 are raised to high physiologic concentrations with a peak in the 12-20 pM range. In contrast, the equivalent activity of GLP-1 receptor agonists is probably achieved at GLP-1 concentrations of 25-30 pM. Both DPP-4 inhibitors and GLP-1 receptor agonists lower fasting and postprandial glucose concentrations, which is done by improving beta-cell function and simulating insulin secretion for a given glucose concentration. Intriguingly, GLP-1 receptor agonists also have powerful effects on intestinal motility, delaying gastric emptying, stimulating the nausea centers in the hypothalamus, and decreasing appetite. These effects are not observed with DPP-4 inhibitors (Vella et al., 2007).

6 The role of genetics in GLP-1 responsiveness

There are individuals who exhibit differential responsiveness to GLP-1-based therapy or GLP-1 infusion.

The earliest suggestion that this may be genetic in origin came from Beinborn et al. (2005) who identified a GLP-1 receptor mutation which altered responsitivity of the GLP-1 receptor to GLP-1 by about 50 % (Beinborn et al., 2005). Subsequently, the suggestion that common genetic polymorphisms in the GLP-1 receptor may affect responsiveness to infused GLP-1 was tested in a population of healthy individuals and indeed, two polymorphisms were identified which significantly altered GLP-1 responsitivity. Of the two SNPs identified, the most profound action was observed for RS3765467, which is an arginine to glutamine change at position 131 of the GLP-1 receptor in axon 4. This has a minor allele frequency of 5 % in Caucasians and, in the particular experiment, had a very profound effect on insulin secretion in response to infused GLP-1 and glucose. In contrast, RS6923761 results in a glycine to serine substitution at position 168 in axon 5. This has a minor allele frequency of about 30 % in Caucasian and, indeed, the individuals who are homozygous for serine at that position have decreased responsiveness to GLP-1 compared to the more common form where individuals are homozygous for glycine (Sathananthan et al., 2010).

7 GLP-1 and bariatric surgery

Another way that GLP-1 may be potentially important in diabetes is as it pertains to bariatric surgery. The commonest form of bariatric surgery undertaken, at least in North America, currently is Roux-en-Y gastric bypass, which creates a small restrictive gastric pouch and diverts nutrients to the distal intestine. The effect of distal delivery of calories results in stimulation of GLP-1 secretion. Individuals after gastric bypass have high concentrations of GLP-1 in response to meal ingestion (Laferrère et al., 2008). Roux-en-Y gastric bypass has aroused interest recently because bypass operations are associated with remission of diabetes in about 40 % of all individuals with type 2 diabetes, and it has been hypothesized that GLP-1 may play a role in this remission. In such circumstances, one of the experimental paradigms used to investigate the contribution of endogenous GLP-1 to insulin secretion in the postprandial period has been to use competitive antagonist of GLP-1 at its cognate receptor. This antagonist is exendin-(9,39) and is actually a derivative of a GLP-1 receptor agonist which is truncated and, therefore, has no significant metabolic effect when it binds the GLP-1 receptor.

In non-diabetic patients after Roux-en-Y gastric bypass, infusion of exendin-(9,39) results in decreased insulin and C-peptide concentrations compared to age-, weight-, and gender-matched controls. Indeed, this results in a small but significant rise in peak and integrated glucose concentrations. These effects are due to small effects on beta-cell function, as manifested by decreases in beta-cell responsitivity. What is interesting is that the component of beta-cell responsitivity that is affected is the one that is dependent upon insulin synthesis and secretion in keeping with the known effects of GLP-1 on insulin synthesis. The converse experimental administration of GLP-1 or GLP-1-based therapies raise the component of insulin secretion that is associated with synthesis and secretion (Shah et al., 2014).

A neglected part of the physiology of insulin secretion is the fact that insulin is actually secreted into the portal vein in a pulsatile fashion, and the amplitude and frequency of insulin pulses are decreased in pathologic states, such as aging, obesity, and type 2 diabetes. GLP-1 may be important when secreted into the portal vein because it may help maintain beta-cell competence as well as beta-cell pulsatility and amplitude. Whether fasting and postprandial insulin secretion or its pulsatility has effects on, for example, hepatic insulin action, thereby explaining the relationship between insulin secretion and action observed in prediabetes, is as yet unknown but is the subject of active investigation (Meier et al., 2005; Matveyenko et al., 2008).

8 Measuring β-cell mass

The final aspect as pertains to beta-cell function is the quest to try and quantify beta-cell mass. At present, this subject is problematic. Initial attempts of quantifying beta-cell mass were quite simple and qualitative as they involved counting islets in autopsy specimens. Since then attempts have been made to undertake invasive testing in humans using pancreatic biopsy. Unfortunately, this method is flawed with complications and rarely provides useful information, therefore it has almost been abandoned completely. Efforts have been made to try and quantify islet mass by extrapolating from pancreatic volume obtained by conventional, noninvasive imaging such as CT scanning of magnetic resonance imaging and subsequent extrapolation of islet number. More recently, efforts have been made to use ligands specific to the islets which then can be labeled either with a fluorescent marker detectable by noninvasive imaging or with a radio-labeled ligand. However, to date there has been no compound identified which binds specifically to the islets.

At the current time, the best paradigm for beta-cell function in vivo is ultimately reductionist in approach; currently islet numbers and islet morphology are less important than how they function in response to a given challenge. It is in this circumstance that a functional test such as an oral glucose tolerance test or a mixed meal test and subsequent mathematical extrapolation of beta-cell function may be important clinically. Our current therapeutic interventions are intended to improve glycaemic control not improving beta-cell health.

Nevertheless, using the current mathematical models to quantify beta-cell function over time may have therapeutic application in the near future with the development of novel therapeutics intended to increase beta-cell mass and function.

Acknowledgments

This manuscript is a summary of the presentation given by Dr A. Vella at the COST BMBS APC held in Malta in April 2014 organized by Prof. G. Di Giovanni.

References

Basu, A., Alzaid, A., Dinneen, S., Caumo, A., Cobelli, C. and Rizza, R. A. (1996). Effects of a change in the pattern of insulin delivery on carbohydrate tolerance in diabetic and nondiabetic humans in the presence of differing degrees of insulin resistance. *J. Clin. Invest.* 97(10), 2351–2361.

Beinborn, M., Worrall, C. I., McBride, E. W. and Kopin, A. S. (2005). A human glucagon-like peptide-1 receptor polymorphism results in reduced agonist responsiveness. *Regul. Pept.* 130(1-2), 1–6.

Bergman, R. N. (1989). Lilly lecture 1989. Toward physiological understanding of glucose tolerance. Minimal-model approach. *Diabetes.* 38(12), 1512–1527.

Bergman, R. N., Ader, M., Huecking, K. and Citters, G. V. (2002). Accurate assessment of beta-cell function: the hyperbolic correction. *Diabetes.* 51 Suppl 1, S212–20.

Breda, E., Cavaghan, M. K., Toffolo, G., Polonsky, K. S. and Cobelli, C. (2001). Oral glucose tolerance test minimal model indexes of beta-cell function and insulin sensitivity. *Diabetes.* 50(1), 150–158.

Breda, E., Toffolo, G., Polonsky, K. S. and Cobelli, C. (2002). Insulin release in impaired glucose tolerance: oral minimal model predicts normal sensitivity to glucose but defective response times. *Diabetes.* 51 Suppl 1, S227–33.

Butler, P. C. and Rizza, R. A. (1991). Contribution to postprandial hyperglycemia and effect on initial splanchnic glucose clearance of hepatic glucose cycling in glucose-intolerant or NIDDM patients. *Diabetes.* 40(1), 73–81.

Campioni, M., Toffolo, G., Shuster, L. T., Service, F. J., Rizza, R. A. and Cobelli, C. (2007). Incretin effect potentiates beta-cell responsivity to glucose as well as to its rate of change: OGTT and matched intravenous study. *Am. J. Physiol. Endocrinol. Metab.* 292(1), E54–60.

Cobelli, C., Man, C. D., Toffolo, G., Basu, R., Vella, A. and Rizza, R. (2014). The oral minimal model method. *Diabetes.* 63(4), 1203–1213.

DeFronzo, R. A. (1988). Lilly lecture 1987. The triumvirate: beta-cell, muscle, liver. A collusion responsible for NIDDM. *Diabetes.* 37(6), 667–687.

Dinneen, S. F., Maldonado, D., Leibson, C. L., Klee, G. G., Li, H., et al. (1998). Effects of changing diagnostic criteria on the risk of developing diabetes. *Diabetes Care.* 21(9), 1408–1413.

Drucker, D. J. and Nauck, M. A. (2006). The incretin system: glucagon-like peptide-1 receptor agonists and dipeptidyl peptidase-4 inhibitors in type 2 diabetes. *Lancet.* 368(9548), 1696–1705.

Ferrannini, E. and Mari, A. (2004). Beta cell function and its relation to insulin action in humans: a critical appraisal. *Diabetologia.* 47(5), 943–956.

Holst, J. J., Bersani, M., Johnsen, A. H., Kofod, H., Hartmann, B. and Orskov, C. (1994). Proglucagon processing in porcine and human pancreas. *J. Biol. Chem.* 269(29), 18827–18833.

Holst, J. J. and Orskov, C. (2001). Incretin hormones–an update. *Scand. J. Clin. Lab. Invest. Suppl.* 234, 75–85.

Laferrère, B., Teixeira, J., McGinty, J., Tran, H., Egger, J. R., et al. (2008). Effect of weight loss by gastric bypass surgery versus hypocaloric diet on glucose and incretin levels in patients with type 2 diabetes. *J. Clin. Endocrinol. Metab.* 93(7), 2479–2485.

Man, C. D., Caumo, A. and Cobelli, C. (2002). The oral glucose minimal model: estimation of insulin sensitivity from a meal test. *IEEE Trans Biomed Eng.* 49(5), 419–429.

Matveyenko, A. V., Veldhuis, J. D. and Butler, P. C. (2008). Adaptations in pulsatile insulin secretion, hepatic insulin clearance, and beta-cell mass to age-related insulin resistance in rats. *Am. J. Physiol. Endocrinol. Metab.* 295(4), E832–41.

Mcintyre, N., Holdsworth, C. D. and Turner, D. S. (1964). New interpretation of oral glucose tolerance. *Lancet.* 2(7349), 20–21.

Meier, J. J., Veldhuis, J. D. and Butler, P. C. (2005). Pulsatile insulin secretion dictates systemic insulin delivery by regulating hepatic insulin extraction in humans. *Diabetes.* 54(6), 1649–1656.

Nesher, R. and Cerasi, E. (2002). Modeling phasic insulin release: immediate and time-dependent effects of glucose. *Diabetes.* 51 Suppl 1, S53–9.

Rossell, R., Gomis, R., Casamitjana, R., Segura, R., Vilardell, E. and Rivera, F. (1983). Reduced hepatic insulin extraction in obesity: relationship with plasma insulin levels. *J. Clin. Endocrinol. Metab.* 56(3), 608–611.

Sathananthan, A., Man, C. D., Micheletto, F., Zinsmeister, A. R., Camilleri, M., et al. (2010). Common genetic variation in GLP1R and insulin secretion in response to exogenous GLP-1 in nondiabetic

subjects: a pilot study. *Diabetes Care*. 33(9), 2074–2076.

Sathananthan, A., Man, C. D., Zinsmeister, A. R., Camilleri, M., Rodeheffer, R. J., et al. (2012). A concerted decline in insulin secretion and action occurs across the spectrum of fasting and postchallenge glucose concentrations. *Clin. Endocrinol. (Oxf)*. 76(2), 212–219.

Shah, M., Law, J. H., Micheletto, F., Sathananthan, M., Man, C. D., et al. (2014). Contribution of endogenous glucagon-like peptide 1 to glucose metabolism after Roux-en-Y gastric bypass. *Diabetes*. 63(2), 483–493.

Vella, A., Bock, G., Giesler, P. D., Burton, D. B., Serra, D. B., et al. (2007). Effects of dipeptidyl peptidase-4 inhibition on gastrointestinal function, meal appearance, and glucose metabolism in type 2 diabetes. *Diabetes*. 56(5), 1475–1480.

Xiang, A. H., Watanabe, R. M. and Buchanan, T. A. (2014). HOMA and Matsuda indices of insulin sensitivity: poor correlation with minimal model-based estimates of insulin sensitivity in longitudinal settings. *Diabetologia*. 57(2), 334–338.